

Synthesis, antimicrobial, and cytotoxicity evaluation of selective growth inhibitors of *Clostridioides difficile*

Bassant Mohamed Said Rateb

Doctor of Philosophy

Aston University

2024

©Bassant Mohamed Said Rateb, 2024

Bassant Mohamed Said Rateb asserts their moral right to be identified as the author of this thesis. This copy of the thesis has been supplied on the condition that anyone who consults it is understood to recognise that its copyright belongs to its author and that no quotation from the thesis and no information derived from it may be published without appropriate permission or acknowledgment.

Aston University

Synthesis, antimicrobial, and cytotoxic evaluation of selective growth inhibitors of
Clostridioides difficile

Thesis Submitted by Bassant Mohamed Said Rateb

For the Degree of Doctor of Philosophy

2024

Abstract

The World Health Organisation has estimated the cost of antimicrobial resistance (AMR) to the global economy to be \$100,000,000,000,000 with AMR becoming the leading cause of death by 2050. *Clostridioides difficile* is a major healthcare-associated infection in the UK, Europe, the USA, and other developed countries. Strains of this microorganism that are less sensitive to the frontline therapies (metronidazole, vancomycin, and fidaxomicin) are emerging, causing great concern and negative prognosis for AMR. Developing new, potent, efficacious antimicrobial agents with a narrow spectrum of activity will provide alternative treatment options for *C. difficile* and AMR. Representative derivatives were prepared in good yield by Knoevenagel condensation of arylaldehydes with an active methylene substrate, in ethanol or water at reflux and without additional catalyst. Compounds were purified, characterised, and assayed against *C. difficile* NCTC 11204 to determine potency, and against *Escherichia coli* NCTC 35218 and *Staphylococcus aureus* NCTC 29213 to determine selectivity. The lead compound 5-[(5-Nitro-2-furyl)methylene]hexahydropyrimidine-2,4,6-trione (**2.10**) gave a minimum inhibitory concentration (MIC) value of 2 µg/mL against *C. difficile* NCTC 11204. Replacement of the nitro group by hydrogen 5-(2-furylmethylene)hexahydropyrimidine-2,4,6-trione (**2.8**) resulted in good selectivity. This inhibitory activity improved further, using isosteres. For example, the replacement of oxygen **2.10** by sulfur 5-[(5-Nitro-2-thienyl)methylene]hexahydropyrimidine-2,4,6-trione (**2.16**) gave a MIC value of 0.5 µg/mL against CD. Replacement of the nitro group in compound **2.16** by hydrogen 5-(thiophen-2-ylmethylene)pyrimidine-2,4,6(1H,3H,5H)-trione (**2.20**) resulted in the most potent compound in the series (MIC = 0.125 µg/mL) albeit with reduced selectivity. The active diene derivatives 5-[(E)-3-(2-Furyl)prop-2-enylidene]hexahydropyrimidine-2,4,6-trione (**2.9**), 5-[(E)-3-(5-Nitro-2-furyl)prop-2-enylidene]hexahydropyrimidine-2,4,6-trione (**2.13**), and 5-[(2-Methoxy-1-naphthyl)methylene]hexahydropyrimidine-2,4,6-trione (**2.21**) demonstrate scope for homologation in the inhibitors. Replacement of the five-membered aryl ring with benzene in compound 5-[(E)-3-(4-Methoxyphenyl)prop-2-enylidene]hexahydropyrimidine-2,4,6-trione (**2.5**) gave excellent selectivity but with reduced growth inhibitory against *C. difficile*. Isosteric modification provided derivatives with improved potency and selectivity against *C. difficile* compared with *S. aureus* and *E. coli*. Six representatives of the lead compounds that were tested for their cytotoxic activity against normal mice liver cells and colorectal cancer cells, where compound **2.8** showed the lowest cytotoxic activity against both cell lines. Of the compounds prepared and evaluated, a subset provided promising development candidates for testing against clinical isolates from patients presenting with *C. difficile* infection, to examine effectiveness against ribotypes that are less sensitive for frontline therapies.

Keywords: *C. difficile*, antimicrobial resistance, Knoevenagel condensation, antimicrobial, minimum inhibitory concentration, selectivity, cytotoxicity, normal mice liver cells, colorectal cancer cells.

Acknowledgments

"And my success is only through Allah. Upon Him, I have relied, and to Him I return." The Quran 11:88 (Surah Hud).

First and foremost, I thank Allah SWT for allowing me to learn and improve in all life aspects. May I in return benefit people with the Knowledge I gained.

I'd like to wholeheartedly thank my supervisors, Dr William Fraser and Dr Tony Worthington. Thank you both for all the support and encouragement that you provided along the way. You both have always been considered and never added extra pressure on me. Thank you for treating me like a daughter; I was lucky to work with both of you in a stress-free environment. You taught me a lot, and you made my PhD journey smooth. Dr Fraser, thank you for all the casual conversations that we had, and for helping me whenever you can. Dr Tony, you are a true warrior and an inspiration; thank you for giving me thesis feedback despite all the pain you are going through. I wish you a complete recovery and a long happy life with your loved ones.

I would also like to thank Dr Isabella Romeo-Melody for teaching me the fundamentals of working in the microbiology lab. I would also like to thank Dr Craig Russell and my colleague Mohamed Al Tahan for illustrating and demonstrating the fundamentals of cytotoxicity. Dr Dan Rathbone, thank you for the constructive feedback and comments on my second-year qualifying report. A huge gratitude to the postdoctoral researchers Dr Subramanian Govindan, Dr Brahman Medapi, and Dr Florian Dato from whom I learned a lot. Thanks to my colleague Dr Aisosa Iyoha and the technical staff, Hayley Shearer and Daniel Burrell, for their support and kindness.

Alhamdulillah for having the best parents anyone can ask for; I am forever grateful for all the sacrifices they have made to see me and my siblings successful and more importantly happy. Thank you both for supporting us morally and financially in every step of our lives. I want to thank my younger brother Ramy for being the kindest heart I know; Jomana and I are lucky to have you as a backbone to rely on. As for my journey companion, my youngest sister Jomana, I could not have survived those 3 years if I did not have you by my side. You were my home away from home, thank you for everything and I hope I make our family proud like you have already done my little genius sister. To my beloved husband Dr Ibrahim Ezz, thank you for all the love and support, for believing in me, and for boosting my always-draining self-esteem. I am lucky to have you by my side forever; you've always been someone I look up to. I hope I become as half as good as you are in my career one day. To all my friends in the UK "Alaa, Zena, Sara, Diana, Nourhan, and Hadeer", thank you for being my happy place. To all my friends in Egypt (a long list to mention) thank you for consistently checking on me and for your encouraging words. Thank you all, I love you all from the bottom of my heart.

List of Abbreviations

°C	Degree Celsius
µg	Microgram
µl	Microlitre
¹³ C NMR	Carbon Nuclear Magnetic Resonance
¹ H NMR	Proton Nuclear Magnetic Resonance
AAD	Antibiotic-Associated Diarrhoea
AMR	Antimicrobial Resistance
APTs	Alkyl Pyrimidinetriones
ATCC	American Type Culture Collection
BNL	Mouse Normal Liver Cells
Caco-2	Colorectal Cancer
CD	<i>Colstridium difficile</i>
CDI	<i>C. difficile</i> Infection
CFU	Colony Forming Unit
CLSI	The Clinical And Laboratory Standards Institute
cm	Centimetre
CPE	Carbapenemase-Producing Enterobacteriaceae
DHODase	Dihydroorotate Dehydrogenase Enzyme
DMEM	Dulbecco's Modified Eagle Medium
DMSO-d6	Deuterated Dimethyl Sulfoxide
ESI	Electron Spray Ionisation
EUCAST	European Committee on Antimicrobial Susceptibility Testing
FAD	Flavin Adenine Dinucleotide
FBS	Fetal Bovine Serum
FDA	Food And Drug Administration
FMN	Flavin Mononucleotide
FMT	Faecal Microbiota Transplantation
g	Gram
GIT	Gastrointestinal Tract
h	Hour

HEK	Human Embryonic Kidney
HMBC	Hetero-Nuclear Multiple Bond-Correlation Spectroscopy
HSQC	Heteronuclear Single Quantum Coherence
Hz	Hertz
IC ₅₀	Inhibitory Concentration 50
IVIg	Intravenous Immunoglobulin
LD ₅₀	Lethal Dose 50
M	Molar
MBC	Minimum Bactericidal Concentration
MH	Mueller-Hinton
MHB	Muller-Hinton Broth
MHz	Mega-Hertz
MIC	Minimum Inhibitory Concentration
ml	Millilitre
mm	Millimetres
mM	Millimolar
mmol	Millimole
MRSA	Methicillin-Resistant <i>Staphylococcus aureus</i>
MS	Mass Spectrometry
MTT	3-(4,5-Dimethylthiazol-2-Yl)-2,5-Diphenyl-2H-Tetrazolium Bromide
OD	Optical Density
OTC	Over The Counter
PFOR	Pyruvate-Ferredoxin Oxidoreductase
ppm	Parts Per Million
RPMI	Roswell Park Memorial Institute
SAR	Structure-Activity Relationship
TLC	Thin-Layer Chromatographic
UMP	Uridine Monophosphate
UTIs	Urinary Tract Infections
UV	Ultraviolet Light
VRE	Vancomycin-Resistant Enterococci

WCB	Wilkins Chalgren Anaerobic Broth
ZOI	Zone of Inhibition
μM	Micromolar
α_{CH}	Alpha Proton's

List of Tables

Table 2. 1. Connectivity deduced from the HMBC spectrum of compound 2.1	39
Table 2. 2. Comparison of the literature melting points in °C of compounds with products isolated in this thesis work using the reported methods	61
Table 2. 3. Comparison of the literature melting points in °C of compounds with products isolated in this thesis work using the reported methods	89
Table 2. 4. Comparison of the literature melting points in °C of compounds with products isolated in this thesis work using the reported methods	113
Table 3. 1. List of Gram-positive and Gram-negative microorganisms, with corresponding American Type Culture Collection number	125
Table 3. 2. List of comparator antimicrobials including the concentration of prepared stock solutions.	126
Table 3. 3. Antimicrobial activities of control drugs against <i>C. difficile</i> and control organisms <i>E. coli</i> and <i>S. aureus</i>	133
Table 3. 4. Antimicrobial activities of aldehydes against <i>C. difficile</i> and control microorganisms <i>E. coli</i> and <i>S. aureus</i>	134
Table 3. 5. The antimicrobial activities of benzylidene barbiturate derivatives against <i>C. difficile</i> and control organisms <i>E. coli</i> and <i>S. aureus</i>	135
Table 3. 6. The antimicrobial activity of allylic barbiturate derivatives against <i>C. difficile</i> and control microorganisms <i>E. coli</i> and <i>S. aureus</i>	138
Table 3. 7. The antimicrobial activity of the Meldrum's acid derivatives against <i>C. difficile</i> and control microorganisms <i>E. coli</i> and <i>S. aureus</i>	140
Table 3. 8. The antimicrobial activity of the five-membered ring derivatives against <i>C. difficile</i> and control organisms <i>E. coli</i> and <i>S. aureus</i>	142
Table 4. 1. Some of the most potent and selective compounds against <i>C. difficile</i> whose cytotoxic activity was evaluated using the MTT assay against BNL and Caco-2 cell lines....	149

List of Figures

Figure 1. 1. Timeline showing the dates of discovery and resistance of some of the most common classes of antibiotics in the past century (Public Health England, 2017).	3
Figure 1. 2. Examples and ring atom numbering of some antimicrobials possessing similar structural features	8
Figure 1. 3. Mechanism of action of metronidazole (Ovung & Bhattacharyya, 2023)	8
Figure 1. 4. The futile cycling in metronidazole reductive activation (left to right) and reductive inactivation (top to bottom)	10
Figure 1. 5. Structure of vancomycin	12
Figure 1. 6. Mechanism of action of vancomycin (Yarlagadda <i>et al.</i> , 2014)	12
Figure 1. 7. The structure of fidaxomicin	14
Figure 1. 8. The reductive activation of nitrofurantoin by flavoprotein reductase enzyme ..	15
Figure 1. 9. Orotate metabolic pathway	19
Figure 1. 10. The fourth and reversible step of <i>de novo</i> pyrimidine biosynthesis	19
Figure 1. 11. DHODase catalytic side with the substrate (blue) and proximal flavine electron acceptor (yellow) (Argyrou <i>et al.</i> , 2000)	22
Figure 1. 12. Hypothetical mechanism of potential prodrug activation and DHODase inhibition.....	23
Figure 2. 1. The resonance forms of the keto/enol tautomers of barbituric acid	27
Figure 2. 2. Grimaux's synthesis of barbituric acid	27
Figure 2. 3. Formation and derivatisation of Meldrum's acid.....	28
Figure 2. 4. The resonating forms of Meldrum's acid carbanion	29
Figure 2. 5. Synthetic route to Meldrum's acid	29
Figure 2. 6. Compound 2.1	32
Figure 2. 7. Compound 2.2	33
Figure 2. 8. Compound 2.3	34
Figure 2. 9. The ¹ H NMR spectra of compounds 2.2 and 2.3	34
Figure 2. 10. Mechanism of action of Wittig reaction	36
Figure 2. 11. The chemical reaction between triphenylphosphine with aldehyde or ketone	37
Figure 2. 12. HMBC spectrum of compound 2.1 indicating the correlation between the ¹ H NMR (horizontal) and ¹³ C NMR (vertical)	39
Figure 2. 13. Compound 2.4	40
Figure 2. 14. Compound 2.5	41
Figure 2. 15. Compound 2.6	42
Figure 2. 16. Compound 2.7	43
Figure 2. 17. Compound 2.8	43
Figure 2. 18. Compound 2.9	44
Figure 2. 19. Compound 2.10	45
Figure 2. 20. Compound 2.11	46
Figure 2. 21. Compound 2.12	47
Figure 2. 22. Compound 2.13	47
Figure 2. 23. Compound 2.14	48
Figure 2. 24. Compound 2.15	49
Figure 2. 25. Compound 2.16	50
Figure 2. 26. Compound 2.17	51
Figure 2. 27. Compound 2.18	52

Figure 2. 28. Compound 2.19	53
Figure 2. 29. Compound 2.20	54
Figure 2. 30. Compound 2.21	54
Figure 2. 31. Compound 2.22	55
Figure 2. 32. Compound 2.23	56
Figure 2. 33. Compound 2.24	56
Figure 2. 34. Compound 2.25	57
Figure 2. 35. Compound 2.26	57
Figure 2. 36. The scheme reported by Barakat <i>et al.</i> (2015).....	59
Figure 2. 37. ¹ H NMR spectra of Michaeladdition product (bottom) and Knoevenagel condensation product (top).....	60
Figure 2. 38. Compound 2.27	62
Figure 2. 39. Compound 2.28	63
Figure 2. 40. Compound 2.29	64
Figure 2. 41. Compound 2.30	64
Figure 2. 42. Significant differences between the ¹ H NMR spectra of 2.16 (blue), 2.27 (red), 2.28 (olive) and 2.30 (green)	66
Figure 2. 43. Significant differences between the ¹³ C NMR spectra of 2.16 (blue), 2.27 (red), 2.28 (olive) and 2.30 (green)	67
Figure 2. 44. Catalytic Knoevenagel condensation mechanism with organic base “piperidine” as an added catalyst.....	68
Figure 2. 45. The predicted Knoevenagel condensation mechanism with no added catalyst	69
Figure 2. 46. Compound 2.31	70
Figure 2. 47. Compound 2.32	71
Figure 2. 48. Compound 2.33	72
Figure 2. 49. Compound 2.34	73
Figure 2. 50. Compound 2.35	74
Figure 2. 51. Compound 2.36	74
Figure 2. 52. Compound 2.37	75
Figure 2. 53. Compound 2.38	76
Figure 2. 54. Compound 2.39	77
Figure 2. 55. Compound 2.40	78
Figure 2. 56. Compound 2.41	79
Figure 2. 57. Compound 2.42	79
Figure 2. 58. Compound 2.43	80
Figure 2. 59. Compound 2.44	81
Figure 2. 60. Compound 2.45	82
Figure 2. 61. Compound 2.46	83
Figure 2. 62. The synthetic route of the production of allylic pyrimidinetrione derivatives using the one pot in situ reaction using benzaldehyde and 2-aminothiophenol to produce 2-phenyl-2,3-dihydrobenzo[d]thiazole which serves as a hydrogen source	85
Figure 2. 63. Keto-enol tautomerisation of the reduced products	86
Figure 2. 64. The ¹ H NMR spectra of Knoevenagel product (2.4) on bottom and the allylic pyrimidinetrione (2.31) on top	86
Figure 2. 65. The ¹ H NMR spectra of Knoevenagel product (2.4) on bottom and the allylic pyrimidinetrione (2.31) on top	87

Figure 2. 66. The ¹ H NMR spectra of compound 2.32, where the NaBH ₄ reduced was placed on bottom and the 2-phenyl-2,3-dihydrobenzo[d]thiazole reduced was placed on top	88
Figure 2. 67. Mechanism of 2-phenyl-2,3-dihydrobenzo[d]thiazole formation in a one-pot reaction.....	90
Figure 2. 68. The predicted mechanism of NaBH ₄ reduction of alkenes	91
Figure 2. 69. Synthesis of propyl bridged aralkylpyrimidinetrioles derivatives	91
Figure 2. 70. Compound 2.47	92
Figure 2. 71. Compound 2.48	93
Figure 2. 72. Compound 2.49	93
Figure 2. 73. Mechanism of action of catalytic hydrogenation using Pd/C	94
Figure 2. 74. Compound 2.50	95
Figure 2. 75. Base-hydrolysis of Knoevenagel products	96
Figure 2. 76. Béchamp reduction mechanism	96
Figure 2. 77. Compound 2.51	97
Figure 2. 78. Compound 2.52	98
Figure 2. 79. Compound 2.53	99
Figure 2. 80. Compound 2.54	100
Figure 2. 81. Compound 2.55	101
Figure 2. 82. Compound 2.56	101
Figure 2. 83. Compound 2.57	102
Figure 2. 84. Compound 2.58	103
Figure 2. 85. Compound 2.59	104
Figure 2. 86. Compound 2.60	104
Figure 2. 87. Compound 2.61	105
Figure 2. 88. Compound 2.62	106
Figure 2. 89. Compound 2.63	107
Figure 2. 90. Compound 2.64	108
Figure 2. 91. Compound 2.65	108
Figure 2. 92. Compound 2.66	109
Figure 2. 93. Compound 2.67	110
Figure 2. 94. Compound 2.69	114
Figure 2. 95. Compound 2.70	115
Figure 2. 96. Compound 2.71	115
Figure 2. 97. Compound 2.72	116
Figure 2. 98. Compound 2.73	117
Figure 2. 99. Compound 2.74	117
Figure 2. 100. Compound 2.75	118
Figure 2. 101. Compound 2.76	118
Figure 2. 102. Compound 2.77	119
Figure 2. 103. Mechanism of imine formation	120
Figure 3. 1. Diagram of the layout of diffusion assay plates, with the tested compounds concentration (mg/ ml) used.....	131
Figure 4. 1. Enzymatic conversion of tetrazolium salt (left, yellow) to the insoluble formazan product (right, purple) by means of NAD(P)H NAD(P)H-dependent oxidoreductase enzymes.	145
Figure 4. 2. Structure of doxorubicin	150

Figure 4. 3. Examples of the MTT assay experiment against BNL (left) and Caco-2 (right) cell lines comprising 9 different drug concentrations of doxorubicin ranging from 0.03-300 µg/ml after 48 hours of drug exposure. The columns show the different drug concentrations in triplicates as labelled on the lid, where the first 3 wells in each figure labelled as (µg/ml) represent the controls..... 150

Figure 4. 4. Graph showing the plot of BNL cell viability % vs concentration of doxorubicin. 151

Figure 4. 5. Graph showing the plot of Caco-2 cell viability % vs doxorubicin concentration. 151

Figure 4. 6. Microscopic imaging showing the cell viability at different doxorubicin concentrations against the BNL cell line, with doxorubicin concentrations of (a) 0 µg/ml as the control; (b) 3 µg/ml; (c) 30 µg/ml; and (d) 100 µg/ml. The dots represent the viable cells that decrease in number with the increase in doxorubicin concentration. 151

Figure 4. 7. Microscopic imaging showing the cell viability at different doxorubicin concentrations against the Caco-2 cell line, with doxorubicin concentrations of (a) 0 µg/ml as the control; (b) 3 µg/ml; (c) 30 µg/ml; and (d) 100 µg/ml. The clusters represent the viable cells that decrease in number with the increase in doxorubicin concentration. 152

Figure 4. 8. Graph showing the plot of BNL cell viability % vs concentration of 2.7 153

Figure 4. 9. Graph showing the plot of Caco-2 viability % vs concentration of 2.7..... 153

Figure 4. 10. Microscopic imaging showing the cell viability at different 2.7 concentrations against the BNL cell line, with 2.7 concentrations of (a) 0 µg/ml as the control; (b) 3 µg/ml; (c) 30 µg/ml; and (d) 100 µg/ml. The dots represent the viable cells that decrease in number with the increase in compound 2.7 concentration..... 153

Figure 4. 11. Microscopic imaging showing the cell viability at different 2.7 concentrations against the Caco-2 cell line, with 2.7 concentrations of (a) 0 µg/ml as the control; (b) 3 µg/ml; (c) 30 µg/ml; and (d) 100 µg/ml. The clusters represent the viable cells that decrease in number with the increase in compound 2.7 concentration. 153

Figure 4. 12. Graph showing the plot of BNL cell viability % vs concentration of 2.8..... 154

Figure 4. 13. Graph showing the plot of Caco-2 viability % vs concentration of 2.8 154

Figure 4. 14. Microscopic imaging showing the cell viability at different 2.8 concentrations against the BNL cell line, with 2.8 concentrations of (a) 0 µg/ml as the control; (b) 3 µg/ml; (c) 30 µg/ml; and (d) 100 µg/ml. The dots represent the viable cells that decrease in number with the increase in compound 2.8 concentration..... 154

Figure 4. 15. Microscopic imaging showing the cell viability at different 2.8 concentrations against the Caco-2 cell line, with 2.8 concentrations of (a) 0 µg/ml as the control; (b) 3 µg/ml; (c) 30 µg/ml; and (d) 100 µg/ml. The clusters represent the viable cells that decrease in number with the increase in compound 2.8 concentration. 155

Figure 4. 16. Graph showing the plot of BNL cell viability % vs concentration of 2.16..... 155

Figure 4. 17. Graph showing the plot of Caco-2 viability % vs concentration of 2.16 155

Figure 4. 18. Microscopic imaging showing the cell viability at different 2.16 concentrations against the Caco-2 cell line, with 2.16 concentrations of (a) 0 µg/ml as the control; (b) 3 µg/ml; (c) 30 µg/ml; and (d) 100 µg/ml. The dots represent the viable cells that decrease in number with the increase in compound 2.16 concentration 156

Figure 4. 19. Microscopic imaging showing the cell viability at different 2.16 concentrations against the Caco-2 cell line, with 2.16 concentrations of (a) 0 µg/ml as the control; (b) 3 µg/ml; (c) 30 µg/ml; and (d) 100 µg/ml. The dots represent the viable cells that decrease in number with the increase in compound 2.16 concentration. 156

Figure 4. 20. Graph showing the plot of BNL cell viability % vs concentration of 2.53.....	157
Figure 4. 21. Graph showing the plot of Caco-2 viability % vs concentration of 2.53	157
Figure 4. 22. Microscopic imaging showing the cell viability at different 2.53 concentrations against BNL cell line, with 2.53 concentrations of (a) 0 µg/ml as the control; (b) 3 µg/ml; (c) 30 µg/ml; and (d) 100 µg/ml. The dots represent the viable cells which decrease in number with the increase in compound 2.53 concentration.....	157
Figure 4. 23. Microscopic imaging showing the cell viability at different 2.53 concentrations against Caco-2 cell line, with 2.53 concentrations of (a) 0 µg/ml as the control; (b) 3 µg/ml; (c) 30 µg/ml; and (d) 100 µg/ml. The dots represent the viable cells which decrease in number with the increase in compound 2.53 concentration.	158
Figure 4. 24. Graph showing the plot of BNL cell viability % vs concentration of 2.58	158
Figure 4. 25. Graph showing the plot of Caco-2 cell viability % vs concentration of 2.58....	158
Figure 4. 26. Microscopic imaging showing the cell viability at different 2.58 concentrations against the BNL cell line, with 2.58 concentrations of (a) 0 µg/ml as the control; (b) 3 µg/ml; (c) 30 µg/ml; and (d) 100 µg/ml. The dots represent the viable cells that decrease in number with the increase in compound 2.58 concentration.....	159
Figure 4. 27. Microscopic imaging showing the cell viability at different 2.58 concentrations against the Caco-2 cell line, with 2.58 concentrations of (a) 0 µg/ml as the control; (b) 3 µg/ml; (c) 30 µg/ml; and (d) 100 µg/ml. The dots represent the viable cells that decrease in number with the increase in compound 2.58 concentration.	159
Figure 4. 28. Graph showing the plot of Caco-2 cell viability % vs concentration of 2.20 ..	160
Figure 4. 29. Graph showing the plot of BNL cell viability % vs concentration of 2.20.....	160
Figure 4. 30. Microscopic imaging showing the cell viability at different 2.20 concentrations against the BNL cell line, with 2.58 concentrations of (a) 0 µg/ml as the control; (b) 3 µg/ml; (c) 30 µg/ml; and (d) 100 µg/ml. The dots represent the viable cell that decreases in number with the increase in compound 2.20 concentration.....	160
Figure 4. 31. Microscopic imaging showing the cell viability at different 2.20 concentrations against the Caco-2 cell line, with 2.58 concentrations of (a) 0 µg/ml as the control; (b) 3 µg/ml; (c) 30 µg/ml; and (d) 100 µg/ml. The dots represent the viable cells that decrease in number with the increase in compound 2.20 concentration.	161
Figure 4. 32. Graph summarising the MIC and IC ₅₀ values of the test compounds against the BNL and Caco-2 cell lines.....	167

List of Schemes

Scheme 2. 2. General scheme for the synthesis of benzylidene barbiturates, and their reduced forms.....	35
Scheme 2. 3. The 2 nd synthetic route of compound 2.16, the right-hand product was the expected compound as reported by Barakat <i>et al.</i> (2015), and the left-hand product was the obtained compound characterised by ¹ H NMR.....	60
Scheme 2. 4. Béchamp reduction of NO ₂ group.....	95
Scheme 2. 5. Meldum's acid derivatives reactions.....	111
Scheme 2. 6. 5-membered rings synthesis scheme.....	120

List of Contents

Chapter 1	1
1. Introduction:.....	1
1.1. Antimicrobial resistance	1
1.2. Causes of antibiotic resistance	1
1.3. Novel approaches to minimise AMR.....	2
1.4. The prevalence of <i>Clostridioides difficile</i> infection	3
1.5. Spread and recurrence of CDI.....	4
1.6. Risk factors associated with CDI	5
1.7. Prevention of CDI.....	6
1.8. Immunity and host defences	6
1.9. Treatment of CDI.....	7
1.9.1. Metronidazole.....	7
1.9.1.1. The biological mechanism of action of metronidazole	8
1.9.1.2. The futile cycling of metronidazole	8
1.9.2. Vancomycin.....	11
Figure 1.6. Mechanism of action of vancomycin (Yarlagadda et al., 2014)	12
1.9.2.1 Comparative studies between metronidazole and vancomycin treatments for CDI ...	12
1.9.3. Fidaxomicin.....	14
1.9.4. Nitrofurantoin	15
1.10. Limitations of antimicrobials in current use.....	16
1.11. Probiotics and faecal microbiota transplantation as treatment options for CDI	16
1.12. Dihydroorotate dehydrogenase enzyme as a potential target	17
1.12.1. The different structural classes of dihydroorotate dehydrogenases.....	20
Aim and objectives	22
Chapter 2	24
2.1. Aldehydes	24
2.1.1. Uses of aldehydes	24
2.1.2. Toxicity of aldehydes.....	24
2.1.2.1. Benzaldehyde.....	25
2.1.2.2. Cinnamaldehyde.....	25
2.2. Barbituric acid.....	25
2.2.1. Grimaux's synthesis of barbituric acid	27
2.3. Meldrum's acid	28

2.3.1. The acidic properties of Meldrum's acid	29
2.3.2. Synthesis of Meldrum's acid	29
Aim of Chapter 2	30
2.4. Materials and methods	31
2.5. Experimental.....	32
2.5.1. Wittig reaction	32
2.5.1.1. Synthesis of Wittig reaction derivatives	32
2.5.1.1.1 (E)-3-(5-Nitrofuran-2-yl)acrylaldehyde (2.1).....	32
2.5.1.1.2. (E)-3-(5-nitrothiophen-2-yl)acrylaldehyde (2.2).....	32
2.5.1.1.3. (2E,4E)-5-(5-nitrothiophen-2-yl)penta-2,4-dienal (2.3).....	33
2.5.1.2. Barbiturates derivatives formation	34
2.5.1.3. Mechanism of the Wittig reaction	35
2.5.1.4. Elongating the olefinic chain of aldehydes by Wittig reaction	37
2.5.2. Synthesis of benzylidene barbiturate derivatives by Knoevenagel condensation.....	39
2.5.2.1. 5-Benzylidenehexahydropyrimidine-2,4,6-trione (2.4)	39
2.5.2.2. 5-[(E)-3-(4-Methoxyphenyl)prop-2-enylidene]hexahydropyrimidine-2,4,6-trione (2.5)	40
2.5.2.3. 5-[(4-Methoxyphenyl)methylene]hexahydropyrimidine-2,4,6-trione (2.6)	41
2.5.2.4. 5-[(E)-3-(4-Nitrophenyl)prop-2-enylidene]hexahydropyrimidine-2,4,6-trione (2.7) ..	42
2.5.2.5. 5-(2-furylmethylene)hexahydropyrimidine-2,4,6-trione (2.8).....	43
2.5.2.6. 5-[(E)-3-(2-Furyl)prop-2-enylidene]hexahydropyrimidine-2,4,6-trione (2.9)	44
2.5.2.7. 5-[(5-Nitro-2-furyl)methylene]hexahydropyrimidine-2,4,6-trione (2.10)	45
2.5.2.8. 5-[(2-Methoxy-1-naphthyl)methylene]hexahydropyrimidine-2,4,6-trione (2.11).....	45
2.5.2.9. 5-[(E)-3-Phenylprop-2-enylidene]hexahydropyrimidine-2,4,6-trione (2.12)	46
2.5.2.10. 5-[(E)-3-(5-Nitro-2-furyl)prop-2-enylidene]hexahydropyrimidine-2,4,6-trione (2.13)	47
2.5.2.11. 5-[[4-[(4-Nitrophenyl)methoxy]phenyl]methylene]hexahydropyrimidine-2,4,6-trione (2.14).....	48
2.5.2.12. 5-[(4-benzyloxyphenyl)methylene]hexahydropyrimidine-2,4,6-trione (2.15).....	49
2.5.2.13. 5-[(5-Nitro-2-thienyl)methylene]hexahydropyrimidine-2,4,6-trione (2.16).....	49
2.5.2.14. 5-[(2-benzyloxy-1-naphthyl)methylene]hexahydropyrimidine-2,4,6-trione (2.17) ..	51
2.5.2.15. 5-(2-naphthylmethylene)hexahydropyrimidine-2,4,6-trione (2.18)	51
2.5.2.16. 5-(2-(Methoxymethoxy)benzylidene)pyrimidine-2,4,6(1H,3H,5H)-trione (2.19)	52
2.5.2.17. 5-(thiophen-2-ylmethylene)pyrimidine-2,4,6(1H,3H,5H)-trione (2.20)	53
2.5.2.18. (E)-5-(3-(5-nitrothiophen-2-yl)allylidene)pyrimidine-2,4,6(1H,3H,5H)-trione (2.21) 54	
2.5.2.19. Attempts to synthesise 5-(4-nitrobenzylidene)pyrimidine-2,4,6(1H,3H,5H)-trione (2.22).....	55

2.5.2.20. Attempts to synthesise (E)-5-(2-methyl-3-phenylallylidene)pyrimidine-2,4,6(1H,3H,5H)-trione (2.23).....	55
2.5.2.21. Attempts to synthesise 5-((5-iodofuran-2-yl)methylene)pyrimidine-2,4,6(1H,3H,5H)-trione (2.24).....	56
2.5.2.22. Attempts to synthesise 5-(1-(2-amino-5-chlorophenyl)-2-oxo-2-phenylethyl)-5-hydroxypyrimidine-2,4,6(1H,3H,5H)-trione (2.25)	56
2.5.2.23. Attempts to synthesise 5-((2E,4E)-5-(5-nitrothiophen-2-yl)penta-2,4-dien-1-ylidene)pyrimidine-2,4,6(1H,3H,5H)-trione (2.26)	57
2.5.3. Discussion of the results from benzylidene barbiturate derivative synthesis and characterisation	57
2.5.4. Knoevenagel condensation between barbituric acid and aldehydes	62
2.5.4.1. 5-((5-nitrothiophen-2-yl)methylene)-2-thioxodihydropyrimidine-4,6(1H,5H)-dione (2.27)	62
2.5.4.2. 1,3-dimethyl-5-[(E)-3-(5-nitro-2-furyl)prop-2-enylidene]hexahydropyrimidine-2,4,6-trione (2.28).....	62
2.5.4.3. (E)-1,3-dimethyl-5-(3-(4-nitrophenyl)allylidene)pyrimidine-2,4,6-trione (2.29)	63
2.5.4.5. 5-((5-nitrothiophen-2-yl)methylene)-1,3-diphenyl-2-thioxodihydropyrimidine-4,6(1H,5H)-dione (2.30) (157)	64
2.5.5. Discussion of benzylidene barbiturate derivatives by Knoevenagel condensation	65
2.5.6. The mechanism of the catalysed Knoevenagel condensation reaction	68
2.5.7. The mechanism of the uncatalysed Knoevenagel condensation reaction	68
2.5.8. Synthesis of exocyclic C=C reduced of benzylidene barbiturate derivatives.....	69
2.5.8.1. 5-Benzylhexahydropyrimidine-2,4,6-trione and its tautomeric form 5-Benzyl-6-hydroxydihydropyrimidine-2,4(1H,3H)-dione (2.31)	69
2.5.8.2. 5-(4-methoxybenzyl)pyrimidine-2,4,6(1H,3H,5H)-trione and its tautomeric form 6-hydroxy-5-(4-methoxybenzyl)pyrimidine-2,4(1H,3H)-dione (2.32).....	70
2.5.8.3. 5-[(2-methoxy-1-naphthyl)methyl]hexahydropyrimidine-2,4,6-trione and its tautomeric form 6-hydroxy-5-((2-methoxy-1-naphthyl)methyl)pyrimidine-2,4(1H,3H)-dione (2.33)	71
2.5.8.4. 5-[(E)-3-(4-methoxyphenyl)allyl]hexahydropyrimidine-2,4,6-trione (2.34)	72
2.5.8.5. 5-[(5-nitro-2-furyl)methyl]hexahydropyrimidine-2,4,6-trione and its tautomeric form 6-hydroxy-5-((5-nitro-2-furyl)methyl)dihydropyrimidine-2,4(1H,3H)-dione (2.35)	73
2.5.8.6. 5-[(E)-3-(5-nitro-2-furyl)allyl]hexahydropyrimidine-2,4,6-trione and its tautomeric form 6-hydroxy-5-5-[(E)-3-(5-nitro-2-furyl)allyl]dihydropyrimidine-2,4(1H,3H)-dione (2.36) .	74
2.5.8.7. 5-[(E)-3-(2-furyl)allyl]-6-hydroxy-1H-pyrimidine-2,4-dione (2.37)	75
2.5.8.8. 5-[[4-[(4-nitrophenyl)methoxy]phenyl]methyl]hexahydropyrimidine-2,4,6-trione (2.38).....	76
2.5.8.9. 5-[[4-benzyloxyphenyl]methyl]hexahydropyrimidine-2,4,6-trione (2.39).....	76
2.5.8.10. 5-[(5-nitro-2-thienyl)methyl]hexahydropyrimidine-2,4,6-trione and its tautomeric form 6-hydroxy-5-[(5-nitro-2-thienyl)methyl]dihydropyrimidine-2,4(1H,3H)-dione	77

(2.40).....	77
2.5.8.11. 5-[(E)-cinnamyl]hexahydropyrimidine-2,4,6-trione and its tautomeric form 6-hydroxy-5-[(E)-cinnamyl]dihydropyrimidine-2,4(1H,3H)-dione (2.41)	78
2.5.8.12. 5-[(3-benzyloxy-2-naphthyl)methyl]hexahydropyrimidine-2,4,6-trione (2.42)	79
2.5.8.13. 5-(2-naphthylmethyl)hexahydropyrimidine-2,4,6-trione and its tautomeric form 6-hydroxy-5-(2-naphthylmethyl)dihydropyrimidine-2,4(1H,3H)-dione (2.43).....	80
2.5.8.14. 5-(2-(methoxymethoxy)benzyl)pyrimidine-2,4,6(1H,3H,5H)-trione (2.44)	81
2.5.8.15. Attempt to synthesise (E)-5-(3-(4-nitrophenyl)allyl)pyrimidine-2,4,6(1H,3H,5H)-trione (2.45).....	82
2.5.8.16. 1,3-dimethyl-5-[(E)-3-(4-nitrophenyl)allyl]hexahydropyrimidine-2,4,6-trione and its tautomeric form (E)-6-hydroxy-1,3-dimethyl-5-(3-(4-nitrophenyl)allyl)dihydropyrimidine-2,4(1H,3H)-dione (2.46)	83
2.5.9. Discussion	84
2.5.10. Mechanism of 2-phenyl-2,3-dihydrobenzo[d]thiazole in a one-pot reaction	89
2.5.11. Mechanism of reduction of exocyclic C=C by NaBH ₄	90
2.5.12. Catalytic hydrogenation with palladium on charcoal.....	91
2.5.13. Synthesis of propyl bridged aralkylpyrimidinetrioes derivatives	91
2.5.13.1. 5-(3-(4-methoxyphenyl)propyl)pyrimidine-2,4,6-trione and its tautomeric form 6-hydroxy-5-(3-(4-methoxyphenyl)propyl)pyrimidine-2,4(1H,3H)-dione (2.47)	91
2.5.13.2. 5-(3-Phenylpropyl)hexahydropyrimidine-2,4,6-trione and its tautomeric form 6-hydroxy-5-(3-Phenylpropyl)pyrimidine-2,4(1H,3H)-dione (2.48)	92
2.5.13.3. Attempts to synthesise 5-(3-(furan-2-yl)propyl)pyrimidine-2,4,6(1H,3H,5H)-trione	93
2.5.14. Mechanism of action of catalytic hydrogenation using Pd/C	94
2.5.15. Discussion of the Pd/C reduced compounds	94
2.5.16. Béchamp reduction	95
2.5.16.1. Attempted syntheses.....	95
2.5.16.1.1. Attempts to synthesise 5-(4-((4-aminobenzyl)oxy)benzylidene)pyrimidine-2,4,6(1H,3H,5H)-trione (2.50).....	95
2.5.17. Discussion	96
2.5.18. Mechanism of action	96
2.5.19. Synthesis of Meldrum's acid derivatives	97
2.5.19.1. 5-[(4-methoxyphenyl)methylene]-2,2-dimethyl-1,3-dioxane-4,6-dione (2.51).....	97
2.5.19.2. [(E)-3-(4-Methoxyphenyl)prop-2-enylidene]-2,2-dimethyl-1,3-dioxane-4,6-dione (2.52)	98
2.5.19.3. 2,2-dimethyl-5-[(E)-3-(4-nitrophenyl)prop-2-enylidene]-1,3-dioxane-4,6-dione (2.53)	99
2.5.19.4. 5-[(E)-3-(2-Furyl)prop-2-enylidene]-2,2-dimethyl-1,3-dioxane-4,6-dione (2.54).....	99
2.5.19.5. 2,2-dimethyl-5-[(E)-3-phenylprop-2-enylidene]-1,3-dioxane-4,6-dione (2.55)	100

2.5.19.6. 5-(2-furylmethylene)-2,2-dimethyl-1,3-dioxane-4,6-dione (2.56)	101
2.5.19.7. (E)-2,2-dimethyl-5-(3-(5-nitrofuran-2-yl)allylidene)-1,3-dioxane-4,6-dione (2.57)	102
2.5.19.8. 2,2-dimethyl-5-((5-nitrothiophen-2-yl)methylene)-1,3-dioxane-4,6-dione (2.58) .	102
2.5.19.9. 2,2-dimethyl-5-(thiophen-2-ylmethylene)-1,3-dioxane-4,6-dione (2.59)	103
2.5.19.10. (E)-2,2-dimethyl-5-(3-(5-nitrothiophen-2-yl)allylidene)-1,3-dioxane-4,6-dione (2.60)	104
2.5.19.11. 5-[(4-benzyloxyphenyl)methylene]-2,2-dimethyl-1,3-dioxane-4,6-dione (2.61) ..	105
2.5.19.12. 2,2-dimethyl-5-[(5-nitro-2-furyl)methylene]-1,3-dioxane-4,6-dione (2.62)	106
2.5.19.13. 5-(2-furylmethyl)-2,2-dimethyl-1,3-dioxane-4,6-dione and its tautomeric form 5- (furan-2-ylmethyl)-6-hydroxy-2,2-dimethyl-1,3-dioxan-4-one (2.63)	106
2.5.19.14. 5-[(E)-3-(4-methoxyphenyl)allyl]-2,2-dimethyl-1,3-dioxane-4,6-dione (2.64)	107
2.5.19.15. 2,2-dimethyl-5-[(E)-3-(4-nitrophenyl)allyl]-1,3-dioxane-4,6-dione (2.65)	108
2.5.19.16. 5-[(E)-3-(2-Furyl)allyl]-2,2-dimethyl-1,3-dioxane-4,6-dione (2.66)	109
2.5.19.17. 5-[(4-methoxyphenyl)methyl]-2,2-dimethyl-1,3-dioxane-4,6-dione (2.67)	110
2.5.20. Meldum's acid derivatives reactions scheme	111
2.5.21. Meldrum's acid discussion	111
2.5.22. Synthesis of five-membered ring derivatives	113
2.5.22.1. Synthesis of (E)-3-((furan-2-ylmethylene)amino)-2-thioxothiazolidin-4-one (2.69)	113
2.5.22.2. Synthesis of (E)-3-amino-5-((5-nitrothiophen-2-yl)methylene)-2-thioxothiazolidin-4- one (2.70)	114
2.5.22.3. Synthesis of (E)-1-((furan-2-ylmethylene)amino)imidazolidine-2,4-dione (2.71)...	115
2.5.22.4. Synthesis of (E)-3-(((5-nitrothiophen-2-yl)methylene)amino)imidazolidine-2,4-dione (2.72)	116
2.5.22.5. Synthesis of (E)-1-((thiophen-2-ylmethylene)amino)imidazolidine-2,4-dione (2.73)	116
2.5.22.6. Attempts to synthesise (Z)-3-(((E)-furan-2-ylmethylene)amino)-5-((5-nitrothiophen- 2-yl)methylene)-2-thioxothiazolidin-4-one	117
2.5.22.7. Attempts to synthesise (Z)-5-((E)-3-(4-nitrophenyl)allylidene)-3-(((E)-5- nitrothiophen-2-yl)methylene)amino)-2-thioxothiazolidin-4-one	117
2.5.22.8. Attempts to synthesise (Z)-3-((2,4-dimethylpentan-3-ylidene)amino)-5-((5- nitrothiophen-2-yl)methylene)-2-thioxothiazolidin-4-one	118
2.5.22.9. Attempts to synthesise 3-((2,4-dimethylpentan-3-ylidene)amino)-2- thioxothiazolidin-4-one	118
2.5.23. Discussion of the 5-membered ring derivatives results	119
2.5.24. 5-Membered rings derivatives synthesis scheme:	120
2.5.25. Mechanism of Schiff bases formation	120
2.5.26. Limitations of chapter 2	121
Chapter 3	122

3.1. Antimicrobial susceptibility testing.....	122
3.1.1. Agar diffusion assay.....	122
3.1.1.1. Purpose.....	122
3.1.1.2. Theory of agar diffusion assay	122
3.1.2. Minimum Inhibitory Concentration	123
3.2. Aim and Objectives	124
3.3. Materials.....	125
3.3.1. Microbial cultures	125
3.3.2. Microbiological media and agar.....	126
3.3.3. Panel of comparator antibacterial agents	126
3.3.4. Dimethyl sulfoxide (DMSO) and sterile distilled water	126
3.3.5. Equipment	126
3.3.6. Preparation of agar and media	127
3.3.6.1. Mueller-Hinton broth	127
3.3.6.2. Mueller-Hinton agar	127
3.3.6.3. Wilkins Chalgren broth	127
3.3.6.4. Wilkins Chalgren agar	127
3.3.6.5. Wilkins Chalgren + 0.1 % w/v Sodium taurocholate agar	128
3.3.7. Test compounds and antibiotic stock solutions.....	128
3.3.8. Preparation of microorganisms for antibacterial activity testing	128
3.3.8.1. Glycerol stocks	128
3.3.8.2. Streak plates.....	128
3.4. Methods	129
3.4.1. Preparation of <i>C. difficile</i> vegetative cell suspensions	129
3.4.2. Diffusion assay for antibacterial susceptibility testing of the synthesised compounds, aldehydes, and the antibiotics controls	129
3.4.3. Minimum inhibition concentrations (MIC) of the synthesised compounds and the comparator antibiotics.....	130
3.4.4. Minimum bactericidal concentrations (MBC).....	130
3.4.5. DMSO control.....	131
3.4.6. Agar diffusion assay.....	131
3.5. Results and discussion.....	132
3.5.1. Antimicrobial susceptibility testing of panel of antimicrobials, aldehydes and synthesised compounds against <i>C. difficile</i> , <i>E coli</i> , and <i>S. aureus</i>	132
3.5.2. Antimicrobial activity assay of some aldehydes	133
3.5.3. Antimicrobial activity of the synthesised compounds	135

3.6. Conclusion	143
3.7. Limitations of the study.....	144
4. Chapter 4.....	145
4.1. Introduction.....	145
4.2. Materials.....	146
4.2.1. Cells and controls	146
4.2.2. MTT Solution preparation and composition.....	146
4.3. Methods	146
4.3.1. Thawing, subculture, and cryopreservation of mouse normal liver cells and colorectal cancer cells	146
4.3.2. Cell count and viability assessment.....	147
4.3.3. Cell culture	147
4.4. Results	148
4.4.1. MTT assay of the positive control against BNL and Caco-2 cells	149
4.4.2. MTT assay of 2.7 against BNL and Caco-2 cells.....	152
4.4.3. MTT assay of 2.8 against BNL and Caco-2 cells.....	154
4.4.4. MTT assay of 2.16 against BNL and Caco-2 cells.....	155
4.4.5. MTT assay of 2.53 against BNL and Caco-2 cells.....	156
4.4.6. MTT assay of 2.58 against BNL and Caco-2 cells.....	158
4.4.7. MTT assay of 2.20 against BNL and Caco-2 cells.....	160
4.5. Discussion	161
4.6. Limitations of the study.....	167
References	168

Chapter 1

1. Introduction:

1.1. Antimicrobial resistance

The misuse of antibiotics over the last few decades has led to a significant global increase in antimicrobial resistance (AMR) (WHO, 2017). Failure of conventional antibiotics to eradicate numerous Gram-positive and Gram-negative pathogens is attributed to their acquired multidrug resistance, which has consequently resulted in higher mortality and morbidity rates within the population. The term 'Superbugs' has been given to bacterial strains that have become problematic or even impossible to eradicate using antibiotics currently used in clinical practice (O'Neill, 2016). Well-documented 'Superbugs' within the clinical practice include Methicillin-resistant *Staphylococcus aureus* (MRSA), carbapenemase-producing Enterobacteriaceae (CPE), and *Clostridioides difficile* to name just a few.

The lack of a method that provides rapid primary detection of the causative pathogens, and their antimicrobial susceptibility patterns in healthcare settings, contributes to the widespread, uncontrolled use of broad-spectrum antibiotics, which could be managed better in most cases (Nathan & Cars, 2014). The emergence of antimicrobial-resistant bacteria can spread easily when the rapid and exponential elevation of resistance coincides with inadequate infection control procedures. Frequent updating of the epidemiological records on AMR of bacterial pathogens will not only facilitate the choice of the appropriate therapeutic schemes but also the development of efficient antimicrobial regimens in hospitals (Singer *et al.*, 2016).

1.2. Causes of antibiotic resistance

The comprehensive etiologic factors leading to AMR are numerous. Inadequate protocols and variability in their use, coupled with the dearth of awareness of proficient antibiotic stewardship, are the fundamentals needed to combat the emergence of antibiotic resistance. The misuse of broad-spectrum antibiotics and their availability as over the counter (OTC) drugs especially in developed countries and through online markets, has compromised their effectiveness (Spellberg & Gilbert, 2014).

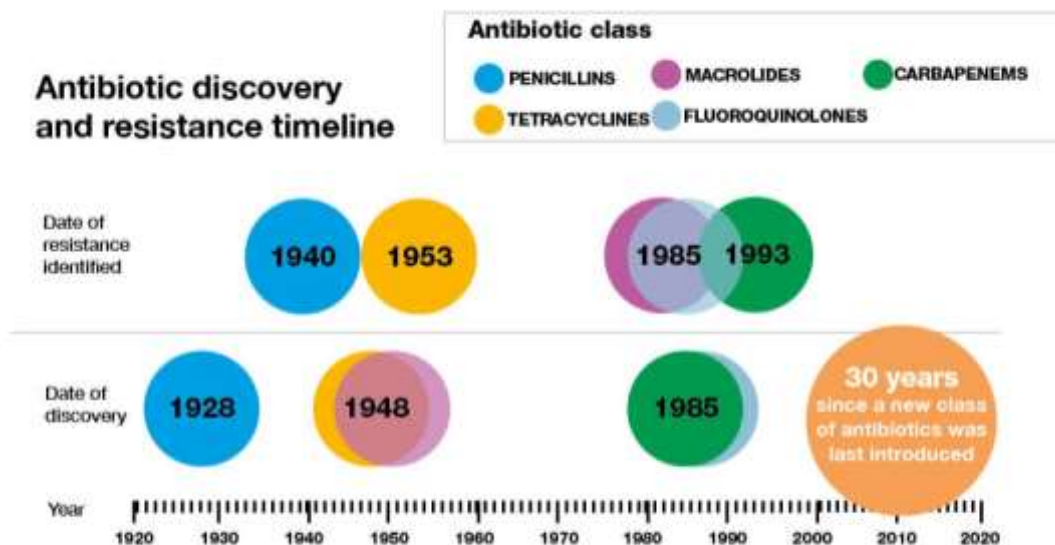
First and foremost, misuse of antibiotics is the primary factor behind resistance outbreaks and progression. Sir Alexander Fleming predicted and stated that the “public will demand [the drug and] then will begin an era ... of abuses” (Aslam *et al.*, 2018). The efficiency of antibiotics is mostly against sensitive bacterial strains whereas the resistant pathogens remain intact to then reproduce and continue to survive in the body. Despite the misuse and all the challenges associated with antibiotic resistance, these agents remain overprescribed, globally. Further to this, numerous aspects concerning the drug indication, drug of choice, and the duration of the course of therapy, are considered incompatible in between 30 to 50% of all the cases (Read & Woods, 2014). Among the main examples of the uncontrolled use of antibiotics worldwide, is their use as growth supplements and prevention of infection in animals.

1.3. Novel approaches to minimise AMR

Discovering approaches to control antimicrobial resistance has been a global challenge for microbiologists and public health specialists for decades. The rate of pathogenic bacterial resistance toward one or more antibiotics has increased extensively, worldwide (Othman *et al.*, 2019) (Figure 1.1). The conventional therapeutic agents and last-resort antibiotics are showing reduced efficacy against infectious, resistant species and strains of microorganisms. Alternative antimicrobial agents are vital to overcome the challenges posed due to the shortage of effective prevention schemes and the limited number of novel antibacterial agents in clinical trials. However, the incentives and enthusiasm of pharmaceutical companies to discover new, novel antibiotics have dissipated over the last few decades (Amaning Danquah *et al.*, 2022). A better comprehension of the bacterial virulence approaches and the molecular routes undertaken by pathogens offers possibilities for innovative tactics to tackle and hinder crucial pathogenicity factors and virulence-allied bacterial characteristics while curtailing the ability to acquire resistance during bacterial evolution. The bacterial virulence-associated factors and pathways that provide potential targets for developing therapeutic agents have been investigated (Amaning Danquah *et al.*, 2022).

Pathogenic bacteria rely on numerous mechanisms to attain antibiotic resistance including altering the uptake of the antibacterial agents, production of enzymes to break down

antibiotics, efflux pumps, modification of antibiotic target sites, and biofilm formation. Development of new generations of antibiotics, combination therapy, discovery of natural



substrates showing antibacterial activity, and use of nanoparticles for drug delivery, are the main approaches by which the serious issue of antibacterial resistance can be tackled (Leffler & Lamont, 2015).

Figure 1. 1. Timeline showing the dates of discovery and resistance of some of the most common classes of antibiotics in the past century (Public Health England, 2017).

1.4. The prevalence of *Clostridioides difficile* infection

It is estimated that 10-25% of nosocomial antibiotic-associated diarrhoea cases are linked to broad-spectrum antibiotics. The symptoms are caused by the Gram-positive, spore-forming, potent toxin-producing, anaerobic bacterium *Clostridioides difficile*. The organism was previously known as *Clostridium difficile* (Lawson, 2016), with the official renaming being approved in 2016 (Czepiel *et al.*, 2019). The new naming indicates the different taxonomic features of this species compared to the other species of the *Clostridium* genus (Garrity, 2006). Various environments can be reservoirs for *C. difficile*, such as symptomatic patients, carriers, contaminated surfaces, healthcare equipment including blood pressure cuffs, and animals' intestinal tracts. The pathogen is transmitted via the fecal-oral route (Leffler, 2015). In 1935, *C. difficile* was initially detected in the stool of a healthy newborn (Hall & O'Toole, 1935); it was classified as a rare, yet non-pathogenic intestinal

microorganism until the 1970s. *C. difficile* started to be regarded as a serious pathogen after antimicrobials were introduced. In 1974, it was observed that 21% of the patients who were administered clindamycin, suffered from diarrhoea, while 50% of cases showed pseudomembranes in the colon (pseudomembranous colitis) when examined by endoscopy (Tedesco *et al.*, 1974). An exponential elevation in the *C. difficile* prevalence was noticed by the end of the 20th century. *C. difficile* ribotype 027, which came from Quebec, caused chaos in several UK hospitals including Stoke, Glasgow, Tunbridge Wells Devon. *C. difficile* infection (CDI) killed hundreds of people and infected thousands. The chief executive of Tunbridge Wells was sacked due to poor infection control policy. The CD ribotype 027 is a hyper-toxin producer and is antimicrobial-resistant (Eggertson, 2004).

1.5. Spread and recurrence of CDI

Administration of broad-spectrum antibiotics to hospitalised patients leads to distortion of the normal gut flora, leaving the gastrointestinal tract (GIT) empty and vulnerable, thus increasing the possibility of acquiring CDI. The CD microorganisms survive in the gut and produce potent proteinaceous toxins that destroy cellular tight junctions in the gut wall, resulting in fluid loss and inflammation. The severity of CDI varies from mild diarrhoea to pseudomembranous colitis, fulminant colitis, and toxic megacolon which can eventually lead to death. There is a high probability of acquiring CDI in those individuals having *C. difficile* asymptomatic colonisation upon their hospital admission. Moreover, these asymptomatic carriers may aid the introduction and the spread of bacterial infection. Consequently, the prevalence of *C. difficile* in healthcare settings increases (Schmidt *et al.*, 2018).

Antimicrobial agents such as metronidazole, vancomycin, and fidaxomicin are administered to treat patients with CDI. However, vancomycin and fidaxomicin are the Food and Drug Administration (FDA)-approved drugs for CDI management. According to the statistical analysis, approximately 15-35% of the cases treated with frontline antimicrobials experience CDI recurrence. The reasons behind episodes of recurrence are not fully understood. However, one of the possible reasons for the high recurrence percentage is the accumulation of antibiotic-resistant spores in the GIT of the patients. After the discontinuation of antimicrobial administration, the spores germinate to form vegetative, toxins-releasing microorganisms. Management of CDI is considered problematic because of the proficiency of *C. difficile* to produce antimicrobial drug-resistant spores. CDI is mediated

primarily by two toxins, TcdA (toxin A) and TcdB (toxin B) (Guery *et al.*, 2019). Toxins TcdA and TcdB can cause changes in the cytoskeleton leading to damage of intestinal cell integrity as toxins possess domains that utilise UDP-glucose to inactivate host Rho GTPases (Paparella *et al.*, 2021). Therefore, *C. difficile* spores serve as the major cause of CDI circulation and recurrence.

1.6. Risk factors associated with CDI

Various risk factors increase the susceptibility of acquiring CDI such as exposure to antimicrobials, hospitalisation, and aging. Antibiotic usage, including the first line of treatment metronidazole and vancomycin, can lead to CDI. However, the broad-spectrum antibiotics associated with the highest CDI incidences are penicillins, cephalosporins, and clindamycin (Owens *et al.*, 2008). Age is also considered a risk factor for the spread of CDI. Studies show that patients 65 years of age or older are 5 to 10 times more susceptible to CDI than younger individuals. The spread of CDI is primarily allied to exposure to healthcare settings; however, studies showed that the number of community-acquired CDI cases has reached approximately 30% of the total number of cases. Colonization of *C. difficile* as a percentage of hospitalised patients varies depending on the country, the extent of hospitalization, and the age of the patients (Owens *et al.*, 2008).

In one study, *C. difficile* colonisation prevalence was estimated to vary from 2.1-20% in the initial days of hospitalisation. It reached 45.4% when the hospitalisation duration lasted longer. In another study, the incidences of colonisation were estimated to vary from 2.1-50% after the first month following hospitalisation. *C. difficile* colonisation ranged from 1-50% after more than a month of hospitalisation (Czepiel *et al.*, 2019).

Colonisation is caused by the ability of the CD spores to remain dormant in the gut of a patient for many months, where the infection can be either symptomatic or asymptomatic. *C. difficile* spores are ubiquitous and can be detected anywhere within healthcare settings. The spread of the pathogen can be controlled by proper hand sanitation using soap and water. In addition, the utilisation of vinyl gloves prevents the transmission of CD spores from healthcare professionals to patients. Many studies failed to prove the hypothesis that demonstrated the link between the decrease in gastric acid and CDI. Inflammatory bowel disease, GIT surgeries, and immunological suppression are some of the other distinct risk factors for CDI (Owens *et al.*, 2008).

1.7. Prevention of CDI

Safety measures should be adhered to for the prevention of the spread of CDI, including the wearing of disposable gloves and gowns, frequent washing of the hands with soap and water by healthcare professionals, and anyone who encounters CDI patients. Alcohol-based products cannot destroy *C. difficile* spores. For optimal prevention, isolation of CDI patients is advisable. If isolation is not possible, direct contact between patients via sharing personal or non-personal items such as books should be prohibited (Worsley, 1998). Surfaces should be disinfected by employing chlorine-based solutions, where the chlorine concentration should range between 1000 (minimum effective concentration) to 5000 ppm (optimal choice). Abiding by infection control measures is necessary in all CDI cases besides the suspected ones, and rooms must be meticulously cleaned and disinfected following the discharge of CDI cases from the healthcare settings (Worsley, 1998).

1.8. Immunity and host defences

The abundance of the normal, healthy gut microbiota acts as the body's first defence mechanism by inhibiting the survival of *C. difficile* *in vitro* and *in vivo* (Borriello, 1990). The acidic nature of the gastric juice and the intestinal peristalsis phenomenon inhibit the viable count of the spores (McFarland *et al.*, 1990). Hence, consuming anti-diarrheal drugs will lead to contrariwise effects as they reduce the peristaltic motility, and subsequent disruption to the clearance of the infectious organism from the body (Kelly & LaMont, 1998).

The extent of the infection duration and the severity of the complications including colitis rely on the humoral immune response (Kelly, 1996). Laboratory experimentation showed that *C. difficile* colitis could be prevented in animal models upon their immunisation against toxin A (Libby *et al.*, 1982). Despite the promising results obtained from immunisation in animals, no sufficient evidence proves their equivalent efficacy against diarrhoea and colitis in humans (Kelly & LaMont, 1998). The colonic secretion of immunoglobulin A antitoxin

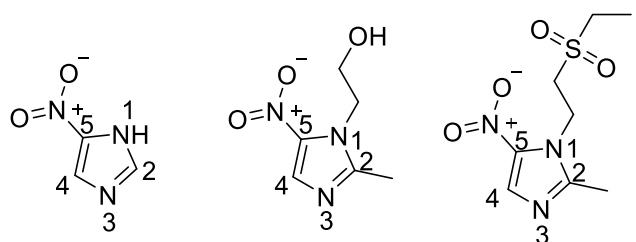
prevents the binding of toxin A to its receptor (Kelly *et al.*, 1992). However, mild colitis or asymptomatic carriage of *C. difficile* can be equated with elevated serum and intestinal antitoxin antibodies (Kelly, 1996). Severe *C. difficile* colitis and episodes of recurrence susceptibility increase with the inadequate immune response (Warny, 1994).

1.9. Treatment of CDI

Termination of antimicrobial usage is the first step in all CDI cases. As a result of the termination of the triggering factor, most antibiotic-associated diarrhoea (AAD) cases and few CDI incidences can be resolved. However, in most CDI cases, additional medical intervention is required. For decades, metronidazole and vancomycin were the only treatments utilised to control CDI. Vancomycin cannot be administered to patients via the intravenous route due to its inability to penetrate the gut mucosa. However, metronidazole and vancomycin can both be given orally and vancomycin, in addition, can be administered through the rectum. The use of intravenous immunoglobulin (IVIg) and colectomy is restricted to severe cases showing poor medical compliance (Mullish & Williams, 2018).

1.9.1. Metronidazole

Several antimicrobials share common structural features including the presence of an electron-withdrawing (oxygen, sulfur, nitrogen) at the N1 position of a heterocyclic 5-membered ring, whilst a nitro group (NO₂) is attached to the C5 position (Figure 1.2.) (O'Brien & Morris, 1971). A wide range of side chains and substituents may be attached to the heterocyclic rings that possess a conjugated, aromatic system, where the lone pair of electrons from nitrogen or another heteroatom is delocalised within the heterocyclic ring. The presence of a NO₂ group in the structure of the derivatives shown in Figure 1.2., is associated with the potential to cause cytotoxicity (Ehlhardt *et al.*, 1987).



1.1 azomycin

1.2 metronidazole

1.3 tinidazole

Figure 1. 2. Examples and ring atom numbering of some antimicrobials possessing similar structural features

1.9.1.1. The biological mechanism of action of metronidazole

The mechanism of action of metronidazole can be summarised in four steps. Initially, the drug diffuses into the cell membranes of the pathogens. The antimicrobial effect of metronidazole is restricted to anaerobic bacteria as metronidazole becomes activated under anaerobic conditions (Figure 1.4.). The second step requires reductive activation of metronidazole creating a concentration gradient that triggers cellular uptake and the activation pathway. In the third step, the cytotoxic derivatives that are formed bind to bacterial DNA strands, causing breakage and the fragmentation of the helix, subsequently inhibiting the synthesis of protein within the bacterium, causing cell death (Figure 1.3.). The fourth and final step involves the breakdown of cytotoxic derivatives of the drug (Weir & Le, 2023).

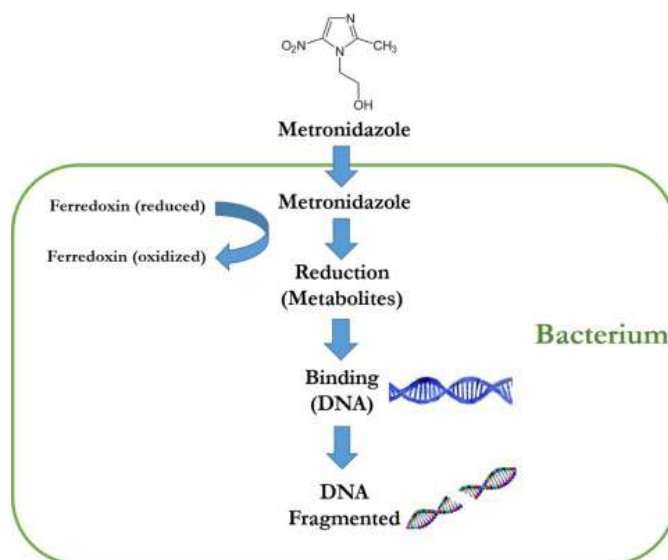


Figure 1. 3. Mechanism of action of metronidazole (Ovung & Bhattacharyya, 2023)

1.9.1.2. The futile cycling of metronidazole

The reduction of the NO₂ group in metronidazole is essential for the activation of the prodrug to generate the active, antibacterial form. The reductive prodrug-activation process

can be achieved by two routes to produce the derivatives essential for activity (Figure 1.4.). Reductive activation of metronidazole occurs upon the reduction of the NO₂ group leading to imidazole fragmentation and cytotoxicity (Bryant & DeLuca, 1991). In the reductive inactivation route, the NO₂ group causes the formation of reduced, a non-toxic amino derivative, compound **1.10**. The resistance mechanism of compound **1.10** is suggested to occur due to the oxygen-insensitive nitroreductases and *nim* genes (Figure 1.4.). A stable, oxygen-insensitive, non-toxic derivative is liberated from the reductive inactivation route in two-electron transfer steps, where six electrons are consumed (Roldán *et al.*, 2008). Ring-fission and formation of transient, cytotoxic derivatives occur upon the consumption of four electrons in the reductive activation pathway (Church *et al.*, 1988). Metronidazole's cytotoxic reductive activation pathway relies on its ability to act as an electron acceptor, hindering the proton motive force, and decreasing the production of APT (Tally *et al.*, 1978). Transient intermediates, compounds **1.5**, **1.6**, and **1.7**, are generated from the reductive activation pathway under the influence of pyruvate-ferredoxin oxidoreductase (PFOR), ferredoxin, flavodoxin, hydrogenase, and effectors of the dissimilatory sulfate pathway. Heterocyclic fission takes place as shown in compound **1.7**, where the dashed lines represent the cleavage site resulting in compounds **1.8** and **1.9** forming. The hypothetical mechanism of the reductive activation suggests the formation of the nitro-free radical in the first step, followed by the formation of nitroso, nitroso-free radical, and hydroxylamine derivatives (**1.5-1.9**; Figure 1.4.). A process of metronidazole regeneration known as futile cycling can be generated upon electron removal from the nitroso radical using oxygen due to the higher affinity of oxygen for electrons compared to metronidazole (Church & Lashley, 1995). The induction of DNA strand breakage in the presence of oxygen can be attributed to the generation of oxygen radicals; this phenomenon can be accelerated by the futile cycling of metronidazole. Oxygen induces the inhibition of uptake of metronidazole (Moore *et al.*, 1995).

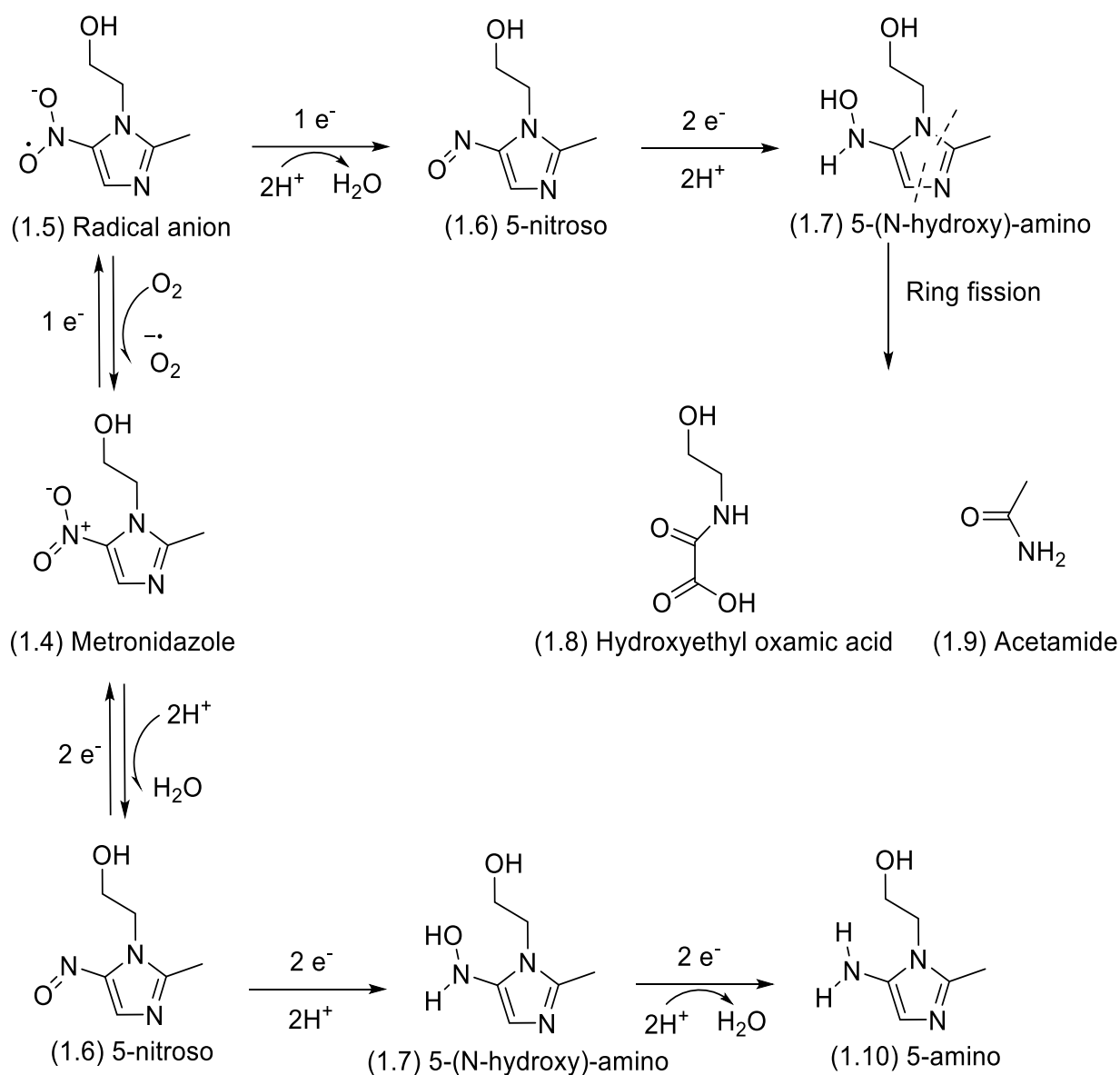


Figure 1. 4. The futile cycling in metronidazole reductive activation (left to right) and reductive inactivation (top to bottom)

1.9.2. Vancomycin

Vancomycin (Figure 1.5.) is a glycopeptide antibacterial drug that was clinically introduced in the late 1950s. It is strictly effective against Gram-positive pathogenic aerobes and anaerobes including *C. difficile* and MRSA (Figure 1.6.). The utilisation of vancomycin has been restricted to patients who are allergic to β -lactam antibiotics. However, the presence of impurities in the preparation of vancomycin contributed to cases of toxicity and erythematous rash resulting in a syndrome known as “red man” (Sivagnanam & Deleu, 2003). These associated adverse effects were later overcome upon improving the purity of the vancomycin. Unfortunately, in 2013, around 20,000 hospitalised patients acquired vancomycin-resistant enterococci (VRE) of which 1,300 deaths were recorded. Vancomycin is composed of a seven-membered peptide chain embedded within a tricyclic ring system to which a disaccharide (vancosamine and glucose) is attached, where the antibacterial properties are dependent upon the presence of the *N*-terminal amino acid, leucine. Vancomycin interacts with the terminal of peptidoglycan precursors to prevent cell wall synthesis (Sivagnanam & Deleu, 2003). Vancomycin resistance developed in VRE is attributable to possession of *vanA* gene which encodes for (D-Ala-D-Lac) or D- Alanine-D-Serine (D-Ala-D-Ser) in the peptidoglycan terminal rather than D-Alanine-D-Alanine (D-Ala-D-Ala) in vancomycin-sensitive microorganisms (Figure 1.6.). Such alterations can lead to variable expressions of glycopeptide resistance. Hence, vancomycin loses its binding affinity because of this alteration to D-Ala-D-Lac by 1,000-fold or D-Ala-D-Ser by 7-fold, compared to the normal cell wall precursors D-Ala-D-Ala (Sivagnanam & Deleu, 2003).

(Guery *et al.*, 2019). Ninety-four patients were involved in the first comparative study between metronidazole and vancomycin. Fifty-two patients were on vancomycin, and 42 were given metronidazole. In this trial both drugs exhibited equal effectiveness and comparable recurrence; it was not blinded and monitoring of episodes of recurrence lasted only for three weeks (Guery *et al.*, 2019).

After a decade, another unblinded study composed of an equal number of patients per study group was published (Guery *et al.*, 2019). The study compared vancomycin, teicoplanin, metronidazole, and fusidic acid. The patients were monitored for 30 days after the termination of drug use. Metronidazole was recommended over vancomycin for CDI despite both showing equal efficacy. Vancomycin was more expensive and there was a higher probability of developing vancomycin-resistant strains of *C. difficile*. Two additional reports showed contradictory results. In a comparative, double-blind, placebo-controlled study, 172 patients were given vancomycin or metronidazole. All patients underwent follow-up for 21 days. Metronidazole and vancomycin total cure percentages were 84% and 97% respectively. Patients having mild symptoms did not show any difference in benefit when taking either medication. Yet, those with severe illness showed a cure rate of 76% in the case of metronidazole use and 97% in the case of vancomycin use. The trial had drawbacks as the recurrence follow-up monitoring only lasted for 21 days. Moreover, the classification of severity in the case studies relied on an unvalidated scoring method. This trial did, however, reflect the efficiency of vancomycin over metronidazole in severe CDI cases (Guery *et al.*, 2019).

An additional trial was carried out to assess a novel toxin-binding polymer known as tolevamer by comparing it to metronidazole and vancomycin (Guery *et al.*, 2019). Five hundred and sixty-three of the patients involved in this study were given tolevamer, while metronidazole and vancomycin were administered to 289 and 266 patients respectively. The results were evaluated in parallel to two well-recognized, randomized controlled trials. The results ranked the drugs vancomycin, metronidazole, and tolevamer from the most to the least effective for the treatment of CDI. Vancomycin was therefore recommended over metronidazole, as it showed greater efficacy and lower CDI recurrence rates (Guery *et al.*, 2019).

1.9.4. Nitrofurantoin

Nitrofurantoin (1.13) (Figure 1.8) is a broad-spectrum antibiotic that is mainly used in the treatment of urinary tract infections (UTIs). According to a study conducted by Ge *et al.* (2018), nitrofurantoin showed the lowest risk of acquiring CDI compared to other antimicrobial agents used such as cefpodoxime, ceftriaxone, clindamycin, and ampicillin. Antimicrobials used for the treatment of UTIs commonly trigger acquiring CDI; nitrofurantoin is therefore considered a safe drug of choice (Ge *et al.*, 2018). Flavoprotein reductase enzyme activates nitrofurantoin within the bacteria (Waller & Sampson, 2018). The first intermediate is formed upon the reduction of nitrofurantoin, where an electron is gained by the NO₂ group at C5 of the furyl ring to produce a nitrofurantoin radical ion. The formed, unstable radical ion undergoes dehydration upon reacting with two protons (Farkas *et al.*, 2020). A highly reactive nucleophile, “nitroso derivative”, is produced from the dehydration of the radical ion intermediate (Figure 1.8). The lone pairs of electrons of nitroso derivative attack the bacterial ribosomal proteins leading to the inhibition of protein synthesis (Huttner & Harbarth, 2017). Moreover, nitrofurantoin targets other bacterial enzymes in charge of the synthesis of DNA, RNA, and other metabolic activities to consequently cause bacterial cell death. Oxidative bacterial cell damage is also believed to be correlated with the radical ion intermediate. Despite having several mechanisms and sites of action, in the early 1950s microorganisms started developing resistance to nitrofurantoin (Huttner & Harbarth, 2017).

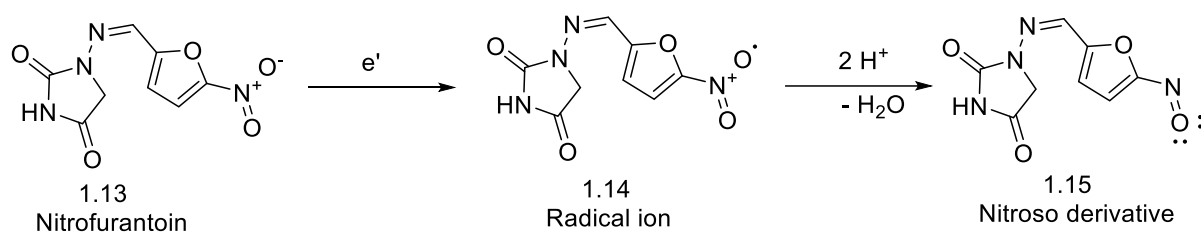


Figure 1. 8. The reductive activation of nitrofurantoin by flavoprotein reductase enzyme

1.10. Limitations of antimicrobials in current use

Metronidazole has become the treatment of choice for CDI over the years when the conventional antimicrobial treatment options fail. Metronidazole is considered a unique drug that ought to be limited in its use owing to its high absorbance, 100% bioavailability in the GIT, and subsequent high potency against a wide range of microbiota that are protective of the GIT. Despite the negligible systemic absorbance of vancomycin, it possesses significant antibacterial activity against other Gram-positive bacteria and limits the protective diversity of the microbiome (Vardanyan & Hruby, 2006).

Moreover, vancomycin and metronidazole showed high failure rates, 14% and 22% respectively, and elevated recurrence of infection in the range of 25-30%. The statistical analysis conducted reflects the inefficiency of both antimicrobials against *C. difficile* spores as well as their negative impact on the protective gut microbiota (Abutaleb & Seleem, 2020). In the last three decades, fidaxomicin represents the only novel treatment for CDI, approved by the FDA. Fidaxomicin displayed the lowest recurrence cases among all the CDI drugs owing to its selectivity against *C. difficile*, yet it is comparatively, very expensive. Despite having been approved by the FDA, vancomycin and fidaxomicin resistance, and reduced sensitivity against these antimicrobials, continue to emerge (Gallagher *et al.*, 2015).

1.11. Probiotics and faecal microbiota transplantation as treatment options for CDI

Restoration of the GIT normal microbiota was a main aim for researchers in the treatment of CDI since the entire forms of AAD disrupt the gut flora. The administration of probiotics was considered a method to reintroduce viable microorganisms into the GIT of patients. There is no sufficient evidence to conclusively show that this use of probiotics is adequate in CDI management, but studies suggest promising value in the management of less severe CDI cases. This probiotic approach faces concerns surrounding the optimum dose and limitations to the bioavailability of the organism used in the formulation (Quraishi *et al.*, 2017).

Faecal microbiota transplantation (FMT) is an additional strategy utilised in severe CDI cases that involves extracting a stool sample from an uninfected donor having normal gut

flora. The samples are treated in the laboratory to give a liquefied bacterial suspension that is administered to the patient via the gut. Many trials have been reported where this method has been applied over the decades (Quraishi *et al.*, 2017). However, the first significant randomised study evaluating the efficiency of the procedure was carried out in 2013. This study involved 3 groups of patients suffering from recurrent CDI; the first group was managed by bowel lavage and FMT afterward. The second group was managed with vancomycin alone, and the third with vancomycin together with bowel lavage. The preliminary results showed that 81% of the first study group had recovered after the FMT. The recovery rates of vancomycin alone and vancomycin and bowel lavages were 31% and 23% respectively. The remaining 19% of the patients who failed to show improvement initially when managed by FMT recovered after a further cycle of treatment. The incidences of CDI recurrence were lower when FMT was administered colonoscopically compared to the use of vancomycin alone (Quraishi *et al.*, 2017).

FMT did not cause any severe side effects, as patients only showed post-operative constitutional symptoms thus supporting this approach as a safe treatment option. Despite this, there is a minimal possibility of CDI transmission, punctures correlated with treatment delivery, and fatality. Some centres in the UK have started to offer FMT services for CDI patients. Expansion of this treatment on a broader scale has not been accomplished due to the high cost of establishing such a service, retention of existing services, and ongoing concerns about the preferred ways to manage and control throughout the UK (Quraishi *et al.*, 2017).

1.12. Dihydroorotate dehydrogenase enzyme as a potential target

The selective targeting of dihydroorotate dehydrogenase enzyme (DHODase) enzyme has proven to be a successful drug discovery pathway that researchers may exploit to deplete the cellular pyrimidine pools (Lucas-Hourani *et al.*, 2017). Species targeting can be achieved as the reduction of L-dihydroorotate by the mammalian DHODase hinges on the reduction of the coupled ubiquinone, allying the pyrimidine biosynthesis pathway to the mitochondrial respiratory chain (Fang *et al.*, 2013). However, the fumarate reductase couples to the cytosolic DHODase to preserve a redox equilibrium (Takashima *et al.*, 2002), giving an insight into the enzyme's regulatory mechanism which may be exploited for selective DHODase inhibition.

The selective DHODase inhibition approach is known to have facilitated the discovery of numerous drugs for the treatment of diseases such as cancer, and immunological disorders, as well as their utilisation as antibacterial, antiviral, and antiparasitic agents (Singh *et al.*, 2017). Libraries of lead compounds have been generated, screened, and evaluated *in vitro*, *in vivo*, and *in silico* (Sykes *et al.*, 2016).

DHODase enzymes isolated from several prokaryotic and eukaryotic organisms have been studied to provide more detailed information about their biochemical mechanisms, structural characteristics, and the similarities and differences between subclasses (Reis *et al.*, 2015). Building research around DHODase targets benefits from the abundance of data on the evolutionary variance of the protein's catalytic, structural, kinetic, dynamic, and functional features.

The necessity for exploiting novel molecular mechanisms for new antimicrobial agents arises from the appearance of bacterial strains showing resistance towards existing antimicrobials and traditional mechanisms of growth inhibition. Researchers aim to overcome antimicrobial resistance by tackling a range of molecular strategies for microbial cell targeting. A successful strategy to terminate cell growth is via the use of antimetabolites. They not only affect cell growth but lead to cell death as well due to the accumulation of metabolic intermediates. In the *de novo* pathway of pyrimidine synthesis in both prokaryotes and eukaryotes, the selective targeting of DHODase provides a way to control pyrimidine biosynthesis (Asai *et al.*, 1983). The amino acid sequence of the DHODase in mammals is sufficiently distinct from that of the prokaryotes to allow potentially selective targeting. Gram-positive and Gram-negative bacteria possess distinct prokaryotic enzymes (Marcinkeviciene *et al.*, 2000). Studies have explored the scope to provide potential inhibitors of DHODase for use as potential treatment options in rheumatology, oncology, and bacteriology.

Biscaro and Belloni first recognised the presence of orotic acid in milk in the early 1900s (Reis, 2017). Further to this, between the late 1940s and early 1950s, orotic acid was experimentally proven to be a precursor for pyrimidine biosynthesis (Reichard, 1952). The initial, detailed exploration of the orotate metabolic pathway is attributed to Lieberman and Kornenberg who examined the anaerobic soil bacterium *Clostridium oroticum* previously known as *Zymobacterium oroticum*. They discovered the fermentation of the orotic acid and

pinpointed the role of L-dihydroorotate, carbamoyl-L-aspartate, and aspartate role in the orotate synthesis and decomposition pathway (Figure 1.9.) (Lieberman & Kornberg, 1953).



Figure 1. 9. Orotate metabolic pathway

In the early 1950s, the DHODase enzyme was successfully isolated from the microorganism *C. roticum* (Lieberman and Kornberg, 1953), followed by purification of the DHODase and determination of the DHODase crystal structure a few years later (Friedmann & Vennesland, 1960). The soluble metalloflavoprotein DHODase enzyme is responsible for catalysing the oxidative conversion of dihydroorotate to orotic acid with concomitant reduction of NAD^+ as the coenzyme (Friedmann & Vennesland, 1960). This fourth requisite step is the only redox reaction in the *de novo* pathway (Figure 1.10.). This step is vital for the biosynthesis of nucleic acid building block precursor, uridine monophosphate (UMP). Aside from salvage pathways, UMP is a prerequisite for the biosynthesis of the pyrimidine nucleotides containing C and T heterocyclic bases. The conversion of orotate to orotidine monophosphate, and later to uridine monophosphate (UMP) in the *de novo* pyrimidine biosynthesis, were revealed as the next steps in the pathway (Cordeiro *et al.*, 2012).

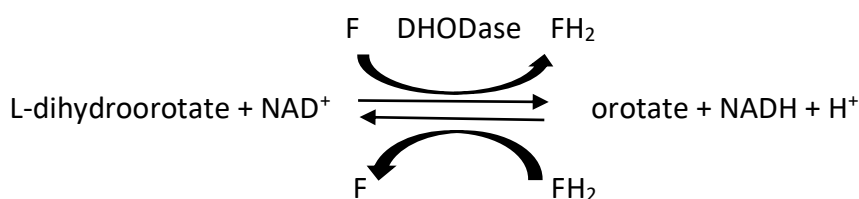


Figure 1. 10. The fourth and reversible step of *de novo* pyrimidine biosynthesis

The presence of iron (Fe), FMN (Flavin mononucleotide), and FAD (flavin adenine dinucleotide) in a ratio of 2:1:1 encompassed within the *C. roticum* DHODase was established provided by Aleman and Handler's (1967) analysis. It was later discovered that the Fe atoms are involved in their roles as a [2Fe-2S] redox cluster in this specific class of DHODase enzyme (Nielsen *et al.*, 1996). It was observed by Friedmann and Vennesland (1960) that the DHODase redox catalysis was directly linked to the enzymatically active flavin prosthetic groups. It was believed that each flavin participates in the interaction with

a coenzyme substrate including nicotinamide adenine dinucleotide/reduced nicotinamide adenine dinucleotide (NAD⁺/NADH+H⁺) as well as dihydroorotate/urotate (O'Donovan & Neuhard, 1970).

When Taylor and Taylor (1964) purified the *E. coli* DHODase, it was experimentally proven in the mid-1960s that DHODase exists as different subtypes, relating to their subcellular positioning and their catalytic characteristics. Unlike the other enzymes studied before the 1960s, *E. coli* DHODase was shown not to be capable of utilizing NAD⁺ as a coenzyme, thus suggesting that a different DHODase subtype existed.

1.12.1. The different structural classes of dihydroorotate dehydrogenases

The amino acid sequence, their cellular positioning, and their preference for coenzyme substrate are the variables that determine the classification of the DHODase enzyme subtypes (Reis *et al.*, 2015). The soluble DHODase enzymes located in the cytosol are grouped in class 1, where class 1 is segmented into two subclasses known as classes 1A and 1B due to the discrete structural and mechanistic properties of the DHODase subtypes. Fumarate was identified as DHODase 1A electron acceptor, where the enzyme is composed of a homodimer constituted of two *PyrD* subunits. This type is prevalent in Gram-positive bacteria such as *Lactococcus lactis* and *Enterococcus faecalis*, archaea, and lower eukaryotes (Reis *et al.*, 2015).

A cysteine residue that acts as a catalytic base was a common feature found in all class 1 DHODase subtypes. While a single *PyrD* gene identical to that of DHODase A, and *PyrK* genes enclosed in the two heterodimers of the heterotetramer was only present in DHODase 1B. Cofactors Fe-S and FAD are enclosed in the *PyrK* along with NAD⁺. NAD⁺ acts as a DHODase 1B electron acceptor (Norager *et al.*, 2002). Class 1B enzymes are also predominant in Gram-positive bacteria for instance *C. roiticum* (Argyrou *et al.*, 2002), *Bacillus subtilis* (Kahler *et al.*, 1999), *L. lactis* (Andersen *et al.*, 1994), and *E. faecalis*. Both, class 1A and 1B were reported to be found only in *Lactococcus lactis* (Andersen *et al.*, 1994), and *Enterococcus faecalis*.

Class 2 DHODase enzymes are monomeric enzymes linked to the eukaryotic inner membrane of mitochondria (Löffler *et al.*, 2002), and in the prokaryotic cytosolic membrane

as in the Gram-negative bacteria *E. coli* (Fagan & Palfey, 2009). Quinone plays the role of electron acceptor in this class 2 DHODase subtype.

A subclass known as class 1S is considered a more distinctive type of DHODase typical of *Sulfolobus solfataricus* (Sørensen & Dandanell, 2002). This type was subcategorised under class 1 according to its localisation in the cytosol. This class is described as a heteromeric enzyme enclosing a catalytic subunit encoded by *pyrD* gene, whereas the electron acceptor subunit is encoded by the *orf* gene (Sørensen & Dandanell, 2002). Despite the ability of this subtype of the enzyme to utilise coenzyme Q and oxygen, the identity of the electron acceptor and the quaternary structure remains unidentified.

It was reported that classes 1A and 1B have approximately 30% of their amino acid sequence in common whilst classes 1 and 2 share approximately 20% of the sequence (Asai *et al.*, 1983). The two classes of DHODase enzymes differ in various ways including subcellular location, the base; cysteine (class 1A/B) or serine (class 2), which is essential for catalysis in the active site, and the electron acceptors employed by the enzymes; NAD⁺, fumarate or quinone. Class 1 and class 2 subtypes owe their variations to the diverse ways in which they interact with electron acceptors and the reduced FMN comma along with the oligomeric state of the enzymes (Singh, 2017).

Enzymatic targeting is a strategy in which selective, species-targeting can be accomplished. The *C. roticum* DHODase was examined by the mechanistic study of the purified enzyme and shown to belong to class 1B, where NAD⁺/NADH acts as an electron acceptor (Argyrou *et al.*, 2000). Located at the active site, cys130 is the nucleophile responsible for the removal of the C5-*pro*-S hydrogen, with concomitant transfer of hydride to flavine, to create the C=C bond in a concerted conversion of dihydroorotic acid to orotic acid (Figure 1.11.). Irreversible inhibition of DHODase from *C. roticum* using arylidene pyrimidinetriones derivatives was achieved (Figure 1.12.) (Fraser, 1990). In this thesis work, we wished to determine whether the arylidene pyrimidinetriones and their derivatives including alkyl pyrimidinetriones (APTs), might also possess growth-inhibitory properties against *C. difficile*.

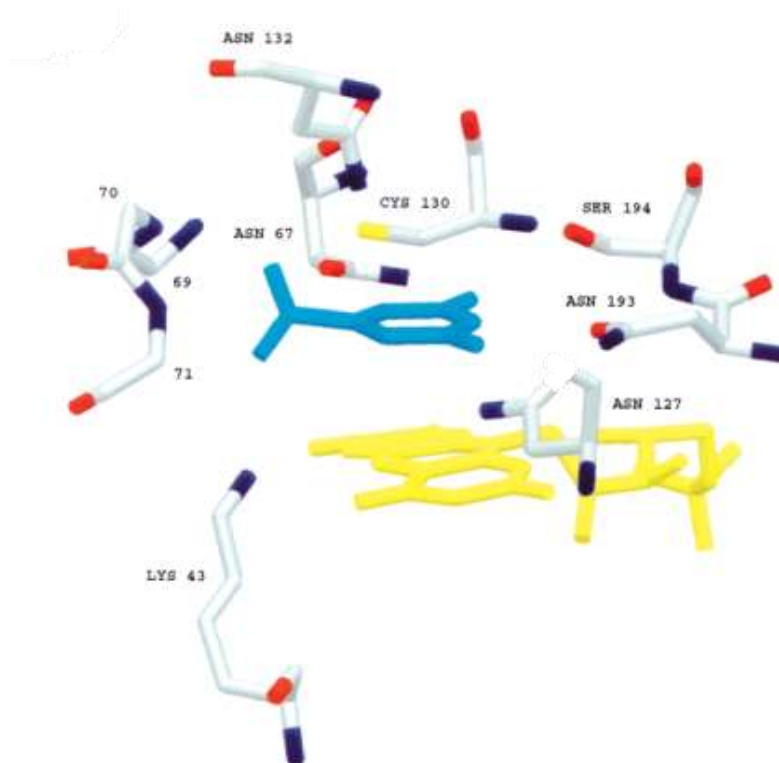


Figure 1. 11. DHODase catalytic side with the substrate (blue) and proximal flavine electron acceptor (yellow) (Argyrou *et al.*, 2000)

Aim and objective

This PhD research aimed to prepare and characterize an extended series of compounds as selective growth inhibitors of *C. difficile* through the evaluation of their antimicrobial and cytotoxicity.

One hypothesis is that APTs have the potential to be surrogate substrates as novel pro-drug inhibitors of DHODase that exploit the enzyme's ability to create C=C bonds. Once bound at the DHODase active site, the benzylic C-C bond in the APT prodrug may conceivably be oxidised to give an exocyclic C=C bond, generating the reactive arylidene at the DHODase active site to which approximal nucleophile can attach, followed by deactivating protonation, leading to irreversible inhibition of the enzyme (Figure 1.12).

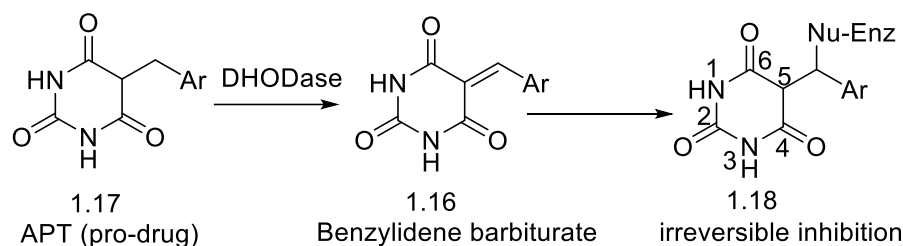


Figure 1. 12. Hypothetical mechanism of potential prodrug activation and DHODase inhibition

Objectives of this research were to:

- Synthesise barbituric acid derivatives as potential selective *C. difficile* inhibitors.
- Examine the significance of the heterocyclic component through synthesis and evaluation of Meldrum's acid derivatives.
- Further examine the significance of the heterocyclic component through the synthesis of 5-membered ring-containing compounds, and nitrofurantoin analogues.
- Characterise the synthesised compounds using ^1H NMR, ^{13}C NMR, IR, and Mass spectroscopic methods.
- Determine the antimicrobial activity and selectivity of the synthesised compounds against *C. difficile*, *E. coli*, and *S. aureus* under anaerobic conditions.
- Evaluate the cytotoxic activity of some representative examples of the lead compounds against two different cell lines: Mouse normal liver cells (BNL) and colorectal cancer (Caco-2).

Chapter 2

2.1. Aldehydes

2.1.1. Uses of aldehydes

The restricted utilisation of aldehydes in the industrial sector results from their toxicity despite being a highly, synthetically useful chemical class of compound. Aldehydes can be chemically obtained via the oxidation of alcohols upon removing hydrogen (dehydrogenation), oxidation of methylbenzene in the case of benzaldehyde, or the reduction of esters (Aljaafari *et al.*, 2022). Aldehydes not only impact both mammalian olfaction and gestation senses, but some aldehydes including cinnamaldehyde attain the ability to bind to the G-protein binding receptors, provoking reaction cascades which in turn induce the perception of senses in mammals as well. Aldehydes are powerful antimicrobial agents as they destroy the exterior bacterial cell membrane.

2.1.2. Toxicity of aldehydes

The mechanism of aldehyde toxicity is still not entirely understood. However, it is judged to arise from the range of factors involving structural aspects, chemical reactivity and target interactions. Despite the negative health impact of aldehydes, humans are regularly exposed to them in everyday life. A study that analysed both the endogenous and exogenous aldehydes based on their electrophilicity and relative softness, revealed that both the soft unsaturated aldehydes and the soft nucleophilic thiolate sites interact with the exact cysteine residues present in enzymes. On the other hand, the interaction between hard aldehydes and hard nucleophiles promotes toxicity by diminishing the roles of macromolecules essential for cytophysiological action. Yet, more in-depth studies are required for a more accurate interpretation of the effect of these interactions on the targets of macromolecules (LoPachin & Gavin, 2014).

2.1.2.1. Benzaldehyde

The aromatic benzaldehyde is part of many industries that deal with cosmetics, food additives, and perfumes. Although aldehydes possess toxic effects, studies have reported that benzaldehyde is safe enough to be utilised in the food industry. Experimental studies on mice and rats have reported an oral lethal dose 50 (LD₅₀) ranging between 0.8 to 0.25 µg/kg showing negligible acute toxicity with minimal or no adverse effect. Yet, ocular and nasal irritation was triggered when rabbits were subjected to vaporized benzaldehyde whereas undiluted benzaldehyde provoked irritation when a drop was added to rabbit eyes, causing oedema, erythema, and pain (Aljaafari *et al.*, 2022).

2.1.2.2. Cinnamaldehyde

Cinnamaldehyde was found to be well tolerated by humans which permits its use in the production of fragrances and the food industry as a flavouring agent. A daily consumption of 1.25 mg/kg is approved by the FDA and the Council of Europe. Unlike the numerous known toxic aldehydes, it was reported that cinnamaldehyde possesses several therapeutic properties. It is used in Chinese medicine for the treatment of gastritis, indigestion, blood circulation disorders, and inflammation (Chen *et al.*, 2019). Moreover, cinnamaldehydes showed some detoxification properties against dangerous agents such as ochratoxin (Aljaafari *et al.*, 2022).

2.2. Barbituric acid

In the pyrimidinetrione ring system of barbituric acid, reversible interconversion of four synchronous, discrete tautomers takes place at equilibrium (Figure 2.1.). Reversible tautomerisation between the keto form, which is characterised by the presence of three carbonyl groups at positions C2, C4, and C6, and the enol form where proton shift occurs giving hydroxyl groups and respective C=C bonds. All the resonance forms possess the exact molecular formula and atom positioning and are discrete only in the placement of electrons (Fahad, 2022). The prevalence of the keto form is higher than the enol form in acid media, unlike in alkaline media, where the enolic form is predominant (Macbeth *et al.*, 1926). Hypothetically, the carbonyl conversion to the keto form can take place either in one, two,

or all three positions depending on the solvent type and the concentration of the hydrogen ion (Fox & Shugar, 1952). Yet, the imide (C=N) bonds are unlikely to be broken due to the high reactivity of the active methylene group, where proton shift from one of the two hydrogens at C5 takes place, first generating a mono-enol form. In 1909, Wood and Anderson managed to elucidate the chemical tautomerisation and the formation of mono-enol form despite failing to isolate any of the tautomers. The formation of isoamide groups (-N=C-OH) correlates with tautomerisation. Such proton shifts are stabilised by both resonance forms of the fully unsaturated heterocyclic ring (Figure 2.1). Barbituric acid itself possesses some acidic properties owing to its structural characteristics such as the active methylene group, flanked by two activating/electron-withdrawing carbonyl groups, conjugated and symmetrical ring, and the relatively stable imino/isoamide groups. Keto and enol forms differ only in the positioning of one or more hydrogen atoms, and the arrangement of double bonds (Maynert & Van, 1950).

The acidic properties of the 5,5-disubstituted barbituric acids are comparatively reduced compared with barbituric acid due to the absence of an active methylene group and the loss of symmetry in the heterocyclic ring. Base catalysis enables the conversion of the keto form to the enol form. For instance, when treating a neutral solution in water with a base, the enol form reacts with the base leading to its depletion in the reaction mixture. To achieve equilibrium, more of the keto form converts to the enol form which becomes sequentially neutralised again via the base (Figure 2.1.) (Nobay & Acquisto, 2014). All the tautomers exist in equilibrium with one another, where structures are differentiated by oscillations of valence electrons and unsaturation. The structure of barbituric acid and its derivatives cannot be fully represented using a single tautomeric form (Figure 2.1.) because of the constant shifts of electrons and protons. A collective contribution is made by all the tautomeric forms to form a hybrid of all the resonating states. The keto form is like that of urea, whereas the tri-enol form manifests a type of resonance like the benzene ring (Figure 2.1.). The comparatively strong acidity of barbituric acid is correlated to the previously mentioned mechanism as the two nitrogen atoms are liable to electron attraction (Fahad, 2022).

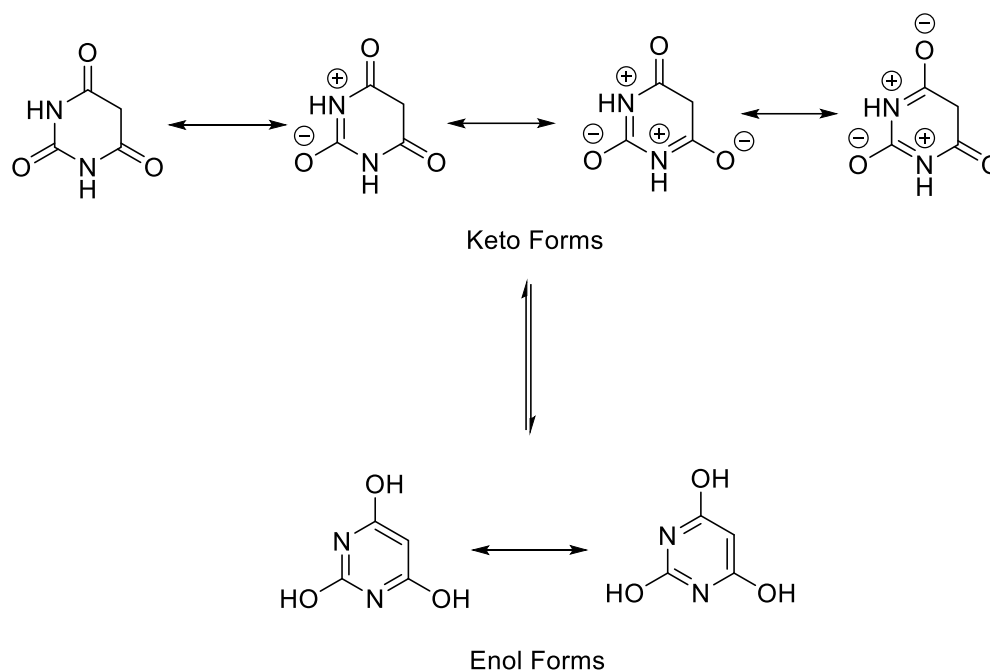


Figure 2. 1. The resonance forms of the keto/enol tautomers of barbituric acid

2.2.1. Grimaux's synthesis of barbituric acid

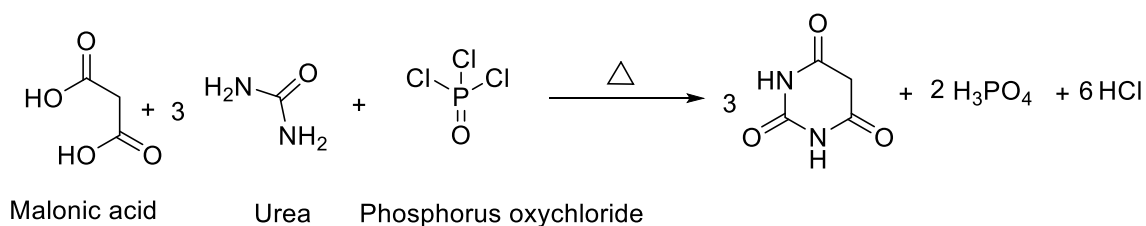


Figure 2. 2. Grimaux's synthesis of barbituric acid

An alternative method (Figure 2.2.) can be utilised for the synthesis of barbituric acid involving the condensation of urea with malonic acid, where the two moles of water produced are afterward absorbed by the phosphorus oxychloride or acetic anhydride (Daneshvar *et al.*, 2018). Barbituric acid alone is non-toxic and has no hypnotic activity. Introducing any functional group at C5 results in the formation of physiologically active compounds. The hypnotic, sedative, or anaesthetic properties are correlated with the di-substitution of the C5 (Daneshvar *et al.*, 2018).

2.3. Meldrum's acid

More than a century ago, Scottish chemist Andrew Meldrum reacted malonic acid and acetone under reflux in the presence of an acid catalyst to give a white solid substance "Meldrum's acid". The first confirmation of the molecular structure was not released till nearly half a century later due to the absence of NMR machines (Dumas & Fillion, 2010). With a pK_a value of nearly 4.9 in water, the reason behind the notable acidic properties of Meldrum's acid remained mysterious until the mid-2000s, when Ohwada observed with computational calculations that the alpha proton's (α_{CH}) orbital is in a proper geometrical alignment with the π^* orbital of the carbonyl groups, leading to a strong, unusually destabilisation of the CH bond in the ground state (Dumas & Fillion, 2010).

A wide range of natural and synthetic bioactive derivatives can be obtained from Meldrum's acid as the acid key building block (Figure 2.3.). The electrophilic attack can easily take place on the hydrogen at the C5 position. Whereas the presence of a carbonyl group at positions 4 and 6 triggers nucleophilic attack. The derivatives obtained from these approaches can be utilised in numerous ways as they undergo decomposition to form ketenes through the loss of acetone and carbon dioxide (Bukhari *et al.*, 2023).

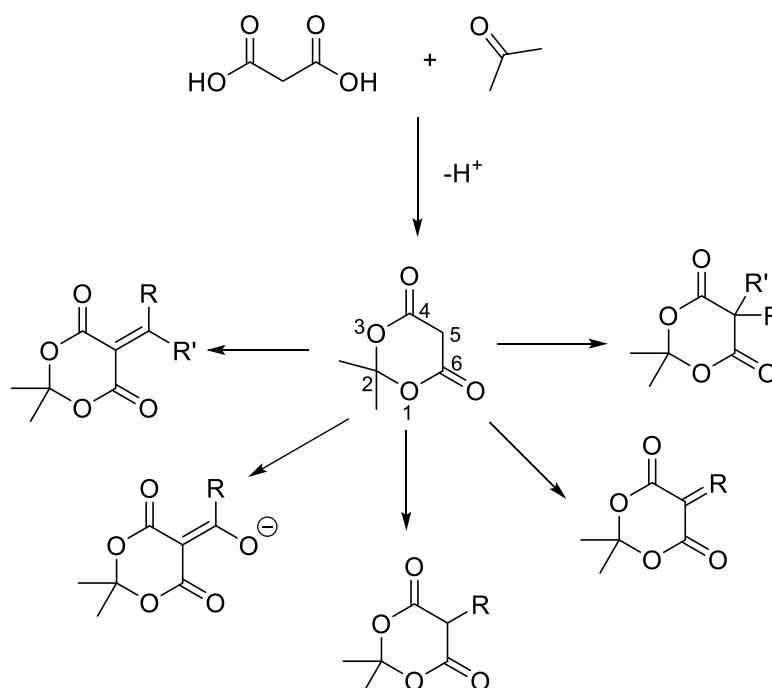


Figure 2. 3. Formation and derivatisation of Meldrum's acid.

2.3.1. The acidic properties of Meldrum's acid

The acidic properties of the heterocyclic ring enable the easy loss of a proton from the methylene group at C5, creating a double bond with the neighbouring carbons (C4 or C6), and a negative charge on the respective oxygen atom. The continuous delocalisation of the double bond between the two carbonyl groups of the anion forms generates resonating stability as shown in Figure 2.4. (McNab, 1978).

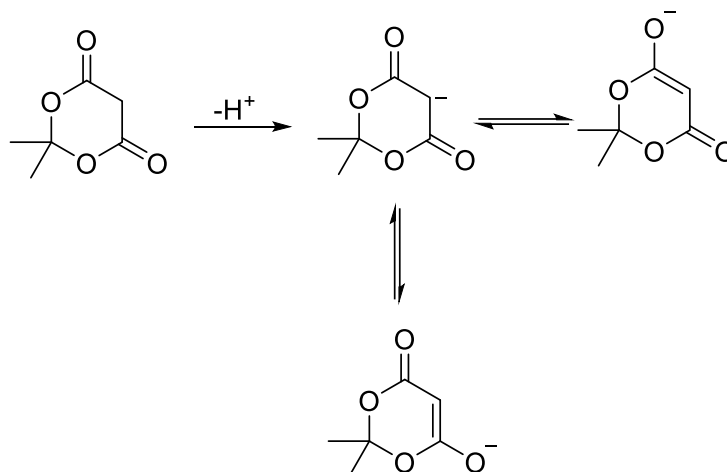


Figure 2. 4. The resonating forms of Meldrum's acid carbanion

2.3.2. Synthesis of Meldrum's acid

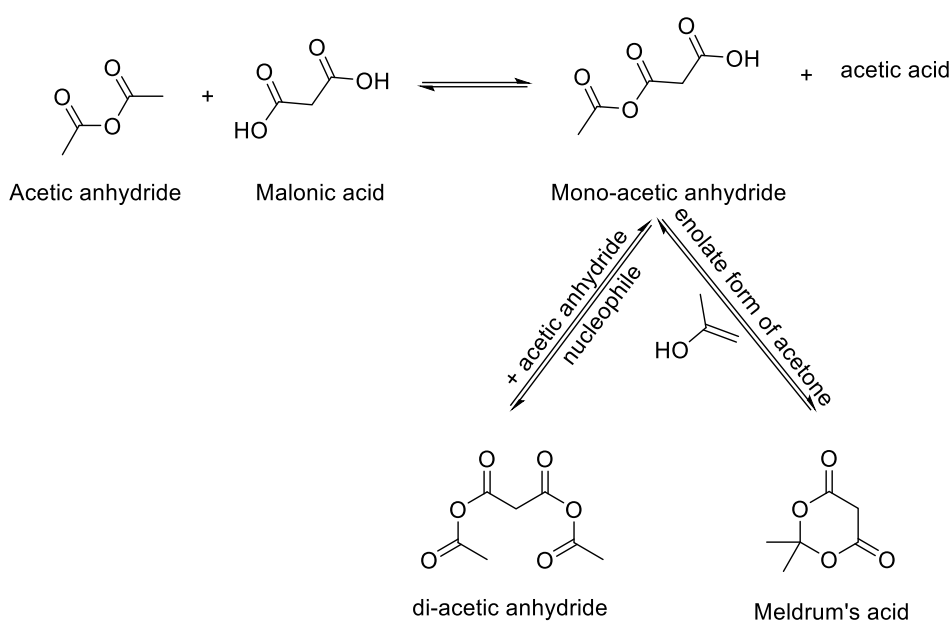


Figure 2. 5. Synthetic route to Meldrum's acid

The mono-acetic anhydride intermediate is produced upon reacting acetic anhydride and malonic acid. The reaction can proceed through two primary routes, wherein the first reaction, the intermediate once formed can further react with an additional equivalent of acetic anhydride to give a di-acetic anhydride, whereas the accompanying pathway involves the reaction of the mono-acetic anhydride with the enolate form of acetone to give Meldrum's acid. The enolate form is formed via acidic catalysis of acetone (Meldrum, 1908). The conversion of di-acetic anhydride to the mono-acetic anhydride intermediate is possible via nucleophiles such as water. The addition of acid catalysts in adequate amounts increases the concentration of the enolate form of acetone and consequently enables Meldrum's acid yield maximization and suppresses the alternative unwanted route to di-acetic acid anhydride (Figure 2.5.). Simultaneously, the addition of acetic anhydride in a controlled, portion-wise manner to the reaction mixture, enhances the yield of Meldrum's acid, as the mono-acetic anhydride intermediate reacts with the enolate form of acetone preferentially, due to the limited amount of acetic anhydride available with which it can react (Relenyi *et al.*, 1986).

Aim of Chapter 2

This part of the research study aimed to synthesise compounds that possess selective antibacterial activity against *C. difficile* to retain the normal gut microbiota that provides defensive properties to the gut. Hence, decreasing the possibility of acquiring CDI and CDI recurrence. Selective aldehydes known for their antimicrobial activity were set into chemical reactions with five or six-membered rings creating a library of compounds that were tested for antimicrobial activity (Chapter 3). The synthesised compounds were characterised by spectroscopic and analytical methods that confirm their structures. Lead compounds that exhibit high efficacy and selectivity against the tested *C. difficile* strain (Chapter 3) may act as potential growth inhibitors to resistant strains such as NAP1/027.

The hypothesis was based on targeting the DHODase enzyme of *C. difficile* despite its unknown X-ray crystal structure. This was to be achieved by synthesising compounds that possess structural features like that of the dihydroorotic acid, thus acting as a competitive antagonist to bind to the DHODase active or allosteric site. According to a study conducted by Fraser (1990), irreversible inhibition of the DHODase enzyme from *C. oroticum* using

arylidene pyrimidinetriones derivatives was achieved. In this work, two libraries of compounds composed of either barbituric acid or Meldrum's acid possessing active methylene groups were reacted with different aromatic aldehydes. Aldehydes are known for their antimicrobial activities; however, they cannot be used as drug candidates on their own because of their potentially high toxicity owing to their reactivity as Michael acceptors. As previously mentioned in Chapter 1, nitrofurantoin is recommended in cases of CDI; accordingly, nitrofurantoin analogues and other five-membered ring analogues were synthesised to evaluate their antibacterial activity (Chapter 3).

2.4. Materials and methods

Reagents and solvents were purchased from Sigma-Aldrich, Fisher Scientific Ltd., and Merck. Oven-dried glassware was used for water-sensitive reactions; the reactions were set under argon (Ar). The reaction-products were monitored under ultraviolet (UV) light ($\lambda = 254/365$ nm) when spotted on a stationary phase composed of silica gel on aluminium foil-backed thin-layer chromatographic (TLC) plates (60 F254, Merck), an aqueous solution of potassium permanganate (KMnO_4) visualisation reagent was used when needed. Crude products were purified by recrystallisation, liquid-liquid extraction, or flash/column chromatography (Merck silica gel 40-70 μm) when needed to obtain the desired products. ^1H and ^{13}C NMR spectra of the synthesised compounds were recorded for structure characterisation using a Bruker Ascend NMR at 400 MHz. Samples were dissolved in deuterated dimethyl sulfoxide (DMSO-d_6). When needed deuterium oxide (D_2O) was added with DMSO to determine exchangeable protons, and spectra and referenced to the solvent peak without the need for an added internal standard. Chemical shifts were reported in parts per million (ppm), and coupling constants in Hertz (Hz), whereas the multiplicities were abbreviated as s = singlet, d = doublet, t = triplet, q = quartet, and m = multiplet. Thermo Scientific Nicolet iS5 FT-IR spectrometer equipped with an ID5 Diamond ATR accessory was used to record the IR spectra of the synthesised compounds, where the intensities of the signals were abbreviated as weak (w), medium (m), and strong (s). Mass spectra were recorded by the National Mass Spectrometry Facility Swansea using Xevo G2-S ASAP or LTQ Orbitrap XL 2. Melting points were measured by a Reichert-Jung Thermo Galen - hot stage microscope coupled with a Pt 100/RTD temperature monitor.

2.5. Experimental

2.5.1. Wittig reaction

2.5.1.1. Synthesis of Wittig reaction derivatives

2.5.1.1.1 (E)-3-(5-Nitrofuranyl)acrylaldehyde (2.1)

One equivalent of 5-Nitro-2-furylaldehyde (0.5 g, 3.54 mmol) and 1.1 equivalent of (triphenylphosphoranylidene)acetaldehyde (PPh₃ acet.) (1.186 g, 3.89 mmol) were added to a dry round-bottom flask. The flask was closed by a rubber cork; a syringe filled with anhydrous magnesium sulfate (MgSO₄) was inserted into the cork. Toluene (10 ml) was added to the syringe and mixed with the anhydrous MgSO₄ to render the solvent anhydrous. The reaction flask was set to reflux (6 h) at 120 °C under Ar. The crude product was purified by flash column chromatography, and the desired compound was extracted (ethyl acetate/petroleum ether, 19:81). The solvent was evaporated under vacuum to give brown crystals of compound **2.1** (0.36 g, 2.15 mmol, 61%). Spectroscopic data was consistent with the literature values, where the reported melting point was 117-120 °C (Meinig *et al.*, 2015).

Molecular Formula C₇H₅NO₄; R_f (ethyl acetate/petroleum ether, 1:4): 0.33.

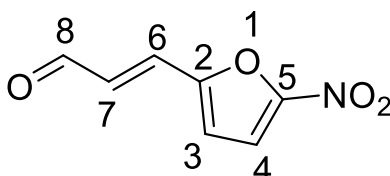


Figure 2. 6. Compound 2.1

¹H NMR (400 MHz, DMSO-d₆) δ= 9.70-9.68 (d, *J*= 7.6 Hz, 1H, -CH₈), 7.78-7.77 (d, *J*= 4.6 Hz, 1H, ArH₄), 7.70-7.66 (d, *J*= 15.9 Hz, 1H, -CH₆), 7.42-7.41 (d, *J*= 3.9 Hz, 1H, ArH₃), 6.76-6.70 (dd, *J*= 15.9, 7.6 Hz, 1H, -CH₇) ppm.

¹³C APT NMR (101 MHz, DMSO-d₆) δ= 193.98 (C 8), 152.87 (C 5), 152.77 (C 2), 136.80 (C 6), 131.18 (C 7), 118.59 (C 3), 115.10 (C 4) ppm.

2.5.1.1.2. (E)-3-(5-Nitrothiophen-2-yl)acrylaldehyde (2.2)

5-Nitro-2-thiophenecarboxyaldehyde (0.5 g, 3.18 mmol) and 0.7 equivalent of PPh₃ acet. (0.7 g, 2.3 mmol) were added to a dry round-bottom flask. The flask was closed with a

rubber cork; a syringe filled with anhydrous magnesium sulfate (MgSO_4) was inserted into the cork. Toluene (10 ml) was added to the syringe and mixed with the anhydrous MgSO_4 to render the solvent anhydrous. The reaction flask was set to reflux (8 h) at 120 °C under Ar. Polar impurities were removed after dissolving the crude in hexane slurry; the hexane-insoluble residue was discarded. The filtrate was collected, and the solvent was evaporated under vacuum. The crude product was further purified using flash column chromatography and the desired compound was extracted (ethyl acetate/hexane, 25:75). The solvents were evaporated under vacuum to give yellow powder of the product **2.2** (0.45 g, 2.4 mmol, 78%). Spectroscopic data was consistent with the literature values (Srivastava *et al.*, 2008). Molecular Formula $\text{C}_7\text{H}_5\text{NO}_3\text{S}$; R_f (ethyl acetate/hexane, 1:4): 0.28.

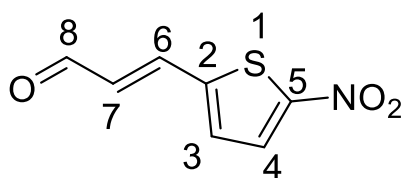


Figure 2. 7. Compound 2.2

^1H NMR (400 MHz, DMSO-d_6) δ = 9.69-9.67 (d, J = 7.5 Hz, 1H, -CH₈), 8.17-8.16 (d, J = 4.3 Hz, 1H, ArH₄), 7.96-7.92 (d, J =15.8 Hz, 1H, -CH₆), 7.73-7.72 (d, J = 4.3 Hz, 1H, ArH₃), 6.92-6.86 (dd, J = 15.8, 7.4 Hz, 1H, -CH₇) ppm.

2.5.1.1.3. (2E,4E)-5-(5-Nitrothiophen-2-yl)penta-2,4-dienal (2.3)

One equivalent of compound 2.2 (0.25 g, 1.59 mmol) and 1.5 equivalent of PPh_3 acet. (0.70 g, 2 mmol) were added to a dry round-bottom flask. The flask was closed by a rubber cork; a syringe filled with anhydrous MgSO_4 was inserted into the cork. Toluene (15 ml) was added to the syringe and mixed with the MgSO_4 to render the solvent anhydrous. The reaction flask was set to reflux (8 h) at 120 °C under Ar. The solvent was evaporated under vacuum, and the crude was purified using flash column chromatography. The desired compound was extracted (ethyl acetate/hexane, 40:60); the solvent was evaporated under pressure to give the product **2.3** (0.15 g, 0.07 mmol, 53%) as an orange powder.

Molecular Formula $\text{C}_9\text{H}_7\text{NO}_3\text{S}$; R_f (ethyl acetate/hexane, 3:7): 0.36.

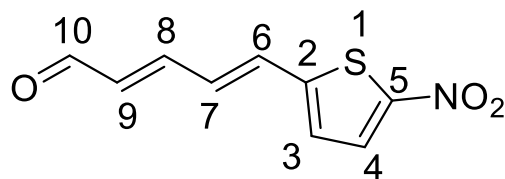


Figure 2. 8. Compound 2.3

^1H NMR (400 MHz, DMSO- d_6) δ = 10.82 (s, 1 H, H 10), 8.94-8.92 (d, J = 7.9, 1H, ArH 4), 8.14-8.12 (d, J = 9.0, 1H, CH 6), 7.90-7.88 (d, J = 7.7, 1H, ArH 3), 7.64-7.59 (m, 1H, CH 8), 7.45-7.41 (m, 1H, CH 7), 7.25-7.23 (d, J = 9.0, 1H, CH 9) ppm.

^{13}C APT NMR (101 MHz, DMSO- d_6) δ =133.73 (C 5), 131.71 (C 2), 132.51 (C 4), 132.48 (C 6), 132.00 (C 3), 131.90 (C8), 129.28 (C7), 129.16 (C9) ppm.

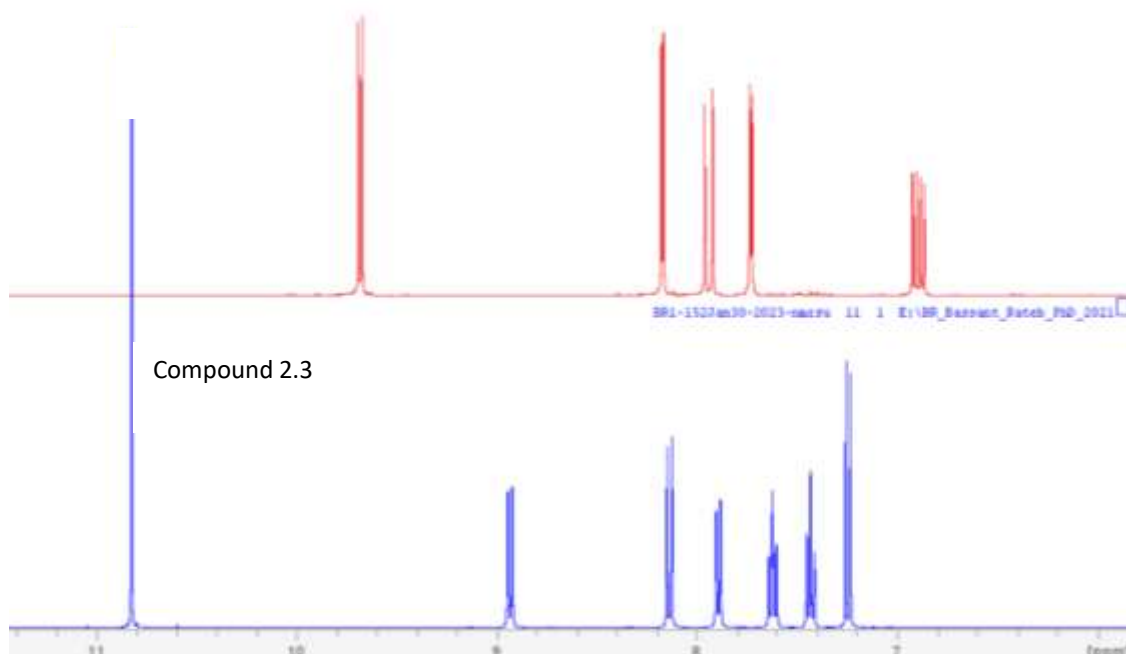
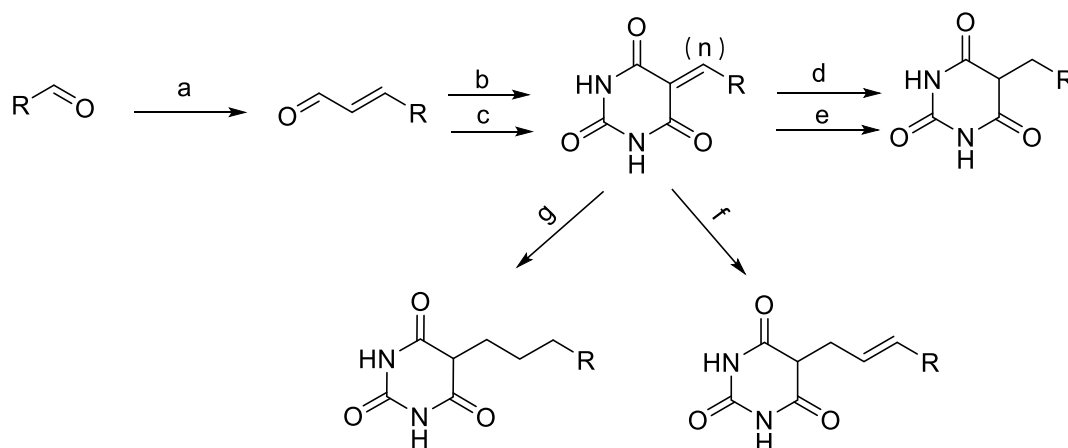


Figure 2. 9. The ^1H NMR spectra of compounds 2.2 and 2.3

2.5.1.2. Barbiturates derivatives formation

The precursors of the target compounds (**2.13**, **2.21**, **2.56**, **2.59**) were made from aldehydes starting materials and (triphenylphosphoranylidene)acetaldehyde to form C=C and C=C-C=C chain-extended derivatives. Knoevenagel condensation reaction was set between a range of these and various other arylaldehydes using barbituric acid as the active methylene substrate, to produce arylidene barbiturates products in good yield. The benzylidene barbiturates were subjected to reduction either with sodium borohydride (NaBH_4) for

selective exocyclic carbon carbon-carbon double bond (C=C) reduction or complete reduction using palladium on charcoal (Pd/C) (Scheme 2.1.).



- a: PPh₃ acet., anhydrous toluene, Ar, reflux
- b: barbituric acid, reflux/ sonicator bath at rt, EthOH
- c: NHEt₂, EthOH
- d: NaBH₄, EthOH
- e: 2-aminothiophenol, benzaldehyde
- f: NaBH₄, EthOH
- g: Pd/C, H₂, EthOH
- (n): number of C=C in the aliphatic bridge

Scheme 2. 1. General scheme for the synthesis of benzylidene barbiturates, and their reduced forms

2.5.1.3. Mechanism of the Wittig reaction

The mechanism of Wittig reactions involves three steps, a nucleophilic attack to the carbonyl group of the aldehyde or ketones, followed by the formation of a four-membered ring, and subsequently, alkene is formed (**Figure 2.12.**) (Byrne, 2012). The phosphonium ylide is a carbanion species, stabilised by the adjacent phosphorus atom. The ionic bonding between the P and C results in the formation of another resonating structure of the ylide form contributing to the carbanion stabilisation. Following the initial carbon-carbon bond formation, two intermediates are formed. The first intermediate is a dipolar, charge-separated betaine species whilst the second intermediate, oxaphosphatane is formed upon cyclisation to form a four-membered heterocyclic structure. Cleavage of oxaphosphatane to give alkene product and accompanying phosphine oxide is exothermic and irreversible (Byrne, 2012).

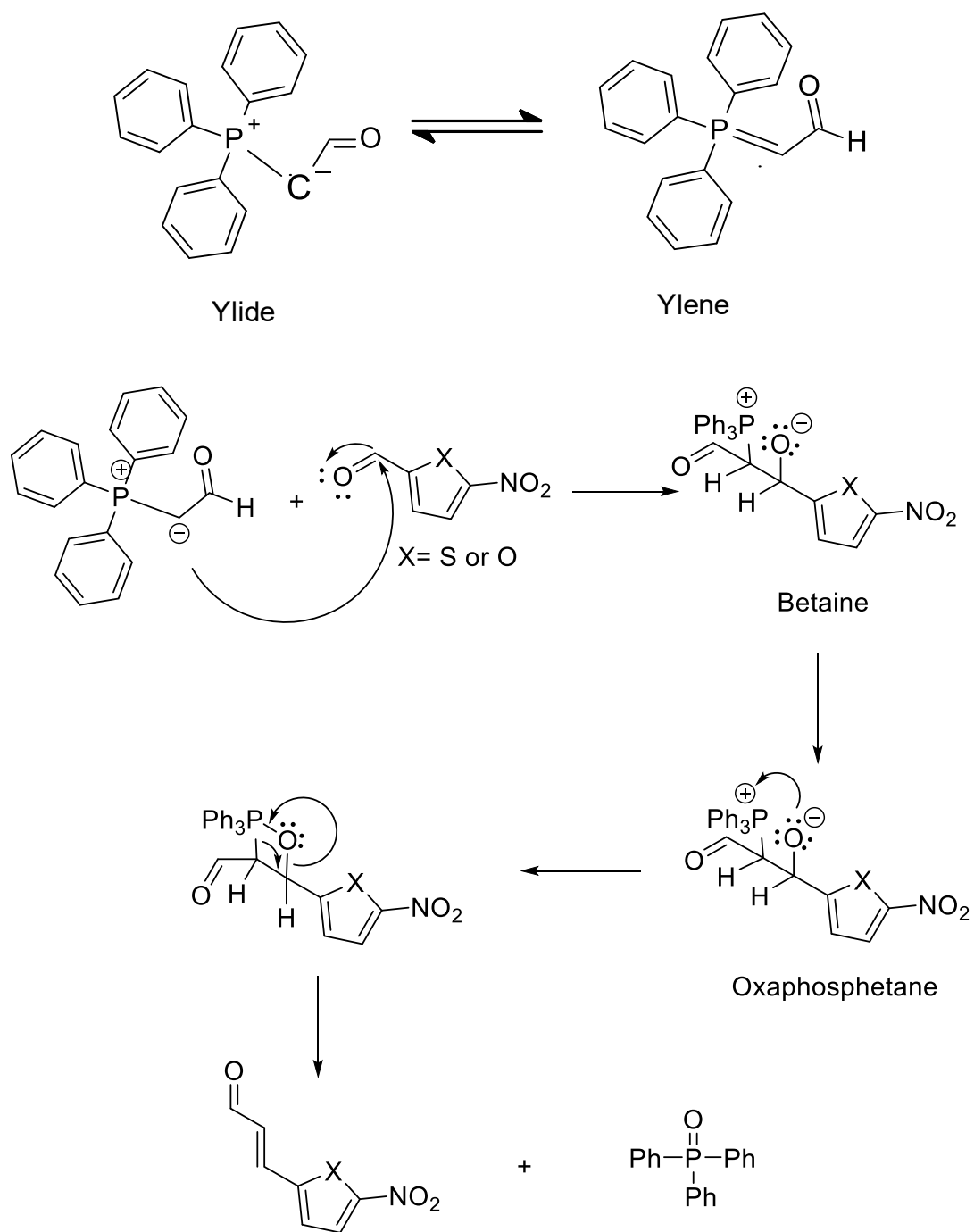


Figure 2. 10. Mechanism of action of Wittig reaction

2.5.1.4. Elongating the olefinic chain of aldehydes by Wittig reaction

In the late 1970s, George Wittig was granted a Nobel prize for a chemical reaction named after him, where an organophosphorus compound, phosphonium ylide is set in reactions with aldehydes and ketones. Wittig reaction forms unsaturated alkenes having a nucleophilic alpha carbon covalently bonded to the electrophilic carbonyl carbon. A principal advantage of alkene synthesis by the Wittig reaction is that the location of the double bond is fixed, in contrast to the mixtures often produced by alcohol dehydration (Ayub & Ludwig, 2016).

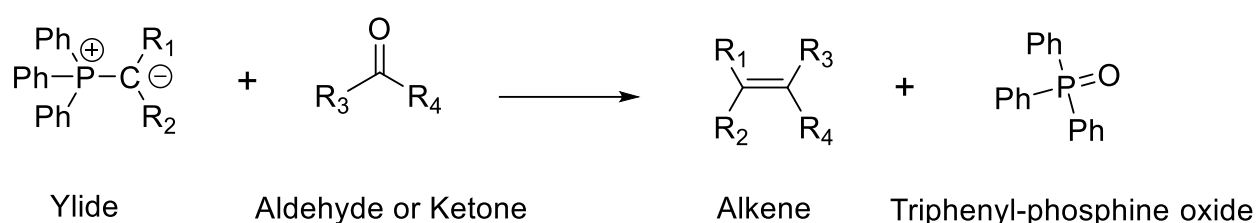


Figure 2. 11. The chemical reaction between triphenylphosphine with aldehyde or ketone

Heterocyclic aldehydes containing five-membered furyl and thiophenyl rings, were set into reacted with PPh_3 under the conventional Wittig mechanism (Vedejs & Peterson, 1994) to give the respective aldehyde derivatives with a longer aliphatic chain in good yields **2.1**, **2.2**, and **2.3** (Scheme 1). The formed aldehydes were used as precursors for the Knoevenagel condensation reaction. Elongating the aliphatic bridge will enable comparative analysis with a shorter chain for a better understanding of the structure-activity relationship (SAR) based on the data from the antimicrobial activity assay (Chapter 3).

The reaction was performed under anhydrous conditions. Toluene was dried using anhydrous MgSO_4 and the reaction was set under Ar. Anhydrous conditions are preferable as moisture influences the relative stabilities of the formed intermediates during the reaction (Ayub & Ludwig, 2016). E-configuration is usually favourable under anhydrous conditions upon reacting a stabilized ylide with aldehyde, unlike the Wittig reaction in water where E/Z selectivity is altered (Ayub & Ludwig, 2016). The reaction products were obtained upon purification with flash/ column chromatography in good yield.

The formation of additional unsaturation in the chain connecting the aldehyde -CHO to the aromatic ring was characterised by ^1H NMR, ^{13}C NMR, Heteronuclear Single Quantum Coherence (HSQC), and Hetero-nuclear Multiple Bond-Correlation Spectroscopy (HMBC). TLC was used as a preliminary indicator for the degree of purity of the products extracted from the column chromatography. Before the Wittig reaction, the C-H in the aldehyde -CHO group appeared as a singlet due to the absence of any neighbouring protons. After the Wittig reaction, compounds **2.1** and **2.2** displayed the presence of a distinctive doublet of doublets (dd) in their proton NMR spectra, corresponding to $\text{O}=\text{CH}-\underline{\text{C}}\text{H}=\text{CH}$, which indicated that the two neighbouring protons coupled together. The second carbon forming the additional alkene appeared as a doublet $\text{O}=\underline{\text{C}}\text{H}-\text{CH}=\text{CH}$. While the aliphatic proton singlet of the starting material appeared as a doublet. Further elongation of the aliphatic chain of compound **2.2** was performed to form compound **2.3**. The doublet peak of $\text{O}=\underline{\text{C}}\text{H}-\text{CH}=\text{CH}$ of compound **2.2** appeared as multiplet, $\text{O}=\text{CH}-\text{CH}=\underline{\text{C}}\text{H}-\text{CH}=\text{CH}$, and $\text{O}=\text{CH}-\underline{\text{C}}\text{H}=\text{CH}-\text{CH}=\text{CH}$ appeared as a dd. Despite having a neighbouring proton three bonds apart, the formyl proton of the aldehyde $\text{O}=\underline{\text{C}}\text{H}-\text{CH}=\text{CH}-\text{CH}=\text{CH}$ appeared as a singlet, this may indicate that these two neighbouring protons are uncoupled as they may be at a 90-degree dihedral angle and the J value can be zero. ^{13}C NMR was used as proof for the expected increase in the number of carbons, which corresponded to the formation of the new alkene in the aliphatic chain. The carbon NMR showed the presence of two additional carbons aligning opposite to the solvent peaks (DMSO); those two peaks correspond to the formed unsaturated alkene. Whereas HMBC was used to show the correlation between carbons bounded to hydrogens which are 2-3 bonds away, thereby the carbon connectivity can be deduced.

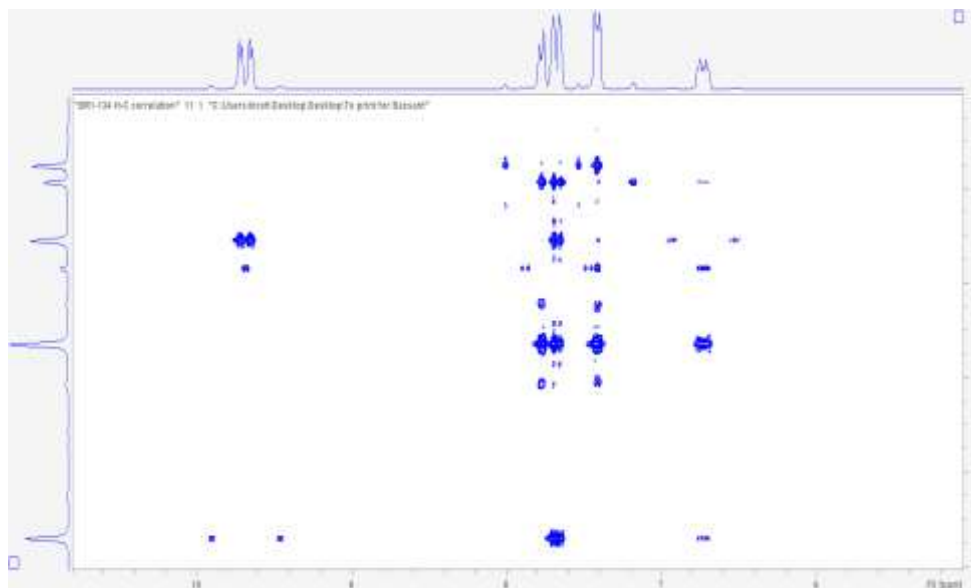


Figure 2. 12. HMBC spectrum of compound 2.1 indicating the correlation between the ^1H NMR (horizontal) and ^{13}C NMR (vertical)

Table 2. 1.Connectivity deduced from the HMBC spectrum of compound 2.1

δ ^1H NMR	HMBC δ ^{13}C NMR	Corresponding Proton
9.70-9.68	136.80 (C 6) 131.18 (C 7)	H 8
7.78-7.77	152.87 (C 5) 118.59 (C 3)	H 4
7.70-7.66	193.98 (C 8) 152.77 (C 2) 131.18 (C 7) 118.59 (C 3)	H 6
7.42-7.41	152.77 (C 2) 136.80 (C 6) 115.10 (C 4)	H 3
6.76-6.70	193.98 (C 8) 152.77 (C 2) 136.80 (C 6) 118.59 (C 3)	H 7

2.5.2. Synthesis of benzylidene barbiturate derivatives by Knoevenagel condensation

2.5.2.1. 5-Benzylidenehexahydropyrimidine-2,4,6-trione (2.4)

A suspension of barbituric acid (0.35 g, 2.7 mmol) in water (5 ml) was heated until dissolved, followed by the addition of benzaldehyde (0.29 g, 2.7 mmol) suspended in ethanol (15 ml). The reaction mixture was heated (3 h) at reflux temperature. After filtration of the precipitated product, the product was washed with cold ethanol (20 ml) and dried overnight under vacuum to give a white solid of compound **2.4** (0.5 g, 2.3 mmol, 85%).

Molecular Formula $C_{11}H_8N_2O_3$; R_f (ethyl acetate/methanol, 9:1): 0.9, melting point: 264 – 268 °C.

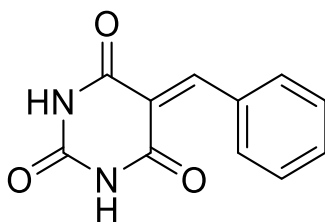


Figure 2. 13. Compound 2.4

1H NMR (400 MHz, DMSO- d_6) δ =11.40 (s, 1H, NH , D_2O exchangeable), 11.24 (s, 1H, NH , D_2O exchangeable), 8.28 (s, 1H, = CH), 8.09 – 8.07 (d, J = 7.4 Hz, 2H, ortho ArHs), 7.55 -7.52 (t, J = 7.2, 1H, para ArH), 7.49 -7.45 (t, J = 7.2, 2H, meta ArHs) ppm.

^{13}C APT NMR (101 MHz, DMSO- d_6) δ =163.8 ($C=O$), 162.0 ($C=O$), 155.1 ($C=CH$), 150.6 ($C=O$), 133.5 (ortho ArCs), 133.1 ($C=CH$), 132.6 (para ArC), 129.5 (meta ArCs), 119.5 ($C=CH-C$) ppm.

IR (ATR): ν = 1658 (s, C=C), 1731 (s, C=O), 2846 (m, CH aliphatic), 3052 (s, CH aromatic), 3208 (s, NH).

2.5.2.2. 5-[(E)-3-(4-methoxyphenyl)prop-2-enylidene]hexahydropyrimidine-2,4,6-trione (2.5)

One equivalent of p- methoxy cinnamaldehyde (0.64 g, 3.9 mmol) was dissolved in ethanol (60 ml), followed by the addition of one equivalent of barbituric acid (0.5g, 3.9 mmol). The reaction flask was sonicated (2 h) at room temperature. The product was collected and purified using flash column chromatography eluting with dichloromethane/ethyl acetate

(81:19). Evaporation of the solvent under vacuum gave the product **2.5** as an orange powder (0.9 g, 3.3 mmol, 85%).

Molecular Formula $C_{14}H_{12}N_2O_4$; R_f (ethyl acetate/methanol, 9:1): 0.85, melting point: >300 °C.

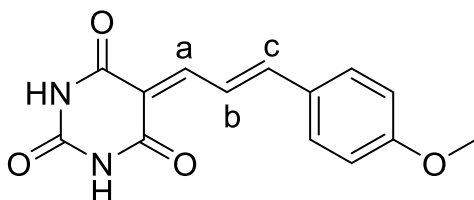


Figure 2. 14. Compound 2.5

1H NMR (400 MHz, DMSO- d_6): δ 11.20 (s, 1H, NH, D_2O exchangeable), 11.15 (s, 1H, NH, D_2O exchangeable), 8.34 – 8.27 (dd, $J = 28.3, 11.9$ Hz, 1H, H_b), 8.00 – 7.97 (d, $J = 11.9$ Hz, 1H, H_a), 7.68 – 7.63 (m, 3H, H_c, ortho ArHs), 7.06-7.04 (d, $J = 8.8$ Hz, 2H, meta ArHs), 3.82 (s, 3H, OCH₃) ppm.

^{13}C APT NMR (101 MHz, DMSO- d_6): δ 163.7 (C=O), 163.5 (C=O), 162.5 (C=O), 155.0 (C_b), 153.8 (C_a), 150.8 (O=C-C=CH), 131.2 (ortho ArCs), 128.5 (CH-C), 122.5 (C_c), 115.3 (meta ArCs), 114.4 (C-OCH₃), 55.9 (OCH₃) ppm.

IR (ATR): $\nu = 1660$ (s, C=C), 1730 (s, C=O), 2844 (m, CH aliphatic), 3066 (s, CH aromatic), 3185 (s, NH).

MS (+ESI) m/z = Found 272.0791 [M] $^+$; calculated for $C_{14}H_{12}N_2O_4$ 272.0792; -0.2 ppm.

MS (+ESI) m/z = Found 273.0867 [M+H] $^+$; calculated for $C_{14}H_{13}N_2O_4$ 273.0870; -1 ppm.

2.5.2.3. 5-[(4-Methoxyphenyl)methylene]hexahydropyrimidine-2,4,6-trione (**2.6**)

A suspension of barbituric acid (0.35 g, 2.7 mmol) in water (5 ml) was heated until dissolved, followed by the addition of anisaldehyde (0.37 g, 2.7 mmol) suspended in ethanol (30 ml). The reaction mixture was heated (5 h) at reflux temperature. After filtration of the precipitated product, the product was washed with cold ethanol (20 ml). The product was dried overnight under vacuum to give a phosphorus yellow solid of compound **2.6** (0.5 g, 2.0475%).

Molecular Formula $C_{12}H_{10}N_2O_4$; R_f (ethyl acetate/hexane, 2:3): 0.7, melting point: 286-289 °C.

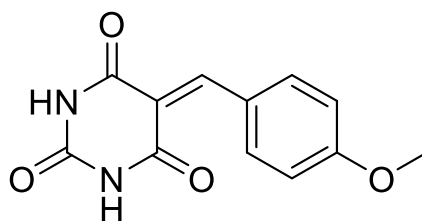


Figure 2. 15. Compound 2.6

1H NMR (400 MHz, DMSO- d_6): δ =11.31 (s, 1H, NH , D_2O exchangeable), 11.18 (s, 1H, NH , D_2O exchangeable), 8.42 – 8.33 (m, 2H, ortho ArHs), 8.26 (s, 1H, = CH), 7.12 – 7.03 (m, 2H, meta ArHs), 3.88 (s, 3H, OCH_3).

^{13}C APT NMR (101 MHz, DMSO- d_6): δ = 164.3 ($C=O$), 163.9 ($C=O$), 162.6 ($C=O$), 155.4 (ortho ArCs), 150.6 ($O=C-C=CH$), 137.9 (=CH), 125.6 (=CH-C), 116.0 ($C-OCH_3$), 114.4 (meta ArCs), 56.1 (OCH_3).

IR (ATR): ν = 1666 (s, C=C), 1723 (s, C=O), 2831 (w, CH aliphatic), 3063 (m, CH aromatic), 3196 (m, NH).

2.5.2.4. 5-[(E)-3-(4-Nitrophenyl)prop-2-enylidene]hexahydropyrimidine-2,4,6-trione (2.7)

A suspension of barbituric acid (0.35 g, 2.7 mmol) in water (5 ml) was heated until dissolved, followed by the addition of p-Nitrocinnamaldehyde (0.48 g, 2.7 mmol) suspended in ethanol (30 ml). The reaction mixture was heated (4 h) at reflux temperature. After filtration of the precipitated product, the product was washed with cold ethanol (20 ml). The product was dried overnight under vacuum to give a phosphorus yellow powder of compound **2.7** (0.705 g, 2.46 mmol, 90%).

Molecular Formula $C_{13}H_9N_3O_5$; R_f (ethyl acetate/hexane, 2:3): 0.75, melting point: >300 °C.

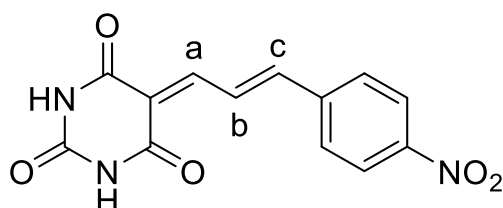


Figure 2. 16. Compound 2.7

^1H NMR (400 MHz, DMSO- d_6): δ = 11.35 (s, 1H, NH, D_2O exchangeable), 11.31 (s, 1H, NH, D_2O exchangeable), 8.55 – 8.48 (dd, J = 15.6, 11.7 Hz, 1H, H_b), 8.30 – 8.27 (d, J = 8.8 Hz, 2H, meta ArHs), 8.00 – 7.97 (d, J = 11.7 Hz, 1H, H_a), 7.89 – 7.87 (d, J = 8.8 Hz, 2H, ortho ArHs), 7.79 – 7.75 (d, J = 15.6 Hz, 1H, H_c) ppm.

^{13}C APT NMR (101 MHz, DMSO- d_6): δ = 163.3 (C=O), 163.2 (C=O), 162.3 (C b), 150.7 (C=O), 149.0 (meta ArCs), 148.4 6 (O=C-C=CH), 141.9 (C-NO₂), 129.8 (C a), 128.2 (ortho ArCs), 124.8 (C_c), 118.3 (CH=CH-C) ppm.

IR (ATR): ν = 1664 (s, C=C), 1743 (m, C=O), 2859 (m, CH aliphatic), 3026 (s, CH aromatic), 3178 (m, NH).

2.5.2.5. 5-(2-furylmethylene)hexahydropyrimidine-2,4,6-trione (2.8)

A suspension of barbituric acid (1 g, 7.8 mmol) in water (10 ml) was heated until dissolved, followed by the addition of furan (0.75 g, 7.8 mmol) suspended in ethanol (60 ml). The reaction mixture was heated (3 h) at reflux temperature. After filtration of the precipitated product, a hexane slurry was made and stirred at room temperature (10 minutes). The residue was collected, and the solid was dried overnight under a vacuum to give a yellow powder of compound **2.8** (1.26 g, 6.08 mmol, 78%).

Molecular Formula $\text{C}_9\text{H}_6\text{N}_2\text{O}_4$; R_f UV active spot (acetic acid/ethyl acetate/methanol, 1:8:1): 0.8, melting point: >300 °C.

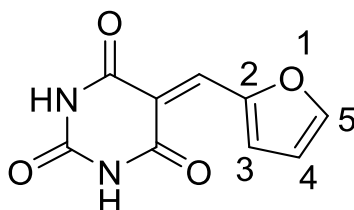


Figure 2. 17. Compound 2.8

^1H NMR (400 MHz, DMSO- d_6): δ = 11.36 (s, 1H, NH, D_2O exchangeable), 11.27 (s, 1H, NH, D_2O exchangeable), 8.48-8.47 (d, J = 3.7 Hz, 1H, H₅), 8.275-7.271 (d, J = 1.6 Hz, 1H, H₃), 8.03 (s, 1H, =CH), 6.93-6.91 (d, J = 2.8 Hz, 1H, H₄) ppm.

^{13}C APT NMR (101 MHz, DMSO- d_6): δ = 163.7 ($\underline{\text{C}}=\text{O}$), 162.5 ($\underline{\text{C}}=\text{O}$), 151.6 ($\underline{\text{C}}_5$), 150.6 ($\underline{\text{C}}_2$), 137.3 ($\underline{\text{C}}=\underline{\text{C}}\text{H}$), 126.9 ($\underline{\text{C}}_3$), 115.6 ($\underline{\text{C}}_4$), 113.3 ($\text{O}=\underline{\text{C}}-\underline{\text{C}}\text{H}$) ppm.

IR (ATR): ν = 1647 (s, C=C), 1741 (m, C=O), 2850 (s, CH aliphatic), 3035 (s, CH aromatic), 3147 (m, NH).

2.5.2.6. 5-[(E)-3-(2-Furyl)prop-2-enylidene]hexahydropyrimidine-2,4,6-trione (2.9)

Furacrolein (0.95 g, 7.77 mmol) was left to dissolve in (60 ml) of ethanol, followed by the addition of one equivalent of barbituric acid (1 g, 7.8 mmol). The reaction mixture was heated (2 h) at reflux temperature. The solvent was discarded by filtration, and a hexane slurry was made of the precipitated product and stirred at room temperature (5 minutes). The residue was collected, and the solid was dried overnight under vacuum to give a dark orange of compound **2.9** (1.3 g, 3.11 mmol, 72.2%).

Molecular Formula $\text{C}_{11}\text{H}_8\text{N}_2\text{O}_4$; R_f (ethyl acetate/methanol, 4:1): 0.9, melting point: 267-268 $^\circ\text{C}$.

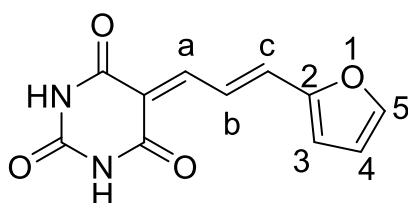


Figure 2. 18. Compound 2.9

^1H NMR (400 MHz, DMSO- d_6): δ = 11.21 (s, 1H, $\underline{\text{N}}\underline{\text{H}}$, D_2O exchangeable), 11.16 (s, 1H, $\underline{\text{N}}\underline{\text{H}}$, D_2O exchangeable), 8.23-8.16 (dd, J = 15.1, 12.3 Hz, 1H, $\underline{\text{H}}\underline{\text{b}}$), 8.00- 7.97 (m, 2H, $\underline{\text{H}}\underline{\text{5}}$ and $\underline{\text{H}}\underline{\text{c}}$), 7.56-7.52 (d, J = 15.1 Hz, 1H, $\underline{\text{H}}\underline{\text{a}}$), 7.03-7.02 (d, J = 3.4 Hz, 1H, $\underline{\text{H}}\underline{\text{3}}$), 6.73-6.71 (dd, J = 3.4, 1.7 Hz, 1H, $\underline{\text{H}}\underline{\text{4}}$) ppm.

^{13}C APT NMR (101 MHz, DMSO- d_6): 163.65 ($\underline{\text{C}}=\text{O}$), 163.56 ($\underline{\text{C}}=\text{O}$), 153.76 ($\underline{\text{C}}\underline{\text{b}}$), 152.23 ($\underline{\text{C}}=\text{O}$), 150.80 ($\underline{\text{C}}_2$), 148.05 ($\underline{\text{C}}_5$), 138.43 ($\underline{\text{C}}\underline{\text{c}}$), 122.46 ($\underline{\text{C}}\underline{\text{a}}$), 118.81 ($\underline{\text{C}}_3$), 116.32 ($\text{O}=\underline{\text{C}}-\underline{\text{C}}$), 114.19 ($\underline{\text{C}}_4$) ppm.

IR (ATR): ν = 1652 (m, C=C), 1685 (m, C=O), 2849 (s, CH aliphatic), 3196 (s, CH aromatic), 3327 (s, NH).

2.5.2.7. 5-[(5-Nitro-2-furyl)methylene]hexahydropyrimidine-2,4,6-trione (2.10)

One equivalent of 5-Nitrofuraldehyde (0.55 g, 3.89 mmol) was left to dissolve in (30 ml) ethanol, and one equivalent of barbituric acid (0.5g, 3.9 mmol). The reaction mixture was heated (4 h) at reflux temperature. The crude was recrystallised in 1,4 dioxane, the crystals were collected and dried overnight under vacuum to give a brown powder of compound **2.10** (0.59 g, 2.35 mmol, 60.5%).

Molecular Formula $C_9H_5N_3O_6$; R_f (ethyl acetate/hexane, 2:3): 0.65, melting point: > 300 °C.

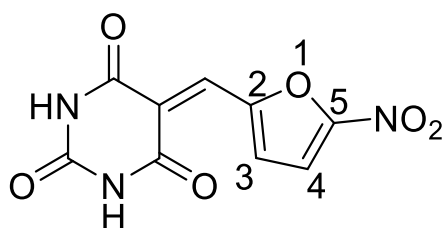


Figure 2. 19. Compound 2.10

1H NMR (400 MHz, DMSO- d_6): δ = 11.58 (s, 1H, NH , D_2O exchangeable), 11.51 (s, 1H, NH , D_2O exchangeable), 8.37-8.36 (d, J = 4.0 Hz, 1H, C 4), 7.85 (s, 1H, C= $\underline{C}H$), 7.83-7.82 (d, J = 4.0 Hz, 1H, C 3) ppm.

^{13}C APT NMR (101 MHz, DMSO- d_6): δ = 162.8 ($\underline{C}=\underline{O}$), 162.1 ($\underline{C}=\underline{O}$), 153.4 ($\underline{C}=\underline{O}$), 150.8 (\underline{C} 5), 150.4 (\underline{C} 2), 134.5 (\underline{C} 4), 125.9 ($=\underline{C}H$), 120.7 ($\underline{C}=\underline{C}H$), 114.7 (\underline{C} 3) ppm.

IR (ATR): ν = 1703 (s, C=C), 1743 (m, C=O), 2850 (m, CH aliphatic), 3081 (s, CH aromatic), 3192 (s, NH).

2.5.2.8. 5-[(2-Methoxy-1-naphthyl)methylene]hexahydropyrimidine-2,4,6-trione (2.11)

2-Methoxy-1-naphthalene (0.72 g, 3.89 mmol) was left to dissolve in (60 ml) ethanol, followed by the addition of one equivalent of barbituric acid (0.5g, 3.9 mmol). The reaction mixture was heated (1 h) at reflux temperature. A yellow powder of compound **2.11** (1 g, 3.38 mmol, 86.6%) was obtained after filtration, where the residue was washed with cold ethanol (20 ml), collected, and dried overnight under vacuum.

Molecular Formula $C_{16}H_{12}N_2O_4$; R_f (ethyl acetate/hexane, 2:3): 0.7, melting point: 238-240 °C.

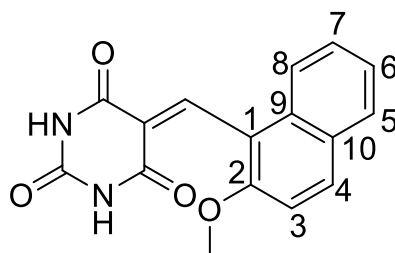


Figure 2. 20. Compound 2.11

^1H NMR (400 MHz, DMSO- d_6): δ = 11.44 (s, 1H, NH, D_2O exchangeable), 11.12 (s, 1H, NH, D_2O exchangeable), 8.53 (s, 1H, C=CH), 8.06-8.04 (d, J = 9.2 Hz, 1H, H 4), 7.91-7.89 (d, J = 7.7 Hz, 1H, H 8), 7.67-7.65 (d, J = 8.5 Hz, 1H, H 5), 7.50-7.48 (d, J = 9.1 Hz, 1H, H 3), 7.45 (m, 1H, H 6), 7.38 (m, 1H, H 7), 3.92 (s, 3H, OCH₃) ppm.

^{13}C APT NMR (101 MHz, DMSO- d_6): δ = 163.2 (C=O), 161.0 (C=O), 155.7 (C=O), 150.6 (C=CH), 149.7 (C=CH), 132.8 (C 4), 131.1 (C 8), 128.8 (C 9), 128.3 (C 10), 127.7 (C 5), 124.5 (C 3), 124.3 (C 7), 122.7 (C 1), 117.2 (C 2), 113.3 (C 6), 56.7 (OCH₃) ppm.

IR (ATR): ν = 16720 (s, C=C), 1743 (m, C=O), 2841 (m, CH aliphatic), 3054 (s, CH aromatic), 3186 (m, NH).

2.5.2.9. 5-[(E)-3-Phenylprop-2-enylidene]hexahydropyrimidine-2,4,6-trione (2.12)

Cinnamaldehyde (0.516 g, 3.9 mmol) was left to dissolve in ethanol (15 ml), followed by the addition of one equivalent of barbituric acid (0.5 g, 3.9 mmol). The reaction mixture was heated (5 h) at reflux temperature. The solvent was discarded by filtration, and a hexane slurry was made of the precipitated product and stirred at room temperature (15 minutes). The residue was collected, and the solid was dried overnight under vacuum to give yellow crystals of compound **2.12** (1.5 g, 5.86 mmol, 75%).

Molecular Formula $\text{C}_{13}\text{H}_{10}\text{N}_3\text{O}_3$; R_f (ethyl acetate/hexane, 2:3): 0.44, melting point: 255 – 258 °C.

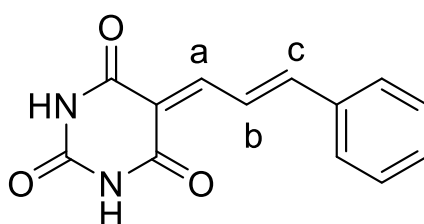


Figure 2. 21. Compound 2.12

^1H NMR (400 MHz, DMSO- d_6): δ =11.27 (s, 1H, NH, D_2O exchangeable), 11.21 (s, 1H, NH, D_2O exchangeable), 8.46 – 8.39 (dd, J = 15.2, 11.8 Hz, 1H, H_b), 8.02 – 7.99 (d, J = 11.8 Hz, 1H, H_a), 7.70 – 7.66 (m, 3H, H_c and ortho ArHs), 7.48-7.47 (m, J = 6.3 Hz, 3H, meta and para ArHs) ppm. ^{13}C APT NMR (101 MHz, DMSO- d_6): δ 163.6 (C=O), 163.4 (C=O), 154.2 (C b), 153.1 (C a), 150.8 (C=O), 135.7 (C=CH), 131.7 (C c), 129.7 (ortho ArCs), 129.0 (meta ArCs), 124.7 (para ArCs), 116.1 (CH-C) ppm.

IR (ATR): ν = 1663 (s, C=C), 1748 (m, C=O), 2850 (w, CH aliphatic), 3074 (s, CH aromatic), 3187 (s, NH).

2.5.2.10. 5-[(E)-3-(5-Nitro-2-furyl)prop-2-enylidene]hexahydropyrimidine-2,4,6-trione (2.13)

5-Nitrofuracrolein (1 g, 3.88 mmol) was left to dissolve in (15 ml) ethanol, followed by the addition of one equivalent of barbituric acid (0.5 g, 3.9 mmol). The reaction mixture was heated (4 h) at reflux temperature. The crude was collected by hot filtration, where the residue was recrystallised by 1,4 dioxane (80 ml). The crystals were collected and dried overnight under a vacuum to give a brown solid of compound **2.13** (1.04 g, 3.75 mmol, 96%).

Molecular Formula $\text{C}_{11}\text{H}_7\text{N}_3\text{O}_6$; R_f (ethyl acetate/hexane, 2:3): 0.2, melting point: > 300 °C.

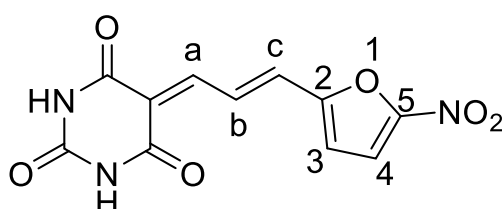


Figure 2. 22. Compound 2.13

^1H NMR (400 MHz, DMSO- d_6): δ = 11.34 (s, 1H, NH, D_2O exchangeable), 11.31 (s, 1H, NH, D_2O exchangeable), 8.45- 8.38 (dd, J = 15.4, 12.0 Hz, 1H, H_b), 7.99- 7.96 (d, J = 12.0 Hz, 1H, H_a), 7.79-7.78 (d, J = 3.9 Hz, 1H, H₄), 7.62- 7.58 (d, J = 15.4 Hz, 1H, H_c), 7.28-7.27 (d, J = 3.9 Hz, 1H, H₃) ppm.

^{13}C APT NMR (101 MHz, DMSO- d_6): δ = 163.2 (C=O), 163.2 (C=O), 153.8 (C 5), 152.8 (C 2), 151.0 (C b), 150.7 (C=O), 135.1 (C a), 128.0 (C=CH), 118.9 (C 4), 118.6 (C 3), 115.4 (C c) ppm.

IR (ATR): ν = 1575 (s, NO₂), 1667 (s, C=C), 1753 (m, C=O), 2822 (w, CH aliphatic), 3139 (m, CH aromatic), 3214 (s, NH).

MS (+ESI) m/z = Found 278.0407 [M+H]⁺; calculated for C₁₁H₈N₃O₆ 278.0413; -2.2 ppm.

2.5.2.11. 5-[[4-[(4-Nitrophenyl)methoxy]phenyl]methylene]hexahydropyrimidine-2,4,6-trione (2.14)

To a stirred solution of p-Nitro-4-benzyloxybenzaldehyde (1 g, 3.88 mmol) in ethanol (20 ml) ethanol, one equivalent of barbituric acid (0.5 g, 3.9 mmol) was then added. The reaction mixture was heated at reflux temperature (3 h), the solvent was discarded by filtration, and a hexane slurry of the precipitated product was stirred at room temperature (15 minutes). The residue was collected, and the solid was dried overnight under vacuum to give a yellow powder of compound **2.14** (1.15 g, 3.56 mmol, 91%). Molecular Formula C₁₈H₁₃N₃O₆; R_f (ethyl acetate/hexane, 2:3): 0.6; melting point: 298 – 301 °C.

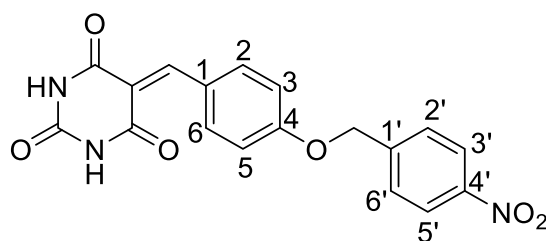


Figure 2. 23. Compound 2.14

¹H NMR (400 MHz, DMSO-d₆): δ = 11.31 (s, 1H, NH, D₂O exchangeable), 11.19 (s, 1H, NH, D₂O exchangeable), 8.37-8.34 (d, J = 9.0 Hz, 2H, H 3, H 5), 8.28-8.26 (d, J = 8.8 Hz, 2H, H 3', H 5'), 8.25 (s, 1H, C=CH), 7.75-7.73 (d, J = 8.8 Hz, 2H, H 2', H 6'), 7.16-7.14 (d, J = 9.0 Hz, 2H, H 2, H 6), 5.42 (s, 2H, O-CH₂) ppm.

¹³C APT NMR (101 MHz, DMSO-d₆): δ = 164.2 (C=O), 162.5 (C=O), 162.3 (C=O), 155.1 (C=CH), 150.6 (C-NO₂), 147.6 (C=CH), 144.7 (C 4), 137.7 (C 3, C 5), 128.8 (C 3', C 5'), 126.1 (C 1), 124.1 (C 2', C 6'), 116.4 (C 1'), 115.1 (C 2, C 6), 68.8 (CH₂) ppm.

IR (ATR): ν = 1525 (s, N-O), 1658 (m, C=C), 1731 (m, C=O), 2864 (m, CH aliphatic), 3041 (m, CH aromatic), 3192 (m, NH).

2.5.2.12. 5-[(4-Benzyloxyphenyl)methylene]hexahydropyrimidine-2,4,6-trione (2.15)

To a stirred solution of benzyloxybenzaldehyde (0.828 g, 3.9 mmol) in ethanol (20 ml), one equivalent of barbituric acid (0.5 g, 3.9 mmol) was added. The mixture was set at reflux temperature (4 h), the solvent was discarded by filtration, and a hexane slurry of the precipitated product was stirred at room temperature (15 minutes). The residue was collected, and the solid was dried overnight under vacuum to give a bright yellow powder of compound **2.15** (1.21 g, 3.75 mmol, 96.3%).

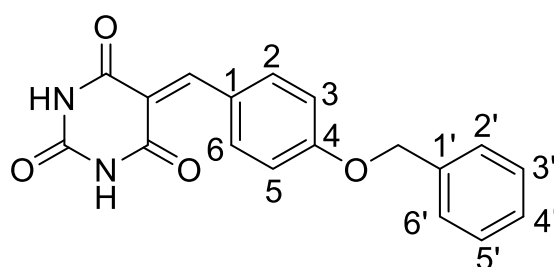


Figure 2. 24. Compound 2.15

Molecular Formula $C_{18}H_{14}N_2O_4$; R_f (ethyl acetate/hexane, 2:3): 0.75; melting point: 283 – 286 °C.

1H NMR (400 MHz, DMSO- d_6): δ = 11.31 (s, 1H, NH, D_2O exchangeable), 11.18 (s, 1H, NH, D_2O exchangeable), 8.37-8.35 (d, J = 9.0 Hz, 2H, H 3, H 5), 8.25 (s, 1H, C=CH), 7.48-7.47 (d, J = 6.8 Hz, 2H, H 2', H 6'), 7.43-7.35 (m, 3H, H 3', H 4', H 5'), 7.15-7.12 (d, J = 9.0 Hz, 2H, H 2, H 6), 5.24 (s, 2H, -OCH₂) ppm.

^{13}C APT NMR (101 MHz, DMSO- d_6): δ = 164.35 (C=O), 162.97 (C=O), 162.61 (C=O), 155.34 (C=CH), 150.66 (C=CH), 138.40 (C 3, C 5), 137.87 (C 4), 128.99 (C 2', C 6'), 128.56 (C 3', C 5'), 128.35 (C 4'), 125.80 (C 2, C 6), 116.13 (C 1'), 115.14 (C 1), 70.12 (OCH₂) ppm.

IR (ATR): ν = 1567 (m, cyclic alkene), 1656 (m, N-H), 1755 (m, C=O), 2858 (m, CH aliphatic), 3038 (m, CH aromatic), 3190 (m, NH).

MS (+ESI) m/z = Found 323.1029 $[M+H]^+$; calculated for $C_{18}H_{15}N_2O_4$ 323.1032; -0.9 ppm.

2.5.2.13. 5-[(5-Nitro-2-thienyl)methylene]hexahydropyrimidine-2,4,6-trione (2.16)

1st method:

5-Nitro-2-thiophenecarboxaldehyde (0.613 g, 3.9 mmol) was dissolved in ethanol (25 ml), followed by the addition of one equivalent of barbituric acid (0.5 g, 3.9 mmol). The mixture was set at reflux temperature (5 h), the solvent was discarded by filtration, and a hexane slurry of the precipitated product was stirred at room temperature (15 minutes). The residue was collected, and the solid was dried overnight under vacuum to give a yellow powder of compound **2.16** (0.9 g, 3.45 mmol, 86%).

2nd method:

5-Nitro-2-thiophenecarboxaldehyde (0.3 g, 1.9 mmol) was suspended in DCM (5 ml) and H₂O (5 ml), followed by the addition of one equivalent of barbituric acid (0.25 g, 1.9 mmol) and diethylamine (NH₂Et₂) (0.14 g, 1.9 mmol). The reaction was set at room temperature (72 h), and the solvent was removed under vacuum. The crude was purified by liquid-liquid extraction using brine and ethyl acetate. The compound was extracted from the aqueous phase (3 X 30 ml), and the compound was dried overnight under vacuum to give **2.16** (0.7, 2.68 mmol, 66.9%).

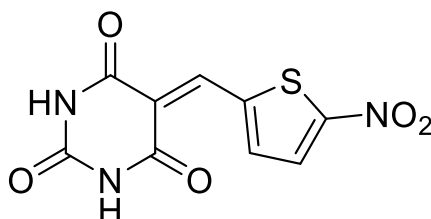


Figure 2. 25. Compound 2.16

Molecular Formula C₉H₆N₃O₅S; R_f (ethyl acetate/hexane, 2:3): 0.4; melting point: >300 °C.

¹H NMR (400 MHz, DMSO-d₆): δ= 11.58 (s, 1H, NH, D₂O exchangeable), 11.52 (s, 1H, NH, D₂O exchangeable), 8.51 (s, 1H, =CH), 8.21-8.18 (d, *J*= 8.2 Hz, 2H, ArHs). ¹³C APT NMR (101 MHz, DMSO-d₆): δ= 163.8 (C=O), 163.0 (C=O), 157.9 (C=O), 150.4 (C-NO₂), 144.4 (C=CH), 143.1 (CH=C-NO₂), 140.9 (C=CH), 128.9 (C=CH-CH=C-NO₂), 117.5 (C-S) ppm.

IR (ATR): ν = 1566 (m, cyclic alkene), 1670 (m, N-H), 1733 (m, C=O), 2900 (m, CH aliphatic), 3060 (s, CH aromatic), 3187 (s, NH) ppm.

MS (+ESI) *m/z* = Found 268.0021 [M+H]⁺; calculated for C₉H₆N₃O₅S 268.0028; -2.6 ppm.

2.5.2.14. 5-[(2-Benzyloxy-1-naphthyl)methylene]hexahydropyrimidine-2,4,6-trione (2.17)

2-Benzyloxy-1-naphthaldehyde (0.51 g, 1.95 mmol) was left to dissolve in (25 ml) ethanol, followed by the addition of one equivalent of barbituric acid (0.25 g, 1.95 mmol). The reaction mixture was set to reflux temperature (4 h), followed by hot filtration. The residue was collected, washed with petroleum ether (2 X 20 ml), and dried under vacuum overnight to give a phosphoric orange powder of compound **2.17** (0.59 g, 1.6 mmol, 82%).

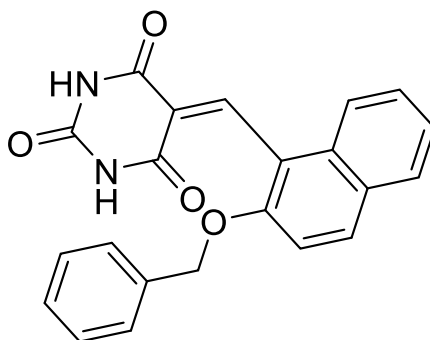


Figure 2. 26. Compound 2.17

Molecular Formula $C_{22}H_{16}N_2O_4$; R_f (dichloromethane/ ethyl acetate, 4:1): 0.45; melting point: 246-249 °C.

1H NMR (400 MHz, DMSO- d_6): δ = 11.41 (s, 1H, NH, D₂O exchangeable), 11.12 (s, 1H, NH, D₂O exchangeable), 8.58 (s, 1H, C=CH), 8.03-8.01 (d, J = 9.1 Hz, 1H, ArH), 7.91-7.89 (d, J = 7.4 Hz, 1H, ArH), 7.68-7.66 (d, J = 8.5 Hz, 1H, ArH), 7.56-7.53 (d, J = 9.1 Hz, 1H, ArH), 7.47-7.32 (m, 7H, ArHs), 2.04 (s, 2H, -CH₂) ppm.

^{13}C APT NMR (101 MHz, DMSO- d_6): δ = 163.13 (C=O), 161.24 (C=O), 154.54 (C=O), 150.73 (C=CH), 149.22 (C=CH), 137.32 (ArC), 132.30 (ArC), 131.40 (ArC), 128.89 (ArC), 128.79 (ArC), 128.61 (ArC), 128.35 (ArC), 127.89 (ArC), 127.60 (ArC), 124.79 (ArC), 124.43 (ArC), 123.37 (ArC), 118.38 (ArC), 114.97 (ArC), 70.95 (OCH₂) ppm.

IR (ATR): ν = 1590 (w, cyclic alkene), 1682 (m, C=O), 2849 (m, CH aliphatic), 3020 (s, CH aromatic), 3193 (s, NH).

MS (+ESI) m/z = Found 373.1182 268.0021 [$M+H$] $^+$; calculated for $C_{22}H_{17}N_2O_4$ 373.1188; -1.6 ppm.

2.5.2.15. 5-(2-Naphthylmethylene)hexahydropyrimidine-2,4,6-trione (2.18)

2-Naphthaldehyde (0.609 g, 3.9 mmol) was left to dissolve in (25 ml) ethanol, followed by the addition of one equivalent of barbituric acid (0.5 g, 3.9 mmol). The mixture was set to reflux temperature (6h), followed by hot filtration. The residue was collected, and the desired product was extracted into ethyl acetate (2 X 30 ml). The organic portions were combined, rinsed with a saturated aqueous solution of NaCl, dried with anhydrous MgSO₄, filtered and the filtrate was collected. The solvent was removed under vacuum and the residue was dried under vacuum to give a fluffy orange solid of compound **2.18** (0.9 g, 3.45 mmol, 72 %).

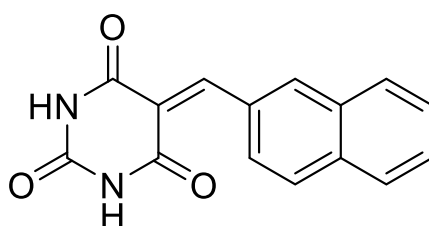


Figure 2. 27. Compound 2.18

Molecular Formula C₁₅H₁₀N₂O₃; R_f (ethyl acetate/ hexane, 2:3): 0.83; melting point: 295-297 °C.

¹H NMR (400 MHz, DMSO-d₆) δ 11.47 (s, 1H, NH, D₂O exchangeable), 11.18 (s, 1H, NH, D₂O exchangeable), 8.80 (s, 1H, C=CH), 8.05-8.00 (m, 2H, ArHs), 7.88-7.82 (m, 2H, ArHs), 7.60-7.54 (m, 3H, ArHs) ppm.

¹³C APT NMR (101 MHz, DMSO-d₆): δ= 163.41 (C=O), 161.44 (C=O), 152.79 (C=CH), 150.82 (C=O), 133.12 (C=CH), 131.48 (ArC), 131.10 (ArC), 129.15 (ArC), 128.78 (ArC), 127.53 (ArC), 126.74 (ArC), 125.37 (ArC), 124.76 (ArC), 122.40 (ArC) ppm.

IR (ATR): ν = 1566 (m, cyclic alkene), 1668 (s, N-H), 1703 (s, C=O), 2851 (s, CH aliphatic), 3046 (s, CH aromatic), 3188 (m, NH).

2.5.2.16. 5-(2-(Methoxymethoxy)benzylidene)pyrimidine-2,4,6(1H,3H,5H)-trione (2.19)

2-Ethoxybenzaldehyde (1.17 g, 7.8 mmol) was left to dissolve in (15 ml) ethanol, followed by the addition of one equivalent of barbituric acid (1 g, 7.8 mmol). The mixture was set to reflux temperature (4 h), the solvent was discarded by filtration, and a hexane slurry of the precipitated product was stirred at room temperature (10 minutes). to give a yellow powder of compound **2.19** (1.85 g, 6.7 mmol, 86%).

Molecular Formula $C_{13}H_{12}N_2O_5$; R_f (ethyl acetate/ hexane, 2:3): 0.89; melting point: 227-230 °C.

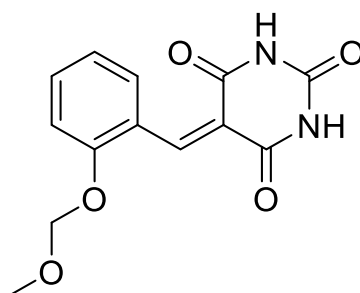


Figure 2. 28. Compound 2.19

1H NMR (400 MHz, DMSO) δ = 11.33 (s, 1H, NH, D_2O exchangeable), 11.15 (s, 1H, NH, D_2O exchangeable), 8.51 (s, 1H, CH), 7.99-7.97 (dd, J = 9.3, 1.4 Hz, 1H, ArH), 7.51-7.47 (m, 1H, ArH), 7.11-7.09 (d, J = 8.0 Hz, 1H, ArH), 6.98-6.94 (t, J = 7.7 Hz, 1H, ArH), 4.18-4.13 (q, J = 6.9 Hz, 2H, CH₂), 1.37-1.34 (t, J = 3.9, 3H, OCH₃) ppm.

^{13}C APT NMR (101 MHz, DMSO- d_6): δ = 163.88 (C=O), 161.95 (C=O), 158.81 (C=O), 150.73 (C=CH), 150.51 (C=CH), 134.52 (ArC), 133.02 (ArC), 122.14 (C-O), 119.84 (ArC), 119.08 (ArC), 112.29 (ArC), 64.50 (O-CH₂-O), 15.03 (O-CH₃) ppm.

IR (ATR): ν = 1565 (m, cyclic alkene), 1671 (s, N-H), 1723 (m, C=O), 2855 (w, CH aliphatic), 3075 (m, CH aromatic), 3194 (m, NH).

2.5.2.17. 5-(Thiophen-2-ylmethylene)pyrimidine-2,4,6(1H,3H,5H)-trione (2.20)

2-Thiophenecarboxaldehyde (0.437 g, 3.9 mmol) was dissolved in ethanol (25 mL), followed by the addition of one equivalent of barbituric acid (0.5 g, 3.9 mmol). The mixture was set at reflux temperature (4 h), followed by hot filtration. The residue was collected, washed with hexane, and dried overnight under vacuum to give a canary yellow powder of compound **2.20** (0.3 g, 1.35 mmol, 68%).

Molecular Formula $C_9H_6N_2O_3S$; R_f (ethyl acetate/hexane, 2:3): 0.3; melting point: > 300 °C.

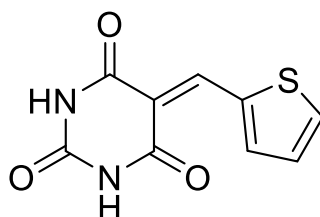


Figure 2. 29. Compound 2.20

^1H NMR (400 MHz, DMSO) δ = 11.30 (s, 1H, NH , D_2O exchangeable), 11.26 (s, 1H, NH , D_2O exchangeable), 8.57 (s, 1H, $=\text{CH}$), 8.29-8.27 (dt, J = 5.1, 1.2 Hz, 1H, ArHs), 8.19-8.17 (dd, J = 4.1, 0.9 Hz, 1H, ArHs), 7.37-7.34 (dd, J = 5.0, 3.8 Hz, 1H, ArHs) ppm.

^{13}C APT NMR (101 MHz, DMSO- d_6): δ = 163.98 (C=O), 163.49 (C=O), 150.70 (C=O), 146.30 ($=\text{CH}$), 146.16 (C 5), 142.57 ($\text{C}=\text{CH}$), 136.80 (C4), 128.84 (C 3), 112.05 (C 2) ppm.

IR (ATR): ν = 1544 (s, cyclic alkene), 1647 (s, N-H), 1689 (m, C=O), 2987 (m, CH aliphatic), 3085 (w, CH aromatic), 3139 (w, NH).

2.5.2.18. (E)-5-(3-(5-Nitrothiophen-2-yl)allylidene)pyrimidine-2,4,6(1H,3H,5H)-trione (2.21)

(5-Nitro-2-thienyl)-2-propenal (0.044 g, 0.24 mmol) was dissolved in ethanol (20 mL), followed by the addition of one equivalent of barbituric acid (0.03 g, 0.24 mmol). The mixture was set to reflux temperature (3 h), followed by hot filtration. The residue was collected and dried overnight under vacuum to give a canary yellow powder of compound **2.21** (0.051 g, 0.177 mmol, 75%).

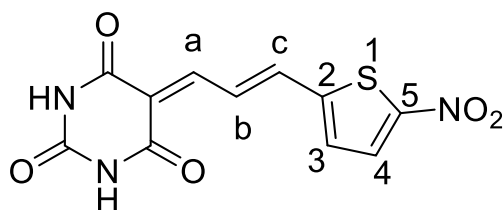


Figure 2. 30. Compound 2.21

Molecular Formula $\text{C}_{11}\text{H}_7\text{N}_3\text{O}_5\text{S}$; R_f (ethyl acetate/hexane, 2:3): 0.3; melting point: > 300 °C.

^1H NMR (400 MHz, DMSO) δ = 11.35 (s, 1H, NH , D_2O exchangeable), 11.31 (s, 1H, NH , D_2O exchangeable), 8.40-8.34 (dd, J = 15.3, 11.7 Hz, 1H, H_b), 8.15-8.14 (d, J = 4.3 Hz, 1H, H_4), 7.94-7.91 (d, J = 11.7 Hz, 1H, H_c), 7.89-7.85 (d, J = 15.3 Hz, 1H, H_a), 7.57-7.55 (d, J = 4.3 Hz, 1H, H_3) ppm.

^{13}C APT NMR (101 MHz, DMSO- d_6): δ = 163.28 ($\text{C}=\text{O}$), 163.23 ($\text{C}=\text{O}$), 152.19 ($\text{C}=\text{O}$), 151.10 (C \underline{b}), 150.71 ($\text{C}=\text{CH}$), 147.52 (C $\underline{5}$), 141.91 (C $\underline{4}$), 131.47 (C \underline{c}), 131.44 (C \underline{a}), 128.34 (C $\underline{3}$), 118.62 (C $\underline{2}$) ppm.

IR (ATR): ν = 1569 (s, cyclic alkene), 1667 (s, N-H), 1732 (m, C=O), 2821 (w, CH aliphatic), 3088 (s, CH aromatic), 3204 (s, NH).

MS (+ESI) m/z = Found 294.0179 $[M+H]^+$; calculated for $C_{11}H_8N_3O_5S$ 294.0185; -2.0 ppm.

2.5.2.19. Attempts to synthesise 5-(4-Nitrobenzylidene)pyrimidine-2,4,6(1H,3H,5H)-trione (2.22)

First attempt:

P- Nitrobenzaldehyde (0.585 g, 3.9 mmol) was dissolved in methanol (15 mL), followed by the addition of one equivalent of water-dissolved (15 ml) barbituric acid (0.5 g, 3.9 mmol). The mixture was set to reflux for 72 hours; followed by hot hot filtration . The crude was collected and purification attempts using column chromatography were made. None of the collected fractions showed the desired product.

Second attempt:

P- Nitrobenzaldehyde (0.3 g, 1.95 mmol) and barbituric acid (0.25 g, 1.95 mmol) were added to a round-bottomed flask, followed by the addition of piperidine (2 drops), ethanol (25 ml). The reaction was set to reflux for 8 hours, the crude was collected after vaporising the solvent. Purification attempts using flash column chromatography were made but with no success.

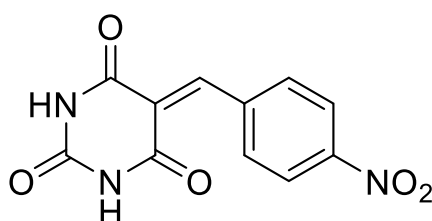


Figure 2. 31. Compound 2.22

2.5.2.20. Attempts to synthesise (E)-5-(2-Methyl-3-phenylallylidene)pyrimidine-2,4,6(1H,3H,5H)-trione (2.23)

α -Methyl-*trans*-cinnamaldehyde (0.57 g, 3.9 mmol) was dissolved in methanol (15 mL), followed by the addition of one equivalent barbituric acid (0.5 g, 3.9 mmol). The mixture was set to reflux for 24 hours; followed by hot filtration . The crude was collected and purification attempts using column chromatography were made. None of the collected fractions showed the desired product.

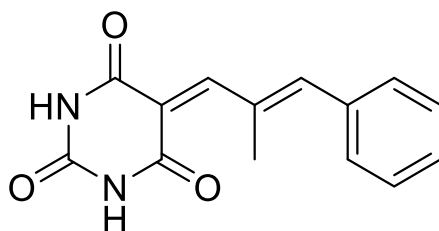


Figure 2. 32. Compound 2.23

2.5.2.21. Attempts to synthesise 5-((5-Iodofuran-2-yl)methylene)pyrimidine-2,4,6(1H,3H,5H)-trione (2.24)

5-Iodo-2-furaldehyde (0.3 g, 1.35 mmol) was dissolved in methanol (15 mL), followed by the addition of one equivalent barbituric acid (0.173 g, 1.35 mmol). The mixture was set to reflux for 36 hours; however, the TLC plates showed no considerable changes under UV light or after impeding the plate in KMNO_4 dye.

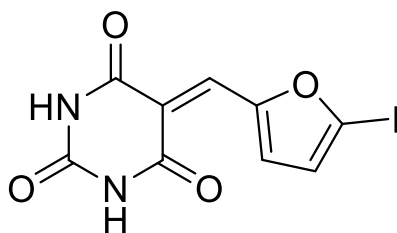


Figure 2. 33. Compound 2.24

2.5.2.22. Attempts to synthesise 5-(1-(2-Amino-5-chlorophenyl)-2-oxo-2-phenylethyl)-5-hydroxypyrimidine-2,4,6(1H,3H,5H)-trione (2.25)

2-Amino-5-chlorobenzophenone (0.452 g, 1.95 mmol) was suspended in dichloromethane (DCM) (5 ml) and H_2O (5 mL), followed by the addition of one equivalent barbituric acid (0.173 g, 1.35 mmol) and 1 equivalent of NH_4Et_2 (0.14 g, 1.95 mmol). The mixture was set at room temperature for 78 hours however, the TLC plates showed no considerable changes under UV light or after impeding the plate in KMNO_4 dye.

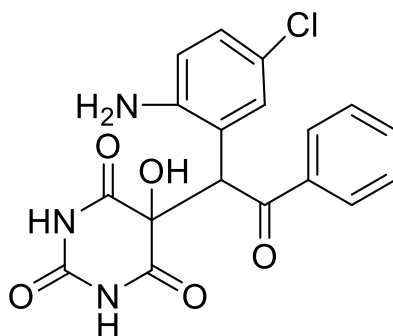


Figure 2. 34. Compound 2.25

2.5.2.23. Attempts to synthesise 5-((2E,4E)-5-(5-Nitrothiophen-2-yl)penta-2,4-dien-1-ylidene)pyrimidine-2,4,6(1H,3H,5H)-trione (2.26)

Compound 2.3 (0.5 g, 2.4 mmol) was left to dissolve in ethanol (30 ml), followed by the addition of one equivalent of barbituric acid (0.3 g, 2.4 mmol). The reaction flask was set and heated at reflux for 24 hours. The reaction was monitored by TLC which showed no considerable changes.

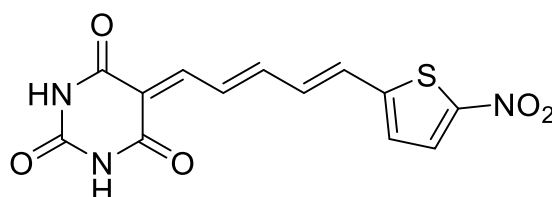


Figure 2. 35. Compound 2.26

2.5.3. Discussion of the results from benzylidene barbiturate derivative synthesis and characterisation

Barbituric acid possesses acidic properties with a pKa value of 4.01 in water. Barbituric acid dissolves partially in water and methanol in accordance with its acidic properties. The active methylene group of barbituric acid (-CH₂ attached to two electron-withdrawing groups) can react with various types of carbonyl compounds including aldehydes and ketones, to form alkenes through Knoevenagel condensation. Studies investigated the production of a single compound when aromatic aldehydes react with barbituric acid in the presence of an acidic or basic catalyst (Jursic, 2001). Uncatalysed Knoevenagel condensation reaction was reported in aqueous or protic solvents (Ferreira *et al.*, 2018). In this study, uncatalysed Knoevenagel condensation at room temperature in a sonicator bath was successful giving

good yields. However, the conventional reflux method was preferred in the absence of a noise-reducing/cancelling cabinet, as the noise correlated with the sonicator bath was not lab-user-friendly.

The benzylidene barbiturate derivatives were characterised by ^1H NMR and ^{13}C NMR. TLC was used as a preliminary tool to detect the formation of the newly formed products and the extent of their purity. ^1H NMR showed that the acidic protons (two protons singlet) of the active methylene group at the C5 of the barbituric acid disappeared when reacted with aldehydes. In ^{13}C NMR, the binding of the barbituric acid moiety with the aldehydes was directly reflected in the total number of peaks appearing in the spectra. In the C13APT spectra where CH_3 , CH appear in the opposite direction to the DMSO-d6 septet and CH_2 , C peaks appear in the same direction as the DMSO-d6 septet, the increase in the total number of peaks aligning with the DMSO peaks in the product compared to the two separate starting materials indicated successful Knoevenagel condensation where the CH_2 in barbituric acid and the formyl $-\text{CHO}$ group of the aldehyde condensed to form a quaternary carbon at C5. In these Knoevenagel products, the keto-form predominated. The tautomeric enol-form was not observed in any arylidene barbiturate derivatives synthesised in this thesis work.

Removal of impurities/residual starting materials from the Knoevenagel products was reported to be successful by simple washing of the solid product with cold methanol. Aldehyde impurities were reported to be removable by crystallisation using solvents such as ethyl acetate or petroleum ether. However, this method cannot separate any unreacted barbituric acid from the reaction mixture (Jursic, 2001). Attempts to purify Knoevenagel products using cold ethanol or methanol were unsuccessful in most cases. This contradicts sentence 1. Barbituric acid impurities were successfully removed upon solubilisation in hot ethanol. Crystallisation attempts using ethyl acetate were not successful. However, non-polar solvents such as hexane or petroleum ether were very effective in most cases in removing any residual aldehyde impurities. Repetition 1,4-Dioxane was used successfully to recrystallise compounds **2.10** and **2.13**. After purification, 1,4-dioxane solvent was judged by NMR to be bound to the product matrix but could be successfully removed under high vacuum by placing it on a rotatory evaporator for 10 minutes. However, uncatalysed Knoevenagel condensation to prepare compounds **2.22-2.26** failed. A study reported the

synthesis of 5-(4-nitrobenzylidene)pyrimidine-2,4,6(1H,3H,5H)-trione (compound **2.22**) using uncatalysed Knoevenagel condensation conditions in ethanol, where the residue was washed with cold ethanol and no further purification was required to give a product yield of 99% (Yang *et al.*, 2022). Several attempts were made in this study to synthesise the same compounds in catalyst-free conditions; however, none of the attempts was successful. The reactions progress was monitored using TLC for 72 hours; they showed mostly starting materials. The accompanying minor spots were judged to be impurities by NMR after separation and isolation by flash column chromatography.

In a study conducted by Barakat *et al.* (2015), a mechanism was reported for Michael addition reaction of N, N-dimethyl barbituric acid with ketone. Diethylamine was used as a base to remove the active methylene group of dimethyl barbituric acid, to give the enolate form. Followed by nucleophilic addition of the enolate form to give the double bond of enone by Michael addition reaction. Unexpected product was obtained when the reaction was carried in in the presence of H₂O (**Figure 2.36.**) (Barakat *et al.*, 2015).

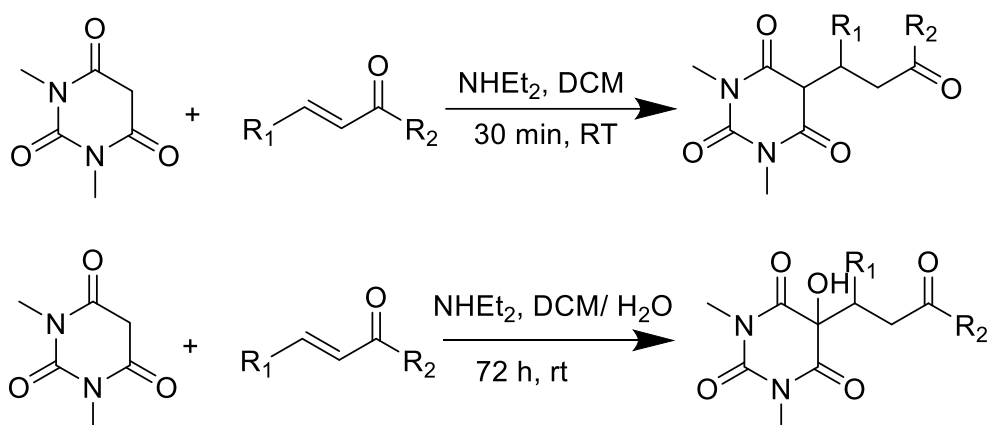
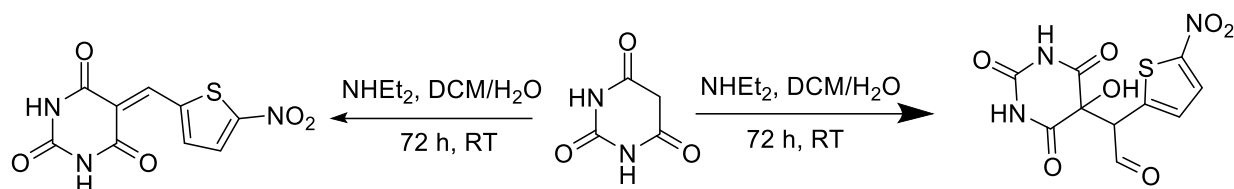


Figure 2. 36. The scheme reported by Barakat *et al.* (2015)

The same procedure was followed in aqueous conditions to synthesise compound **2.25**, where the N,N-dimethyl barbituric acid was replaced with barbituric acid. However, the TLC analysis of the reaction mixture did not show any significant change from the starting materials. In the second attempt to prepare compound **2.16**, barbituric acid was set to react with the arylaldehyde using the same procedure reported by Barakat *et al.* (2015) where the use of aqueous conditions was hoped to create the characteristic hydroxyl group at C5 in the corresponding product (**Scheme 2.2**). However, the isolated product was found to be identical to that obtained by the Knoevenagel condensation reaction conditions. The

identity of the synthesised compound was confirmed by ^1H NMR and was compared with the compound obtained by the Knoevenagel condensation reaction (**Figure 2.37.**). No sign of a deshielded proton representing the hydroxyl group or the two doublets representing the $\text{CH}-\text{CH}=\text{O}$ or $\text{CH}-\text{CH}=\text{O}$ were observed.



Scheme 2. 2. The 2nd synthetic route of compound 2.16, the right-hand product was the expected compound as reported by Barakat *et al.* (2015), and the left-hand product was the obtained compound characterised by ^1H NMR.

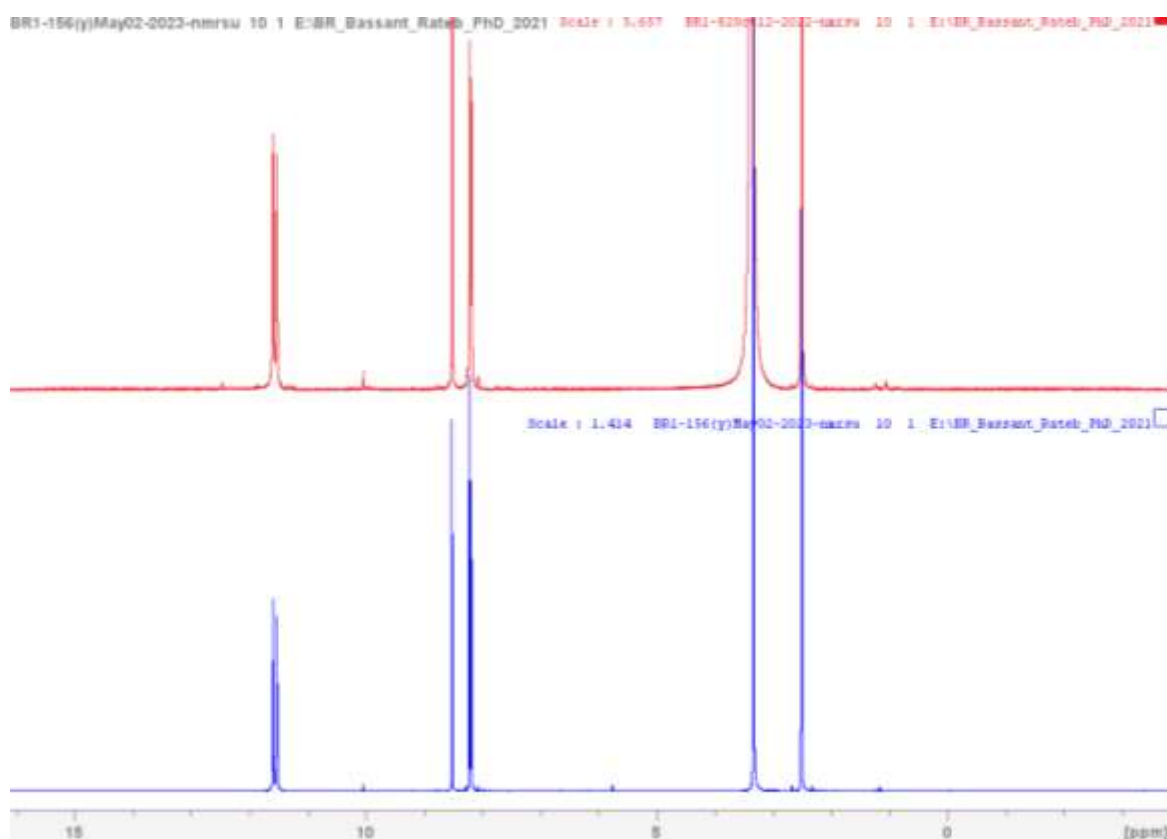


Figure 2. 37. ^1H NMR spectra of Michael addition product (bottom) and Knoevenagel condensation product (top)

The conventional uncatalysed Knoevenagel condensation method failed in the attempted synthesis of compound **2.23**. The reaction was monitored using TLC for 24 hours however, most starting material was present with a new spot. The compound corresponding to the new spot was isolated by flash column chromatography but proved not to be the desired product according to NMR analysis. A study reported the synthesis of compound **2.23** in different conditions, where the starting materials were irradiated in a microwave oven for 1 minute, and the crude was purified by simple filtration by washing with water and ether to give a 96% yield of the desired product (Reddy & Nagaraj, 2007).

In an attempt to synthesise a compound possessing a halogen at C5 heterocyclic five-membered ring as in compound **2.24**, uncatalysed Knoevenagel failed. Only starting material was present when investigated with ¹H NMR. A study was conducted by Prousek (1993) where it was claimed that the same compound **2.24** was obtained in 60% yield.

Table 2. 2. Comparison of the literature melting points in °C of compounds with products isolated in this thesis work using the reported methods

Compound	Reported mp	References	Found mp
2.4	256	Khurana & Vij, 2010	264-268
2.5	268	Reddy & Nagaraj, 2007	>300
2.6	279	Li <i>et al.</i> , 2006	286-289
2.7	266-268	Wang <i>et al.</i> , 2015	>300
2.8	280	Jursic, 2001	>300
2.9	260-261	Reddy & Nagaraj, 2007	267-268
2.10	>300	Wang <i>et al.</i> , 2015	>300
2.12	228	Khurana & Vij, 2010	255-257
2.19	260-262	Vieira <i>et al.</i> , 2011	227-230
2.20	330-333	Owen, 1950	>300

Some of the synthesised compounds were reported in the literature. The obtained melting points were compared with those reported in articles, some inconsistencies were observed

(Table 3.2.). These deviations may be correlated to impurities, residual solvents in the samples, or the different methods or equipment employed to determine the melting point.

2.5.4. Knoevenagel condensation between barbituric acid and aldehydes

2.5.4.1. 5-((5-Nitrothiophen-2-yl)methylene)-2-thioxodihydropyrimidine-4,6(1H,5H)-dione (2.27)

5-Nitro-2-thiophenecarboxaldehyde (0.55 g, 3.49 mmol) was dissolved in ethanol (15 mL), followed by the addition of one equivalent of 2-thiobarbituric acid (0.55 g, 3.46 mmol). The mixture was set to reflux temperature (4 h); followed by hot filtration and washing with cold ethanol. The residue was collected and dried overnight under vacuum to give a brown powder of compound **2.27** (0.051 g, 0.177 mmol, 75%).

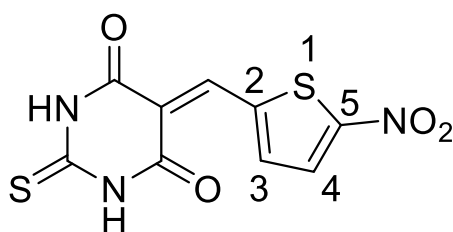


Figure 2. 38. Compound 2.27

Molecular Formula $C_9H_5N_3O_4S_2$; R_f (ethyl acetate/hexane, 4:1): 0.85; melting point: > 300.

1H NMR (400 MHz, DMSO- d_6): δ = 12.65 (s, 1H, NH, D_2O exchangeable), 12.60 (s, 1H, NH, D_2O exchangeable), 8.52 (s, 1H, =CH), 8.23-8.21 (m, 2H, ArHs) ppm. ^{13}C APT NMR (101 MHz, DMSO- d_6): δ =178.94 (C=S), 161.69 (C=O), 161.27 (C=O), 158.29 (C=CH), 145.06 (C=CH), 143.51 (C4), 141.05 (C5), 129.08 (C3), 117.56 (C2) ppm.

IR (ATR): ν = 1562 (s, cyclic alkene), 1651 (s, N-H), 1705 (m, C=O), 2978 (w, CH aliphatic), 3108 (s, CH aromatic), 3201 (s, NH).

MS (+ESI) m/z = Found 283.9792 [$M+H$] $^+$; calculated for $C_9H_6N_3O_4S_2$ 283.9800; -2.8 ppm.

2.5.4.2. 1,3-Dimethyl-5-[(E)-3-(5-nitro-2-furyl)prop-2-enylidene]hexahydropyrimidine-2,4,6-trione (2.28)

5-Nitro-2-furanacrolein (0.26 g, 1.55 mmol) was left to dissolve in (15 ml) ethanol, followed by the addition of one equivalent of 1,3-Dimethylbarbituric acid (0.25 g, 1.6 mmol). The

mixture was heated to reflux temperature for (2h), followed by hot filtration . The residue was washed with hexane (3x20 ml), collected, and left to dry under vacuum to give fluffy dark orange powder of compound **2.28** (0.4 g, 1.42 mmol, 88%).

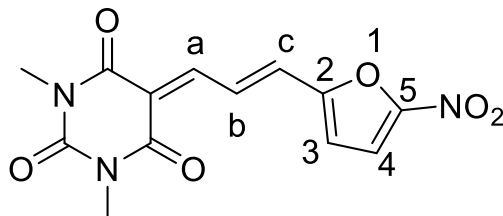


Figure 2. 39. Compound 2.28

Molecular Formula $C_{13}H_{11}N_3O_6$; R_f (ethyl acetate/ hexane, 2:3): 0.4; melting point: 256-259.

1H NMR (400 MHz, DMSO- d_6) δ = 8.49-8.43 (dd, J = 15.4, 12.7 Hz, 1H, H_b), 8.08-8.05 (d, J = 12.7 Hz, 1H, H_a), 7.80-7.79 (d, J = 3.9 Hz, 1H, H₄), 7.68-7.64 (d, J = 15.4 Hz, 1H, H_c), 7.31-7.30 (d, J = 3.9 Hz, 1H, H₃), 3.218 (s, 3H, CH₃), 3.215 (s, 3H, CH₃) ppm.

^{13}C APT NMR (101 MHz, DMSO- d_6): δ = 162.05 (C=O), 161.82 (C=O), 153.80 (C=CH), 151.85 (C_b), 151.55 (c₅), 135.57 (C_a), 128.16 (C₄), 118.75 (C_c), 118.54 (C₂), 115.41 (C₃), 28.82 (N-CH₃), 28.30 (N-CH₃) ppm.

IR (ATR): ν = 1581 (m, cyclic alkene), 1651 (s, N-H), 1727 (m, C=O), 2810 (w, CH aliphatic), 3066 (m, CH aromatic), 3117 (w, NH).

MS (+ESI) m/z = Found 306.0720 [$M+H$] $^+$; calculated for $C_{13}H_{12}N_3O_6$ 306.0726; -2.0 ppm.

2.5.4.3. (E)-1,3-Dimethyl-5-(3-(4-nitrophenyl)allylidene)pyrimidine-2,4,6-trione (2.29)

1,3-Dimethyl-5-[(E)-3-(4-nitrophenyl)prop-2-enylidene]hexahydropyrimidine-2,4,6-trione

To a stirred solution of *p*-Nitrocinnamaldehyde (1.135 g, 6.4 mmol) in ethanol (20 ml), one equivalent of 1,3-Dimethylbarbituric acid (1 g, 6.4 mmol) was then added. The mixture was heated at reflux temperature for (7 h), followed by hot filtration . The crude mixture was purified by flash column chromatography using dichloromethane/ethyl acetate (81:19). The desired compound was collected, and the solvent was evaporated under pressure to give a bright yellow powder of compound **2.29** (0.9 g, 2.86 mmol, 45%).

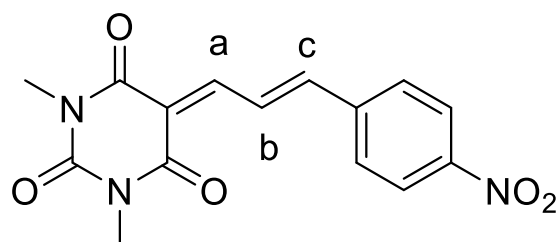


Figure 2. 40. Compound 2.29

Molecular Formula $C_{15}H_{13}N_3O_5$; R_f (Dichloromethane/ ethyl acetate, 4:1): 0.85; melting point: 296-299.

1H NMR (400 MHz, DMSO) δ = 8.63-8.56 (dd, J = 15.4, 11.7 Hz, 1H, H_b), 8.33-8.30 (d, J = 8.6 Hz, 2H, meta ArHs), 8.11-8.08 (d, J = 11.6 Hz, 1H, H_a), 7.95-7.93 (d, J = 8.3 Hz, 2H, ortho ArHs), 7.89-7.85 (d, J = 15.6 Hz, 1H, H_c), 3.22 (s, 6H, -CH₃ X 2) ppm.

IR (ATR): ν = 1590 (m, cyclic alkene), 1661 (s, N-H), 1710 (w, C=O), 2968 (w, CH aliphatic), 3080 (w, CH aromatic), 3110 (w, NH).

The reported melting point was >235 (Gorovoy *et al.*, 2014).

2.5.4.5. 5-((5-Nitrothiophen-2-yl)methylene)-1,3-diphenyl-2-thioxodihydropyrimidine-4,6(1H,5H)-dione (2.30) (157)

To a stirred solution of 5-Nitro-2-thiophenecarboxaldehyde (0.265 g, 1.68 mmol) in ethanol (20 ml), one equivalent of 1,3-Diphenyl-2-thiobarbituric acid (0.5 g, 1.68 mmol) was then added. The mixture was heated at reflux temperature (9 h), followed by hot filtration. The crude mixture was purified by flash column chromatography using hexane/ethyl acetate (28:22). The desired compound was collected, and the solvent was evaporated under pressure to give a brown powder of compound **2.30** (0.5 g, 1.15 mmol, 68%).

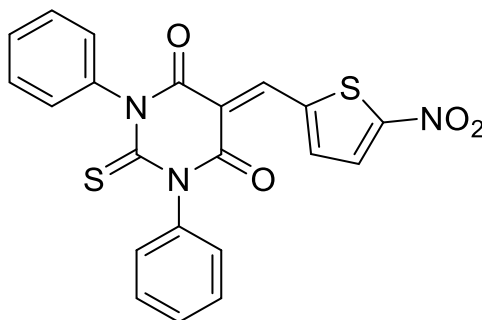


Figure 2. 41. Compound 2.30

Molecular Formula $C_{21}H_{13}N_3O_4S_2$; R_f (Hexane/ ethyl acetate, 3:2): 0.43.

1H NMR (400 MHz, DMSO) δ = 8.72 (s, 1H, C=CH), 8.30-8.29 (d, J = 4.7 Hz, 1H, CH-C-NO₂), 8.25-8.24 (d, J = 4.7 Hz, 1H, S-C=CH), 7.53-7.31 (m, 10 Hs, ArHs) ppm. ^{13}C APT NMR (101 MHz, DMSO-d₆): δ = 181.17 (C=S), 161.18 (C=O), 160.90 (C=O), 158.55 (C-NO₂), 146.73 (C=CH), 144.03 (CH-C-NO₂), 140.71 (N-C), 140.58 (N-C), 139.87 (C=CH), 129.59 (S-C=CH), 129.52 (ArC), 129.35 (ArC), 129.21 (ArC), 129.16(ArC), 128.87 (ArC), 128.75 (ArC), 118.09 (C-S) ppm.

2.5.5. Discussion of benzylidene barbiturate derivatives by Knoevenagel condensation

Barbituric acid derivatives were set in a reaction with aldehydes which exhibited the highest antimicrobial activity against *C. difficile* (Chapter 3) to produce Knoevenagel condensation reaction products. Modifying some functional groups would provide a comparative analysis and a better understanding of the SAR.

The reaction was set in ethanol at reflux temperature to give a good yield. Compound **2.27** was purified by washing it with cold ethanol. The aldehyde impurities of compound **2.28** were insoluble in ethanol but soluble in hexane because of their non-polar characteristics. As for compounds **2.29** and **2.30** purification using column chromatography was essential.

The electrophilic changes that the aromatic substitution caused to N, N-dimethylbenzylidene barbiturates, thiobenzylidene barbiturates, and 1,3-diphenyl-2-thiobenzylidene barbiturates compared to benzylidene barbiturates were observed through their 1H NMR chemical shifts. The C=S at position C2 of thiobenzylidene barbiturates (**2.27**) caused the corresponding protons of the two NHs to be further deshielded compared to **2.16** despite oxygen being more electron withdrawing than sulfur. The spectrum of N, N-dimethylbenzylidene barbiturates (**2.28**) was characterised by the presence of a 6 protons singlet representing the dimethyl protons in the aliphatic region. While the N-phenols of **2.30** were observed as 10 protons multiplets in the aromatic region. This electrophilic shift was also observed in ^{13}C NMR spectra, where the C=S of **2.27** was more deshielded compared to the C=O groups of **2.16**. The aliphatic dimethyl groups of **2.27** were observed as two peaks in the aliphatic region opposing the DMSO peaks confirming that the carbons are attached to an odd number of protons.

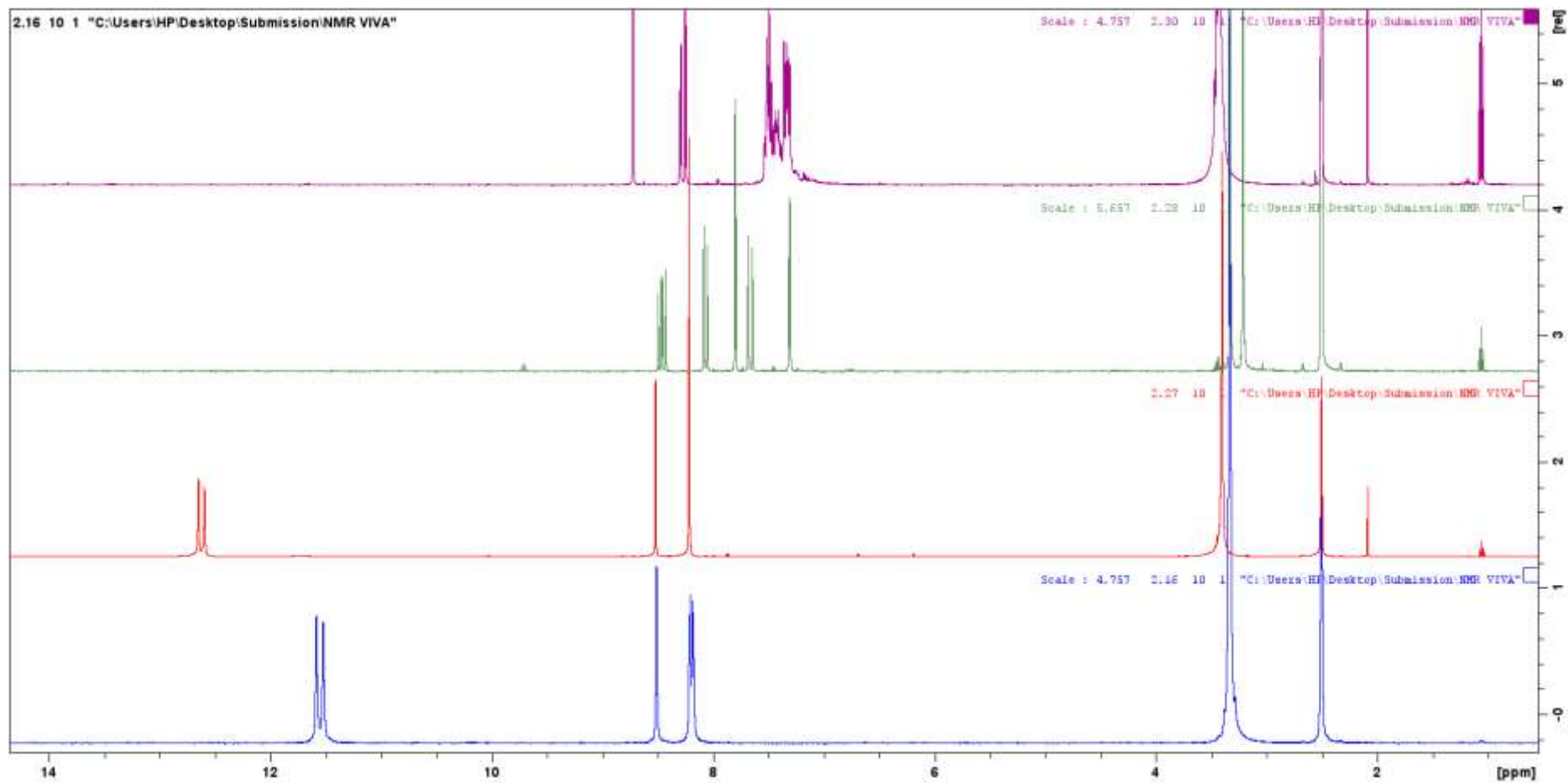


Figure 2. 42. Significant differences between the ¹H NMR spectra of 2.16 (blue), 2.27 (red), 2.28 (olive) and 2.30 (green)

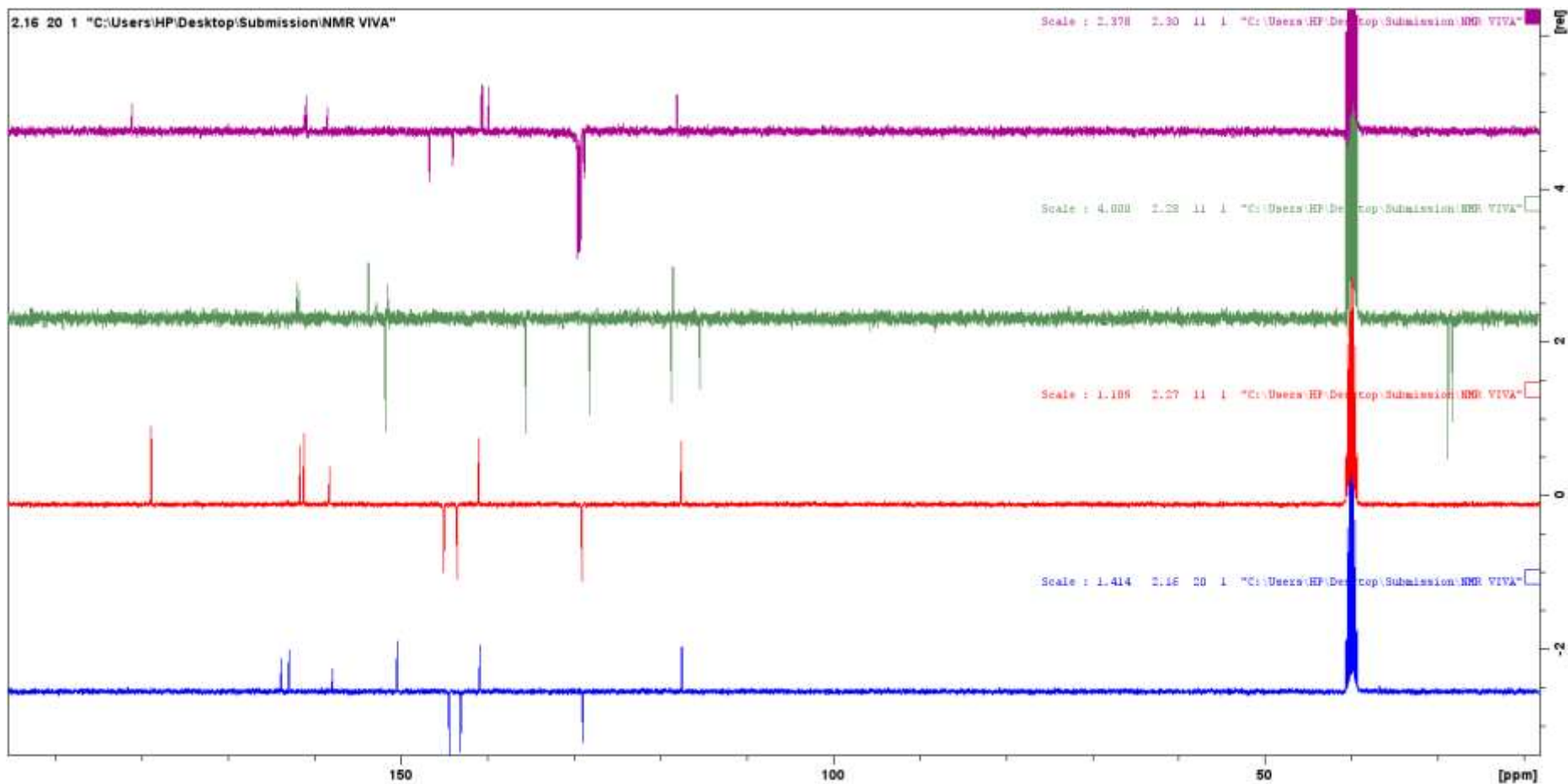


Figure 2. 43. Significant differences between the ^{13}C NMR spectra of 2.16 (blue), 2.27 (red), 2.28 (olive) and 2.30 (green)

2.5.6. The mechanism of the catalysed Knoevenagel condensation reaction

The catalysed version of this reaction involves the utilisation of weak bases, such as amines and basic salts, for their catalytic properties (Ferreira *et al.*, 2018). The carbanion is formed upon the deprotonation of the active methylene group promoted by the added base; followed by an electrophilic attack on the carbanion intermediate to the carbonyl group of the arylaldehyde. The base-catalysed Knoevenagel condensation cause a considerable level of toxicity (Dandia *et al.*, 2016). Studies aimed to develop catalysts possessing reduced toxic impact on the environment, easier separation from the reaction mixture, retrieval and reuse, and high stability under vacuum and temperature (Ferreira *et al.*, 2018). The Heterogeneous catalysts showed the highest success among the other alternatives (Srivastava *et al.*, 2017).

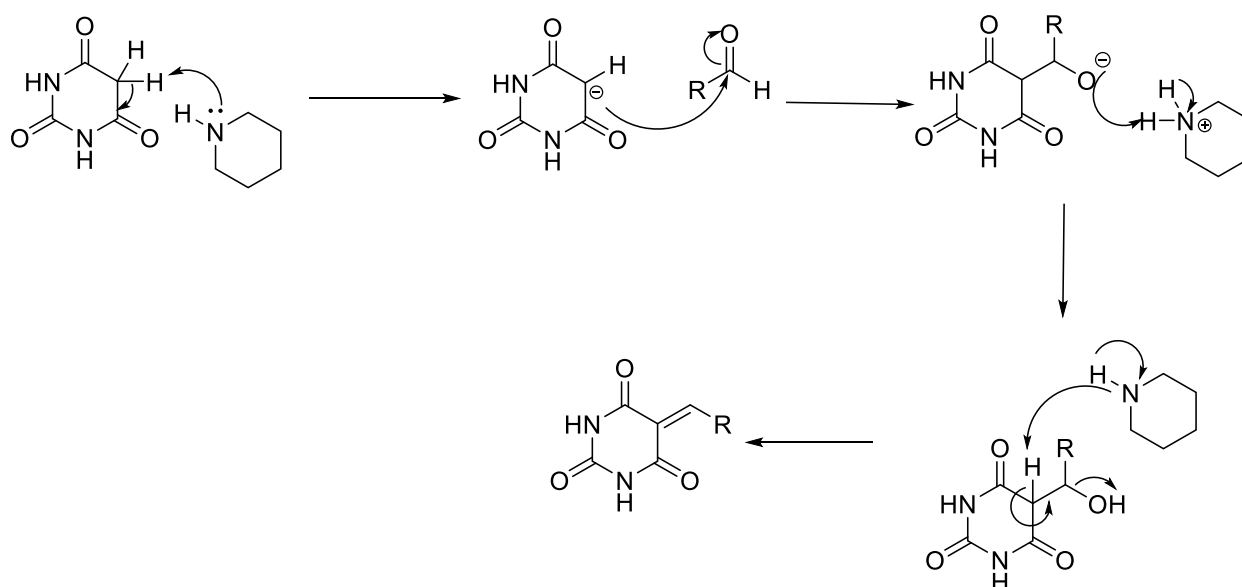


Figure 2. 44. Catalytic Knoevenagel condensation mechanism with organic base “piperidine” as an added catalyst.

2.5.7. The mechanism of the uncatalysed Knoevenagel condensation reaction

Various studies reported eco-friendly procedures, abiding by the criteria of green chemistry including Knoevenagel condensation (Dandia *et al.*, 2016). A simple, solvents catalysed, and catalyst-free reaction between barbituric acid and α,β -conjugated aromatic aldehydes in the presence of a green-solvent, water, or a protic solvent such as ethanol or methanol. The

reaction flask is left to reflux for several hours to a few days at room temperature, where the reaction is traced by thin-layer chromatography (TLC) (Sachar *et al.*, 2009).

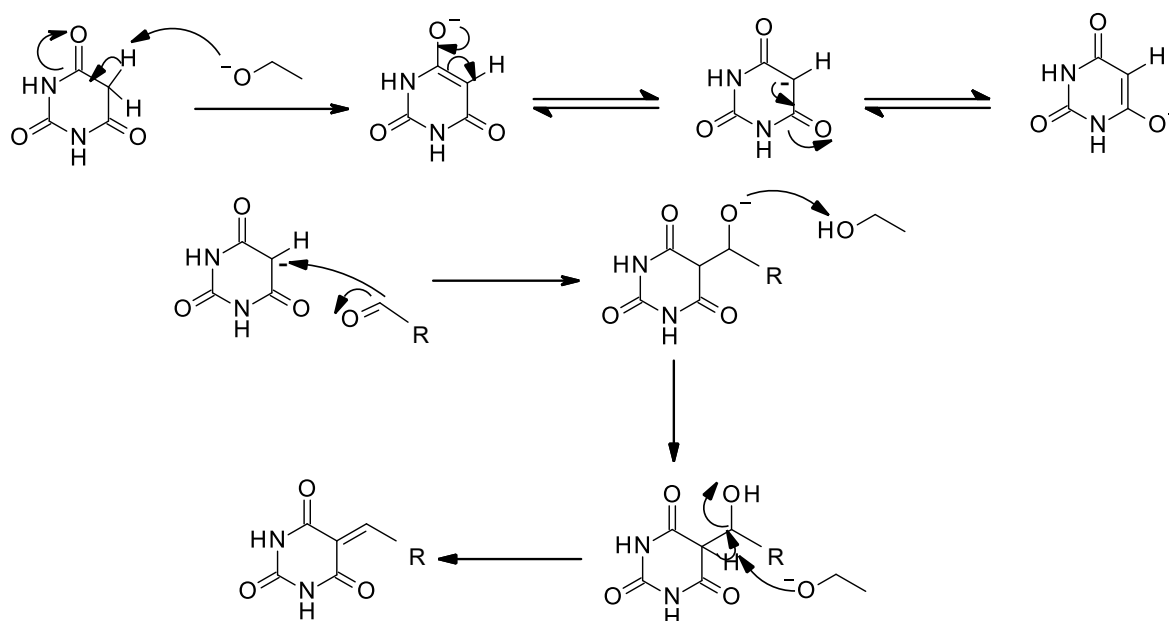


Figure 2. 45. The predicted Knoevenagel condensation mechanism with no added catalyst

Benzylidene barbiturates possess a polarized exocyclic $\text{C}=\text{C}$, polarisation is endorsed by its conjugation with the two neighbouring carbonyl groups and with the aromatic ring. The electronic properties and the position of the aromatic ring substitution alter the polarisation state; $\text{C}=\text{C}$ polarization relies on the charge differences of the involved atoms. The $\text{C}=\text{C}$ located between $\text{C}5$ and $\text{C}7$ and in conjugation with the two $\text{C}=\text{O}$ groups are the main reactive sites of benzylidene barbiturate derivatives (Figueroa-Villar & Vieira, 2013).

2.5.8. Synthesis of exocyclic $\text{C}=\text{C}$ reduced of benzylidene barbiturate derivatives

2.5.8.1. 5-Benzylhexahydropyrimidine-2,4,6-trione and its tautomeric form 5-Benzyl-6-hydroxydihydropyrimidine-2,4(1H,3H)-dione (2.31)

Five equivalents of NaBH_4 (0.308 g, 8.15 mmol) were added portion-wise to the ethanol suspension (30 ml) of **2.4** (0.35 g, 1.63 mmol). The reaction mixture was initially left in an ice bath (0°C) for 5 minutes and then stirred overnight at room temperature. The PH of the mixture was adjusted to 4-5 4M aqueous HCl , the desired compound appeared as a

suspended particle; the aqueous phase was collected and filtered where the residue was further washed by water. Compound **2.31** was dried overnight to give a white powder (0.2 g, 0.92 mmol, 57%).

Molecular Formula $C_{11}H_{10}N_2O_3$; R_f (acetic acid/ methanol/ water, 1:4:5): 0.5; melting point: 203-206 °C.

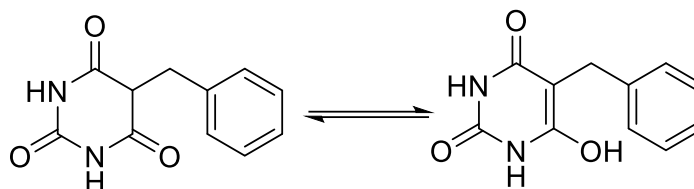


Figure 2. 46. Compound 2.31

1H NMR (400 MHz, DMSO- d_6): δ 11.18 (s, 2H, $NH \times 2$, D_2O exchangeable), 7.27 – 7.08 (m, 5H, ArHs), 3.91 (broad s, 1H, $\underline{C}H-CH_2$), 3.26 (broad s, 2H, $CH-\underline{C}H_2$), ppm.

^{13}C APT NMR (101 MHz, DMSO- d_6): δ = 170.42 ($\underline{C}=O$), 151.01 ($\underline{C}=O$), 137.86 ($CH_2-\underline{C}$), 129.33 (ortho ArCs), 128.77 (meta ArCs), 127.17 (para ArCs), 49.77 ($\underline{C}H-CH_2$), 33.76 ($CH-\underline{C}H_2$) ppm.

IR (ATR): ν = 1563 (s, cyclic alkene), 1668 (m, N-H), 1743 (m, C=O), 2871 (m, CH aliphatic), 3011 (m, CH aromatic), 3234 (m, NH).

2.5.8.2. 5-(4-Methoxybenzyl)pyrimidine-2,4,6(1H,3H,5H)-trione and its tautomeric form 6-Hydroxy-5-(4-methoxybenzyl)pyrimidine-2,4(1H,3H)-dione (2.32)

Three equivalents of $NaBH_4$ (0.08 g, 2.1 mmol) were added portion-wise to the ethanol suspension (30 ml) of **2.6** (0.26 g, 0.69 mmol). The reaction mixture was initially left in an ice bath (0 °C) for 5 minutes and then stirred overnight at room temperature. The PH of the mixture was adjusted to 4-5 4M aqueous HCl, the compound was then extracted from the aqueous phase water (3 x 30 ml). The desired compound appeared as a suspended particle; the aqueous phase was collected and filtered where the residue was further washed by water. Compound **2.32** was dried overnight to give a white powder (0.17 g, 0.69 mmol, 65%).

Molecular Formula $C_{12}H_{12}N_2O_3$; R_f (dichloromethane/ ethyl acetate 1:1): 0.2; melting point: >300 °C.

2nd attempt:

One equivalent benzaldehyde (0.3 g, 2.86 mmol) and 2-aminothiophenol (0.36 g, 2.87 mmol) were added to a water suspension of **2.6** (0.7 g, 2.86 mmol). The reaction was left to reflux for 4 hours, the crude was collected and purified by extraction from the aqueous phase (3 x H₂O). The compound was concentrated by solvent evaporation under vacuum and left to dry overnight under vacuum h to give a white powder of compound **2.32** (0.5 g, 2 mmol, 71%). Some polar impurities were detected in the ¹H NMR and TLC.

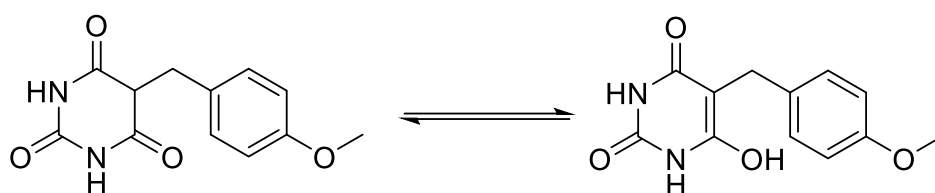


Figure 2. 47. Compound 2.32

¹H NMR (400 MHz, DMSO-d₆): δ = 11.17 (s, 2H, NH X2, D₂O exchangeable), 7.00-6.98 (d, J = 8.7 Hz, 2H, ortho ArHs), 6.82-6.80 (d, J = 8.7 Hz, 2H, meta ArHs), 6.55 (s, 1H, tautomeric OH), 3.82 (broad s, 1H, CH-CH₂), 3.70 (broad s, 3H, OCH₃), 3.20 (broad s, 2H, CH-CH₂) ppm.

¹³C APT NMR (101 MHz, DMSO-d₆): δ = 170.51 (C=O), 158.50 (C=O), 151.01 (CH₂-C), 130.48 (ortho ArCs), 129.38 (CH₂-C), 114.14 (meta ArCs), 55.40 (OCH₃), 50.02 (CH-CH₂), 33.29 (CH-CH₂) ppm.

IR (ATR): ν = 1510 (s, cyclic alkene), 1633 (s, N-H), 1679 (s, C=O), 2917 (m, CH aliphatic), 3005 (m, CH aromatic), 3121 (w, NH).

2.5.8.3. 5-[(2-Methoxy-1-naphthyl)methyl]hexahydropyrimidine-2,4,6-trione and its tautomeric form 6-Hydroxy-5-((2-methoxy-1-naphthyl)methyl)pyrimidine-2,4(1H,3H)-dione (2.33)

Three equivalents of NaBH₄ (0.153 g, 4 mmol) were added portion-wise to the ethanol suspension (30 ml) of **2.11** (0.4 g, 0.69 mmol). The reaction mixture was initially left in an ice bath (0 °C) for 5 minutes and then stirred overnight at room temperature. The PH of the mixture was adjusted to 4-5 4M aqueous HCl; the compound was then extracted from the aqueous phase water (3 x 30 ml), collected, and filtered. Compound **2.33** was dried overnight to give white crystals (0.3 g, 1 mmol, 75%).

Molecular Formula $C_{16}H_{14}N_2O_4$; R_f (butanol/acetic acid/water, 4:1:5): 0.7; melting point: 179-182 °C.

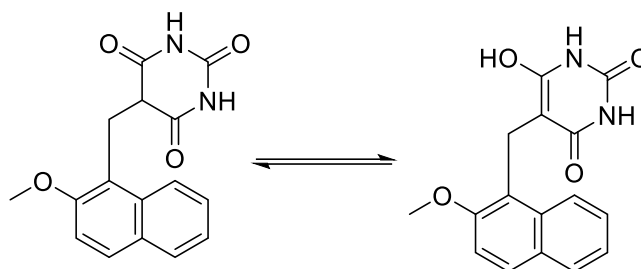


Figure 2. 48. Compound 2.33

1H NMR (400 MHz, DMSO- d_6): δ = 11.09 (s, 2H, NH X2, D_2O exchangeable), 7.99 – 7.97 (d, J = 8.5 Hz, 1H, ArH), 7.87 – 7.85 (d, J = 8.8 Hz, 2H, ArHs), 7.53 – 7.49 (t, J = 16.6 Hz, 1H, ArH), 7.41 – 7.39 (d, J = 9.0 Hz, 1H, ArHs), 7.37 – 7.34 (t, J = 15.6 Hz, 1H, ArH), 3.83 (s, 3H, OCH_3), 3.62 – 3.55 (m, 3H, $CH-CH_2$, $CH-CH_2$) ppm.

^{13}C APT NMR (101 MHz, DMSO- d_6): δ = 170.61 ($C=O$), 155.46 ($C=O$), 151.72 (ArC), 133.08 (ArC), 129.19 (ArC), 129.09 (ArC), 128.96 (ArC), 127.00 (ArC), 123.56 (ArC), 123.12 (ArC), 117.99 (ArC), 113.78 (ArC), 56.50 (OCH_3), 49.08 ($CH-CH_2$), 26.85 ($CH-CH_2$) ppm.

1H NMR (400 MHz, pyridine- d_5): δ = 13.37 (s, 2H, NH X2), 8.40 (broad s, 1H, ArH), 7.88 – 7.85 (broad d, J = 8.773 Hz, 2H, ArHs), 7.50 – 7.46 (t, J = 15.173 Hz, 1H, ArH), 7.36 – 7.33 (t, J = 15.6 Hz, 2H, ArHs), 4.18 (broad s, 3H, $CH-CH_2$, $CH-CH_2$), 3.80 (s, 3H, OCH_3).

IR (ATR): ν = 1623 (m, N-H), 1685 (s, C=O), 2841 (m, CH aliphatic), 3070 (m, CH aromatic), 3206 (m, NH).

2.5.8.4. 5-[(E)-3-(4-Methoxyphenyl)allyl]hexahydropyrimidine-2,4,6-trione (2.34)

Three equivalents of $NaBH_4$ (1.2 g, 8.98 mmol) were added portion-wise to ethanol (25 ml) suspended Knoevenagel product **2.5** (0.52 g, 1.38 mmol). The reaction mixture was initially left in an ice bath (0 °C) for 15 minutes and then stirred overnight at room temperature. The pH of the mixture was adjusted to 4-5 with 4M aqueous HCl. The desired compound was found as suspended particles in the aqueous phase; the residue was collected after filtration under low pressure and further washed with water and methanol. Yellow powder of compound **2.34** (0.2004 g, 3.58 mmol, 25%) was obtained.

Molecular Formula $C_9H_7N_3O_5S$; R_f (butanol/acetic acid/water, 4:1:5): 0.7; melting point: 190-193 °C.

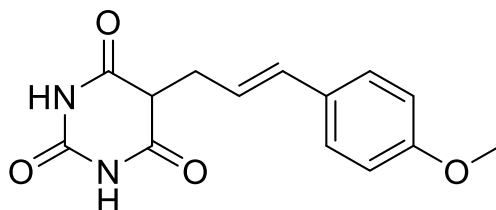


Figure 2. 49. Compound 2.34

1H NMR (400 MHz, DMSO) δ = 11.22 (s, 2H, NH, D_2O exchangeable), 7.28-7.26 (d, J = 8.7 Hz, 2H, ortho ArHs), 6.87-6.85 (d, J =8.7 Hz, 2H, meta ArHs), 6.39-6.35 (d, J = 15.8 Hz, 1H, $CH_2-CH=CH$), 5.99-5.92 (dt, J = 15.8, 8.4 Hz, 1H, $CH_2-CH-CH$), 3.73 (s, 3H, OCH_3), 3.72-3.70 (t, J = 5.0 Hz, 1H, $CH-CH_2$), 2.81-2.78 (t, J = 5.8 Hz, 2H, $CH-CH_2$) ppm.

^{13}C NMR (101 MHz, DMSO- d_6): δ = 170.40 ($C=O$), 159.20 ($C=O$), 151.30 ($CH-C$), 132.68 (ortho ArCs), 129.73 ($C-OCH_3$), 127.72 (meta ArCs), 122.79 ($CH_2-CH-CH$), 114.48 ($CH_2-CH-CH$), 55.55 (OCH_3), 48.73 ($CH-CH_2$), 31.77 ($CH-CH_2$) ppm.

IR (ATR): ν = 1512 (m, cyclic alkene), 1605 (w, N-H), 1711 (m, C=O), 2988 (w, CH aliphatic), 3050 (m, CH aromatic), 3209 (s, NH).

2.5.8.5. 5-[(5-Nitro-2-furyl)methyl]hexahydropyrimidine-2,4,6-trione and its tautomeric form 6-hydroxy-5-((5-nitrofuran-2-yl)methyl)dihydropyrimidine-2,4(1H,3H)-dione (2.35)

Five equivalents of $NaBH_4$ (0.308 g, 8.15 mmol) were added portion-wise to ethanol (30 ml) suspended Knoevenagel product **2.10** (0.2 g, 1.63 mmol). The reaction mixture was initially left in an ice bath (0 °C) for 15 minutes and then stirred overnight at room temperature. The PH of the mixture was adjusted to 4-5 with 4M aqueous HCl. The desired compound was extracted from the aqueous phase; the solvent was evaporated under vacuum and dried overnight to give a brown powder of **2.35** (0.1 g, 3.58 mmol, 50 %). The compound was tested without further purification.

Molecular Formula $C_9H_7N_3O_6$; R_f (butanol/acetic acid/water, 4:1:5): 0.6, 0.3; melting point: >300 °C.

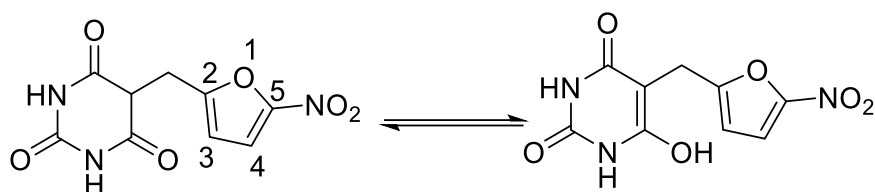


Figure 2. 50. Compound 2.35

^1H NMR (400 MHz, DMSO) δ = 9.24 (s, 2H, NH_2 , D_2O exchangeable), 7.54-7.53 (d, J = 3.7 Hz, 1H, H 4), 6.27-6.26 (d, J =3.7 Hz, 1H, H 3), 3.49 (broad s, 3 H, $\text{CH}-\text{CH}_2$, $\text{CH}-\text{CH}_2$) ppm.

^{13}C NMR (101 MHz, DMSO- d_6): δ = 165.12 ($\text{C}=\text{O}$), 164.81 ($\text{C}=\text{O}$), 152.64 (C 5), 115.70 (C 4), 109.97 (C 3), 79.43 (C 2), 25.30 ($\text{CH}-\text{CH}_2$), 23.29 ($\text{CH}-\text{CH}_2$) ppm.

IR (ATR): ν = 1568 (s, cyclic alkene), 1682 (m, N-H), 1704 (m, C=O), 2987 (s, CH aliphatic), 3193 (m, NH).

Vernallis *et al.*, reported this compound in a patent submitted in 2010.

2.5.8.6. 5-[(E)-3-(5-Nitro-2-furyl)allyl]hexahydropyrimidine-2,4,6-trione and its tautomeric form 6-Hydroxy-5-5-[(E)-3-(5-nitro-2-furyl)allyl]dihydropyrimidine-2,4(1H,3H)-dione (2.36)

Three equivalents of NaBH_4 (0.409 g, 10.8 mmol) were added portion-wise to ethanol (20 ml) suspended Knoevenagel product **2.13** (1 g, 3.6 mmol). The reaction mixture was initially left in an ice bath (0 °C) for 15 minutes and then stirred overnight at room temperature. The PH of the mixture was adjusted to 4-5 with 4M aqueous HCl. The desired compound was extracted from the aqueous phase; the solvent was evaporated under vacuum, washed with acetone, and dried overnight to give a brown powder of **2.36** (0.8 g, 2.86 mmol, 78%). No further purification was made.

Molecular Formula $\text{C}_{11}\text{H}_8\text{N}_3\text{O}_7$; R_f (butanol/acetic acid/water, 4:1:5): 0.5, 0.4; melting point: >300 °C.

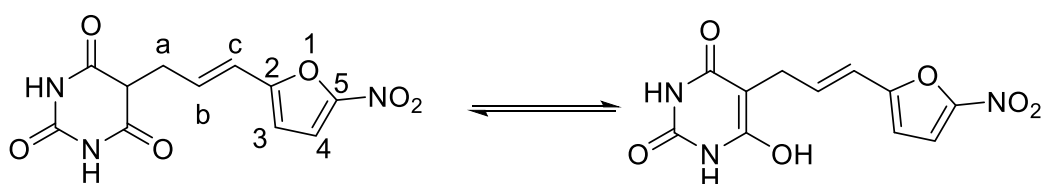


Figure 2. 51. Compound 2.36

^1H NMR (400 MHz, DMSO- d_6): δ = 9.01 (s, 2H, NH_2 , D_2O exchangeable), 7.67-7.66 (d, J = 3.5 Hz, 1H, H 4), 6.729- 6.720 (d, J = 3.5 Hz, 1H, H 3), 6.59-6.52 (dt, J = 15.8, 6.2 Hz, 1H, H b),

6.24-6.20 (d, $J= 15.8$ Hz, 1H, H c), 3.47-3.43 (broad t, $J= 6.8$ Hz, 1H, $\underline{\text{CH}}\text{-CH}_2$), 3.00-2.99 (d, $J= 5.6$ Hz, 2H, CH-CH_2) ppm.

δ ^{13}C NMR (101 MHz, DMSO- d_6): $\delta= 164.64$ ($\underline{\text{C}}=\text{O}$), 157.83 ($\underline{\text{C}}=\text{O}$), 152.59 (C 5), 141.27 (C 4), 116.35 (C 3), 115.06 (C b), 109.78 (C c), 80.97 (C 2), 56.48 (tautomeric form), 27.28 (CH-CH_2), 19.01 ($\underline{\text{CH}}\text{-CH}_2$) ppm.

IR (ATR): $\nu = 1568$ (s, cyclic alkene), 1682 (m, N-H), 1704 (m, C=O), 2987 (s, CH aliphatic), 3193 (m, NH).

Vernallis *et al.*, reported this compound in a patent submitted in 2010.

2.5.8.7. 5-[(E)-3-(2-Furyl)allyl]-6-hydroxy-1H-pyrimidine-2,4-dione (2.37)

Three equivalents of NaBH_4 (0.44 g, 11.6 mmol) were added portion-wise to ethanol (20 ml) suspended Knoevenagel product **2.9** (0.9 g, 3.9 mmol). The reaction mixture was initially left in an ice bath (0 °C) for 15 minutes and then stirred overnight at room temperature. The pH of the mixture was adjusted to 4-5 with 4M aqueous HCl. The desired compound was extracted from the aqueous phase; the solvent was evaporated under vacuum, washed with acetone, and dried overnight to give a brown powder of **2.37** (0.5 g, 2.13 mmol, 55%). The compound required further purification, yet no further purification was made.

Molecular Formula $\text{C}_{11}\text{H}_{10}\text{N}_2\text{O}_4$; R_f (butanol/acetic acid/water, 4:1:5): 0.4 and 0.1; melting point: >300 °C.

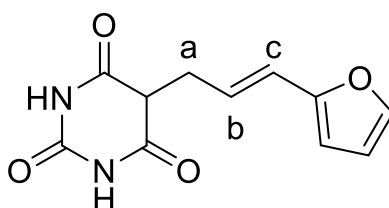


Figure 2. 52. Compound 2.37

^1H NMR (400 MHz, DMSO- d_6): $\delta= 8.94$ (s, 2H, $\underline{\text{NH}}$ X2, D_2O exchangeable), 7.48 – 7.47 (d, $J= 1.6$ Hz, 1H, H c), 6.39 – 6.38 (dd, $J=3.2, 1.8$ Hz, 1H, H b), 6.18 – 6.17 (m, 2H, ArHs), 3.3 (underneath H_2O peak, $\underline{\text{CH}}\text{-CH}_2$) 2.90-2.88 (d, $J= 4.6$, 2H, CH-CH_2), 1.60 (s, 3H, impurities) ppm.

^{13}C NMR (101 MHz, DMSO- d_6): $\delta= 164.64$ (C=O), 154.04 (C=O), 152.60 (impurities), 141.66 (C a), 131.97 (C b), 116.48 (ArC), 111.68 (ArC), 105.57 (ArC), 82.18 (ArC), 26.71 (CH-CH_2), 25.77 ($\underline{\text{CH}}\text{-CH}_2$) ppm.

IR (ATR): ν = 1581 (m, cyclic alkene), 1781 (m, C=O), 2948 (w, CH aliphatic), 3340 (m, NH).

2.5.8.8. 5-[[4-[(4-Nitrophenyl)methoxy]phenyl]methyl]hexahydropyrimidine-2,4,6-trione (2.38)

To arylidene barbituric acid derivative 2.14 (1 g, 2.72 mmol) suspended in ethanol (20 ml) were added three equivalents of NaBH₄ (0.31 g, 8.19 mmol), portion-wise. The reaction mixture was initially left in an ice bath (0 °C). The mixture was then stirred overnight at room temperature. The pH of the mixture was adjusted to 4-5 in a 4M aqueous HCl, the desired compound appeared as a suspended particle, and the aqueous phase was collected and filtered. The residue was further washed with water. No further purification was carried out due to the high polarity of the desired compound and the remaining impurities. The desired compound was dried overnight under vacuum to give a white powder of compound **2.38** (0.6 g, 1.85 mmol, 60%). Molecular Formula C₁₈H₁₅N₃O₆; R_f (butanol/acetic acid/water, 4:1:5): 0.3, 0.1; melting point: >300 °C.

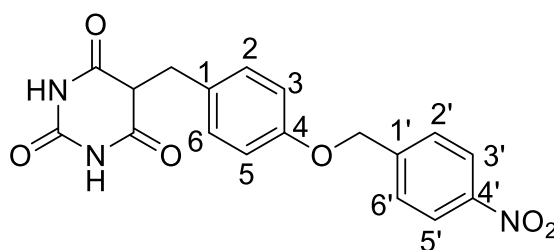


Figure 2. 53. Compound 2.38

¹H NMR (400 MHz, DMSO-d₆): δ = 11.17 (s, 2 H, NH, D₂O exchangeable), 8.25–8.23 (d, J = 8.7 Hz, 2H, ArHs), 7.71–7.62 (d, J = 8.7, 2H, ArHs), 7.02–7.00 (d, J = 8.7 Hz, 2H, ArHs), 6.93–6.91 (d, J = 8.7 Hz, 2H, ArHs), 5.22 (s, 2H, O-CH₂), 3.85-3.83 (t, J = 9.6 Hz, 1H, CH-CH₂), 3.20-3.19 (d, J = 4.7 Hz, 2H, CH-CH₂) ppm.

¹³C NMR (101 MHz, DMSO-d₆): δ =170.45 (C=O), 157.22 (C=O), 151.01 (C4), 147.44 (C-NO₂), 145.83 (impurities), 145.51 (C 1'), 130.59 (C 3', C 5'), 130.19 (C 1), 128.72 (C 3, C 5), 124.04 (C 2', C 6'), 115.11 (C 2, C 6), 68.43 (OCH₂), 49.98 (CH-CH₂), 33.13 (CH-CH₂) ppm.

IR (ATR): ν = 1508 (s, N-O), 1761 (m, C=O), 2988 (m, CH aliphatic), 3050 (m, CH aromatic), 3181 (m, NH).

Vernallis *et al.*, reported this compound in a patent submitted in 2010.

2.5.8.9. 5-[(4-Benzyloxyphenyl)methyl]hexahydropyrimidine-2,4,6-trione (2.39)

Three equivalents of NaBH₄ (0.422 g, 11.15 mmol) were added portion-wise to ethanol (25 ml) suspended Knoevenagel product **2.15** (1.2 g, 3.72 mmol). The reaction mixture was initially left in an ice bath (0 °C), the mixture was then stirred overnight at room temperature. The pH of the mixture was adjusted to 4-5 a 4M aqueous HCl; the compound was then extracted from the aqueous phase water (3 x 30 ml). The desired compound was extracted from the aqueous phase under low pressure; the residue was further washed with acetone. Due to the high polarity of the residue, no further purification was performed. White powder of compound **2.39** (1.16 g, 3.58 mmol, 97%) was obtained.

Molecular Formula C₁₈H₁₆N₂O₄; R_f (ethyl acetate/methanol, 4:1): 0.4; 0.3; melting point: 216 – 218 °C.

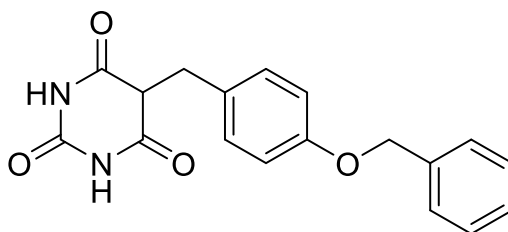


Figure 2. 54. Compound 2.39

¹H NMR (400 MHz, DMSO) δ= 11.17 (s, 2H, NH, D₂O exchangeable), 7.43-7.32 (m, 5H, ArHs), 7.00-6.98 (d, *J*=8.6 Hz, 2H, ArHs), 6.91-6.88 (d, *J*= 8.6 Hz, 2H, ArHs), 5.03 (s, 2H, -OCH₂), 3.85-3.82 (t, *J*= 9.5 Hz, 1H, CH-CH₂), 3.20-3.19 (d, *J*= 4.7 Hz, 2H, CH-CH₂) ppm.

¹³C NMR (101 MHz, DMSO-d₆): δ= 170.48 (C=O), 157.67 (C=O), 151.02 (C4), 137.52 (C3, C5), 130.51 (C2, C6), 129.72 (C 1), 128.86 (C2', C6'), 128.27 (C3', C5'), 128.20 (C4'), 115.03, 69.12 (OCH₂), 50.01 (CH-CH₂), 33.21 (CH-CH₂) ppm.

IR (ATR): ν = 1567 (m, cyclic alkene), 1656 (m, N-H), 1755 (m, C=O), 2858 (m, CH aliphatic), 3026 (m, CH aromatic), 3216 (m, NH).

Guerin, et al. reported this compound in 1999.

2.5.8.10. 5-[(5-Nitro-2-thienyl)methyl]hexahydropyrimidine-2,4,6-trione and its tautomeric form 6-Hydroxy-5-[(5-nitro-2-thienyl)methyl]dihydropyrimidine-2,4(1H,3H)-dione (2.40)

Three equivalents of NaBH₄ (1.2 g, 8.98 mmol) were added portion-wise to ethanol (25 ml) suspended Knoevenagel product **2.16** (0.8 g, 2.99 mmol). The reaction mixture was initially

left in an ice bath (0 °C) for 15 minutes and stirred overnight at room temperature. The PH of the mixture was adjusted to 4-5 with 4M aqueous HCl. The desired compound was extracted from the aqueous phase and further washed with water and methanol. Due to the high polarity of the residue, no further purification was performed. Brown powder of **2.40** (0.2004 g, 3.58 mmol, 25%) was obtained.

Molecular Formula C₉H₇N₃O₅S; R_f (butanol/acetic acid/water, 4:1:5): 0.45, 0.3; melting point: >300 °C.

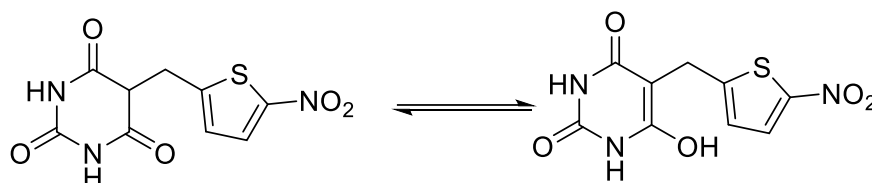


Figure 2. 55. Compound 2.40

¹H NMR (400 MHz, DMSO-d₆): δ= 11.36 (s, 1H, NH, D₂O exchangeable), 10.62 (s, 1H, NH, D₂O exchangeable), 7.94-7.93 (d, *J* = 3.9 Hz, 1H, ArHs), 6.99-6.98 (d, *J* = 4.1 Hz, 1H, ArHs), 4.28 (broad s, 1H, CH-CH₂), 3.80 (broad d, 2 H, CH-CH₂), 2.50 (s, 0.64H, impurities).

IR (ATR): ν =1512 (m, cyclic alkene), 1605 (w, N-H), 1711 (m, C=O), 2988 (w, CH aliphatic), 3050 (m, CH aromatic), 3209 (s, NH).

2.5.8.11. 5-[(E)-Cinnamyl]hexahydropyrimidine-2,4,6-trione and its tautomeric form 6-Hydroxy-5-[(E)-cinnamyl]dihydropyrimidine-2,4(1H,3H)-dione (2.41)

Three equivalents of NaBH₄ (0.117 g, 3.09 mmol) were added portion-wise to ethanol (20 ml) suspended Knoevenagel product **2.12** (0.25 g, 1.03 mmol). The reaction mixture was initially left in an ice bath (0 °C) for 15 minutes and then stirred overnight at room temperature. The PH of the mixture was adjusted to 4-5 with 4M aqueous HCl. The desired compound was extracted from the aqueous phase. The aqueous residue was then washed with acetone, where the desired compound was collected from the filtrate and dried overnight under vacuum. Yellow powder of **2.41** (0.12 g, 0.489 mmol, 48 %) was obtained.

Molecular Formula C₁₃H₁₂N₂O₃; R_f (butanol/acetic acid/water, 4:1:5): 0.8.

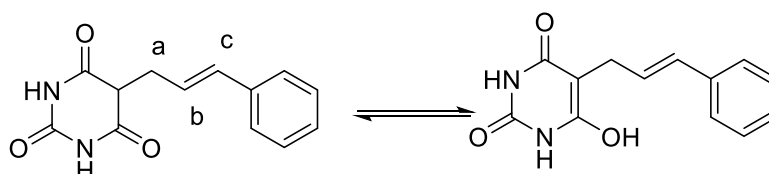


Figure 2. 56. Compound 2.41

^1H NMR (400 MHz, DMSO) δ = 11.23 (s, 2H, NH, D₂O exchangeable), 7.36-7.22 (m, 5H, ArHs), 6.52 (s, 1H, -OH, tautomeric form), 6.46-6.42 (d, J =15.8 Hz, 1H, Ha, tautomeric form), 6.18-6.10 (dt, J = 15.8, 7.1 Hz, 1H, Hb), 3.77-3.74 (t, J = 5.0 Hz, 1H, H5), 2.84-2.81 (t, J = 5.8 Hz, 2H, Ha) ppm.

^{13}C APT NMR (101 MHz, DMSO-d₆): δ = 170.33 ($\underline{\text{C}}=\text{O}$), 151.31 ($\underline{\text{C}}=\text{O}$), 137.08 ($\text{CH}-\underline{\text{C}}$), 133.04 (ArC), 129.05 (ArC), 127.87 (ArC), 126.48 (Cb), 125.59 (Cc), 48.61 ($\underline{\text{C}}\text{H}-\text{CH}_2$), 31.51 ($\text{CH}-\underline{\text{C}}\text{H}_2$) ppm.

The spectroscopic data of the compound was reported by Kalita and Deka (2018).

2.5.8.12. 5-[(3-Benzyloxy-2-naphthyl)methyl]hexahydropyrimidine-2,4,6-trione (2.42)

Three equivalents of NaBH₄ (0.091 g, 2.42 mmol) were added portion-wise to ethanol (20 ml) suspended Knoevenagel product **2.11** (0.3 g, 0.8 mmol). The reaction mixture was initially left in an ice bath (0 °C) for 15 minutes and stirred overnight at room temperature. The PH of the mixture was adjusted to 4-5 with 4M aqueous HCl. The desired compound was extracted from the organic phase i.e., ethyl acetate (3 x 30 ml), rinsed with a saturated aqueous solution of NaCl, dried with anhydrous MgSO₄, filtered and the filtrate was collected. The solvent was removed at low pressure and the residue obtained was dried under vacuum to give yellowish crystals of **2.42** (0.25 g, 0.68 mmol, 85%).

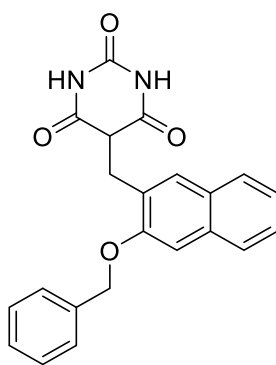


Figure 2. 57. Compound 2.42

Molecular Formula C₂₂H₁₈N₂O₄; R_f (butanol/acetic acid/water, 4:1:5): 0.48; melting point: 97-99 °C.

^1H NMR (400 MHz, DMSO-d₆): δ = 11.10 (s, 2H, NH, D₂O exchangeable), 8.00-7.98 (d, J = 8.5 Hz, 1H, ArHs), 7.87-7.82 (t, J = 18.6 Hz, 2H, ArHs), 7.53-7.32 (m, 8H, ArHs), 5.28 (s, 2H, -OCH₂), 3.67-3.62 (m, 3H, -CH, -CH₂) ppm.

^{13}C APT NMR (101 MHz, DMSO-d₆): δ = 170.62 (C=O), 154.50 (C=O), 151.66 (ArC), 137.89 (ArC), 133.17 (ArC), 129.24 (ArC), 129.04 (ArC), 128.96 (ArC), 128.87 (ArC), 128.07 (ArC), 127.65 (ArC), 126.99 (ArC), 123.70 (ArC), 123.23 (ArC), 119.02 (ArC), 115.09 (ArC), 70.58 (OCH₂), 49.11 (CH-CH₂), 31.15 (impurities), 27.16 (CH-CH₂) ppm.

IR (ATR): ν =1631 (m, N-H), 1693 (s, C=O), 2846 (m, CH aliphatic), 3059 (m, CH aromatic), 3196 (m, NH).

2.5.8.13. 5-(2-Naphthylmethyl)hexahydropyrimidine-2,4,6-trione and its tautomeric form 6-Hydroxy-5-(2-naphthylmethyl)dihydropyrimidine-2,4(1H,3H)-dione (2.43)

Three equivalents of NaBH₄ (0.106 g, 2.8 mmol) were added portion-wise to ethanol (20 ml) suspended Knoevenagel product 2.18 (0.25 g, 0.93 mmol). The reaction mixture was initially left in an ice bath (0 °C) for 15 minutes and then stirred overnight at room temperature. The PH of the mixture was adjusted to 4-5 with 4M aqueous HCl. The desired compound was extracted from the aqueous phase i.e., water (3 x 30 ml). The solvent was removed at low pressure and the residue obtained was rinsed with acetone and dried under vacuum to give a white powder of **2.43** (0.18 g, 0.67 mmol, 71.4%).

Molecular Formula C₁₅H₁₂NO₃; R_f (butanol/acetic acid/water, 4:1:5): 0.85; melting point: 196-199 °C.

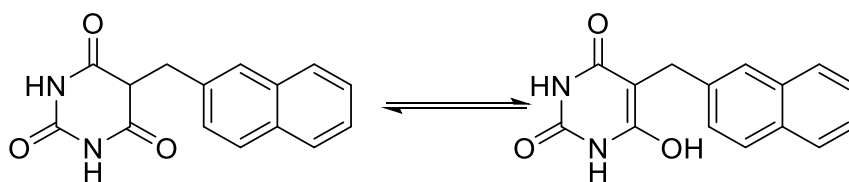


Figure 2. 58. Compound 2.43

^1H NMR (400 MHz, DMSO) δ = 11.18 (s, 2H, NH, D₂O exchangeable), 8.17-7.12 (m, 7H, ArHs, Hb. Hc), 3.99 (broad s, 1H, CH-CH₂), 3.69 (broad s, 2H, CH-CH₂) ppm. ^{13}C NMR (101 MHz, DMSO-d₆): δ = 170.68 (C=O), 151.30 (C=O), 134.80 (ArC), 133.83 (ArC), 131.91 (ArC), 129.06 (ArC), 127.57 (ArC), 127.12 (ArC), 126.62 (ArC), 126.10 (ArC), 125.78 (ArC), 123.95 (ArC), 49.34 (CH-CH₂), 30.42 (CH-CH₂) ppm.

IR (ATR): ν =1507 (m, cyclic alkene), 1626 (s, N-H), 1729 (s, C=O), 2975 (m, CH aliphatic), 3011 (m, CH aromatic), 3099 (w, NH).

2.5.8.14. 5-(2-(Methoxymethoxy)benzyl)pyrimidine-2,4,6(1H,3H,5H)-trione (2.44)

Three equivalents of NaBH₄ (0.2 g, 5.43 mmol) were added portion-wise to ethanol (20 ml) suspended Knoevenagel product **2.19** (0.5 g, 1.81 mmol). The reaction mixture was initially left in an ice bath (0 °C) for 15 minutes and then stirred overnight at room temperature. The PH of the mixture was adjusted to 4-5 with 4M aqueous HCl. The desired compound was extracted from the organic phase i.e., hexane (3 x 30 ml), rinsed with a saturated aqueous solution of NaCl, dried with anhydrous MgSO₄, filtered and the filtrate was collected. The solvent was removed at low pressure and the residue obtained was dried under vacuum to give a buff powder 0.22 g, 0.79 mmol, 44 % was obtained.

Molecular Formula C₁₃H₁₄N₂O₅; R_f (butanol/acetic acid/water, 4:1:5): 0.5; melting point: 69-70 °C.

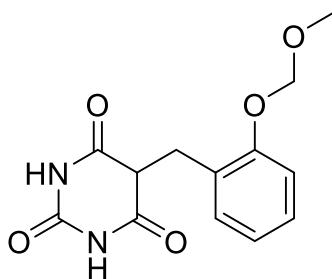


Figure 2. 59. Compound 2.44

¹H NMR (400 MHz, DMSO) δ = 11.04 (s, 2 H, NHs), 7.17-7.14 (t, J = 14.8 Hz, 1H, ArH), 6.99-6.97 (d, J = 6.9 Hz, 1H, ArH), 6.91-6.89 (d, J = 7.9 Hz, 1H, ArH), 6.82-6.78 (t, J = 14.6 Hz, 1H, ArH), 4.01-3.96 (d, J = 19.8 Hz, 2H, OCH₂), 3.79-3.64 (t, J = 11.9, 1H, CH-CH₂), 3.2-3.19 (d, J = 4.8, 2H, CH-CH₂), 1.34-1.31 (t, J = 13.4, 3H, OCH₃) ppm.

¹³C APT NMR (101 MHz, DMSO-d₆): δ = 170.44 (C=O), 156.97 (C=O), 151.43 (ArC), 130.67 (ArC), 128.36 (ArC), 125.93 (ArC), 120.31 (ArC), 111.71 (ArC), 63.57 (OCH₂), 48.63 (CH-CH₂), 29.66 (CH-CH₂), 14.95 (OCH₃) ppm.

IR (ATR): ν =1590 (w, cyclic alkene), 1684 (s, N-H), 1769 (m, C=O), 2873 (w, CH aldehydic), 2977 (w, CH aliphatic), 3074 (m, CH aromatic), 3161 (w, NH).

2.5.8.15. Attempt to synthesise (E)-5-(3-(4-Nitrophenyl)allyl)pyrimidine-2,4,6(1H,3H,5H)-trione (2.45)

One equivalent benzaldehyde (0.39 g, 3.67 mmol) and 2-aminothiophenol (0.46 g, 3.67 mmol) were added to a water suspension of **2.6** (1 g, 2.69 mmol). The reaction was left to reflux for 4 hours, the crude was collected, and purified by extraction from the aqueous phase (3 X H₂O). The compound was concentrated by solvent evaporation under vacuum and left to dry overnight under vacuum to give a white powder (0.7 g, 2.56 mmol, 70%).

Molecular Formula C₁₃H₁₁N₃O₅; R_f (butanol/acetic acid/water, 4:1:5): 0.4.

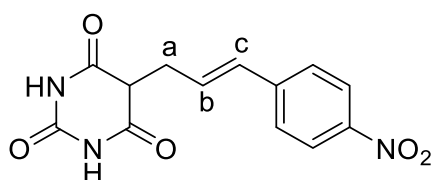


Figure 2. 60. Compound 2.45

¹H NMR (400 MHz, DMSO-d₆): δ= 11.24 (s, 2H, NH, D₂O exchangeable), 8.16-8.14 (d, *J*= 8.7 Hz, 2H, meta ArHs), 7.65-7.63 (d, *J*=8.9 Hz, 2H, ortho ArHs), 6.62-6.58 (d, *J*= 15.9 Hz, 1H, H_c), 6.51-6.44 (m, 1H, H_b), 3.87-3.85 (t, *J*= 10.4 Hz, 1H, CH-CH₂), 2.89-2.87 (t, *J*= 11.7 Hz, 2H, H_a) ppm. ¹³C APT NMR (101 MHz, DMSO) δ= 170.12 (C=O), 151.31 (C=O), 146.66 (C-NO₂), 143.99 (CH-C), 132.03 (meta ArCs), 130.93 (ortho ArCs), 127.44 (C_c), 124.36 (C_b), 48.34 (CH-CH₂), 31.03 (C_a) ppm.

IR (ATR): ν =1588 (s, cyclic alkene), 1688 (s, C=O), 2839 (w, CH aliphatic), 3077 (m, CH aromatic), 3223 (m, NH).

MS (+ESI) *m/z* = Found 290.0771 [M+H]⁺; calculated for C₁₃H₁₂N₃O₅ 290.0777; -2.1 ppm (the desired compound).

MS (+ESI) *m/z* = Found 292.0936 [M+H+2H]⁺; calculated for C₁₅H₁₆N₃O₅ 292.0933; 1.0 ppm (might be resulted from complete reduction).

MS (+ESI) *m/z* = Found 288.0614 [M+H-2H]⁺; calculated for C₁₃H₁₀N₃O₅ 288.0620; -2.1 ppm (Knoevenagel impurities).

2.5.8.16. 1,3-Dimethyl-5-[(E)-3-(4-nitrophenyl)allyl]hexahydropyrimidine-2,4,6-trione and its tautomeric form (E)-6-Hydroxy-1,3-dimethyl-5-(3-(4-nitrophenyl)allyl)dihydropyrimidine-2,4(1H,3H)-dione (2.46)

Three equivalents of NaBH₄ (0.55 g, 14.5 mmol) were added portion-wise to ethanol (20 ml) suspended Knoevenagel product **2.29** (1.54 g, 4.89 mmol). The reaction mixture was initially left in an ice bath (0 °C) for 15 minutes and then stirred overnight at room temperature. The PH of the mixture was adjusted to 4-5 with 4M aqueous HCl. The desired compound was extracted from the aqueous phase i.e., water (3 x 30 ml). The solvent was removed at low pressure and the residue was washed with acetone (2 x 20 ml). The compound was extracted after crystallisation and dried under vacuum to give a yellow solid of **2.46** (0.41 g, 1.4 mmol, 27.4%).

Molecular Formula C₁₅H₁₅N₃O₅; R_f (butanol/acetic acid/water, 4:1:5): 0.9; melting point: >300 °C.

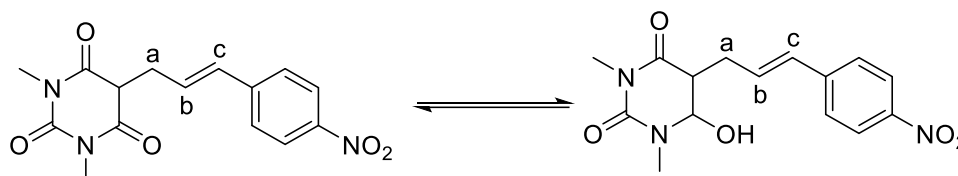


Figure 2. 61. Compound 2.46

¹H NMR (400 MHz, DMSO) δ= 8.12-8.09 (d, *J* = 6.5 Hz, 2H, meta ArHs), 7.58-7.55 (d, *J* = 6.5 Hz, 2H, ortho ArHs), 6.58-6.50 (dt, *J* = 15.8, 6.5 Hz, 1H, H_b), 6.40-6.36 (d, *J* = 15.8 Hz, 2H, H_c), 3.36 (s, 6H, CH₃ X₂), 3.11-3.09 (dd, *J* = 6.5, 1.2 Hz, 2H, H_a).

¹³C APT NMR (101 MHz, DMSO-d₆): δ= 162.35 (C=O), 153.45 (C), 145.84 (C=O), 145.80 (C-NO₂), 139.00 (meta ArCs), 126.75 (ortho ArCs), 125.84 (C b), 124.30 (C c), 81.91 (CH-C), 28.90 (C-CH₂), 27.36 (N-CH₃ X₂).

IR (ATR): ν =1598 (s, cyclic alkene), 1677 (s, C=O), 2846 (w, CH aliphatic), 3065 (m, CH aromatic).

MS (+ESI) *m/z* = Found 316.1081 [M+H-2H]⁺; calculated for C₁₅H₁₆N₃O₅ 316.1090; -2.8 ppm (minor Knoevenagel impurities).

MS (+ESI) m/z = Found 318.1081 $[M+H]^+$; calculated for $C_{15}H_{16}N_3O_5$ 318.1090; -2.8 ppm.

MS (+ESI) m/z = Found 320.1234 $[M+H+2H]^+$; calculated for $C_{15}H_{18}N_3O_5$ 320.1246; -23.7 ppm (might be resulted from complete reduction).

2.5.9. Discussion

Regioselective reduction of the exocyclic C=C of the Knoevenagel products was successfully achieved in this part of the synthetic route of this project. The reduction was achieved by two distinct mechanisms, sodium borohydride reduction and one pot in situ transfer hydrogen. The initial hypothesis was based on the enzymatic oxidation of allylic derivatives by DHODase enzyme upon binding to the active site generating the active benzylidene barbiturate derivatives. Herein, the allylic pyrimidinetriones were synthesised to check the validity of the hypothesis based on their antimicrobial activity readings (Chapter 3).

The reduction of alkenes to the corresponding alkanes can be achieved by employing numerous approaches including direct hydrogenation with an external hydrogen source, metal catalysis, or catalytic hydrogen transfer methods which can utilise either the solvent or a reagent as a hydrogen source. Reduction of unsaturated hydrocarbons using hydride reagents including $NaBH_4$ is another approach. $NaBH_4$ is considered a particularly valuable reagent, owing to its mild nature, easy handling, and low cost. However, its activity is limited to the reduction of unsaturated aliphatic chains (Tran *et al.*, 2009). In the early 1960s, Brown elaborated that the borohydride reduces the metal salts generating active metals that catalyse the hydrolysis of the borohydride producing H_2 gas and sequentially hydrogenating the alkenes (Brown & Brown, 1962).

Kalita and Deka (2017) reported the production of 5-monoalkyl barbiturates using a metal-free and catalyst-free procedure relying on the in-situ generation of 2-phenyl-2,3-dihydrobenzo[d]thiazole in a one-pot reaction. Water was used in Knoevenagel condensation owing to its benign, natural, low-cost, non-toxic, and non-flammable properties. The in-situ reduction provided by this protocol is considered a valuable route as it minimised the purification steps and provided mild reaction conditions.

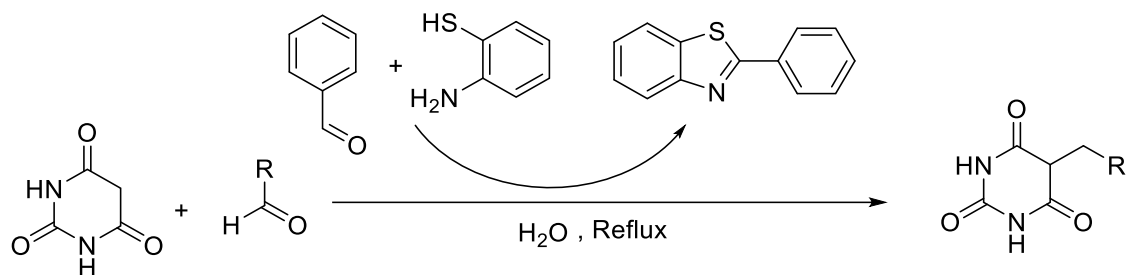


Figure 2. 62. The synthetic route of the production of allylic pyrimidinetrione derivatives using the one pot in situ reaction using benzaldehyde and 2-aminothiophenol to produce 2-phenyl-2,3-dihydrobenzo[d]thiazole which serves as a hydrogen source

To form the allylic pyrimidinetrione derivatives by NaBH_4 reduction method shown in scheme 2.1, the benzylidene barbiturate derivatives were suspended in ethanol at room temperature, followed by the addition of the reducing agent (NaBH_4) portion-wise. A tube containing CaCl_2 granules was attached to the flask nozzle to entrap the liberated hydrogen. A significant change in the benzylidene barbiturate starting material to a lighter colour was observed after a few minutes indicating a decrease in the electron conjugation, supporting the reduction of the $\text{C}=\text{CH}-\text{Ar}$ bond to $\text{CH}-\text{CH}_2\text{Ar}$. Selective exocyclic reduction of dienes ($\text{C}=\text{CH}-\text{CH}$) giving monoenes ($\text{CH}-\text{CH}_2-\text{CH}$) from dienes was achieved by NaBH_4 .

The allylic derivatives obtained from reduction were primarily characterised by ^1H NMR, ^{13}C NMR, IR, and melting point. Some compounds were further analysed by mass spectroscopy. Some difficulties were faced during the purifying attempts because of the polar nature of the produced allylic derivatives and some of the impurities. Purification using column chromatography was not beneficial in this case due to the acidic properties of the silica used for separation. The only purification method employed for this reaction was liquid-liquid extraction, because of the polar properties of both the products and the impurities. Purification via column chromatography was avoided to prevent the production of silica impurities. Some of the products possessed some impurities which could not be purified by the conventional methods.

The ^1H NMR spectrum of the Knoevenagel products was compared to that of the allylic pyrimidinetriones; compounds **2.4** and **2.31** were used as examples to illustrate the changes (Figure 2.64.). ^1H NMR spectra showed that the 2 proton singlets of the two NHs were merged into a two-proton singlet. The exocyclic one proton singlet of $\text{C}=\underline{\text{C}}\text{H}-\text{Ar}$ disappeared after the reduction, and two peaks appeared in the aliphatic region representing the $\underline{\text{C}}\text{H}-$

$\text{CH}_2\text{-Ar}$. The $\text{CH-CH}_2\text{-Ar}$ was expected to appear as a triplet and the $\text{CH-CH}_2\text{-Ar}$ was expected to appear as a doublet; unlike the expected splitting the two peaks appeared as broad singlets. The broad peaks indicate reversible tautomerisation between the keto and enol forms (Figure 2.63.). Moreover, the aromatic protons were more shielded compared to the Knoevenagel products due to the loss of conjugation. However, the hydroxyl group (OH) of the enol form did not appear in the spectrum.

As for the ^{13}C NMR spectra, the 3 carbonyl groups appeared as two peaks after reduction, unlike the Knoevenagel products where the C=O groups appear as 3 peaks, which indicates that two of the three C=O groups are at the same chemical shift. The exocyclic C=CH peak disappeared after reduction and was replaced by the CH-CH_2 and CH-CH_2 peaks in the aliphatic region which validated of the reduction of the aliphatic bridge (Figure 2.65).

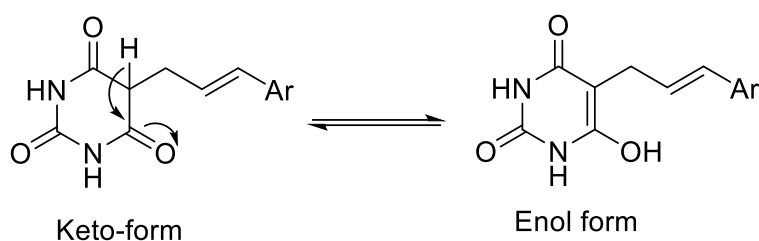


Figure 2. 63. Keto-enol tautomerisation of the reduced products

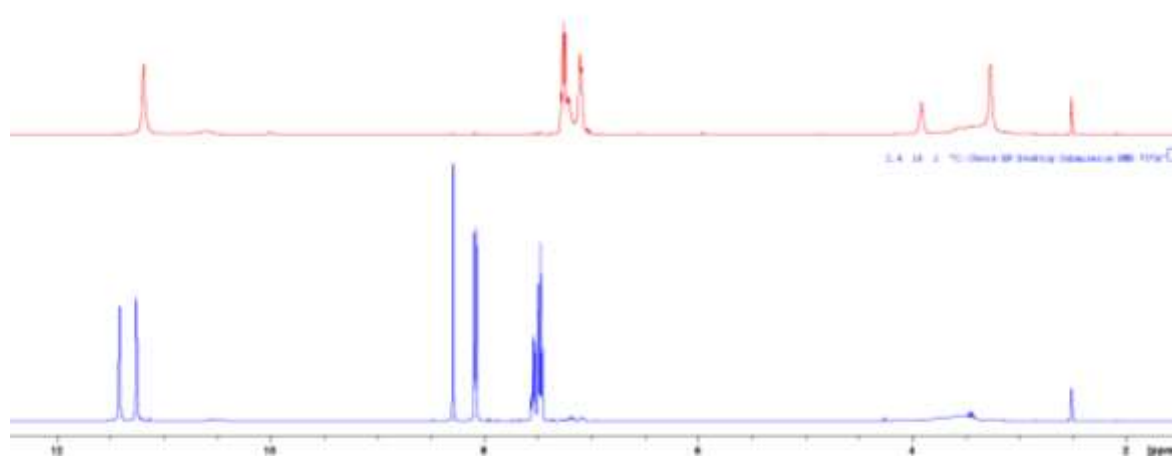


Figure 2. 64. The ^1H NMR spectra of Knoevenagel product (2.4) on bottom and the allylic pyrimidinetrione (2.31) on top

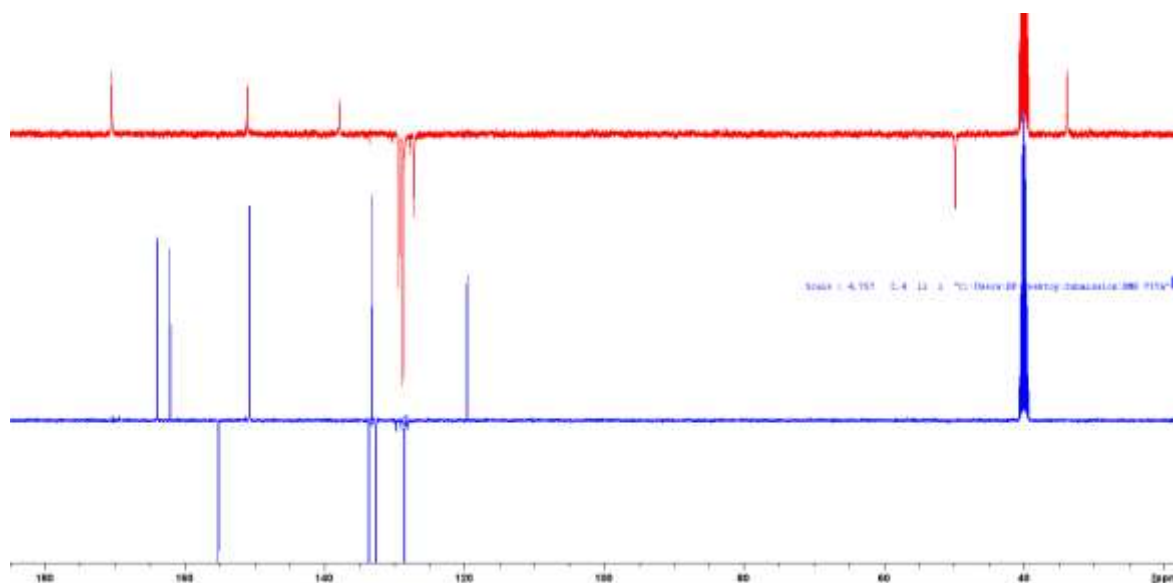


Figure 2. 65. The ^{13}C NMR spectra of Knoevenagel product (2.4) on bottom and the allylic pyrimidinetrione (2.31) on top

Reductions was attempted using the NaBH_4 and 2-phenyl-2,3-dihydrobenzo[d]thiazole in one-pot reaction. The TLC showed some impurities that were challenging to remove by liquid-liquid extraction because of the polar nature of both the desired compound and the impurities. Despite the presence of impurities, ^1H NMR spectrum was interesting as the peak representing the $\text{CH}-\text{CH}_2$ disappeared which might give an indication that the enol form is predominant. Moreover, the splitting of $\text{CH}-\text{CH}_2$ appeared as a singlet, which proves the predominance on the enol form in this case and the conversion of the $\text{CH}-\text{CH}_2$ to $\text{C}-\text{CH}_2$. The NaBH_4 reduced version spectrum displayed both configurations. Moreover, unlike compound 2.31, the hydroxyl group of the enol-form appeared in the ^1H NMR spectra of compound 2.32 at 6.55 ppm.

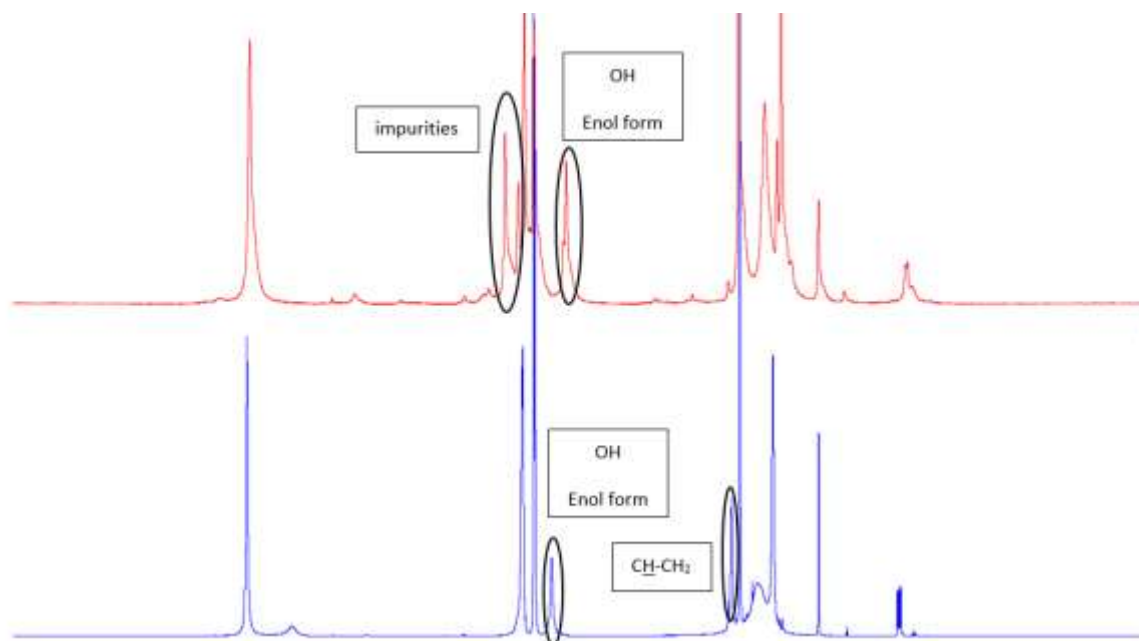


Figure 2. 66. The ^1H NMR spectra of compound **2.32**, where the NaBH_4 reduced was placed on bottom and the 2-phenyl-2,3-dihydrobenzo[d]thiazole reduced was placed on top

The ^1H NMR spectrum of compound **2.33** shows both keto and enol configurations. This finding was confirmed when pyridine d_5 was used as a solvent, since the pyridine peaks and the moisture peaks appear away from the aliphatic region to prevent the overlapping of the moisture and the aliphatic peaks. However, the peaks appeared as broad singlets which indicated tautomerisation. The OH group of the enol form did not appear as clear as that of **2.32**, yet a very tiny peak with a negligible integration at 6.57 ppm in DMSO-d_6 .

NaBH_4 reduction of **2.34** caused a regioselective reduction of the exocyclic $\text{C}=\text{CH}$ of the diene aliphatic bridge. The ^1H NMR displayed on the keto form, where the $\text{CH}-\text{CH}_2-\text{CH}$ produced after reduction appeared as a one proton doublet overlapping with the 3-proton singlet of the methoxy group (OCH_3), and $\text{CH}-\text{CH}_2-\text{CH}$ appeared as two proton triplet. As for $\text{CH}-\text{CH}_2-\text{CH}=\text{CH}$ appeared as doublet of triplet. Compound **2.36** displayed the same spectral features, and a small broad singlet peak integrating for 0.5 proton appeared at 4.38 ppm which probably represent the OH group of the enol tautomeric form.

The moisture peak of compound **2.35** overlapped with the aliphatic peaks of the $\text{CH}-\text{CH}_2$; however, the ^{13}C NMR confirmed the reduction. Yet, some polar impurities were detected. Compound **2.35**, **2.37** and **2.41** required further purification via high performance liquid chromatography (HPLC) as the conventional methods failed due to the high polarity of the

desired compound and the impurities. However, the two tautomeric forms were observed in the form of broad peaks.

^1H NMR Compounds **2.38** and **2.39** showed starting material impurities; non-polar impurities could have been avoided by further washing with a non-polar solvent. However, the minor polar impurities required HPLC. The Keto configuration alone appeared in the spectra, as $\text{CH}-\text{CH}_2$ splitting appeared as a triplet and $\text{CH}-\text{CH}_2$ appeared as a doublet.

Compound **2.40**, **2.41**, and **2.46** displayed both tautomeric configurations, where its peaks appeared as broad singlets in the aliphatic region. While **2.42** and **2.44** spectrum were consistent with the keto configuration; however, the ^{13}C of **2.42** showed an extra small peak in the aliphatic region which indicate the presence of minor impurities.

The MS of compound **2.46** showed the presence of residual Knoevenagel product that could be prevented by further washing with non-polar solvent. A $[\text{M}+\text{H}-2\text{H}]^+$ peak appeared in the MS which might indicate that the reaction led to a complete reduction to the aliphatic chain as well, leading to the formation of a mixture.

Table 2. 3. Comparison of the literature melting points in °C of compounds with products isolated in this thesis work using the reported methods

Compound	Reported mp	References	Found mp
2.31	212.5-214	Ramachary <i>et al.</i> , 2008	203-206
2.32	204-207	Vieira <i>et al.</i> , 2011	200-205

2.5.10. Reduction mechanism using 2-phenyl-2,3-dihydrobenzo[d]thiazole in a one-pot reaction

In the first step, benzylidene barbiturate derivatives are formed upon reacting barbituric acid with aldehydes via Knoevenagel condensation. In the second step, 2-aminothiophenol reacts with benzaldehyde forming 2-phenyl-2,3-dihydrobenzo[d]thiazole, which acts as a hydrogen source for hydrogenation transfer (Figure 2.67.).

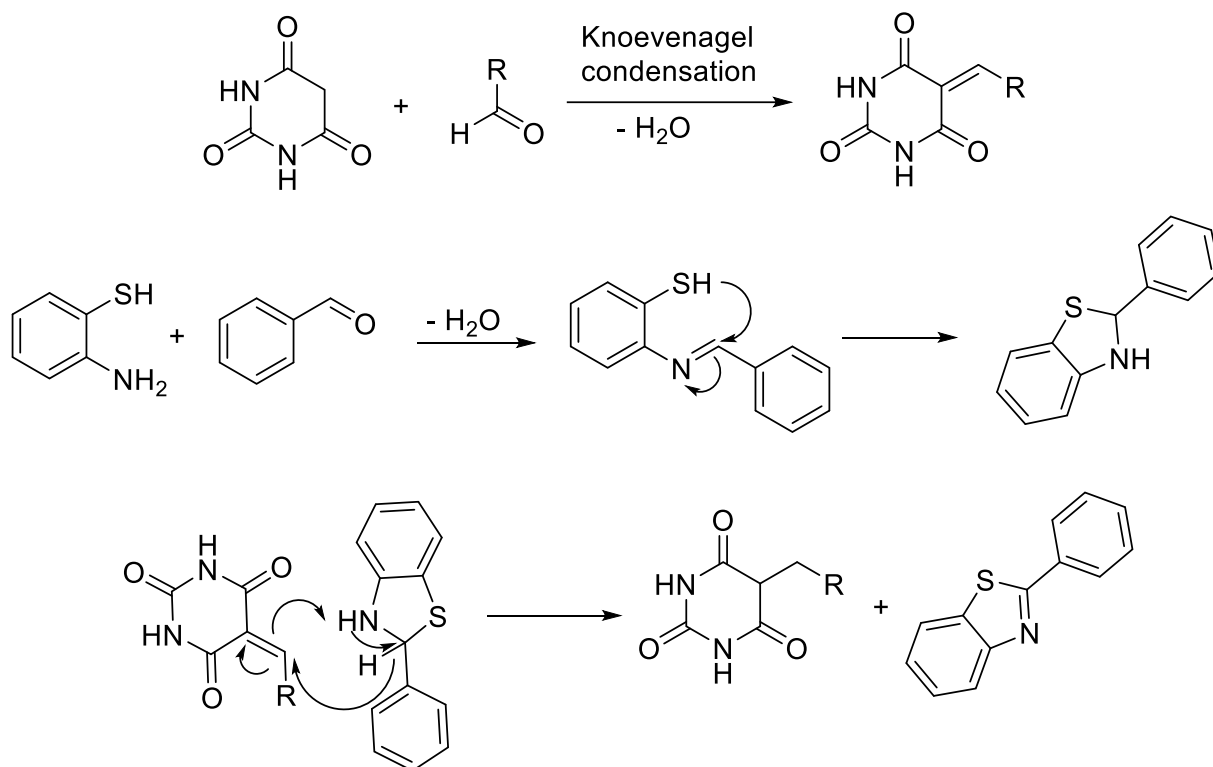


Figure 2. 67. Mechanism of 2-phenyl-2,3-dihydrobenzo[d]thiazole formation in a one-pot reaction

2.5.11. Mechanism of reduction of exocyclic C=C by NaBH₄

Reduction (NaBH₄) of aldehydes and ketones involves two steps. Initially, H⁻ detaches from the nucleophilic borohydride, followed by H⁻ addition to the partially positive carbon of the carbonyl group. The first step results in the formation of alkoxides salt and BH₃. The second step involves the protonation of the alkoxide by water or an acid-forming alcohol (Suzuki *et al*, 2009).

Selective reduction of the exocyclic C=C of arylidene barbituric acid derivatives was reduced by NaBH₄ in the presence of ethanol as a solvent (Levesque *et al*, 1993). However, the exact mechanism was not reported in literature.

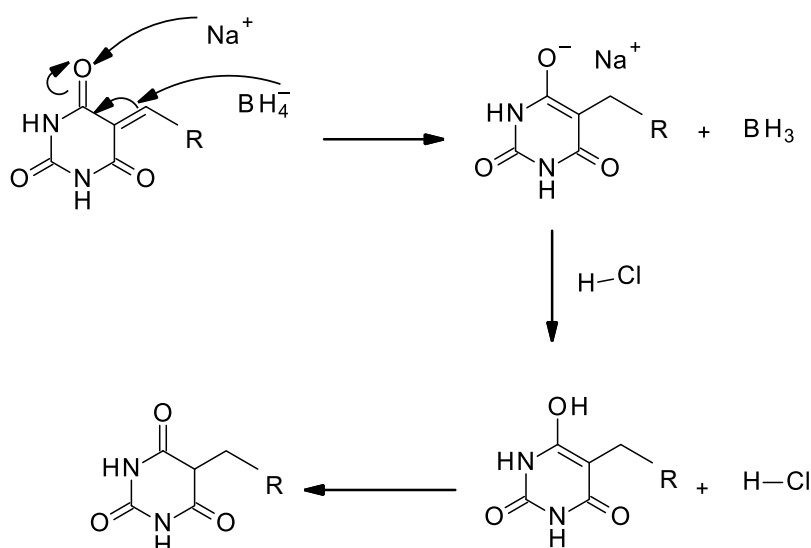


Figure 2. 68. The predicted mechanism of NaBH₄ reduction of alkenes

2.5.12. Catalytic hydrogenation with palladium on charcoal

Catalytic hydrogenation was achieved (scheme 2.1) using 10% palladium on charcoal (Pd/C) in ethanol containing the suspension of Knoevenagel diene starting material. Reduction of alkenes into alkanes results in the formation of a highly stable product, having lower energy compared to the starting unsaturated compound; hence, the reaction is exothermic. The presence of a catalyst is a cornerstone for the hydrogenation reaction (Mironenko *et al.*, 2020).

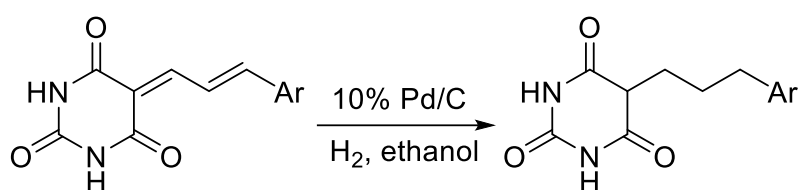


Figure 2. 69. Synthesis of propyl bridged aralkylpyrimidinetriones derivatives

2.5.13. Synthesis of propyl bridged aralkylpyrimidinetriones derivatives

2.5.13.1. 5-(3-(4-Methoxyphenyl)propyl)pyrimidine-2,4,6-trione and its tautomeric form 6-Hydroxy-5-(3-(4-methoxyphenyl)propyl)pyrimidine-2,4(1H,3H)-dione (2.47)

Compound **2.5** (2g, 1.2 mmol) was left to dissolve in ethanol (60 ml). Pd/C (10%, 0.2 g) was then added, sonicated at room temperature, and hydrogen gas was introduced to the

reaction flask after the removal of oxygen by vacuum. The reaction was left to stir for 5 hours at room temperature. The catalyst was filtered off by celite and washed with ethanol, where the filtrate was collected and the solvent was evaporated and dried under vacuum overnight to obtain a yellow solid (0.5 g, 7.35 mmol, 25%).

Molecular Formula $C_{14}H_{16}N_2O_4$; R_f (butanol/acetic acid/water, 4:1:5): 0.87; melting point: 180-183.

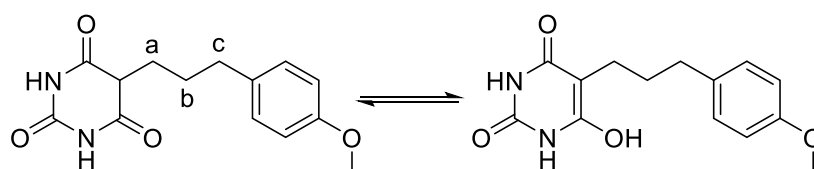


Figure 2. 70. Compound 2.47

1H NMR (400 MHz, DMSO- d_6): δ 11.20 (s, 2H, NH , D_2O exchangeable), 7.08 – 7.06 (d, J = 7.5 Hz, 2H, ortho ArHs), 6.83 – 6.81 (d, J = 7.6 Hz, 2H, meta ArHs), 3.71 (s, 3H, OCH_3), 3.53 (broad s, 1H, $CH-CH_2$), 2.49 (broad s, 2H, Hb), 1.89 (broad s, 2H, Ha), 1.52 (broad s, 2H, Hc) ppm.

^{13}C NMR (400 MHz, DMSO- d_6): δ 170.9 (C=O), 157.8 (C=O), 151.3 (CH_2-C), 133.8 ($C-OCH_3$), 129.6 (ortho ArCs), 114.1 (meta ArCs), 55.3 (OCH_3), 48.3 ($CH-CH_2$), 34.4 (Cb), 28.5 (Ca), 28.1 (Cc) ppm.

IR (ATR): ν = 1511 (m, C=C), 1697 (s, C=O), 2969 (w, CH aliphatic), 3085 (m, CH aromatic), 3238 (m, NH).

MS (+ESI) m/z = Found 276.1105 [M] $^+$; calculated for $C_{14}H_{16}N_2O_4$ 277.1183; -1.4 ppm.

MS (+ESI) m/z = Found 277.1179 [$M+H$] $^+$; calculated for $C_{14}H_{17}N_2O_4$ 277.1183; -1.4 ppm.

2.5.13.2. 5-(3-Phenylpropyl)hexahydropyrimidine-2,4,6-trione and its tautomeric form 6-Hydroxy-5-(3-phenylpropyl)pyrimidine-2,4(1H,3H)-dione (2.48)

Compound 2.18 (0.5 g, 2 mmol) was left to dissolve in ethanol (60 ml). Pd/C (10%, 0.05 g) was added, the reaction flask was sonicated at room temperature, and hydrogen gas was introduced to the reaction flask after the removal of oxygen by vacuum. The reaction was stirred for 6 hours at room temperature. The catalyst was filtered off by celite and washed with ethanol, where the filtrate was collected, and the solvent was evaporated and dried under vacuum overnight to obtain a white powder (0.3 g, 60%).

Molecular Formula $C_{13}H_{14}N_2O_3$; R_f (butanol/acetic acid/water, 4:1:5): 0.75; melting point: 165-168.

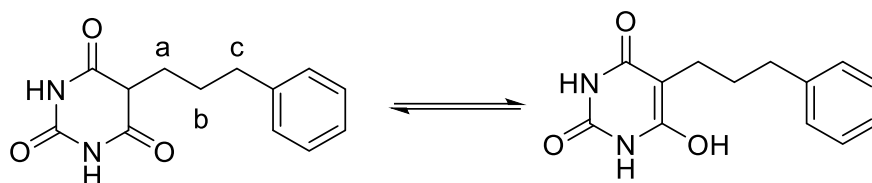


Figure 2. 71. Compound 2.48

1H NMR (400 MHz, DMSO- d_6): δ = 11.19 (s, 2H, NH , D_2O exchangeable), 7.28 – 7.25 (m, 2H, ArHs), 7.18 – 7.16 (m, 3H, ArHs), 3.56 – 3.54 (t, J = 9.4 Hz, 1H, $CH-CH_2$), 2.58 – 2.54 (t, J = 15.2 Hz, 2H, Hc), 1.93 – 1.90 (m, 2H, Ha), 1.61-1.53 (m, 2H, Hb) ppm.

^{13}C APT NMR (400 MHz, DMSO- d_6): δ = 170.90 ($C=O$), 151.34 ($C=O$), 142.05 (CH_2-C), 128.72 (ArCs), 128.70 (ArCs), 126.21 (ArC), 48.30 ($CH-CH_2$), 35.35 (Ca), 28.36 (Cc), 28.14 (Cb) ppm.

IR (ATR): ν = 1453 (m, C=C), 1697 (s, C=O), 2941 (w, CH aliphatic), 3082 (m, CH aromatic), 3239 (s, NH).

MS (+ESI) m/z = Found 247.1083 [M] $^+$; calculated for $C_{14}H_{16}N_2O_4$ 277.1183; -1.4 ppm.

MS (+ESI) m/z = Found 263.1029 [$M+O+H$] $^+$; calculated for $C_{13}H_{15}N_2O_4$ 263.1032; 2.4 ppm.

2.5.13.3. Attempts to synthesise 5-(3-(Furan-2-yl)propyl)pyrimidine-2,4,6(1H,3H,5H)-trione

Compound 2.9 (0.9 g, 3.9 mmol) was left to dissolve in ethanol (60 ml). Pd/C (10%, 0.09 g) was added, the reaction flask was sonicated at room temperature, and hydrogen gas was introduced to the reaction flask after the removal of oxygen by vacuum. The reaction was stirred for 8 hours at room temperature. The catalyst was filtered off by celite and washed with ethanol, where the filtrate was collected, and the solvent was evaporated and dried under vacuum overnight; however, the attempt failed.

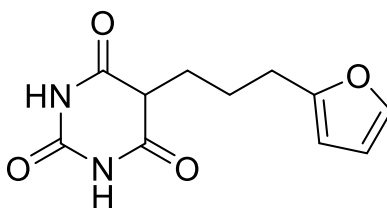


Figure 2. 72. Compound 2.49

2.5.14. Mechanism of action of catalytic hydrogenation using Pd/C

Homolytic cleavage of hydrogen gas in the presence of the insoluble catalyst Pd/C leads to the conversion of the catalyst to the liquid state, where each hydrogen atom adheres to the surface of the catalyst creating metal-hydrogen bonds. Followed by the attachment of the alkene to the Pd/C surface, the π bond breaks, and a hydrogen atom binds to each of the two-carbon forming C-H. Both alkene and the hydrogens are oriented on the catalyst's flat surface, causing an obligatory syn addition of the two hydrogens on the same side (Mironenko *et al.*, 2020).

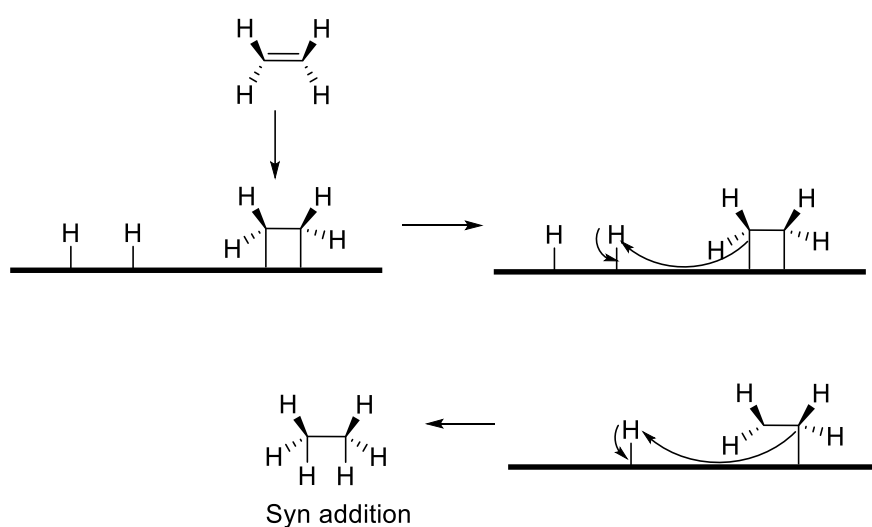


Figure 2. 73. Mechanism of action of catalytic hydrogenation using Pd/C

2.5.15. Discussion of the Pd/C reduced compounds

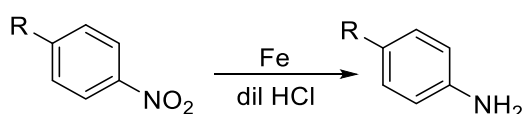
Compounds **2.48** and **2.49** displayed both the keto and enol configurations upon the complete reduction of the aliphatic bridge. The broad peaks presenting the aliphatic bridge in the ^1H NMR and ^{13}C NMR aliphatic regions.

Pd/C was found to be unsuitable for the reduction of furan containing Knoevenagel products. It not only reduces the aliphatic chain but also caused the hydrogenation and opening of the furan ring. Furan ring is subjected to successive hydrogenation of carbons starting from the α -carbon, adjacent β -carbon, second β -carbon, and then the second α -carbon to form THF. Ring-opening is induced upon the reduction of the first α -carbon of

furan. Hence, hydrofuran is the reaction intermediate of furan ring hydrogenation (Wang *et al.*, 2014).

2.5.16. Béchamp reduction

Béchamp reduction reaction involves the reduction of an aromatic NO₂ group to the corresponding amine in the presence of Fe and diluted acid. Reducing the nitro group would indicate the impact of the presence of a nitro group on the antimicrobial activity (Chapter 3).



Scheme 2. 3. Béchamp reduction of NO₂ group

2.5.16.1. Attempted syntheses

2.5.16.1.1. Attempts to synthesise 5-(4-((4-Aminobenzyl)oxy)benzylidene)pyrimidine-2,4,6(1H,3H,5H)-trione (2.50)

Compound 2.14 (0.3 g, 0.9 mmol) was added to a round bottom flask, followed by the addition of 4 equivalents of iron (0.221 g, 3.9 mmol). Water (35 ml) and conc. HCl (15 ml) was added dropwise in the first 30 minutes. The reaction was set for 8 hours, the reaction mixture was then cooled down at room temperature. The mixture was poured into a beaker, the solution was neutralised with diluted NaOH to form ferric hydroxide (Fe (OH)₃) sludge. Ethyl acetate (75 ml) was added, and the mixture was stirred (5 minutes) followed by the extraction of the organic phase. The solvent was dried over MgSO₄, evaporated and dried under vacuum overnight.

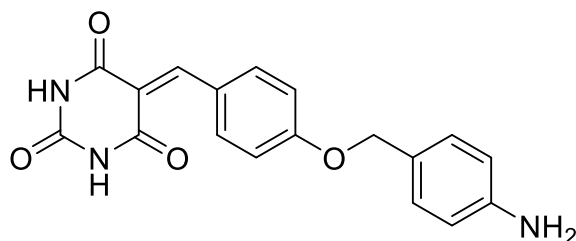


Figure 2. 74. Compound 2.50

2.5.17. Discussion

The C=C bond of the benzylidene barbiturate derivatives is sensitive in the presence of acids and bases because of the conjugated effects on the C=C-C=O functional group. As a result, the Knoevenagel product can be converted to the starting materials if NaOH is charged in the solution (Yang *et al.*, 2022). Hydrolysis was proven in our study as the aldehyde fragment of the Knoevenagel product was extracted from the organic phase as proven by ^1H NMR. Another study stated that treating barbituric acid with hot bases can easily hydrolyse the bonds between NH and C=O producing ammonia (NH_3), carbon dioxide (CO_2) and an alkali malonate (Aljaafari *et al.*, 2022) (Figure 2.75).

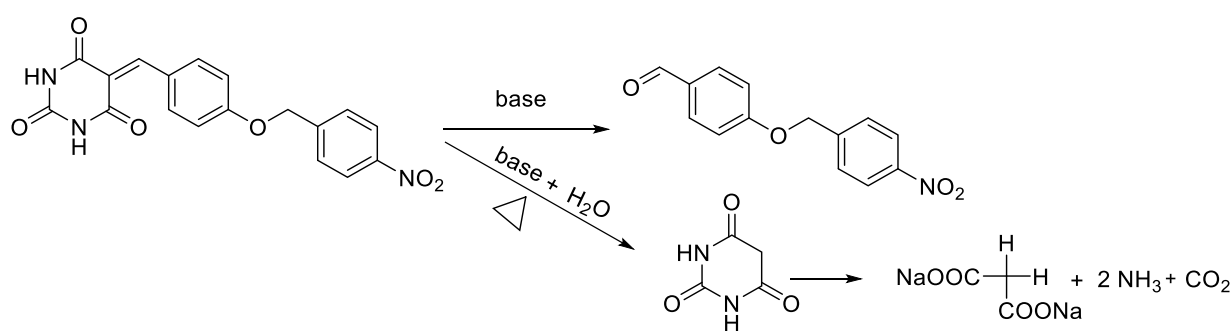


Figure 2.75. Base-hydrolysis of Knoevenagel products

2.5.18. Mechanism of action

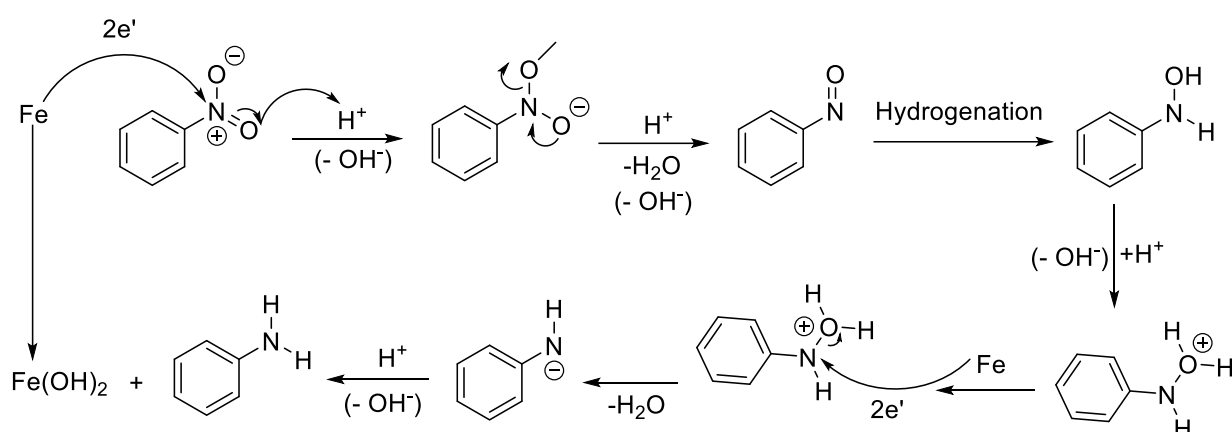


Figure 2.76. Béchamp reduction mechanism

Hydrogen ion is liberated from the reaction of acid and water in the first step of the Béchamp reaction. HCl and formic acid are commonly used acids in this reaction. Formic acid is preferable over HCl as the halogen possessed by the acid is quite reactive and therefore may react with the aromatic ring (Popat & Padhiyar, 2013). The NO₂ group is then reduced to nitroso group, which undergoes hydrogenation forming a hydroxylamino group prior to further reduction to amine (Wang, 2010).

2.5.19. Synthesis of Meldrum's acid derivatives

2.5.19.1. 5-[(4-Methoxyphenyl)methylene]-2,2-dimethyl-1,3-dioxane-4,6-dione (2.51)

Anisaldehyde (0.47 g, 3.46 mmol) was left to dissolve in (25 ml) ethanol, followed by the addition of one equivalent of Meldrum's acid (0.5 g, 3.46 mmol). The mixture was set at reflux temperature (8 h), and the solvent was then evaporated under vacuum to give a yellow oil. The crude was purified using flash column chromatography and the desired compound was eluted with dichloromethane/ethyl acetate (24:1). The solvents were evaporated under pressure to give bright yellow powder of 2.51 (0.6 g, 2.5 mmol, 67 %).

Second attempt for yield optimisation:

Anisaldehyde (0.944 g, 7.34 mmol) was suspended in (15 ml) of distilled water, followed by the addition of one equivalent of Meldrum's acid (1 g, 7.34 mmol). The mixture was set to reflux (5 h), followed by hot filtration and drying the residue overnight under vacuum to give **2.51** (1.4 g, 5.34 mmol, 77 %).

Molecular Formula C₁₄H₁₄O₅; R_f (dichloromethane/ethyl acetate, 4:1): 0.8; melting point: 110-112 °C.

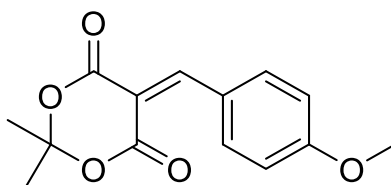


Figure 2. 77. Compound 2.51

¹H NMR (400 MHz, DMSO) δ= 8.32 (s, 1H, -CH), 8.24-8.22 (d, *J*= 8.9 Hz, 2H, ArHs), 7.11-7.08 (d, *J*= 8.9 Hz, 2H, ArHs), 3.88 (s, 3H, -OCH₃), 1.74 (s, 6H, -CH₃ X2) ppm. ¹³C APT NMR (400 MHz, DMSO) δ= 164.48 (C=O), 163.59 (C=O), 160.56 (C=CH), 157.07 (C=CH), 137.55 (ortho

ArCs), 124.90 ($\underline{\text{C}}\text{-C}_2\text{H}_6$), 114.77 (meta ArCs), 111.93 ($\underline{\text{C}}\text{-OCH}_3$), 104.60 (CH $\underline{\text{C}}$), 56.28 (O $\underline{\text{C}}\text{H}_3$), 27.38 ($\underline{\text{C}}\text{H}_3$ X2) ppm.

IR (ATR): ν = 1573 (s, cyclic alkene), 1709 (s, C=O), 2848 (w, CH aldehydic) 2997 (w, CH aliphatic), 3107 (w, CH aromatic).

2.5.19.2. [(E)-3-(4-Methoxyphenyl)prop-2-enylidene]-2,2-dimethyl-1,3-dioxane-4,6-dione (2.52)

p-Methoxycinnamaldehyde (0.56 g, 3.45 mmol) was left to dissolve in (25 ml) ethanol, followed by the addition of one equivalent of Meldrum's acid (0.5 g, 3.46 mmol). The mixture was heated at reflux temperature (3 h), followed by hot filtration. The residue was added to hexane (30 ml) to form a slurry at room temperature for 20 minutes to remove the hexane-soluble aldehyde impurities. The product was collected after filtration and left to dry under vacuum to give an orange powder of compound **2.52** (0.9 g, 3.45 mmol, 86%).

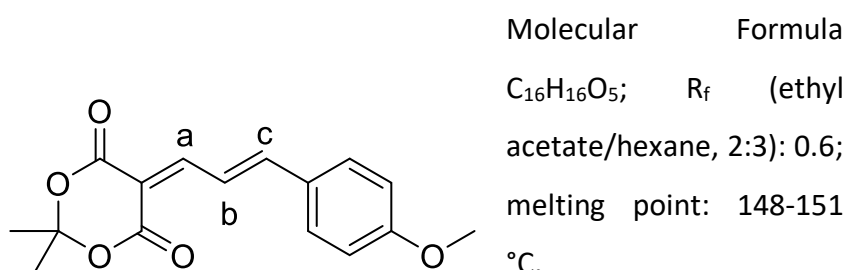


Figure 2. 78. Compound 2.52

^1H NMR (400 MHz, DMSO- d_6): δ = 8.18-8.15 (d, J = 11.9 Hz, 1H, H a), 8.07-8.00 (dd, J = 11.9, 15.0 Hz, 1H, H b), 7.83-7.79 (d, J = 15.0 Hz, 1H, H c), 7.70-7.68 (d, J = 8.8 Hz, 2H, ortho ArHs), 7.08-7.06 (d, J = 8.8 Hz, 2H, meta ArHs), 3.84 (s, 3H, -O $\underline{\text{C}}\text{H}_3$), 1.70 (s, 6H, - $\underline{\text{C}}\text{H}_3$ X2) ppm. ^{13}C APT NMR (101 MHz, DMSO- d_6): δ =162.9 (C=O), 162.8 (C=O), 160.9 ($\underline{\text{C}}\text{=CH}$), 158.2 (C a), 155.4 (C b), 131.7 (C c), 128.1 (CH=CH $\underline{\text{C}}$), 122.2 (ortho ArCs), 115.4 (meta ArCs), 110.0 ($\underline{\text{C}}\text{-C}_2\text{H}_6$), 104.8 ($\underline{\text{C}}\text{-OCH}_3$), 56.0 (O $\underline{\text{C}}\text{H}_3$), 27.4 ($\underline{\text{C}}\text{H}_3$ X2) ppm.

IR (ATR): ν = 1556 (m, cyclic alkene), 1705 (s, C=O), 2941 (w, CH aliphatic), 3051 (w, CH aromatic).

2.5.19.3. 2,2-dimethyl-5-[(E)-3-(4-nitrophenyl)prop-2-enylidene]-1,3-dioxane-4,6-dione (2.53)

p-Nitrocinnamaldehyde (0.614 g, 3.46 mmol) was suspended in (20 ml) distilled water, followed by the addition of one equivalent of Meldrum's acid (0.5 g, 3.46 mmol). The mixture was heated to reflux (6 h), followed by hot filtration. The residue was further washed with hexane (20 ml), where the product was dried overnight under vacuum to give **2.53** (0.57 g, 1.88 mmol, and 54%).

Molecular Formula C₁₅H₁₃NO₆; R_f (ethyl acetate/hexane, 2:3): 0.5; melting point: 149-152 °C.

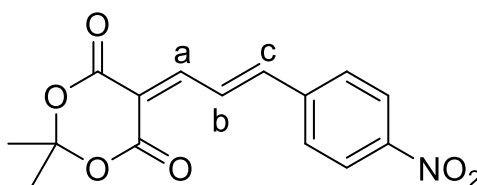


Figure 2. 79. Compound 2.53

¹H NMR (400 MHz, DMSO) δ= 8.32-8.29 (d, *J*= 2.30 Hz, 2H, meta ArHs), 8.24-8.20 (d, *J*= 2.1 Hz, 1H, ortho ArHs), 8.20-8.17 (d, *J*= 11.043 Hz, 1H, H_c) 7.96-7.89 (m, 3H, H_a and H_b), 1.73 (s, 6H, -CH₃ X2) ppm.

¹³C APT NMR (101 MHz, DMSO-d₆): δ= 162.37 (C=O), 160.50 (C=O), 155.75 (meta ArCs), 150.46 (C_a), 148.80 (C-NO₂), 141.46 (C=CH), 130.17 (C_c), 127.88 (c_b), 124.82 (ortho ArCs), 114.66 (C-C₂H₆), 105.41 (CH=CH-C), 27.60 (CH₃ X2) ppm.

IR (ATR): *ν* = 1520 (s, cyclic alkene), 1597 (m, NO₂), 1716 (s, C=O), 2998 (w, CH aliphatic), 3077 (w, CH aromatic).

2.5.19.4. 5-[(E)-3-(2-Furyl)prop-2-enylidene]-2,2-dimethyl-1,3-dioxane-4,6-dione (2.54)

2-Furanacrolein (0.42 g, 3.43 mmol) was dissolved ethanol (20 ml), followed by the addition of one equivalent of Meldrum's acid (0.5 g, 3.46 mmol). The mixture was heated at reflux temperature (3 h), followed by hot filtration. The residue was collected and purified via flash column chromatography using dichloromethane/ethyl acetate (93:7) to give brown crystals of **2.54** (0.54 g, 2.17 mmol, 63%).

Molecular Formula $C_{13}H_{12}O_5$; R_f (dichloromethane/ethyl acetate, 4:1): 0.9; melting point: 134-137 °C.

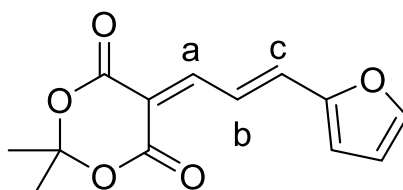


Figure 2. 80. Compound 2.54

^1H NMR (400 MHz, DMSO) δ = 8.19-8.16 (d, J = 12.2 Hz, 1H, H a), 8.038-8.0384 (d, J = 1.4 Hz, 1H, ArH 5), 7.96-7.89 (dd, J = 15.0, 12.2 Hz, 1H, H b), 7.70-7.66 (d, J = 15.0 Hz, 1H, H c), 7.138-7.13 (d, J = 15.0 Hz, 1H, ArH 3), 6.76-7.65 (dd, J = 5.3, 1.7 Hz, 1H, ArH 4), 1.69 (s, 6H, -CH₃) ppm.

^{13}C APT NMR (101 MHz, DMSO- d_6): δ = 162.75 (C=O), 160.94 (C=O), 156.97 (C a), 151.98 (C=CH), 148.75 (C 5), 139.75 (C b), 122.01 (C c), 119.98 (C 3), 114.45 (C 4), 110.91 (C=C₂H₆), 104.91 (C 2), 27.49 (CH₃ X2) ppm.

IR (ATR): ν = 1624 (s, cyclic alkene), 1703 (s, C=O), 2841 (m, CH aliphatic), 3062 (m, CH aromatic).

2.5.19.5. 2,2-Dimethyl-5-[(E)-3-phenylprop-2-enylidene]-1,3-dioxane-4,6-dione (2.55)

Cinnamaldehyde (0.458 g, 3.46 mmol) was left to dissolve in (20 ml) ethanol, followed by the addition of one equivalent of Meldrum's acid (0.5 g, 3.46 mmol). The mixture was heated at a reflux temperature (10 h). Ethanol was removed under vacuum and the crude mixture was purified by flash column chromatography using dichloromethane/petroleum ether (3:22). The desired compound was collected, and the solvent was evaporated under pressure to give a yellow needle crystal of **2.55** (0.35 g, 0.13 mmol, 39.4).

Second attempt for yield optimisation:

Cinnamaldehyde (0.458 g, 3.46 mmol) was suspended in (15 ml) of distilled water, followed by the addition of one equivalent of Meldrum's acid (0.5 g, 3.46 mmol). The mixture was heated at reflux temperature (3 h), followed by hot filtration and drying the product overnight under vacuum to give **2.55** (0.41 g, 1.58 mmol, 45.8%).

Molecular Formula $C_{15}H_{14}O_4$; R_f (ethyl acetate/hexane, 2:3): 0.71; melting point: 89-92 °C.

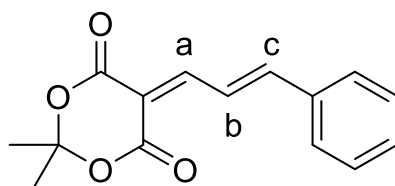


Figure 2. 81. Compound 2.55

^1H NMR (400 MHz, DMSO) δ = 8.22-8.11 (m, 2H, H b and H a), 7.86-7.83 (d, J = 14.2 Hz, 1H, H c), 7.72-7.70 (m, 2H, ArHs), 7.52-7.49 (m, 3H, ArHs), 1.71 (s, 6H, -CH₃) ppm.

^{13}C APT NMR (101 MHz, DMSO- d_6): δ = 162.66 (C=O), 160.76 (C=O), 157.43 (C a), 154.65 (C b), 135.39 (C=CH), 132.17 (C c), 129.83 (ArC), 129.39 (ArC), 124.42 (ArC), 112.19 (C=C₂H₆), 105.11 (CH=CH-C), 27.54 (CH₃ X2) ppm.

IR (ATR): ν = 1563 (s, cyclic alkene), 1597 (m, N-O), 1708 (s, C=O), 2979 (w, CH aliphatic), 3062(w, CH aromatic).

2.5.19.6. 5-(2-Furylmethylene)-2,2-dimethyl-1,3-dioxane-4,6-dione (2.56)

2-Furaldehyde (0.67 g, 7.34 mmol) was suspended in (20 ml) distilled water, followed by the addition of one equivalent of Meldrum's acid (1 g, 7.34 mmol). The mixture was set at reflux temperature (5 h), the crude was purified by means of flash column chromatography and the desired compound was extracted using ethyl acetate/ petroleum ether (1:9). The solvents were evaporated under pressure to give an ash brown powder of **2.56** (1.42 g, 4.2 mmol, 60.7%).

Molecular Formula $\text{C}_{11}\text{H}_{10}\text{O}_5$; R_f (ethyl acetate/ petroleum ether, 1:4): 0.75; melting point: 75-77 °C.

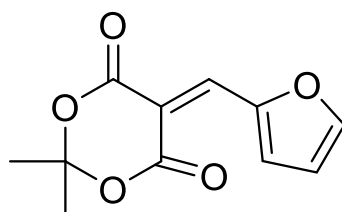


Figure 2. 82. Compound 2.56

^1H NMR (400 MHz, DMSO) δ = 8.33-8.32 (d, J = 1.2 Hz, 2H, H 5), 8.27-8.26 (d, J = 3.8 Hz, 2H, H 3), 8.13 (s, 1H, C=H), 6.96-6.95 (dddd, 1H, H 4), 1.72 (s, 6H, -CH₃ X 2) ppm.

^{13}C APT NMR (101 MHz, DMSO- d_6): δ = 163.07 ($\underline{\text{C}}=\text{O}$), 160.12 ($\underline{\text{C}}=\text{O}$), 152.41 ($\underline{\text{C}}_5$), 149.83 ($\underline{\text{C}}=\text{CH}$), 139.94 ($\underline{\text{C}}_3$), 128.09 ($\text{C}=\underline{\text{C}}\text{H}$), 115.96 (C_4), 108.34 ($\underline{\text{C}}-\text{C}_2\text{H}_6$), 104.95 ($\underline{\text{C}}_2$), 27.42 ($\underline{\text{C}}\text{H}_3 \times 2$) ppm.

IR (ATR): ν = 1582 (s, cyclic alkene), 1702 (s, C=O), 3002 (w, CH aliphatic), 3117 (w, CH aromatic).

2.5.19.7. (E)-2,2-Dimethyl-5-(3-(5-nitrofuran-2-yl)allylidene)-1,3-dioxane-4,6-dione (2.57)

5- Nitrofuracrolein (0.2 g, 1.12 mmol) was suspended in (20 ml) of distilled water, followed by the addition of one equivalent of Meldrum's acid (0.16 g, 1.11 mmol). The mixture was heated at reflux temperature (7 h), followed by hot filtration . The residue was collected, washed with hexane, and dried overnight under vacuum to give a brown powder of **2.57** (0.174 g, 0.59 mmol, 73.7 %).

Molecular Formula $\text{C}_{20}\text{H}_{18}\text{O}_5$; R_f (ethyl acetate/hexane, 2:3): 0.6; melting point: 205-208 °C.

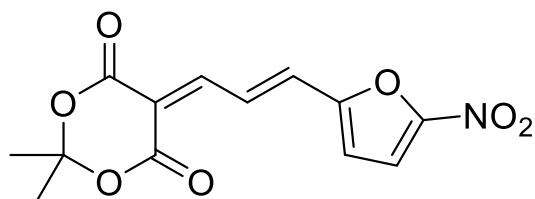


Figure 2. 83. Compound 2.57

^1H NMR (400 MHz, DMSO) δ = 8.20-8.17 (d, J = 12.0 Hz, 1H, $\underline{\text{H}}_a$), 8.13-8.06 (dd, J = 14.8, 12.00 Hz, 1H, $\underline{\text{H}}_b$), 7.81-7.80 (d, J = 3.9 Hz, 1H, $\underline{\text{H}}_4$), 7.73-7.69 (d, J = 14.8 Hz, 1H, $\underline{\text{H}}_c$), 7.38-7.37 (d, J = 3.9 Hz, 1H, $\underline{\text{H}}_3$), 1.72 (s, 6H, $-\underline{\text{C}}\text{H}_3$) ppm.

^{13}C APT NMR (101 MHz, DMSO- d_6): δ = 162.27 ($\underline{\text{C}}=\text{O}$), 160.51 ($\underline{\text{C}}=\text{O}$), 154.46 ($\underline{\text{C}}_a$), 153.36 ($\underline{\text{C}}-\text{NO}_2$), 1533.30 ($\underline{\text{C}}=\text{CH}$), 136.36 (C_b), 127.44 (C_4), 119.40 (C_c), 115.31 (C_3), 115.12 ($\underline{\text{C}}-\text{C}_2\text{H}_6$), 105.46 ($\underline{\text{C}}_2$), 27.60 ($\underline{\text{C}}\text{H}_3 \times 2$) ppm.

IR (ATR): ν = 1586 (s, cyclic alkene), 1716 (s, C=O), 2995 (w, CH aliphatic), 3053 (w, CH aromatic).

2.5.19.8. 2,2-Dimethyl-5-((5-nitrothiophen-2-yl)methylene)-1,3-dioxane-4,6-dione (2.58)

5- Nitro-2-thiophenecarboxyaldehyde (0.545 g, 3.46 mmol) was left to dissolve in (35 ml) of ethanol, followed by the addition of one equivalent of Meldrum's acid (0.5 g, 3.46 mmol).

The mixture was heated at reflux temperature (10 h). Ethanol was evaporated under vacuum to give a brown oil. The crude mixture was purified by flash column chromatography ethyl acetate/hexane (1:9) to give a canary yellow powder of compound **2.58** (0.23 g, 0.81 mmol, 23%).

Second attempt for yield optimisation:

5-Nitro-2-thiophenecarboxyaldehyde (0.545 g, 3.46 mmol) was suspended in (15 ml) distilled water, followed by the addition of one equivalent of Meldrum's acid (0.5 g, 3.46 mmol). The mixture was heated at reflux temperature (4 h), followed by hot filtration and drying the product overnight under vacuum to give (0.84 g, 2.96 mmol, 86%).

Molecular Formula $C_{11}H_9NO_6S$; R_f (ethyl acetate/hexane, 2:3): 0.67; melting point: 218-220 °C.

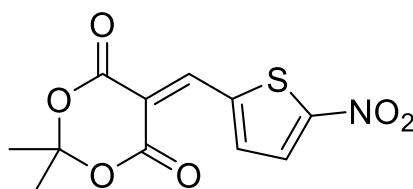


Figure 2. 84. Compound 2.58

1H NMR (400 MHz, DMSO- d_6): δ = 8.71 (s, 1H, =CH), 8.24 (broad s, 2H, H 4 and H 3), 1.75 (s, 6H, -CH₃ X2) ppm. ^{13}C APT NMR (101 MHz, DMSO- d_6): 161.98 (C=O), 161.41 (C=O), 158.31 (=CH), 147.80 (C=CH), 143.97 (C 4), 140.03 (C 5), 129.02 (C 3), 113.21 (C-C₂H₆), 105.96 (C 2), 27.57 (CH₃ X2) ppm.

IR (ATR): ν = 1590 (s, cyclic alkene), 1704 (s, C=O), 3002 (w, CH aliphatic), 3114 (m, CH aromatic).

2.5.19.9. 2,2-Dimethyl-5-(thiophen-2-ylmethylene)-1,3-dioxane-4,6-dione (2.59)

2-Thiophenecarboxaldehyde (0.389 g, 3.46 mmol) was suspended in distilled water (25 ml), followed by the addition of one equivalent of Meldrum's acid (0.5 g, 3.46 mmol). The mixture was set at reflux temperature (4 h), followed by hot filtration. The residue was collected, washed with hexane, and dried overnight under vacuum to give the buff powder of compound **2.59** (0.7 g, 2.94 mmol, 84.7%).

Molecular Formula $C_{11}H_{10}O_4S$; R_f (ethyl acetate/hexane, 2:3): 0.68; melting point: 179-181 °C.

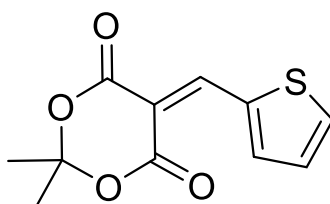


Figure 2. 85. Compound 2.59

1H NMR (400 MHz, DMSO) δ = 8.71 (s, 1H, =CH), 8.38-8.37 (d, J = 4.7 Hz, 1H, H 5), 8.27-8.26 (d, J = 3.8 Hz, 1H, H 3), 7.40-7.38 (t, J = 8.8 Hz, 1H, H 4), 1.72 (s, 6H, -CH₃) ppm. ^{13}C APT NMR (400 MHz, DMSO) δ = 163.14 (C=O), 161.25 (C=O), 149.11 (C=CH), 147.03 (C 5), 143.31 (C 3), 136.30 (C=CH), 129.10 (C 4), 107.44 (C-C₂H₆), 104.95 (C 2), 27.38 (CH₃ X2) ppm.

IR (ATR): ν = 1557 (s, cyclic alkene), 1711 (s, C=O), 2978 (w, CH aliphatic), 3090 (m, CH aromatic).

2.5.19.10. (E)-2,2-Dimethyl-5-(3-(5-nitrothiophen-2-yl)allylidene)-1,3-dioxane-4,6-dione (2.60)

(5-Nitro-2-thienyl)-2-propenal (0.04 g, 0.22 mmol) was suspended in distilled water (30 ml), followed by the addition of one equivalent of Meldrum's acid (0.032 g, 0.22 mmol). The mixture was heated at reflux temperature (3 h), followed by hot filtration. The product was collected and dried overnight under vacuum to give brown crystals of **2.60** (0.052 g, 0.17 mmol, 77.6 %).

Molecular Formula $C_{13}H_{11}O_6S$; R_f (ethyl acetate/hexane, 1:4): 0.83; melting point: 200-203 °C.

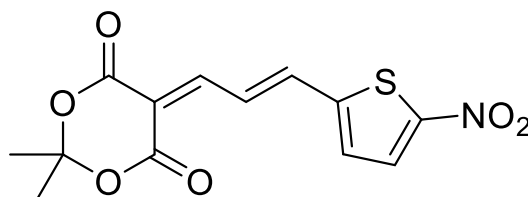


Figure 2. 86. Compound 2.60

^1H NMR (400 MHz, DMSO) δ = 8.16-7.96 (m, 4H, H a, H b, H 4 and H c), 7.64-7.63 (d, J = 2.0 Hz, 1H, H 3), 1.72 (s, 6H, -CH₃) ppm.

^{13}C APT NMR (101 MHz, DMSO- d_6): δ = 162.27 (C=O), 160.52 (C=O), 154.70 (C a), 152.79 (C 5), 146.84 (C=CH), 143.28 (C b), 132.11 (C 4), 131.39 (C c), 127.82 (C 3), 114.73 (C-C₂H₆), 105.47(C 2), 27.62 (CH₃ X2) ppm.

IR (ATR): ν = 1588 (m, cyclic alkene), 1721 (s, C=O), 2921 (s, CH aliphatic), 3054 (w, CH aromatic).

2.5.19.11. 5-[(4-Benzyloxyphenyl)methylene]-2,2-dimethyl-1,3-dioxane-4,6-dione (2.61)

4-Benzyloxybenzaldehyde (1.47 g, 7.34 mmol) was suspended in (20 ml) distilled water, followed by the addition of one equivalent of Meldrum's acid (1 g, 7.34 mmol). The mixture was heated at reflux temperature (6 h). After filtration, the crude was purified using flash column chromatography and the desired compound was extracted at ethyl acetate/petroleum ether (1:4). The solvents were evaporated under vacuum to give a buff powder of compound **2.61** (1.42 g, 4.2 mmol, 60.7%).

Molecular Formula $\text{C}_{20}\text{H}_{18}\text{O}_5$; R_f (ethyl acetate/ petroleum ether, 1:4): 0.6; melting point: >300.

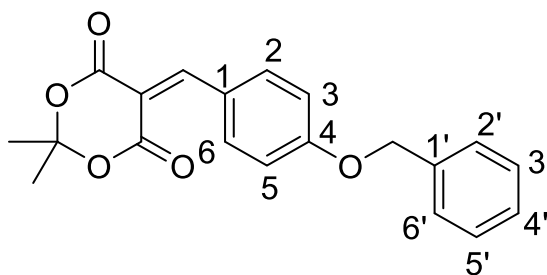


Figure 2. 87. Compound 2.61

^1H NMR (400 MHz, DMSO- d_6): δ = 8.31 (s, 1H, C=CH), 8.23-8.21 (d, J = 8.9 Hz, 2H, 3, 5 ArHs), 7.48-7.47 (d, J = 7.0 Hz, 2H, 2', 6' ArHs), 7.43-7.34 (m, 3H, 3', 4', 5' ArHs), 7.18-7.16 (d, J = 9.9 Hz, 2H, 2, 6 ArHs), 5.26 (s, 2H, CH₂), 1.74 (s, 6H, -CH₃ X2) ppm.

δ ^{13}C APT NMR (101 MHz, DMSO-d₆): δ = 163.56 ($\underline{\text{C}}=\text{O}$), 163.50 ($\underline{\text{C}}=\text{O}$), 160.55 ($\underline{\text{C}}=\text{CH}$), 156.98 ($\underline{\text{C}}=\text{CH}$), 137.48 (C3, C5), 136.71 (C 4), 129.00 (C2', C6'), 128.59 (C 4'), 128.35 (C3', C5'), 125.05 (C1'), 115.51 (C2, C6), 112.08 (C1), 104.62 ($\underline{\text{C}}-\text{C}_2\text{H}_6$), 70.20 ($\underline{\text{O}}\text{CH}_2$), 27.38 ($\underline{\text{C}}\text{H}_3$ X2) ppm.

Spectroscopic data were consistent with the literature values (Forst & Hartely, 2009).

2.5.19.12. 2,2-Dimethyl-5-[(5-nitro-2-furyl)methylene]-1,3-dioxane-4,6-dione (2.62)

5- Nitrofuraldehyde (0.978 g, 7.34 mmol) was suspended in (15 ml) distilled water, followed by the addition of one equivalent of Meldrum's acid (1 g, 7.34 mmol). The mixture was heated at reflux temperature (3 h), followed by hot filtration where the residue was collected to form a hexane slurry. The residue was left to dry under vacuum overnight to give a black powder of compound **2.62** (1.4 g, 5.34 mmol, 77%).

Molecular Formula $\text{C}_{11}\text{H}_9\text{NO}_7$; R_f (dichloromethane/ethyl acetate, 3:1): 0.8; melting point: >300 °C.

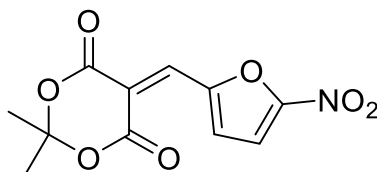


Figure 2. 88. Compound 2.62

^1H NMR (400 MHz, DMSO) δ = 8.16-8.15 (d, J = 4.0 Hz, 1H, ArHs), 8.03 (s, 1H, = $\underline{\text{C}}\text{H}$), 7.86-7.85 (d, J = 4.0 Hz, 1H, ArHs), 1.75 (s, 6H, - $\underline{\text{C}}\text{H}_3$ X2) ppm.

^{13}C APT NMR (400 MHz, DMSO) δ = 162.06 ($\underline{\text{C}}=\text{O}$), 159.45 ($\underline{\text{C}}=\text{O}$), 153.64 ($\underline{\text{C}}-\text{NO}_2$), 149.77 ($\underline{\text{C}}=\text{CH}$), 137.80 ($\underline{\text{C}}\text{H}=\text{C}-\text{NO}_2$), 126.54 ($\underline{\text{C}}\text{H}-\text{CH}$), 116.27 ($\text{CH}-\underline{\text{C}}$), 114.59 ($\text{C}=\underline{\text{C}}\text{H}$), 105.79 ($\underline{\text{C}}-\text{C}_2\text{H}_6$), 27.60 ($\underline{\text{C}}\text{H}_3$ X2) ppm.

IR (ATR): ν = 1616 (m, cyclic alkene), 1703 (s, C=O), 2862 (m, CH aliphatic), 3054 (m, CH aromatic).

2.5.19.13. 5-(2-Furylmethyl)-2,2-dimethyl-1,3-dioxane-4,6-dione and its tautomeric form 5-(Furan-2-ylmethyl)-6-hydroxy-2,2-dimethyl-1,3-dioxan-4-one (2.63)

Three equivalents of NaBH_4 (0.1 g, 2.64 mmol) were added portion-wise to an ethanol (20 ml) suspended Knoevenagel product **2.56** (0.2 g, 0.9 mmol). The reaction mixture was initially left in an ice bath (0 °C) for 15 minutes and then stirred overnight at room temperature. The pH of the mixture was adjusted to 4-5 with 4M aqueous HCl. The desired

compound was extracted from the organic phase i.e., petroleum (3x30 ml), rinsed with a saturated aqueous solution of NaCl, dried with anhydrous MgSO₄, filtered and the filtrate was collected. The solvent was removed at vacuum and the obtained product was dried under vacuum to give a brown powder of **2.63** (0.065 g, 0.79 mmol, 32 %).

Molecular Formula C₁₁H₁₂O₅; R_f (butanol/acetic acid/water, 4:1:5): 2 spots 0.77 and 0; melting point: >300 °C.

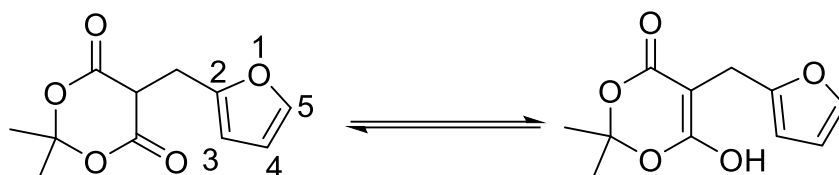


Figure 2. 89. Compound 2.63

¹HNMR (400 MHz, DMSO) δ = 7.488-7.485 (d, J = 1.0 Hz, 1H, H5), 6.52 (broad s, 2H, CH-CH₂), 6.35-6.33 (dd, J = 3.0, 1.9 Hz, 1H, H4), 6.09-6.08 (d, J = 2.6 Hz, H3), 4.84-4.81 (t, J = 9.6 Hz, 1H, CH-CH₂), 1.82 (s, 3H, -CH₃), 1.65 (s, 3H, -CH₃) ppm.

¹³C APT NMR (101 MHz, DMSO-d₆): δ = 165.76 (C=O X2), 111.04 (C5), 107.95 (C4), 106.85 (C3), 105.45 (C-C₂H₆), 45.20 (CH-CH₂), 28.29 (CH₃), 26.40 (CH₃), 24.85 (CH-CH₂) ppm.

IR (ATR): ν = 1704 (s, C=O), 2928 (w, CH aliphatic), 3198 (m, OH enol form).

2.5.19.14. 5-[(E)-3-(4-Methoxyphenyl)allyl]-2,2-dimethyl-1,3-dioxane-4,6-dione (**2.64**)

Three equivalents of NaBH₄ (0.098 g, 2.6 mmol) were added portion-wise to ethanol (20 ml) suspended Knoevenagel product **2.52** (0.25 g, 0.87 mmol). The reaction mixture was initially left in an ice bath (0 °C) for 15 minutes and stirred overnight at room temperature. The pH of the mixture was adjusted to 4-5 with 4M aqueous HCl. The desired compound was extracted from the organic phase i.e., ethyl acetate (3x30 ml) after drying it over anhydrous MgSO₄ and collecting the filtrate. The residual Knoevenagel product was washed away with hexane, and ethanol insoluble impurities were removed upon washing the residue with ethanol (2x10ml). Yellow powder of compound **2.64** (0.12 g, 0.489 mmol, 48 %) was obtained.

Molecular Formula C₁₆H₁₈O₅; R_f (butanol/acetic acid/water, 4:1:5): 0.9; melting point: 103-106 °C. The compound was reported by Hayashi *et al.*, 2011.

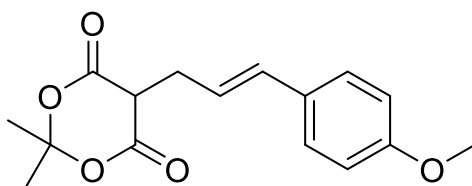


Figure 2. 90. Compound 2.64

^1H NMR (400 MHz, DMSO) δ = 7.30-7.28 (d, J = 8.7 Hz, 2H, ortho ArHs), 6.88-6.86 (d, J = 8.7 Hz, 2H, meta ArHs), 6.46-6.42 (d, J = 15.8 Hz, 1H, CH-Ph), 6.09-6.02 (dt, J = 15.8, 6.9 Hz, 1H, $\text{CH}_2\text{-CH}$), 4.69-4.66 (t, J = 4.9 Hz, 1H, CH-CH_2), 3.74 (s, 3H, $-\text{OCH}_3$), 2.83-2.80 (t, J = 5.4 Hz, 2H, CH-CH_2), 1.81 (s, 3H, $-\text{CH}_3$), 1.66 (s, 3H, $-\text{CH}_3$) ppm.

^{13}C APT NMR (101 MHz, DMSO- d_6): δ =166.00 (C=O), 132.56 (ortho ArCs), 129.90 (CH-C), 127.65 (meta ArCs), 123.49 (CH=CH-Ph), 114.46 (CH=CH-Ph), 144.36 (C-OCH_3), 105.36 ($\text{C-C}_2\text{H}_6$), 55.54 (CH-CH_2), 46.42 (OCH_3), 29.30 (CH-CH_2), 28.35 (CH_3), 26.39 (CH_3) ppm.

IR (ATR): ν = 1510 (m, cyclic alkene), 1738 (s, C=O), 2838 (w, aldehydic CH), 2933 (w, CH aliphatic), 3030 (w, CH aromatic).

2.5.19.15. 2,2-Dimethyl-5-[(E)-3-(4-nitrophenyl)allyl]-1,3-dioxane-4,6-dione (2.65)

Three equivalents of NaBH_4 (0.075 g, 1.98 mmol) were added portion-wise to ethanol (20 ml) suspended Knoevenagel product **2.53** (0.2 g, 0.65 mmol). The reaction mixture was initially left in an ice bath (0 °C) for 15 minutes and stirred overnight at room temperature. The pH of the mixture was adjusted to 4-5 with 4M aqueous HCl. The desired compound was extracted from the organic phase i.e., ethyl acetate (3X30 ml), rinsed with a saturated aqueous solution of NaCl, dried with anhydrous MgSO_4 , filtered and the filtrate was collected. The solvent was removed under vacuum and the residue obtained was dried under vacuum to give a white powder of compound **2.65** (0.14 g, 0.48 mmol, 68.3 %).

Molecular Formula $\text{C}_{15}\text{H}_{15}\text{NO}_6$; R_f (butanol/acetic acid/water, 4:1:5): 0.91; melting point: 126-130 °C.

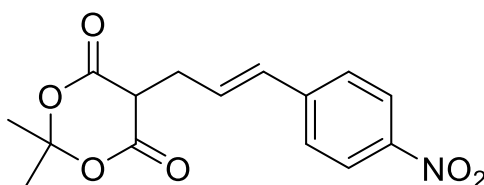


Figure 2. 91. Compound 2.65

^1H NMR (400 MHz, DMSO) δ = 8.18-8.16 (d, J = 8.8 Hz, 2H, meta ArHs), 7.66-7.64 (d, J = 8.8 Hz, 2H, ortho ArHs), 6.70-6.66 (d, J = 16.0 Hz, 1H, CH=CH), 6.59-6.51 (dt, J = 15.9, 6.7 Hz, 1H, CH=CH-Ph), 4.75-4.72 (t, J = 5.1 Hz, 1H, CH-CH₂), 2.91-2.89 (t, J = 5.5 Hz, 2H, CH-CH₂), 1.83 (s, 3H, -CH₃), 1.68 (s, 3H, -CH₃) ppm.

^{13}C APT NMR (101 MHz, DMSO-d₆): δ = 165.85 (C=O), 146.63 (C-NO₂), 144.14 (CH=CH-C), 132.34 (CH=CH-Ph), 130.91 (CH=CH-Ph), 127.38 (meta ArCs), 124.40 (ortho ArCs), 105.46 (C-C₂H₆), 46.05 (CH-CH₂), 29.29 (CH-CH₂), 28.39 (CH₃), 26.26 (CH₃) ppm.

IR (ATR): ν = 1590 (m, cyclic alkene), 1736 (s, C=O), 2949 (w, CH aliphatic), 3112 (m, CH aromatic).

MS (+ESI) m/z = Found 306.0972 [M+H]⁺; calculated for C₈H₇N₄O₄S 306.0978; -2 ppm.

2.5.19.16. 5-[(E)-3-(2-Furyl)allyl]-2,2-dimethyl-1,3-dioxane-4,6-dione (2.66)

Three equivalents of NaBH₄ (0.114 g, 3.02 mmol) were added portion-wise to ethanol (20 ml) suspended Knoevenagel product **2.54** (0.25 g, 1 mmol). The reaction mixture was initially left in an ice bath (0 °C) for 15 minutes and stirred overnight at room temperature. The pH of the mixture was adjusted to 4-5 with 4M aqueous HCl. The desired compound was extracted from the organic phase i.e., petroleum ether (3x30 ml), rinsed with a saturated aqueous solution of NaCl, dried with anhydrous MgSO₄, filtered and the filtrate was collected. The solvent was removed at low pressure and the residue obtained was dried under vacuum to give dark brown crystals of **2.66** (0.23 g, 0.92 mmol, 90.6 %).

Molecular Formula C₁₃H₁₂O₅; R_f (butanol/acetic acid/water, 4:1:5): 0.85; melting point: 107-110 °C. The compound was reported by Hayashi *et al.*, 2011.

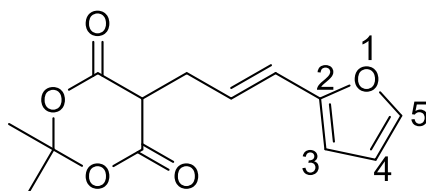


Figure 2. 92. Compound 2.66

^1H NMR (400 MHz, DMSO) δ = 7.57-7.56 (d, J = 1.5 Hz, 1H, CH=CH-), 6.45-6.44 (dd, J = 2.6, 1.8 Hz, 1H, H 4), 6.40-6.34 (m, 2H, H 5, H 3), 6.08-6.01 (dt, J = 15.8, 7.2, 1H, CH₂-CH=CH-), 4.72-

4.69 (t, $J = 4.9$ Hz, 1H, CH-CH_2), 2.82-2.79 (t, $J = 6.5$ Hz, 2H, CH-CH_2), 1.81 (s, 3H, $-\text{CH}_3$), 1.67 (s, 3H, $-\text{CH}_3$) ppm.

^{13}C APT NMR (101 MHz, DMSO- d_6): $\delta = 165.89$ ($\text{C}=\text{O}$), 152.41 (C2), 142.80 ($\text{CH}=\text{CH-}$), 124.55 (C4), 121.91 (C3), 111.96 (C, 108.09, 105.42 ($\text{C-C}_2\text{H}_6$), 46.35 (CH-CH_2), 28.93 (CH-CH_2), 28.33 (CH_3), 26.29 (CH_3) ppm.

IR (ATR): $\nu = 1567$ (s, cyclic alkene), 1704 (m, $\text{C}=\text{O}$), 2987(m, CH aliphatic), 3205 (m, CH aromatic).

2.5.19.17. 5-[(4-Methoxyphenyl)methyl]-2,2-dimethyl-1,3-dioxane-4,6-dione (2.67)

Three equivalents of NaBH_4 (0.2 g, 5.28 mmol) were added portion-wise to ethanol (20 ml) suspended Knoevenagel product **2.51** (0.49 g, 1.87 mmol). The reaction mixture was initially left in an ice bath (0°C) for 15 minutes and then stirred overnight at room temperature. The pH of the mixture was adjusted to 4-5 with 4M aqueous HCl. The desired compound was extracted from the organic phase i.e., petroleum ether (3X30 ml), rinsed with a saturated aqueous solution of NaCl, dried with anhydrous MgSO_4 , filtered and the filtrate was collected. The solvent was removed at low pressure and the residue obtained was dried under vacuum to give a fluffy white solid of **2.67** (0.37 g, 1.4 mmol, 75.5 %).

Molecular Formula $\text{C}_{14}\text{H}_{16}\text{O}_5$; R_f (butanol/acetic acid/water, 4:1:5): 0.5; melting point: $69-70^\circ\text{C}$.

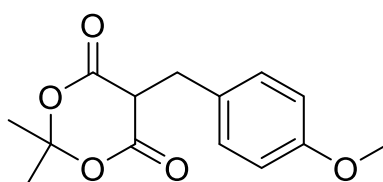


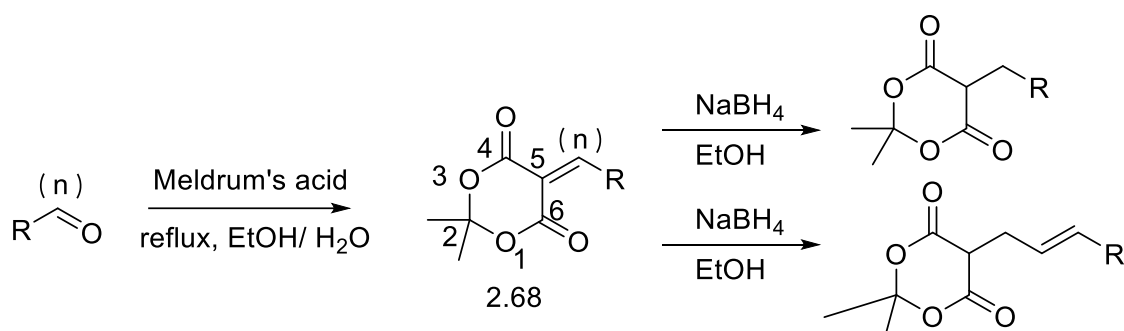
Figure 2. 93. Compound 2.67

^1H NMR (400 MHz, DMSO) $\delta = 7.17-7.15$ (d, $J = 8.5$ Hz, 2H, ArHs), 6.84-6.81 (d, $J = 8.6$ Hz, 2H, ArHs), 4.75-4.72 (t, $J = 9.8$ Hz, 1H, H5), 3.71 (s, 3H, OCH_3), 3.23-3.22 (d, $J = 4.8$ Hz, 2H, $-\text{CH}_2$), 1.79 (s, 3H, $-\text{CH}_3$), 1.57 (s, 3H, $-\text{CH}_3$) ppm.

^{13}C APT NMR (400 MHz, DMSO) $\delta = 166.16$ ($\text{C}=\text{O}$), 158.33 (CH_2-C), 130.84 (ortho ArCs), 130.15 (C-OCH_3), 113.98 (meta ArCs), 105.33 ($\text{C-C}_2\text{H}_6$), 55.43 (OCH_3), 47.68 (CH-CH_2), 30.82 (CH-CH_2), 28.31 (CH_3), 26.66 (CH_3) ppm.

IR (ATR): $\nu = 1540$ (s, cyclic alkene), 1742 (s, $\text{C}=\text{O}$), 2967(w, CH aliphatic), 3000 (w, CH aromatic).

2.5.20. Meldrum's acid derivatives reactions scheme



(n) : number of C=C in the aliphatic chain

Scheme 2. 4. Meldrum's acid derivatives reactions

2.5.21. Meldrum's acid discussion

Knoevenagel condensation products were prepared as reported by Jursic (2001). When the Knoevenagel condensation reaction involved electron-rich aromatic aldehydes, special precautions were abided as reported by Jurisic *et al.* (2018), as an adduct formed of two rather than one Meldrum's acid can be easily added to these aldehydes. This adduct formation is caused due to the high reactivity of the formed α, β -conjugates to Michael acceptors (Jurisic *et al.* 2018). To avoid adduct formation, the Knoevenagel condensation reaction was set in aqueous media as reported by Deb & Bhuyan (2005). The same approach was used in this study between Meldrum's acid and electron-rich aromatic aldehydes as the starting materials were partially soluble in water, unlike the Knoevenagel condensation products that were less soluble. Precipitation of the Knoevenagel product in water prevented the addition of a second Meldrum's acid.

The Knoevenagel condensation of Meldrum's acid produced derivatives with a moderate percentage yield (23-45%). The percentage yield was enhanced upon using water as a reaction solvent, as simple washing with water was sufficient to remove the residual impurities and no further purification was required in most cases except compounds **2.56** and **2.61**, where column chromatography was required. Column chromatography was used as a purification technique for Knoevenagel condensation reaction in ethanol, subsequently

loss of product took place as presented in the synthesis of compounds **2.51**, **2.54**, **2.55** and **2.58**.

Some common spectral features were deduced from the ^1H NMR spectra of the Knoevenagel benzylidene Meldrum's acid derivatives, where the two methyl groups at position 2 of compound **2.68** appear as 6 proton singlets in the aliphatic regions which indicate that they both have the same chemical shift. However, following the exocyclic reduction of the diene aliphatic bridge, the 2 methyl groups appeared as distinct peaks as 3 proton singlet each. The same finding was observed in the ^{13}C NMR spectra of the Knoevenagel and exocyclic reduced derivatives. As for the two-carbonyl group at positions 4 and 6 of compound **2.68**, they were observed as 2 different peaks in the ^{13}C spectra of the Knoevenagel products. Yet, the two peaks merged into one peak following the reduction process.

The spectroscopic data of the reported compounds were compared with the synthesised products. The novel compounds were further analysed by MS, where the obtained molecular weight matched the expected. The expected parent molecular ion was not detected in compounds **2.54**, **2.57**, and **2.60** despite the structural confirmation by ^1H NMR and ^{13}C NMR. However, potential fragments of the parent compound were detected, this might result from the ionisation power of the mass spectrometer which might have been sufficient to fragment these compounds.

The exocyclic $\text{C}=\underline{\text{C}}\text{H}$ proton of the mono-ene derivatives appeared as a one proton singlet, while the diene aliphatic bridge was observed as three protons. The splitting of $\text{C}=\underline{\text{C}}\text{H}-\text{CH}=\text{CH}$ appeared as a doublet, $\text{C}=\text{CH}-\underline{\text{C}}\text{H}=\text{CH}$ appeared as a doublet of doublet and $\text{C}=\text{CH}-\text{CH}=\underline{\text{C}}\text{H}$ appeared as a doublet. After reduction, the keto form was more the more predominant form as the peaks appeared as sharp peaks unlike the benzylidene barbiturate derivatives which appeared a broad peaks. The splitting of $\underline{\text{C}}\text{H}-\text{CH}_2-\text{CH}=\text{CH}$ appeared as a one proton triplet, $\text{CH}-\underline{\text{C}}\text{H}_2-\text{CH}=\text{CH}$ appeared as two proton triplet, $\text{CH}-\text{CH}_2-\underline{\text{C}}\text{H}=\text{CH}$ appeared as a doublet of triplet and $\text{CH}-\text{CH}_2-\text{CH}=\underline{\text{C}}\text{H}$ appeared as a one proton doublet. The only exception was compound **2.62** where the two tautomeric forms were observed, as the $\text{CH}-\underline{\text{C}}\text{H}_2$ appeared as a highly deshielded two protons broad singlet. On the other hand, $\underline{\text{C}}\text{H}-\text{CH}_2$ appeared as a one proton triplet. The reason behind the highly deshielding effect might be resulted from the high electron density of the surrounding functional groups.

Some minor impurities were detected in the ^1H NMR spectra of the reduced forms; however, as previously mentioned purification via HPLC was required due to the high polarity of the desired compounds.

Table 2. 4. Comparison of the literature melting points in °C of compounds with products isolated in this thesis work using the reported methods

Compound	Reported mp	References	Found mp
2.51	124	Tahmassebi <i>et al.</i> , 2009	203-206
2.52	147	Insuasty <i>et al.</i> , 2005	148-151
2.53	196	Insuasty <i>et al.</i> , 2005	152-155
2.55	104-106	Tahmassebi <i>et al.</i> , 2009	89-92
2.56	97	Tahmassebi <i>et al.</i> , 2009	75-77
2.58	221-225	Herzog, 1977	218-220
2.59	196-197	Mohite & Bhat, 2013	179-181
2.62	157	Herzog, 1977	>300
2.63	91	Chau <i>et al.</i> , 2017	>300
2.67	82-85	Forst <i>et al.</i> , 2009	69-70

Some of the synthesised compounds were reported in the literature. The obtained melting points were compared with those reported in articles, and some inconsistencies were observed (Table 2.4.). These deviations may be correlated to impurities, residual solvents in the samples, or the different methods or equipment employed to determine the melting point.

2.5.22. Synthesis of five-membered ring derivatives

2.5.22.1. Synthesis of (E)-3-((Furan-2-ylmethylene)amino)-2-thioxothiazolidin-4-one (2.69)

In a round bottom flask, 3-Aminorhodanine (0.25 g, 1.68 mmol) was dissolved in distilled water (10 ml) and acetic acid (100 μl). The reaction flask was sonicated at room temperature for 5 minutes via ultrasonic cleaner (Thomas Scientific, UK). Furfural (0.162 g, 1.68 mmol) was added to the mixture portion-wise and left to sonicate at room temperature (45 minutes). The mixture was filtered, and the residue was rinsed with ice-cold distilled water

(2x30 ml). The residue was collected and dried overnight under vacuum to give a mustard yellow powder of **2.69** (0.2 g, 0.88 mmol, 52.6 %).

Molecular Formula $C_9H_5N_3O_4S_2$; R_f (ethyl acetate/hexane, 2:3): 0.47; melting point: 85-88 °C.

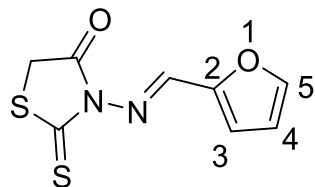


Figure 2. 94. Compound 2.69

1H NMR (400 MHz, DMSO- d_6): δ = 8.55 (s, 1H, N=CH), 8.097-8.092 (d, J = 1.7 Hz, 1H, H 5) , 7.38-7.37 (d, J = 2.9 Hz, 1H, H 3) , 6.80-6.79 (dd, J = 2.9, 1.7 Hz, 1H, H 4), 4.34 (s, 2H, CH₂) ppm.

^{13}C NMR (101 MHz, DMSO) δ = 197.23 (C=S), 170.10 (C=O), 158.82 (N=CH), 148.87 (C 5), 147.51 (C 2), 121.79 (C 3), 113.54 (C 4), 35.16 (S-CH₂) ppm.

MS (+ESI) m/z = Found 226.9944 [M+H]⁺; calculated for $C_8H_7N_2O_2S_2$ 226.9949; -2.2 ppm.

2.5.22.2. Synthesis of (E)-3-Amino-5-((5-nitrothiophen-2-yl)methylene)-2-thioxothiazolidin-4-one (2.70)

3-Aminorhodanine (0.5 g, 3.37 mmol) was left to dissolve in hot ethanol, followed by the addition of 5-Nitro-2-thiophenecarboxaldehyde (0.53 g, 3.37 mmol). The reaction mixture was set at reflux temperature (2 h), and the residue was collected after filtration under vacuum. The residue was further purified by suspending the residue in a hexane slurry to wash away the aldehyde impurities. The residue was recollected and dried overnight under a high vacuum to give a fluffy orange solid of compound **2.70** (0.7 g, 2.4 mmol, 72.2 %).

Molecular Formula $C_9H_5N_3O_3S_3$; R_f (ethyl acetate/hexane, 2:3): 0.6; melting point: 208-211 °C.

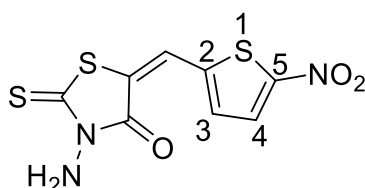


Figure 2. 95. Compound 2.70

^1H NMR (400 MHz, DMSO- d_6): δ = 8.25-8.24 (d, J = 4.3, 1H, H 4), 8.16 (s, 1H, N=CH), 7.76-7.75 (d, J = 4.4 Hz, 1H, H 3), 5.97 (s, 2H, NH₂) ppm.

IR (ATR): ν = 1600 (w, NH bending), 1696 (s, C=O), 2744 (w, CH aliphatic), 3022 (m, CH aromatic), 3322-3211 (m, NH stretching).

MS (+ESI) m/z = Found 287.9565 [M+H]⁺; calculated for C₈H₆N₃O₃S₃ 287.9571; -2.1 ppm.

2.5.22.3. Synthesis of (E)-1-((Furan-2-ylmethylene)amino)imidazolidine-2,4-dione (2.71)

1- Aminohydrantoin hydrochloride (0.25 g, 1.64 mmol) was dissolved in distilled water (10 ml) and acetic acid (100 μ l). The reaction flask was sonicated at room temperature for 5 minutes; furfural (0.1585 g, 1.64 mmol) was added to the mixture portion-wise and left to sonicate at room temperature for 1 hour. The mixture was filtered, and the residue was rinsed with ice-cold distilled water (3X20 ml). The residue was collected and dried overnight under vacuum to give a white powder of 0.262 g, 1.14 mmol, 69 %.

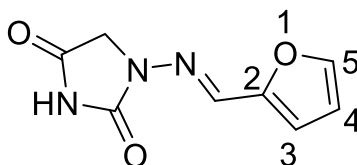


Figure 2. 96. Compound 2.71

Molecular Formula C₈H₇N₃O₃; R_f (ethyl acetate/hexane, 2:3): 0.19; melting point: 278-280 °C.

^1H NMR (400 MHz, DMSO- d_6): δ = 11.24 (s, 1H, NH), 7.828-7.825 (d, J = 1.1 Hz, 1H, H 5), 7.69 (s, 1H, N=CH), 6.84-6.83 (d, J = 2.9 Hz, 1H, H 3), 6.63-6.62 (dd, J = 2.9, 1.1 Hz, 1H, H 4), 4.32 (s, 2H, CH₂) ppm.

δ ^{13}C APT NMR (400 MHz, DMSO) δ = 169.40 (N=C=O), 153.78 (CH₂-C=O), 149.98 (C 2), 145.30 (C 5), 133.66 (N=CH), 113.39 (C 3), 112.58 (C 4), 49.31 (CH₂) ppm.

IR (ATR): ν = 1695 (s, C=O), 2913 (w, CH aliphatic), 3029 (m, CH aromatic), 3136 (m, NH).

The spectroscopic data were consistent with the literature values (Tantawy & Gad, 1991).

2.5.22.4. Synthesis of (E)-3-(((5-Nitrothiophen-2-yl)methylene)amino)imidazolidine-2,4-dione (2.72)

1-Aminohydrantoin hydrochloride (0.258 g, 1.7 mmol) and 5-Nitro-2-thiophenecarboxaldehyde (0.268 g, 1.7 mmol) were dissolved in ethanol (20 ml). The reaction was set to reflux for 3 hours. The reaction mixture was filtered on hot where the residue was collected and rinsed with cold hexane (3x30 ml). The residue was collected and dried overnight under vacuum to give a white powder of compound **2.72** (0.38 g, 1.5 mmol, 88.1 %).

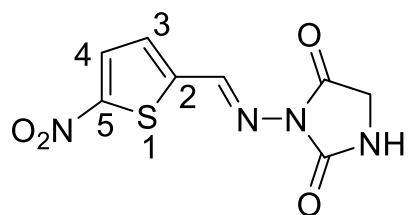


Figure 2. 97. Compound 2.72

Molecular Formula $C_8H_6N_4O_4S$; R_f (ethyl acetate/hexane, 2:3): 0.17; melting point: 273-276 °C.

1H NMR (400 MHz, DMSO- d_6): δ = 11.44 (s, 1H, NH), 8.12-8.11 (d, J = 4.3 Hz, 1H, H 4), 8.03 (s, 1H, N=CH), 7.46-7.45 (d, J = 4.3 Hz, 1H, H3), 4.35 (s, 2H, CH₂) ppm.

^{13}C APT NMR (101 MHz, DMSO) δ = 169.07 (N-C=O), 153.57 (CH₂-C=O), 150.95 (C 2), 147.00 (C 5), 136.97 (N=CH), 131.08 (C 3), 129.45 (C 4), 49.72 (CH₂) ppm.

IR (ATR): ν = 1704 (s, C=O), 2919 (w, CH aliphatic), 3070 (m, CH aromatic), 3180 (broad m, NH).

MS (+ESI) m/z = Found 255.0184 [M+H]⁺; calculated for $C_8H_7N_4O_4S$ 255.0188; -1.6 ppm.

2.5.22.5. Synthesis of (E)-1-((Thiophen-2-ylmethylene)amino)imidazolidine-2,4-dione (2.73)

1-Aminohydrantoin hydrochloride (0.5 g, 3.3 mmol) and 2-Thiophenecarboxaldehyde (0.37 g, 3.3 mmol) were dissolved in ethanol (20 ml). The reaction was set to reflux for 4 hours. The reaction mixture was filtered on hot where the residue was collected and rinsed with

cold hexane (3x30 ml). The residue was collected and dried overnight under vacuum to give a white powder of 0.6 g, 2.87 mmol, 87 %.

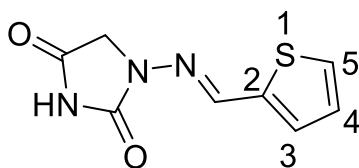


Figure 2. 98. Compound 2.73

^1H NMR (400 MHz, DMSO- d_6): δ = 11.23 (s, 1H, NH), 8.03 (s, 1H, N=CH), 7.64-7.63 (d, J = 5.9 Hz, 1H, H 5), 7.41-7.40 (dd, J = 3.6, 1.0 Hz, 1H, H 4), 7.14-7.12 (dd, J = 5.0, 3.5 Hz, 1H, H 3), 4.33 (s, 2H, CH₂) ppm.

δ ^{13}C APT NMR (400 MHz, DMSO) δ = 169.40 (N-C=O), 153.78 (CH₂-C=O), 149.98 (C 2), 145.30 (C 5), 133.66 (N=CH), 113.39 (C 4), 112.58 (C 3), 49.31 (CH₂) ppm.

IR (ATR): ν = 1704 (s, C=O), 2919 (w, CH aliphatic), 3070 (m, CH aromatic), 3180 (broad m, NH).

2.5.22.6. Attempts to synthesise (Z)-3-(((E)-Furan-2-ylmethylene)amino)-5-((5-nitrothiophen-2-yl)methylene)-2-thioxothiazolidin-4-one

Compound 2.69 (0.123 g, 0.43 mmol) and 5-Nitro-2-thiophenecarboxaldehyde (0.0412 g, 0.43 mmol) were dissolved in ethanol (20 ml). The reaction was set at reflux temperature (48 h). The reaction was monitored by TLC; however, no change was observed.

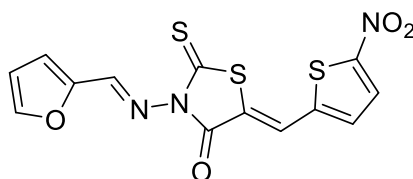


Figure 2. 99. Compound 2.74

2.5.22.7. Attempts to synthesise (Z)-5-((E)-3-(4-Nitrophenyl)allylidene)-3-(((E)-5-nitrothiophen-2-yl)methylene)amino)-2-thioxothiazolidin-4-one

Compound 2.72 (0.13 g, 0.45 mmol) and *p*-Nitrocinnamaldehyde (0.08 g, 0.45 mmol) were dissolved in ethanol (20 ml). The reaction was set at reflux temperature (36 h). The reaction was monitored by TLC; however, no change was observed.

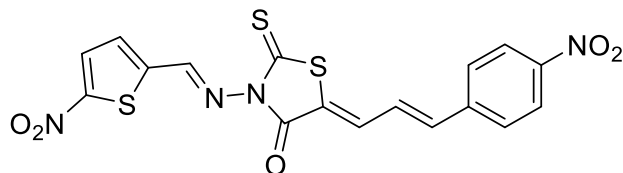


Figure 2. 100. Compound 2.75

2.5.22.8. Attempts to synthesise (Z)-3-((2,4-Dimethylpentan-3-ylidene)amino)-5-((5-nitrothiophen-2-yl)methylene)-2-thioxothiazolidin-4-one

Compound 2.70 (0.2, 0.69 mmol) was dissolved in distilled water (10 ml) and acetic acid (100 μ l). The reaction flask was sonicated at room temperature for (5 minutes), 2,4 Dimethyl-3-pentanone (0.079 g, 0.69 mmol) was added to the mixture portion-wise and left to sonicate at room temperature for (3 h). The reaction was monitored by TLC; however, no change was observed.

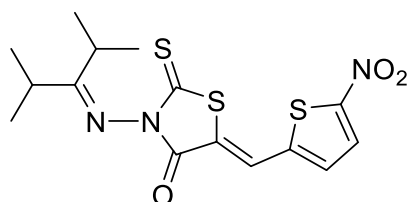


Figure 2. 101. Compound 2.76

2.5.22.9. Attempts to synthesise 3-((2,4-Dimethylpentan-3-ylidene)amino)-2-thioxothiazolidin-4-one

1-Aminohydrantoin hydrochloride (0.5 g, 3.29 mmol) was dissolved in distilled water (10 ml) and acetic acid (100 μ l). The reaction flask was sonicated at room temperature (5 minutes), 2,4-dimethyl-3-pentanone (0.376 g, 3.29 mmol) was added to the mixture portion-wise and sonicated at room temperature (3 h). The reaction was monitored by TLC; however, no change was observed.

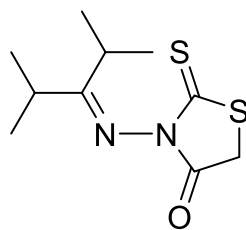


Figure 2. 102. Compound 2.77

2.5.23. Discussion of the 5-membered ring derivatives results

Nitrofurantoin (**1.13**) is one of the treatments that have been used recently against *C. difficile*. In this section, a furantoin derivative was synthesised to determine the impact of the NO₂ on the antimicrobial activity. Additionally, other 5 membered ring derivatives were synthesised to correlate the ring size to the antimicrobial activity (Chapter 3). An addition reaction between hydrazine derivatives and carbonyl compounds were set in a reaction as described by Gallardo-Garrido *et al.* (2020).

The hydrazine derivatives addition reaction with aldehydes as shown in **2.68** and **2.70** was set in water, where the acetic acid was added to catalyse the reaction. The two hydrazine derivatives, 3-aminorhodamine and 1-aminohydrantoin hydrochloride used as starting materials to synthesise compounds **2.68** and **2.70** respectively possessed two active sites, the amino group and the active methylene group. The two products were proven to bind to the amino group of the hydrazine derivative using ¹H NMR and ¹³C NMR.

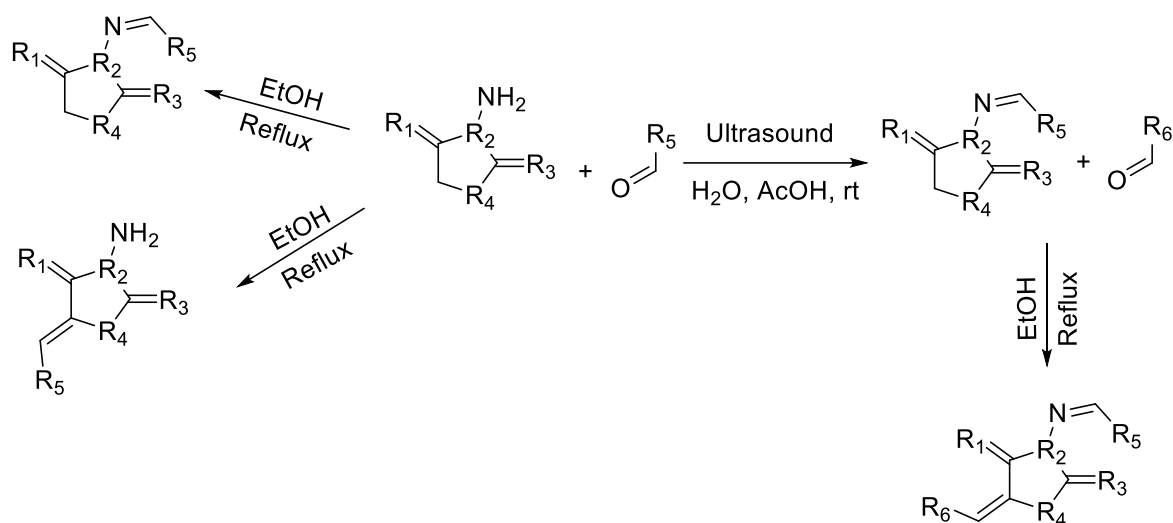
The only ¹H NMR spectral difference to determine the binding site was the shielding range, as the amino group (NH₂) possess a higher electronegativity compared the active methylene group. Therefore, the free unbind NH₂ group was slightly more deshielded compared to the CH₂ group. The NH₂ group cannot appear in the ¹³C NMR; therefore, no peak would appear in the aliphatic range if the active methylene group bonded to the carbonyl group leaving the NH₂ free. Compounds **2.68** and **2.70** showed a peak aligned with the DMSO in the aliphatic range; it was deduced that the aldehydes bound to the NH₂ group leaving the CH₂ group free.

Compounds **2.71** and **2.72** displayed the same outcome when the reaction was set to reflux temperature in the presence of ethanol as a solvent. ¹³C NMR showed a peak in the aliphatic region aligned with the DMSO peaks which correspond to the free CH₂. Moreover, the CH₂

groups appeared at 4.3 ppm unlike compound **2.69**, where binding took place on the CH₂ and the NH₂ peak appeared deshielded at 5.97 ppm.

Numerous attempts were made to attach an extra aldehyde to the active CH₂ using Knoevenagel condensation or NH₂ by nucleophilic addition to determine their antimicrobial activity; however, all the attempts failed.

2.5.24. 5-Membered rings derivatives synthesis scheme



Scheme 2. 5. 5-membered rings synthesis scheme

2.5.25. Mechanism of Schiff bases formation

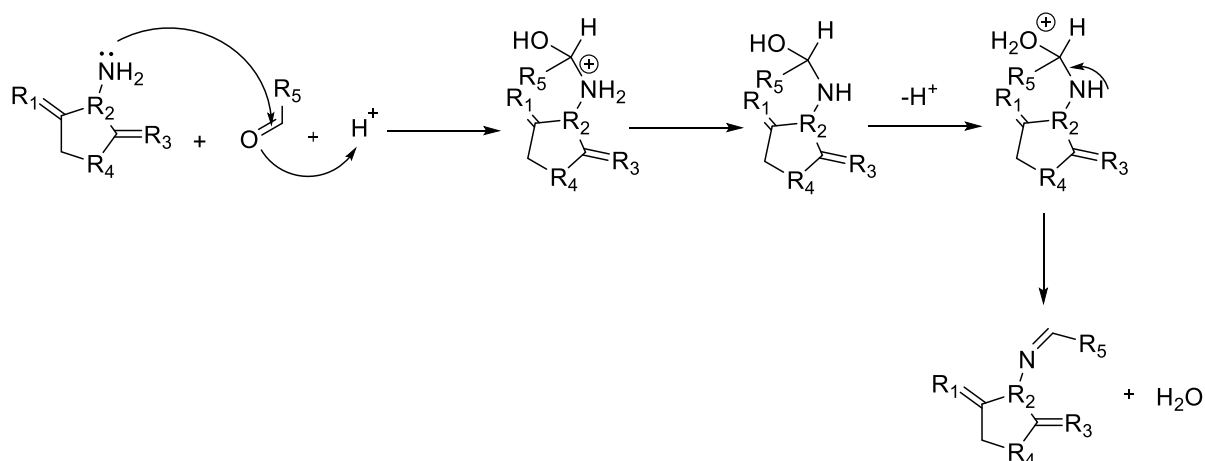


Figure 2. 103. Mechanism of imine formation

The aldehyde is protonated by the acetic acid, making the C=O more electrophilic and liable to nucleophilic attack by the NH₂ group of aminohydrantoin or aminorhodanine, leading to the formation of carbinolamine intermediate. The intermediate undergoes dehydration to form Schiff bases.

2.5.26. Limitations of chapter 2

- Some of the NaBH₄ reduced compounds could be further purified via HPLC.
- The exact mechanism of action and the target of the synthesised compounds were not confirmed. The target's identity would facilitate the synthesis of compounds with potential high efficacy and affinity towards the receptor employing computational chemistry.

Chapter 3

3.1. Antimicrobial susceptibility testing

The synthesised compounds (Chapter 2) were tested to evaluate their antimicrobial activity against the target microorganism *C. difficile* and two control microorganisms *E. coli* and *S. aureus* employing agar diffusion assay and minimum inhibitory concentration assay (MIC).

3.1.1. Agar diffusion assay

3.1.1.1. Purpose

The extent of sensitivity or resistance of microorganisms to potential antimicrobial compounds or drugs was traditionally estimated by a susceptibility means of test known as the Kirby-Bauer disk diffusion test. This method aided clinicians in the determination of appropriate treatment to be taken by their patients. The test is carried out by growing the microorganisms on nutrient agar, where filter paper discs impregnated with the compound or tested drugs are placed on the surface of the agar. The ability of the tested compounds to form a clear zone around the placed disc (zone of inhibition) is an indirect method to estimate the extent of the compounds' inhibitory effect (Hudzicki, 2009).

3.1.1.2. Theory of agar diffusion assay

A known concentration of a potential antimicrobial agent is impregnated in a 6-mm filter paper disk. It is then placed on the surface of an appropriate agar eg. Mueller-Hinton (MH); water instantly diffuses from MH agar to the disk after its placement. The tested compound then diffuses into the surrounding agar. The extraction rate of the potential antimicrobial agent outside the disk is higher than its diffusion rate over the agar. Therefore, the concentration of the tested compound is inversely proportional to the distance. The optimal concentration can be found close to the disc with an exponential decrease in concentration as the distance increases (Weinstein & Clinical and Laboratory Standards Institute, 2018).

The diffusion and solubility characteristics and the molecular weight of the tested compound in MH agar are some of the factors affecting the diffusion rate. The rate of diffusion of the compounds having high molecular weight tends to be slower than those with the lower ones. These factors contribute to the forming a distinct zone size that indicates the microorganisms' susceptibility to the test compound. When inoculation occurs

before the placement of disks on the surface of the agar, the growth of the pathogen and diffusion of the antimicrobial agents take place simultaneously. If the bacteria can overcome the emplaced potential antimicrobial agent, it will grow normally. The depth of the agar is inversely proportional to the diameter of the zone of inhibition (ZOI). The deeper the layer, the smaller the ZOI as the potential antimicrobial agent diffuses in 3D (Hudzicki, 2009).

3.1.2. Minimum Inhibitory Concentration

The lowest concentration of a drug required to hinder the visible growth of pathogens after incubation is called the minimum inhibitory concentration (MIC). This method is considered the most reliable experiment to test the sensitivity of the pathogens to antimicrobial compounds. MIC is also considered the standard evaluator for the remaining susceptibility tests. MICs evaluate the unfamiliar resistance incidences. MIC can also provide decisive results when other methods fail. It is used for in vitro testing of potentially novel antimicrobial agents, and the determination of the MIC breakpoints of the different antimicrobials. MIC is preferable for compounds having poor diffusion through the loading disc or the agar in the disc diffusion method. The lowest concentration that visually kills pathogens after subculture on drug-free agar is known as the minimum bactericidal concentration (MBC) (Andrews, 2001).

Agar and broth dilution are the most reliable methods used to estimate the MIC values of a potential antimicrobial agent or the bacteriostatic/bactericidal activity of antibiotics. In broth dilution, nutrient broth having known exponentially increasing or decreasing drug concentrations is inoculated with definite known, or standard, concentration of microorganisms. Followed by incubation of the 96-well plate (containing microorganisms and antimicrobial(s)), any observed turbidity signifies the resistance of pathogens to the tested drug. The degree of antimicrobial sensitivity to the drugs clinically can be classified in one of the following categories; susceptible, intermediate, or resistant. Various institutions such as the Clinical and Laboratory Standards Institute (CLSI) (Clinical and Laboratory Standards Institute, 2006) and the European Committee on Antimicrobial Susceptibility Testing (EUCAST) (EUCAST of the ESCMID, 2003) issue the standardised classification of the drugs.

The exact concentration that separates a drug from being resistant or susceptible to a definite pathogen is known as the breakpoint. MIC is not the only factor that determines the breakpoints, the drugs' pharmacodynamics, pharmacokinetics, and clinical results are also

considered. Medicinal malfunction and resistance are attained from drugs having a value above the breakpoint. However, a high chance of therapeutic efficacy is associated with drugs falling within the susceptible range. As for those categorised in the intermediate class, their effectiveness is ambiguous. If the MIC value against a pathogen exceeds the wild type, it will be a species with developed antimicrobial resistance. Sufficient data can be obtained from the continuous observation of MIC values. It will facilitate the detection of deviations of the tested drug or species having distinct susceptibility, where minor fluctuations can be critical (Wiegand *et al.*, 2008).

3.2. Aim and Objectives

Chapter 3 aimed to investigate the antimicrobial efficacy of the synthesised compounds (Chapter 2) against the target microorganism *C. difficile*.

The preliminary evaluation included the following steps:

- Determination of the MIC of some aldehydes.
- Preparation of the stock solutions of the synthesised compounds.
- Selection of two control microorganisms representing a Gram-positive and Gram-negative pathogens to test the antimicrobial efficacy of the synthesised compounds.
- Assessment of the antimicrobial efficacy by the agar diffusion assay to assess the zones of inhibition of the synthesised compounds against the target and control pathogens.
- Comparison of the antimicrobial efficacy of the synthesised compounds through the zones of inhibition against two of the first line of treatments of *C. difficile*.

Following the preliminary assay, the antimicrobial efficacy of the synthesised compounds was primarily determined through the following assays:

- Determination of the minimum inhibitory and bactericidal concentrations (MIC/ MBC) of the synthesised compounds against the three pathogens.
- Compare MIC/ MBC values of the synthesised compounds against two of the first line of treatments of *C. difficile*.
- Creation of a structure-activity relationship based on the antimicrobial activity against *C. difficile*.

To detect the possible correlation between the synthesised compounds and DHODase enzyme inhibition through:

- Assessment of the effect of pyrimidine rescue on *C. difficile* survival rate upon treating the different drugs concentrations with 0.1% (μM) uridine.

3.3. Materials

3.3.1. Microbial cultures

A panel of American Type Culture Collection (ATCC) microorganisms, including a facultative aerobe Gram-positive, a facultative anaerobe Gram-negative, and a strict anaerobic Gram-positive microorganism, was selected to test the efficacy and selectivity of the synthesised compounds against a panel of known comparator antimicrobials currently utilised as the first line of treatment (Table 3.1.). The facultative aerobe and facultative anaerobe were set as the controls for this study, whilst the strict anaerobe was the test microorganism. The selection was determined based on the abundance of these microorganisms in the targeted organ i.e., the normal gut microbiota. In addition, they can indicate each of the compound's efficacy against both Gram-positive and Gram-negative species.

Table 3. 1. List of Gram-positive and Gram-negative microorganisms, with corresponding American Type Culture Collection number

Microorganism	Gram-staining	Aerobe/ Anaerobe	American Type Culture Collection (ATCC)
<i>Escherichia coli</i>	Negative	Facultative anaerobe	35218
<i>Staphylococcus aureus</i>	Positive	Facultative anaerobe	29213
<i>Clostridium difficile</i>	Positive	Strict aerobe	11204

3.3.2. Microbiological media and agar

Muller-Hinton broth (MHB) (Oxoid Ltd®) was utilised as the culture media for both *E. coli* and *S. aureus*, and Wilkins Chalgren anaerobic broth (WCB) (Oxoid Ltd®) was used as the culture media of *C. difficile* used. Mueller-Hinton agar (MHA) was used in this study for antibacterial susceptibility testing and storage of *E. coli* and *S. aureus*, and Wilkins Chalgren agar (WCA) (Oxoid Ltd®) was used for *C. difficile*.

3.3.3. Panel of comparator antibacterial agents

Two of the first-line clinical treatments for *C. difficile* were selected for comparative antimicrobial susceptibility testing on MHA and MIC assay (Table 3.2.). The antibiotics were purchased from Sigma-Aldrich in the form of powder and were stored in accordance with the manufacturer's guidelines. The prepared stock solutions were stored at 4°C until required.

Table 3. 2. List of comparator antimicrobials including the concentration of prepared stock solutions.

Antimicrobial	Susceptibility test (stock solution concentration mg/ml)	MIC (stock solution concentration µg/ ml)
Nitrofurantoin	20.48	2048
Metronidazole	20.48	2048

3.3.4. Dimethyl sulfoxide (DMSO) and sterile distilled water

All the synthesised compounds were dissolved in DMSO (Merck, Germany) to give liquid stock solutions. DMSO was stored at room temperature. Stock solutions were further diluted with autoclaved distilled water to generate the different concentration ranges for MIC assay.

3.3.5. Equipment

Optical density (OD) readings of microorganism concentrations (Table 3.1.) were taken using spectrophotometer (Jenway Geneva Plus UV). The DG 250 anaerobic workstation (Don Whitely Scientific UK) was used to incubate the microtitre plate for MIC assay under anaerobic conditions.

3.3.6. Preparation of agar and media

Agar and media were prepared following the manufacturer's instructions and sterilised using an autoclave.

3.3.6.1. Mueller-Hinton broth

In accordance with manufacturer's instructions MHB (5.25 g) was fully dissolved in distilled water (250 mL). The solution was sterilised by placing it in an autoclave for 30 minutes at 121°C, MHB was then stored at room temperature.

3.3.6.2. Mueller-Hinton agar

MHA (19 g) was fully dissolved in distilled water (500 mL). The solution was sterilised by placing it in an autoclave for 30 minutes at 120°C. The culture media bottle was left to cool down in a water bath to 55°C before pouring into sterile petri dishes. The petri dishes were stored at 4°C in an inverted position once the agar was set.

3.3.6.3. Wilkins Chalgren broth

WCB (8.27 g) was fully dissolved in distilled water (250 mL). The solution was sterilised by placing it in an autoclave for 30 minutes at 120°C, WCB was then stored at room temperature.

3.3.6.4. Wilkins Chalgren agar

WCA (21.55 g) was fully dissolved in distilled water (500 mL). The solution was sterilised by placing it in an autoclave for 30 minutes at 120°C. The culture media bottle was left to cool down in a water bath to 55°C before pouring into sterile petri dishes. The petri dishes were stored at 4°C in an inverted position once the agar was set.

3.3.6.5. Wilkins Chalgren + 0.1 % w/v Sodium taurocholate agar

WCA (4.18 g) and 97 % sodium taurocholate (0.1 g) were fully dissolved in distilled water (97 mL). The solution was sterilised by placing it in an autoclave for 30 minutes at 120°C. The culture media bottle was left to cool down in a water bath to 55°C before pouring into sterile petri dishes. The petri dishes were stored at 4°C in an inverted position once the agar was set.

3.3.7. Test compounds and antibiotic stock solutions

Aqueous stock solutions of 20.48 mg/mL were prepared for the agar diffusion assay, where the compounds were vortexed in DMSO. Whereas aqueous stock solutions of 2048 µg/mL were prepared for the MIC assay, where the compounds were vortexed in sterile distilled water and 5% DMSO. The stock solutions were stored at 4 °C in sterile specimen containers until required.

3.3.8. Preparation of microorganisms for antibacterial activity testing

The list of microorganisms (Table 3.1.) selected for this study was obtained from the culture collection maintained by Aston University's Microbiology Research Group; the microorganisms were stored on Microbank beads (Pro-Lab Diagnostics) at -80°C until required for testing.

3.3.8.1. Glycerol stocks

The panel of microorganisms were stored by taking a single colony (Table 3.1.) and mixing them into Microbank vials containing plastic beads and a glycerol-based cryo-preserved medium (Pro-Lab Diagnostics, UK), followed by their storage in the freezer at -80°C until required for testing.

3.3.8.2. Streak plates

A single bead was taken from the desired Microbank vial, followed by streak plating and inoculating each microorganism on the appropriate culture agar. Microbial growth was

obtained upon the incubation of the inoculated plates overnight at 37°C and then stored at 4°C until required.

3.4. Methods

3.4.1. Preparation of *C. difficile* vegetative cell suspensions

C. difficile spores stored on beads at -80°C were inoculated on WCA containing 0.1 % sodium taurocholate in anaerobic conditions (DG 250 anaerobic workstation, Don Whitely Scientific UK) for 48 hours. The procedure reported by Shetty *et al.* (1999) for spore suspensions was followed. Sodium taurocholate was added to the agar to induce the formation of vegetative cells of *C. difficile*. A single colony was isolated and incubated in WCB for 24 hours at 37°C.

3.4.2. Diffusion assay for antibacterial susceptibility testing of the synthesised compounds, aldehydes, and the antibiotics controls

The susceptibility of the chosen panel of microorganisms (Table 3.1.) against the control, synthesised compounds, and aldehydes (Tables 3.3., 3.4., 3.5.) were primarily tested through the agar diffusion assay method. Nutrient agar (MHA or WCA) were surface inoculated with a swab previously dipped in a suspension of each microorganism. A semi-confluent microbial growth was obtained after incubating the nutrient agar plates overnight in appropriate conditions.

Replacing the discs with wells cut into the agar was the only minor alteration made to the conventional disc diffusion method. Wells act as drug reservoirs when cut into the inoculated agar. In the wells' formation approach, the spread of the drugs only relies on their ability to diffuse through the nutrient agar, unlike the disc approach which relies on the diffusion through both the discs and agar. The antimicrobial agents were dispensed into the wells until they reached the surface of the microorganism-inoculated agar. The concentration of the tested compounds was set at 20.48 mg/ml; the compounds were vortexed in 100% DMSO. Despite the antimicrobial activity of 100% DMSO, it did not interfere with the results owing to its observed poor diffusion through MHA and WCA upon experimentation. The drug-containing wells were left to dry, followed by the inversion of the plates and incubation in anaerobic conditions at 37°C for 24 hours. The diameter of the

ZOI was measured and recorded in millimetres (mm). The experiment was undertaken in triplicate. Blank wells and wells containing 100% DMSO were used as a control.

3.4.3. Minimum inhibition concentrations (MIC) of the synthesised compounds and the comparator antibiotics

Following the CLSI guidelines, broth microdilution was utilised to determine the MICs of the tested compounds (Patel et al., 2015). In 96 wells microtiter plates, stock solutions of the potential antimicrobial agents were diluted to a 2-fold concentration of 100 μ l in nutrient broth to give exponentially decreasing drugs' concentrations range of 1024 μ g/ml – 0.25 μ g/ml. All wells were inoculated with 100 μ l of the tested microorganism at 10^6 CFU (colony forming unit)/ml concentration in nutrient broth to give a final pathogen concentration of $\approx 6 \times 10^5$ CFU/ mL of *E. coli*, $\approx 7 \times 10^5$ CFU/ ml for of *S.aureus*, and 5×10^5 CFU/ ml of *C. difficile*. Therefore, the drugs' concentration was further diluted to a final range of 512-0.125 μ g/ml. Samples from nutrient broths, diluted microorganisms, and drug controls were taken to act as controls. All MIC trials were made in triplicate for results verification. The plates were placed in anaerobic cabinets for incubation at 37°C for 24 hours for *E. coli* and *S. aureus*, while *C. difficile* was incubated for 48 hours. After incubation, the presence of turbidity in any of the wells indicates pathogen growth. Blanking of turbidity was observed in some assays due to the high pigmentation of some of the potential antimicrobial agents. Streak plating of the wells onto nutrient agar was therefore required to determine the MIC value. MICs were recorded through observing the lowest concentration of antibacterial agents that displayed no turbidity. The trials were monitored by MHB, drugs, and pathogen controls.

3.4.4. Minimum bactericidal concentrations (MBC)

MBC values were sometimes recorded by placing 20 μ L of each well showing no turbidity on the suitable nutrient agar and spreading with a sterile inoculation loop. The agar plates were incubated anaerobically overnight at 37°C. Samples were taken after agitating the wells components to guarantee effective transferal to the plates. MBCs were recorded as the lowest concentration of antibacterial agent that displayed no growth on nutrient agar.

3.4.5. DMSO control

For results verification, drugs-free trials were conducted to ensure that the concentration of DMSO alone did not interfere with the MIC or MBC readings. DMSO ranging from 0.5– 50% (v/v) in nutrient and Wilken's Chagren broth (MHB, WCB) was tested against the panel of microorganisms (Table 3.1.).

3.4.6. Agar diffusion assay

Replacing the discs with wells was the only minor alteration made to the conventional disc diffusion method. Wells act as drug reservoirs when cut into the inoculated agar. In the wells' formation approach, the spread of the drugs only relies on their ability to diffuse through the agar. In the disc approach, the rate of drugs' diffusion depends on their diffusion through both the discs and agar. The test antimicrobial agents are filled into the wells until they reach the surface of the microorganisms-inoculated agar, where the concentration was set at 20.48 mg/ml. Despite the well-documented antimicrobial activity of 100% DMSO, it did not interfere with the results when used to dissolve the test drugs as DMSO does not diffuse through the agar. The dissolving drugs were left to dry, followed by the inversion of the plates, and incubation overnight at 37°C. The diameter of the ZOI was measured and recorded on the following day. Drug-free wells were used as a control.

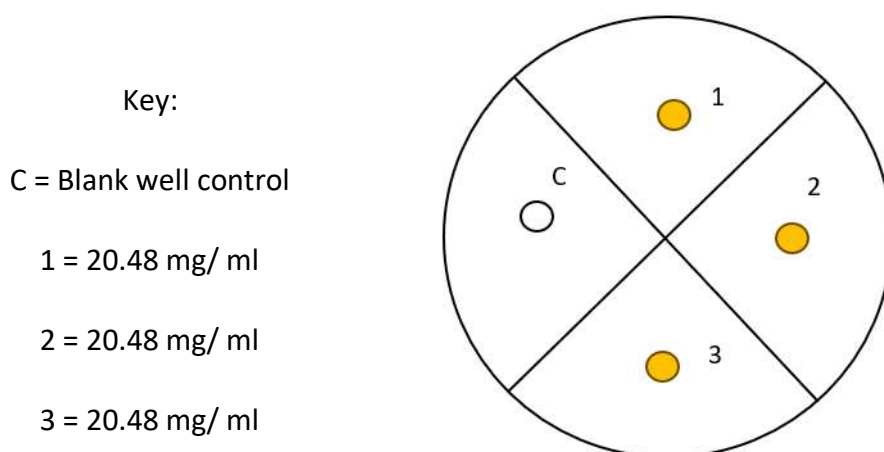


Figure 3. 1. Diagram of the layout of diffusion assay plates, with the tested compounds concentration (mg/ml) used.

3.5. Results and discussion

In this chapter, the antimicrobial activity of all the synthesised compounds were tested against the target microorganism *C. difficile* and the control microorganisms *E. coli*, *S. aureus*. The aim was to determine the compounds that exhibited the highest efficacy and selectivity against *C. difficile*. The MIC readings enabled a better understanding of the common structural features, and a SAR correlation was deduced.

3.5.1. Antimicrobial susceptibility testing of panel of antimicrobials, aldehydes and synthesised compounds against *C. difficile*, *E coli*, and *S. aureus*

Metronidazole (1.4) is a first line of treatment of CDI; therefore, it was chosen as a control for this comparative activity analysis with the synthesised products to evaluate their antimicrobial activities in anaerobic conditions. Metronidazole did not show any antibacterial activity against *E. coli*, and *S. aureus* when tested in aerobic conditions. Metronidazole is commonly utilised in the treatment of infectious diseases caused by anaerobic pathogens; its antimicrobial activity is evaluated when kept in anaerobic conditions to activate the futile cycle (Dione *et al.*, 2015). *E. coli* and *S. aureus* are facultative anaerobes that can tolerate anaerobic conditions. The diffusion assay and the MIC were repeated in anaerobic conditions, where Metronidazole showed its efficacy as an antimicrobial agent against the two control organisms. Nitrofurantoin (1.13) has been used lately not only for UTIs but for the management of CDI as well (Ge *et al.*, 2018).

The concentration of the tested compounds for the diffusion assay was set at 20.48 mg/ml; the compounds were dissolved in 100% DMSO. The absolute DMSO was used as a control for results validation to ensure that the DMSO did not interfere with the readings. The experiments were made in triplicate per compound to determine the ZOI in mm. Whereas the serial dilution of the tested compounds for the MIC assay were set at concentrations ranging between 512 – 0.125 µg/ml.

Table 3. 3. Antimicrobial activities of control drugs against *C. difficile* and control organisms *E. coli* and *S. aureus*

Controls	<i>E. coli</i>		<i>S. aureus</i>		<i>C. difficile</i>	
	ZOI (mm)	MIC ($\mu\text{g/ml}$)	ZOI (mm)	MIC ($\mu\text{g/ml}$)	ZOI (mm)	MIC ($\mu\text{g/ml}$)
1.4	20	512	10	>512	62	0.5
1.13	30	MBC = 4 MIC = 4	0	MBC = 8 MIC = 8	34	1

Compound **1.4** showed the highest efficacy and selectivity against *C. difficile*. The recorded MIC against *C. difficile* was a thousand times less than *E. coli* and *S. aureus*. However, compound **1.13** exhibits high potency against the tested microorganisms and narrow selectivity compared to **1.4**. Despite the high efficacy and selectivity of metronidazole against the tested strain of *C. difficile*, strain NAP1/027 was found to be resistant to the first line of treatment including metronidazole (Fatima & Aziz, 2019). As a result, synthesising drugs that might have a different mechanism of action was essential.

3.5.2. Antimicrobial activity assay of some aldehydes

Toxic adducts in cellular proteins involving DNA cross-links are generated from the addition reactions of aldehydes that exhibit electrophilic properties with thiols and amines. Cellular aldehydes are naturally abundant during the intermediate metabolism of natural compounds and drugs (Kuykendall, 2010). Despite the toxic effect of aldehydes as therapeutic agents, they can be involved in chemical reactions to benefit from their antimicrobial activity and overcome the possible side effects. Herein, the antimicrobial activity of some of those aldehydes were evaluated to give an insight of their contribution to the antimicrobial properties of the synthesised compounds. The antimicrobial activity of some of the utilised aldehydes was tested anaerobically to assess their contribution to the antimicrobial activity of the synthesised compounds. The concentration of the tested aldehydes for the diffusion assay was set at 20.48 mg/ml; the aldehydes were dissolved in 100% DMSO. The absolute DMSO was used as a control for results validation to ensure that the DMSO did not interfere with the readings. The serial dilution of the tested aldehydes for

the MIC assay was set at concentrations ranging between 512 – 0.125 µg/ml. The ZOI and MIC were carried out in triplicate (**Table 3.4.**).

Table 3. 4. Antimicrobial activities of aldehydes against *C. difficile* and control microorganisms *E. coli* and *S. aureus*

Aldehydes	<i>E. coli</i>		<i>S. aureus</i>		<i>C. difficile</i>	
	ZOI (mm)	MIC (µg/ml)	ZOI (mm)	MIC (µg/ml)	ZOI (mm)	MIC (µg/ml)
Benzaldehyde	0	128	0	>512	14	256
p-Methoxy benzaldehyde	10	512	0	>512	11	256
p-Methoxy cinnamaldehyde	20	>512	24	512	26	16
p-Nitro cinnamaldehyde	19	>512	28	64	34	2
Furaldehyde	0	>512	18	>512	11	256
5-Nitro furaldehyde	40	MIC = 5 MBC= 156	54	MIC = 8 MBC= 64	70	1
Furacrolein	20	256	17	>512	34	16
2-Methoxy-1-naphthaldehyde	0	>512	11	>512	15	>512
4-Benzyloxybenzaldehyde	0	>512	0	>512	0	512

The results showed that benzaldehyde is mostly active against *E. coli*, while its activity is 2-fold less against *C. difficile*. Replacing the para-substituted proton with a methoxy group (OCH₃) as in p-Methoxybenzaldehyde decreased the efficiency against *E. coli* by 2-fold. P-Methoxy cinnamaldehyde was highly selective against *C. difficile*, where its MIC against *C. difficile* was 32 times less than that recorded against *S. aureus*. Replacing the OCH₃ group with a NO₂ group increased the efficacy against *S. aureus* and *C. difficile*; however, the selectivity decreased.

The heterocyclic furan ring exhibited some antimicrobial activity against *C. difficile*, where the MIC value was 256 µg/ml. Adding a NO₂ group in the C5 of the furan ring showed a huge

enhancement in the antimicrobial activity against the three microorganisms. It was deduced that adding a NO₂ group in the C5 increases the antimicrobial activity but decreases the selectivity. The extra aliphatic C=C in furacrolein increased the antimicrobial efficacy against *C. difficile* by 16-fold compared to furan.

2-Methoxy-1-naphthaldehyde showed no antimicrobial activity against the three microorganisms in the tested concentration ranges, which indicates steric hindrance. 4-Benzyloxybenzaldehyde showed limited antimicrobial activity against *C. difficile* with an MIC value of 512 µg/ml.

3.5.3. Antimicrobial activity of the synthesised compounds

The antimicrobial activity of the synthesised compounds was evaluated anaerobically against *E. coli*, *S. aureus*, and *C. difficile* by agar diffusion assay and MIC. The concentration of the tested compounds for the diffusion assay was set at 20.48 mg/ml; the compounds were dissolved in 100% DMSO. The ZOI was measured in mm and the MIC was measured in µg/ml. Whereas the serial dilution of the tested compounds for the MIC assay was set at concentrations ranging between 512 – 0.125 µg/ml. The ZOI and MIC assays were carried out in triplets. SAR based on the efficiency and selectivity of tested compounds against *C. difficile* was deduced based on the obtained results.

Table 3. 5. The antimicrobial activities of benzylidene barbiturate derivatives against *C. difficile* and control organisms *E. coli* and *S. aureus*

[Table 3.5 redacted from open access version]

The aim of this study was to target *C. difficile* selectively; therefore, the smaller the MIC value against *C. difficile* and the greater that scored against *E. coli* and *S. aureus*, the greater the selectivity. The antimicrobial activity of the synthesised compounds was mainly based on the MIC readings, as some compounds had poor diffusion across the agar.

Regarding SAR, the presence of a benzene ring linked to an unsaturated monoene aliphatic chain in **2.4** led to a moderate selective growth inhibition of *C. difficile* (Table 3.5.). Elongating the aliphatic bridge between the aromatic rings with an additional unsaturated CH=CH, as in **2.12**, had no impact on the antimicrobial activity against *C. difficile*. However, the selectivity of **2.12** was lost, as it was more effective against *S. aureus*.

The addition of an electron-donating substrate (OCH₃ group) at the para-position of the benzene ring in compound **2.6** increased the electro-positivity hence induced a positive

inductive (+I) effect and a positive mesomeric (+M) effect. The antimicrobial activity of **2.6** against *C. difficile* was enhanced by 2-fold compared to an unsubstituted benzene ring, whilst sustaining the selectivity. The presence of an OCH₃ group can give two types of interactions with the receptor, where the compound can either employ the oxygen's lone pairs of electrons as a hydrogen bond acceptor or the hydrogen to act as a hydrogen bond donor. When the aliphatic chain was elongated with an extra unsaturated CH=CH bond as in **2.5**, the selective antibacterial activity against *C. difficile* increased by 8-fold. This may indicate that the elongated substrate binds with higher affinity to the active site or gives an umbrella effect by binding to the allosteric site of the receptor. The addition of an ethoxy group at position 2 of the benzene ring showed some antimicrobial activity against *C. difficile* with a MIC value of 512 µg/ml.

The presence of an electron-withdrawing group (NO₂) at the para-position of the benzene ring linked to unsaturated propene in the aliphatic region in compound **2.7** enhanced the antimicrobial activity against *C. difficile* by 8-fold. However, the selectivity decreased as the compound showed an inhibitory effect against *S. aureus*. Yet, the concentration required to inhibit *S. aureus* is 128 times greater than that needed to inhibit *C. difficile*; therefore, selective inhibition could be achieved. The NO₂ group induces negative inductive (-I) and negative mesomeric (-M) effects. NO₂ group acts as a hydrogen bond acceptor when interacting with the receptor.

Replacing the aromatic six-membered ring with a heterocyclic 5-membered furan ring in compound **2.8**, increased the potency against *C. difficile* by 32-fold. This indicated that minimising the ring size may enhance the antimicrobial activity against *C. difficile*. This high potency might be attributed to the presence of an electron-withdrawing group (oxygen) which might have employed its lone pairs of electrons to act as a hydrogen bond acceptor upon binding to the receptor. Furthermore, an electron-withdrawing NO₂ group at the fifth position of the furan ring in **2.10** increased the potency against *C. difficile* by 8-fold. However, the selectivity has dramatically declined by around 51-fold compared to the unsubstituted furan ring. Nevertheless, selective inhibition of *C. difficile* can still be achieved, as its MIC observed against *C. difficile* was five times less than *E. coli* and *S. aureus*.

Replacing the oxygen with sulfur in the heterocyclic 5-membered ring of **2.20** caused moderate antimicrobial activity against *E. coli* and *S. aureus* with a recorded MIC value of 512 µg/ml. Compound **2.20** was highly potent against *C. difficile* with a MIC of 0.25 µg/ml.

Adding a NO₂ group to the 5th position of the thiophene ring of **2.16** increased the efficacy against *E. coli* and *S. aureus*; however, the selectivity against *C. difficile* decreased. Elongating the aliphatic bridge with an additional unsaturated CH=CH spacer of **2.21**, decreased the efficacy against the three microorganisms.

Elongating the aliphatic bridge with an additional unsaturated CH=CH spacer between the six-membered ring and the unsubstituted furan ring in **2.9** decreased the efficacy against *C. difficile* by 2-fold compared to **2.8**. A narrow selectivity and non-discriminative high potency were achieved when a NO₂ group was added to the C5 of the furacrolein ring in **2.13**.

In compound **2.11**, the steric bulkiness and hydrophobicity of the aromatic group increased by adding a naphthalene ring instead of 5 and 6-membered rings, where the methoxy group in position 2 can act as a hydrogen bond donor or acceptor upon interacting with the receptor. This compound showed a selective inhibition of *C. difficile* with a moderate potency. Similarly, the aromatic bulkiness hindered the antimicrobial activity against the three microorganisms in compounds **2.14**, **2.15**, **2.17**, and **2.18**.

Substituting the C=O group at position 2 of the barbituric acid moiety of **2.16** with a C=S in compound **2.27** did not cause any change against *E. coli*; however, the antimicrobial activity against *S. aureus* decreased by 2-fold and against *C. difficile* by 8-fold.

When the hydrogens of the two NHs at position 1 and 3 of the barbituric acid moiety of **2.13** were replaced with two methyl groups in compound **2.28**, its antimicrobial activity against *E. coli* decreased by 4-fold and decreased against *C. difficile* by 16-fold. However, its antimicrobial activity against *S. aureus* increased by 2-fold.

When the hydrogens of the two NH at position 1 and 3 of the barbituric acid moiety of **2.7** were replaced with two methyl groups in compound **2.29**, its antimicrobial activity decreased against *S. aureus* by 2-fold and decreased against *C. difficile* by 256-fold. It was deduced that replacing the two NH with two N-CH₃ caused a decrease in the antimicrobial activity against the targeted microorganism *C. difficile*.

Table 3. 6. The antimicrobial activity of allylic barbiturate derivatives against *C. difficile* and control microorganisms *E. coli* and *S. aureus*

[Table 3.6 redacted from open access version]

The aim behind synthesising allylic barbiturate derivatives was to test the effect of reducing the exocyclic C=CH on the antimicrobial activity of a panel of test microorganisms. The hypothesis of this study was based on the ability of the allylic derivatives to act as pro-drugs, where enzymatic oxidation would take place once they bind to the DHODase active site giving the active form. The results showed a large decline in the antimicrobial activity against the three microorganisms after reducing the aliphatic chain. Most allylic compounds did not exhibit any antimicrobial activity against the test microorganisms when tested between the concentration ranges of 512-0.125 µg/ml. Compound 2.42 exhibited a MIC value of 256 µg/ml against *S. aureus* and *C. difficile*, while a MIC value of 64 µg/ml was recorded for compound 2.32 against *C. difficile*. Compound 2.45 was only active against *S.*

aureus with a MIC value of 128 µg/ml. The MIC values of the allylic barbiturate derivatives disprove the original pro-drugs hypothesis.

Table 3. 7. The antimicrobial activity of the Meldrum's acid derivatives against *C. difficile* and control microorganisms *E. coli* and *S. aureus*

[Table 3.7 redacted from open access version]

Barbituric acid was replaced with Meldrum's acid in this synthesised batch of compounds to estimate the necessity of barbituric acid's functional groups on the antimicrobial activity. In terms of interaction with the receptor, barbituric acid possesses two NH groups at positions 1, and 3 which can act as either a hydrogen bond donor or acceptor. While the C=O can act as a hydrogen bond acceptor. On the other hand, Meldrum's acid possesses two O groups at

positions 1 and 3 which can act as a hydrogen bond acceptor. The two methyl groups at position 2 of Meldrum's acid can bind to hydrophobic pockets.

It was observed that none of the Meldrum's acid possesses any antimicrobial activity against any of the three tested microorganisms except for the derivatives possessing a NO₂ group. Therefore, the presence of NO₂ is essential for the antimicrobial activity against *E. coli*. Numerous derivatives showed no growth inhibition against *S. aureus* or *C. difficile* including compounds **2.51**, **2.52**, **2.56**, **2.59**, and **2.61**. Moreover, compound **2.64** was the only derivative possessing an aliphatic allylic bridge that showed antimicrobial activity against *C. difficile*.

Replacing the barbituric acid moiety of compound **2.7** with a Meldrum's acid in compound **2.53** led to a decrease in the antimicrobial activity against *C. difficile* by 2-fold. Moreover, a decrease in the selectivity against *C. difficile* occurred as **2.53** enhanced antimicrobial activity against *S. aureus* by 4-fold.

Compound **2.9** possessed equal efficacy, but more selectivity against *C. difficile* compared to compound **2.54**. Whereas compound **2.55** showed higher activity compared to the benzylidene barbiturate derivative **2.12**; however, **2.12** was more selective against *C. difficile*. The benzylidene Meldrum's acid derivative **2.57** showed less antimicrobial activity and less selectivity compared to compound **2.13**.

As for compound **2.60**, it showed lower activity and equal selectivity against *C. difficile* compared to compound **2.21**. Compound **2.62** showed a decrease in the antimicrobial activity against *C. difficile* by 2-fold; however, it was two-fold more selective against *E. coli* and *S. aureus*. The only benzylidene Meldrum's acid derivative that exhibited higher activity and selectivity against *C. difficile* compared to its corresponding benzylidene barbiturate derivative **2.16** was compound **2.58**. Based on the MIC reading, it can be deduced that the benzylidene barbiturate derivative had an advantage over the benzylidene Meldrum's acid derivative in most cases except compound **2.58**.

Table 3. 8. The antimicrobial activity of the five-membered ring derivatives against *C. difficile* and control organisms *E. coli* and *S. aureus*

[Table 3.8 redacted from open access version]

As deduced from the previous MIC values obtained in this study, NO₂ containing compounds possess high, non-selective antimicrobial activity. Since compound **1.13** is one of the safest treatments used for *C. difficile*, furantoin derivative was synthesised to determine the impact of NO₂ on the antimicrobial activity. The results showed that furantoin **2.71** lost its antimicrobial activity against the three tested microorganisms. This finding gave an edge to the synthesised compounds over **1.13** as the synthesised compounds are not nitro group dependent. When the oxygen of position 1 of the furan ring of **1.13** was replaced with sulfur, the antimicrobial activity against *C. difficile* increased by 8-fold; however, no major change in the selectivity was observed. Whereas compounds **2.69**, **2.73**, and **2.80** showed some limited yet selective inhibitory effect against *C. difficile*.

Uridine (0.1 mM) was added to different concentration ranges between 256 – 4 µg/ml of some lead compounds to detect the correlation between the tested compounds and the inhibition of the DHODase enzyme. Uridine gets phosphorylated to nucleotides, which are essential for the synthesis of DNA and RNA. Therefore, restoration of the bacterial growth would be observed if the compounds rely on the DHODase inhibition pathway. However, no changes were observed after leaving the 96-well plates in anaerobic condition for 48 hours.

3.6. Conclusion

Based on the obtained results, it was deduced that the presence of a nitro substitution in the fifth position of a five-membered heterocyclic or the para-position of a six-membered aromatic ring increased the antimicrobial activity; however, the selectivity this study was aiming for dramatically decreased against *C. difficile*. Despite the decrease in the selectivity accompanied with the presence of the nitro-group, all the synthesised compounds exhibited the highest efficacy against *C. difficile* compared to the controls *E. coli* and *S. aureus*. Moreover, the antimicrobial activity did not completely vanish upon the removal of the nitro-groups, which indicated that the benzylidene barbiturates and the benzylidene Meldrum's acid derivatives are not NO₂ group dependent. Unlike the benzylidene barbiturates and the benzylidene Meldrum's acid derivatives, nitrofurantoin was proven to be NO₂ group dependent; thereby these findings indicate that they may not exhibit the exact inhibitory mechanism.

Steric hindrance was reflected in the decrease in the antimicrobial activity accompanied by the presence of a bulky group attached to the aliphatic chain. Additionally, a complete loss of the antimicrobial activity was obtained upon the saturation of the exocyclic C=C or the complete reduction of the aliphatic bridge linking the aromatic rings to benzylidene barbiturates or the benzylidene Meldrum's acid derivatives. Therefore, the hypothesis that the allylic derivatives might act as prodrugs, where the active arylidene form is generated by enzymatic oxidation upon binding to the DHODase active site was not verified.

The benzylidene barbiturates derivatives exhibited a slightly higher antimicrobial activity, especially against *C. difficile* compared with the benzylidene Meldrum's acid derivatives. This indicated that the presence of a hydrogen bond acceptor at position 2 or the presence of a hydrogen bond donor at positions 1 and 3 of barbituric acid moiety enhances the antimicrobial activity. Substituting the hydrogens in positions 1 and 3 of the barbituric acid moiety of the benzylidene barbiturates decreased their antimicrobial activity; it can be deduced that hydrophobic interactions are not required at these positions.

Finally, uridine (0.1 mM) was added to 96-well plates after placing different concentration ranges between 256 – 4 µg/ml of some lead compounds with *C. difficile* to detect the correlation between the tested compounds and the inhibition of the DHODase enzyme. No changes were observed when compared to the uridine-free wells, which indicates that the

mechanism of *C. difficile* inhibition does not relate to the inhibition of DNA, RNA, or proteins.

3.7. Limitations of the study

For wider data collection, the antimicrobial activity of the lead compounds could be tested against other strains of *C. difficile* including the resistant strain ribotype 027. Additionally, to confirm the selectivity of the lead compounds, other anaerobic bacteria included in the composition of the normal gut microbiota should be tested. Despite the high efficacy and selectivity of some synthesised compounds; however, their mechanism of action and their target were not detected in this study.

Chapter 4

4.1. Introduction

The assessment of cell viability, cytotoxicity, and proliferation became possible by the 1980s after Mosmann established the 3-(4,5-dimethylthiazol-2-yl)-2,5-diphenyl-2H-tetrazolium bromide (MTT) assay. This MTT assay was highly sensitive and avoided the need for the traditional radioactive isotope method requiring the incorporation of the radioactive ^3H -thymidine isotope (Maehara *et al.*, 1987). Any alteration in the number of viable cells is directly correlated with mitochondrial activity, as this activity is constant in most of the cells that remain viable. This colorimetric MTT assay relies on the enzymatic reduction of the yellow tetrazolium salt **4.1** to the purple, water-insoluble, ring-opened formazan structure **4.2** (Figure 4.1.) caused by the NAD(P)H-dependent oxidoreductase enzymes present in the mitochondria of viable cells (Van Meerloo *et al.*, 2011).

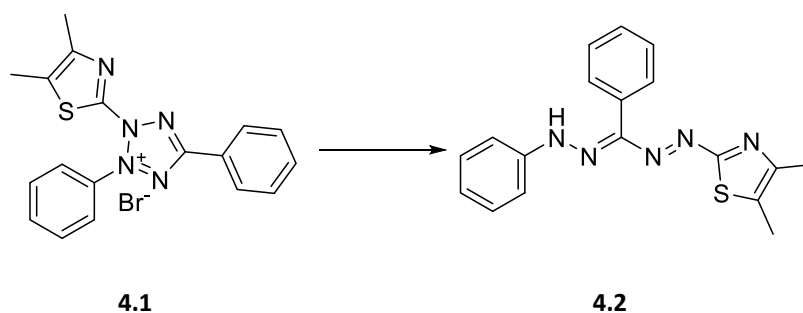


Figure 4. 1. Enzymatic conversion of tetrazolium salt (left, yellow) to the insoluble formazan product (right, purple) by means of NAD(P)H NAD(P)H-dependent oxidoreductase enzymes.

Solubilising agents such as DMSO are added to guarantee complete dissolution of the insoluble formazan crystals, where the resulting, purple-coloured solution can be quantified by means of a multi-well spectrophotometer. Hence, any change in viable cell count can be quantified by determining the concentration of formazan as measured by the OD readings. The intensity of the formazan colour is directly proportional to the quantity of viable, metabolically active cells that remain. The impact of the compounds being evaluated for cytotoxicity in the MTT assay method can be assessed on the chosen cell lines quantitatively by comparing the OD values obtained from the wells in a plate containing incubated cells exposed to test compounds compared with the OD values measured for control wells containing only the incubated cells, in the absence of test compound. Any reduction in the quantity of viable, dividing cells indicates inhibition in cell growth due to the test compound

thereby giving a direct measure of the sensitivity of the chosen cell line to the test compound.

The term IC_{50} is defined as the cytotoxic concentration sufficient to kill fifty percent of the viable cells compared to the growth of the drug-free control (Van Tonder *et al.*, 2015). The determination of the IC_{50} values of each compound in this study would provide the adequate therapeutic dose that causes the least possible damage to the normal cell lines.

The purpose of this part of the PhD research study was to determine the IC_{50} values of representative examples of the lead compounds synthesised (Chapter 2) and evaluated (Chapter 3) against BNL and Caco-2 cell lines. This facilitated a qualitative SAR determination based on comparisons with data obtained in parallel using doxorubicin, as cytotoxic, positive control alongside metronidazole and nitrofurantoin as pertinent reference compounds that were controls used in the antimicrobial work (Chapter 3).

4.2. Materials

4.2.1. Cells and controls

The MTT experiments were performed in a class 2B bio-cabinet. Incubation (37 °C) was undertaken in a complete media in CO₂ (5%).

4.2.2. MTT Solution preparation and composition

Phosphate buffered saline (10 ml) was added to MTT powder (500 mg) and the mixture was left to stir in the dark for (1 h, approximately). The solution was filtered through a 0.22 µm filter and stored at -20°C as aliquots (10 ml).

4.3. Methods

4.3.1. Thawing, subculture, and cryopreservation of mouse normal liver cells and colorectal cancer cells

Cell thawing, subculture, and cryopreservation were performed by Nawah Scientific Inc. (Mokatam, Egypt). BNL and Caco-2 cells were thawed by gentle agitation in a water bath (37°C) before centrifugation at room temperature (5 minutes). Following centrifugation, BNL cell pellets were gently resuspended in Dulbecco's Modified Eagle Medium (DMEM) (500 µl), while Caco-2 cells were resuspended in Roswell Park Memorial Institute (RPMI) media. Both media were supplemented with streptomycin (100 mg/ml), penicillin (100 units/ml), and heat-inactivated fetal bovine serum (FBS) (10%). The cell cultures were

further diluted to a total volume of (10 ml) and transferred to a flask (25 cm³) placed in a humidified CO₂ (5% v/v) atmosphere, at 37 °C. The cells were transferred to a flask (75 cm³) upon reaching 75-80% confluence. Subculturing was an essential step to follow when 75-80% confluence was reached, to retain the viability of the cells. Adherent cells were then washed gently with PBS (10 mM Na₂HPO₄, 1.8 mM KH₂PO₄, 137 mM NaCl, and 2.7 mM KCl, pH 7.4) after discarding the old media. To detach the adherent cells from the surface, trypsin/EDTA (0.5 mg/ml trypsin with 0.2 mg/ml EDTA pH 7.0-7.6) in PBS were added to the flask and then incubated (37°C) for 5 minutes with 5% CO₂. Trypsin inactivation occurred upon resuspending the cells with the culture media.

This exact procedure of cell washing, and detachment was repeated for the cryopreservation process. Cells were further diluted to 5 x 10⁶ cells/ml in a freezing medium (5% DMSO in FBS). Aliquots (1 ml) were then transferred to cryovials, before placing them in MrFrosty Freezing Containers with isopropanol overnight (-80°C, 18 h). For long-term storage, the aliquots were placed in a vapour phase liquid nitrogen tank.

4.3.2. Cell count and viability assessment

The cell suspension (50 µl) was stained with trypan blue (0.1%, 50 µl) to quantify the viable cells using a haemocytometer. The live cells were observed as bright spots, where the cell viability was calculated as a percentage of the total number of cells including both the dead and live cell populations.

4.3.3. Cell culture

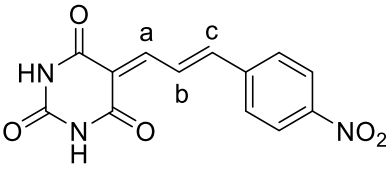
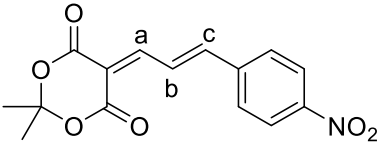
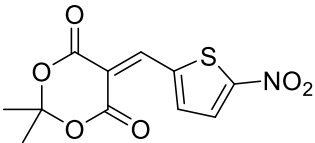
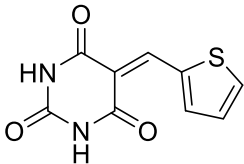
BNL and Caco-2 were grown to 80% confluence before detaching the cells with trypsin as described in section (4.3.1.). Cells were then centrifugated for 10 minutes, where BNL cell pellets were resuspended in DMEM media, and Caco-2 cells were resuspended in RPMI; trypan blue was further added for viable cell counting. Cells were diluted to 5 x 10⁴ cells/ml; wells were seeded with aliquots of 100 µl 5 x 10⁴ cells/ml to give 5 x 10³ cells/well. The 96 well plates were incubated for 24 hours at 37°C in the presence of 5% CO₂. The old media was discarded and replaced with 100 µl of fresh media containing a specified range of drug concentrations. The drug concentrations were as follows; 0.03 µg/ml, 0.1 µg/ml, 0.3 µg/ml, 1 µg/ml, 3 µg/ml, 10 µg/ml, and 30 µg/ml. The plates were swirled for 5 seconds to mix the components and the media aspirated after 48 hours of drug exposure. The drug-containing

media were aspirated, and each well was washed with 100 μ l of PBS. MTT stock solution (20 μ l of 1 mg/ml) was then added to each well, followed by plate incubation at 37 °C and 5% CO₂ for 4 hours. 100 μ l of absolute DMSO was utilised to solubilise the formazan crystals. The absorbance of the formazan solutions was recorded at λ_{max} 570 nm by a multi-well plate reader (BMG LABTECH FLUOstar® Omega).

4.4. Results

Six compounds (Table 4.1.), representative of the most potent and selective compounds prepared (Chapter 2) and evaluated for antimicrobial activity (Chapter 3) in this thesis work, were selected for the MTT assay against two cell lines (BNL and Caco-2). The selection of compounds was based on their encouraging MIC values from the antimicrobial evaluation (Chapter 3). The MTT assay was undertaken in triplicate; seeding the plates with sufficient cell density was a prerequisite to ensure that the absorbance fell within the linear range, with minimal error to detect changes in cell viability after the incubation of cells with MTT and consequent formazan solubilisation. A cell density of 5×10^3 cells/well was appropriate to note any deviation in the total cell count compared to the negative control.

Table 4. 1. Some of the most potent and selective compounds against *C. difficile* whose cytotoxic activity was evaluated using the MTT assay against BNL and Caco-2 cell lines.

Compound	Structure
2.7	
2.8	
2.16	
2.53	
2.58	
2.20	

4.4.1. MTT assay of the positive control against BNL and Caco-2 cells

Doxorubicin (Figure 4.2.) was used as a cytotoxic, positive control for the assay against BNL and Caco-2 cells for the comparative study against a selection of the synthesised lead compounds (Chapters 2 and 3). Serial dilution of seven different drug concentrations was made to assess the percentage viability of cells (Figure 4.3.). The effect of the different concentrations of doxorubicin on the cell viability of BNL and Caco-2 cells after 48 hours of drug exposure was established using an MTT assay. The dose-response curve plots the cell viability % (y-axis) against drug concentration in ($\mu\text{g/ml}$) on the x-axis. After 48 hours at a doxorubicin concentration of 0.1 $\mu\text{g/ml}$ and less,

no substantial decline in BNL cell viability was observed. However, an approximate 60% reduction in BNL cell viability was observed at a doxorubicin concentration of only 0.3 $\mu\text{g/ml}$ (Figure 4.4.). An IC_{50} of 0.21 $\mu\text{g/ml}$ was recorded for doxorubicin (Figure 4.4.). As for Caco-2 cells, an IC_{50} value of 34.32 $\mu\text{g/ml}$ was recorded after their exposure to doxorubicin for 48 hours (Figure 4.5.). Microscopic images were taken of the control cells and treated cells of both cell lines after their exposure to the drug at concentrations of 3 $\mu\text{g/ml}$, 30 $\mu\text{g/ml}$, and 100 $\mu\text{g/ml}$ (Figures 4.6. and Figure 4.7.).

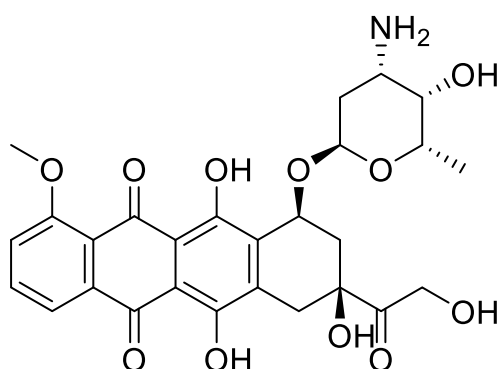


Figure 4. 2. Structure of doxorubicin

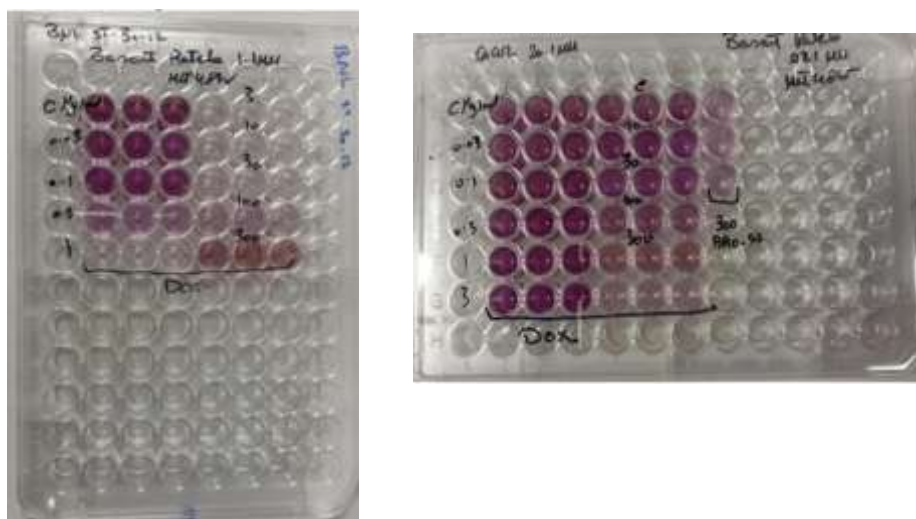


Figure 4. 3. Examples of the MTT assay experiment against BNL (left) and Caco-2 (right) cell lines comprising 9 different drug concentrations of doxorubicin ranging from 0.03-300 $\mu\text{g/ml}$ after 48 hours of drug exposure. The columns show the different drug concentrations in triplicates as labelled on the lid, where the first 3 wells in each figure labelled as ($\mu\text{g/ml}$) represent the controls.

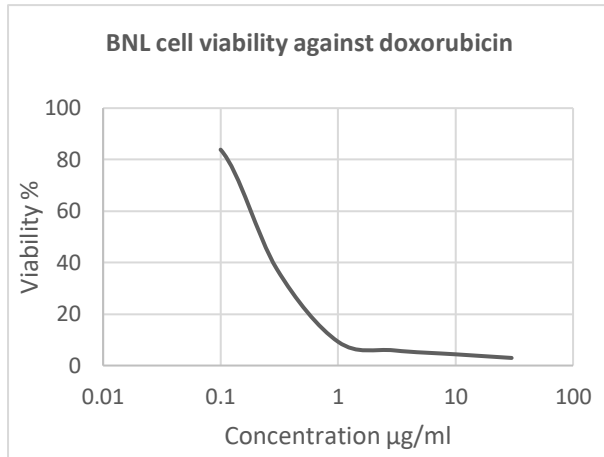


Figure 4. 4. Graph showing the plot of BNL cell viability % vs concentration of doxorubicin.

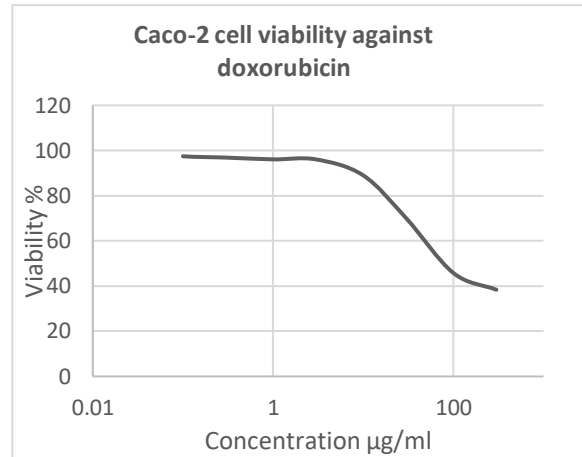


Figure 4. 5. Graph showing the plot of Caco-2 cell viability % vs doxorubicin concentration.

a

B

c

d

Figure 4. 6. Microscopic imaging showing the cell viability at different doxorubicin concentrations against the BNL cell line, with doxorubicin concentrations of (a) 0 µg/ml as the control; (b) 3 µg/ml; (c) 30 µg/ml; and (d) 100 µg/ml. The dots represent the viable cells that decrease in number with the increase in doxorubicin concentration.

a B c d

Figure 4. 7. Microscopic imaging showing the cell viability at different doxorubicin concentrations against the Caco-2 cell line, with doxorubicin concentrations of (a) 0 µg/ml as the control; (b) 3 µg/ml; (c) 30 µg/ml; and (d) 100 µg/ml. The clusters represent the viable cells that decrease in number with the increase in doxorubicin concentration.

4.4.2. MTT assay of 2.7 against BNL and Caco-2 cells

After exposure (48 h) to compound 2.7, No significant decrease in BNL cell viability was observed until the concentration reached 30 µg/ml, where approximately 30% cell death was observed (Figure 4.10.). An IC₅₀ of 42.12 µg/ml was recorded (Figure 4.8.). Conversely, Caco-2 cells exhibit high sensitivity to compound 2.7, where an approximate 30% cell death rate was observed, at a drug concentration of 10 µg/ml (Figure 4.11.). A notable decrease in the cell survival rate was further observed, where a drug concentration of 12.39 µg/ml was sufficient to reduce initial cell density by 50% (Figure 4.9.). Microscopic imaging was performed on the treated BNL and Caco-2 cell lines after exposure to drug concentrations of 3 µg/ml, 10 µg/ml, and 100 µg/ml (Figure 4.10. and Figure 4.11.).

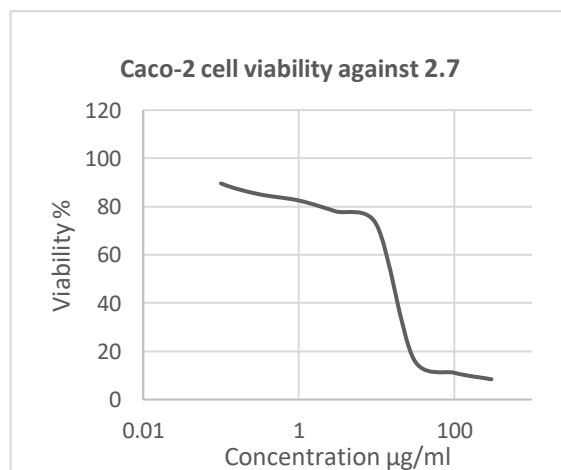
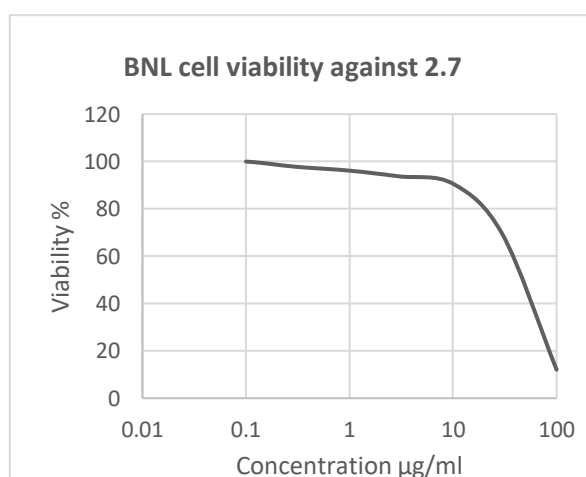


Figure 4. 8. Graph showing the plot of BNL cell viability % vs concentration of 2.7

Figure 4. 9. Graph showing the plot of Caco-2 viability % vs concentration of 2.7

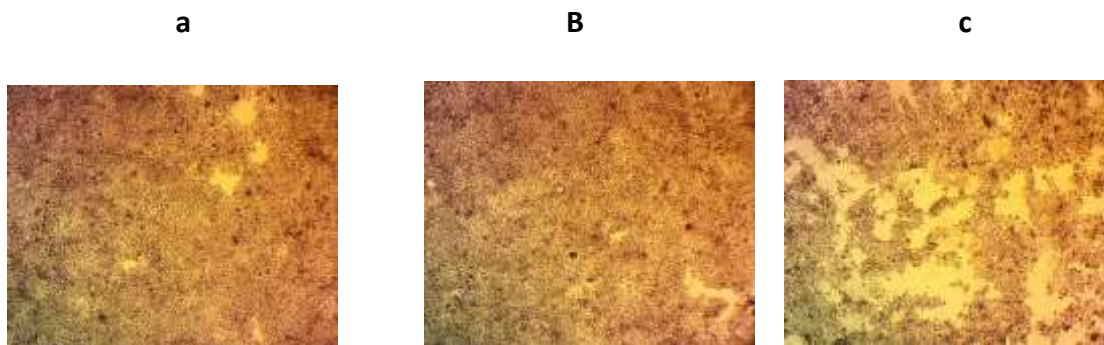


Figure 4. 10. Microscopic imaging showing the cell viability at different 2.7 concentrations against the BNL cell line, with 2.7 concentrations of (a) 0 $\mu\text{g/ml}$ as the control; (b) 3 $\mu\text{g/ml}$; (c) 30 $\mu\text{g/ml}$; and (d) 100 $\mu\text{g/ml}$. The dots represent the viable cells that decrease in number with the increase in compound 2.7 concentration.

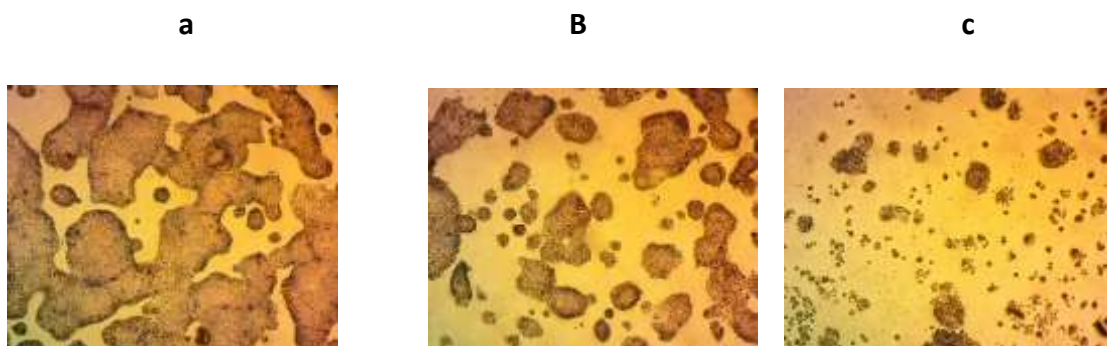


Figure 4. 11. Microscopic imaging showing the cell viability at different 2.7 concentrations against the Caco-2 cell line, with 2.7 concentrations of (a) 0 $\mu\text{g/ml}$ as the control; (b) 3 $\mu\text{g/ml}$; (c) 30 $\mu\text{g/ml}$; and (d) 100 $\mu\text{g/ml}$. The clusters represent the viable cells that decrease in number with the increase in compound 2.7 concentration.

4.4.3. MTT assay of 2.8 against BNL and Caco-2 cells

After exposure (48 h) to compound 2.8; the least cytotoxic effect against BNL cell lines with an IC_{50} of 123.94 $\mu\text{g}/\text{ml}$ was demonstrated (Figure 4.12.). Caco-2 cell lines also showed a high level of survival stability against compound 2.8, where an exponential reduction in cell viability was observed. Less than 25% cell death was evident at concentrations lower than 100 $\mu\text{g}/\text{ml}$, with an IC_{50} of 150 $\mu\text{g}/\text{ml}$ (Figure 4.13.). Microscopic imaging of the treated cells against both BNL and Caco-2 cell lines after exposure to drug concentrations of 3 $\mu\text{g}/\text{ml}$, 30 $\mu\text{g}/\text{ml}$, and 100 $\mu\text{g}/\text{ml}$ were recorded (Figure 4.14. and Figure 4.15.).

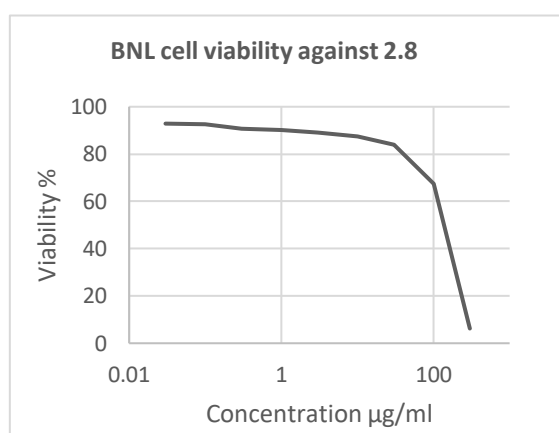


Figure 4. 12. Graph showing the plot of BNL cell viability % vs concentration of 2.8

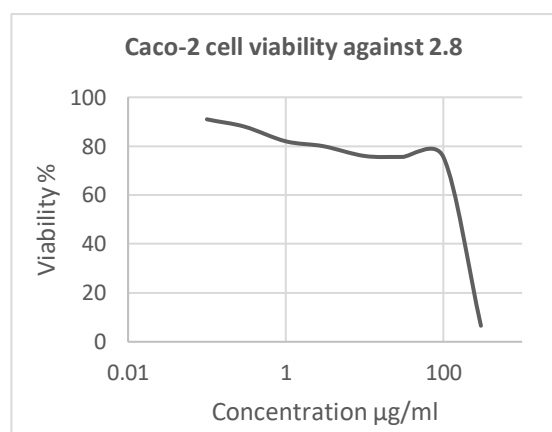


Figure 4. 13. Graph showing the plot of Caco-2 viability % vs concentration of 2.8

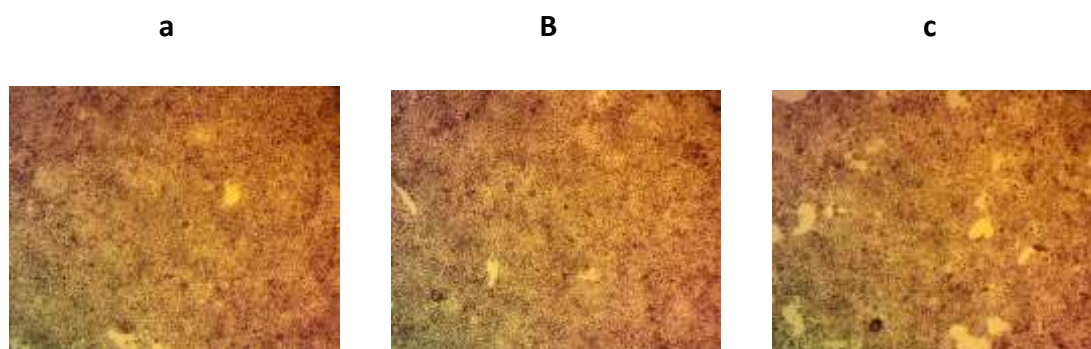


Figure 4. 14. Microscopic imaging showing the cell viability at different 2.8 concentrations against the BNL cell line, with 2.8 concentrations of (a) 0 $\mu\text{g}/\text{ml}$ as the control; (b) 3 $\mu\text{g}/\text{ml}$; (c) 30 $\mu\text{g}/\text{ml}$; and (d) 100 $\mu\text{g}/\text{ml}$. The dots represent the viable cells that decrease in number with the increase in compound 2.8 concentration.

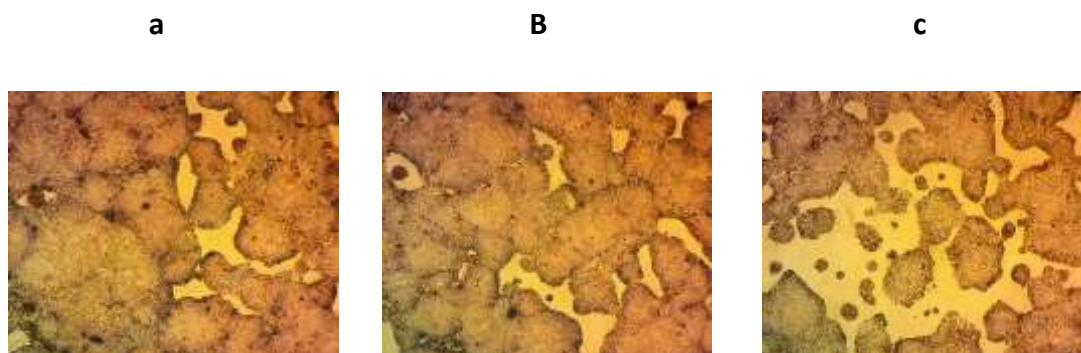


Figure 4. 15. Microscopic imaging showing the cell viability at different 2.8 concentrations against the Caco-2 cell line, with 2.8 concentrations of (a) 0 $\mu\text{g/ml}$ as the control; (b) 3 $\mu\text{g/ml}$; (c) 30 $\mu\text{g/ml}$; and (d) 100 $\mu\text{g/ml}$. The clusters represent the viable cells that decrease in number with the increase in compound 2.8 concentration.

4.4.4. MTT assay of 2.16 against BNL and Caco-2 cells

After exposure (48 h) to compound 2.16, an exponential decrease in the BNL cell viability was recorded when increasing the drug concentration, where an IC_{50} of 42.45 $\mu\text{g/ml}$ was observed (Figure 4.16.). As for the Caco-2 cell lines, a gradual decrease in the cell viability was observed until the drug concentration reached 10 $\mu\text{g/ml}$. A notable decline in the cell viability was then observed and an IC_{50} of 13.68 $\mu\text{g/ml}$ was reached (Figure 4.17.). Microscopic imaging of the treated cells after exposure to drug concentrations of 3 $\mu\text{g/ml}$,

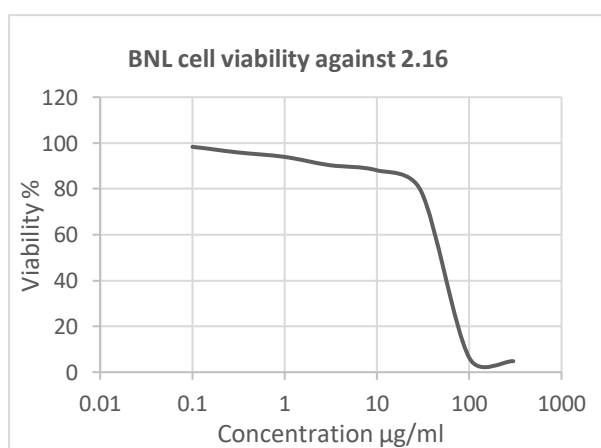


Figure 4. 16. Graph showing the plot of BNL cell viability % vs concentration of 2.16

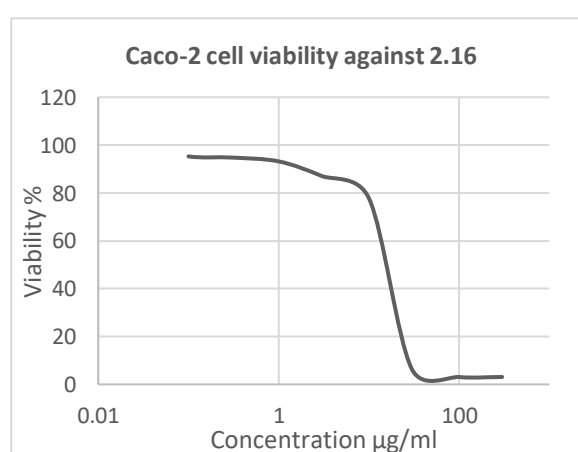


Figure 4. 17.Graph showing the plot of Caco-2 viability % vs concentration of 2.16

30 $\mu\text{g/ml}$, and 100 $\mu\text{g/ml}$ were recorded (Figure 4.18. and Figure 4.19.).

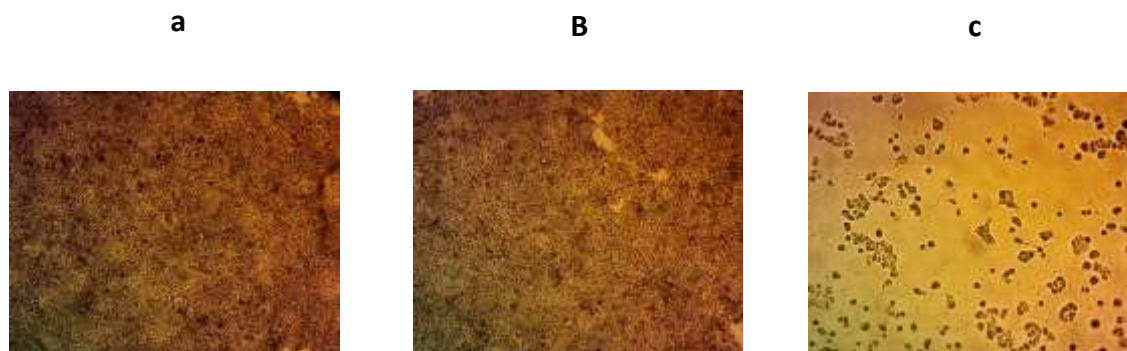


Figure 4. 18. Microscopic imaging showing the cell viability at different 2.16 concentrations against the Caco-2 cell line, with 2.16 concentrations of (a) 0 $\mu\text{g/ml}$ as the control; (b) 3 $\mu\text{g/ml}$; (c) 30 $\mu\text{g/ml}$; and (d) 100 $\mu\text{g/ml}$. The dots represent the viable cells that decrease in number with the increase in compound 2.16 concentration

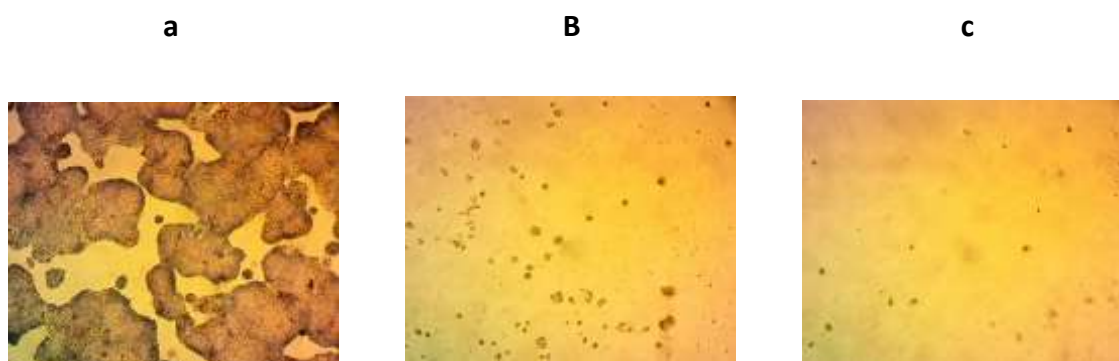


Figure 4. 19. Microscopic imaging showing the cell viability at different 2.16 concentrations against the Caco-2 cell line, with 2.16 concentrations of (a) 0 $\mu\text{g/ml}$ as the control; (b) 3 $\mu\text{g/ml}$; (c) 30 $\mu\text{g/ml}$; and (d) 100 $\mu\text{g/ml}$. The dots represent the viable cells that decrease in number with the increase in compound 2.16 concentration.

4.4.5. MTT assay of 2.53 against BNL and Caco-2 cells

Less than 10% decrease in cell viability after the BNL cell line was treated with compound 2.53 at concentrations of up to 30 $\mu\text{g/ml}$ for 48 hours. Viable BNL cells decreased to 65% at a drug concentration of 100 $\mu\text{g/ml}$ with a recorded IC_{50} of 117.98 $\mu\text{g/ml}$ (Figure 4.20.). Caco-2 cell lines displayed higher sensitivity to this compound 2.53, where an IC_{50} of 38.88 $\mu\text{g/ml}$ was obtained (Figure 4.21). Microscopic images of the treated cells against the BNL and

Caco-2 cell lines after drug exposure to 3 $\mu\text{g/ml}$, 30 $\mu\text{g/ml}$, and 100 $\mu\text{g/ml}$ concentrations are shown in figures (4.22.) and (4.23.).

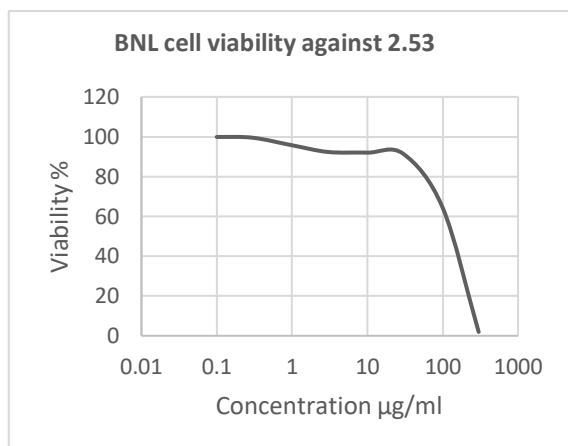


Figure 4. 20. Graph showing the plot of BNL cell viability % vs concentration of 2.53

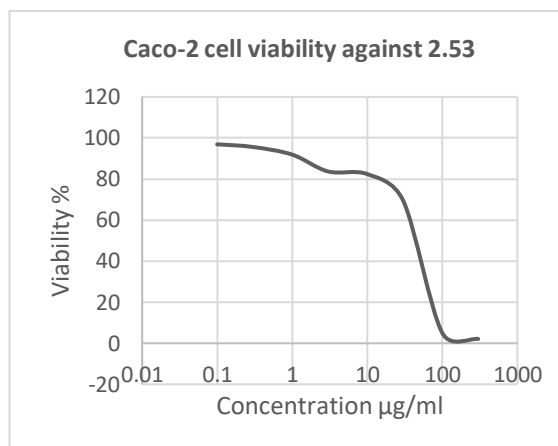


Figure 4. 21. Graph showing the plot of Caco-2 viability % vs concentration of 2.53

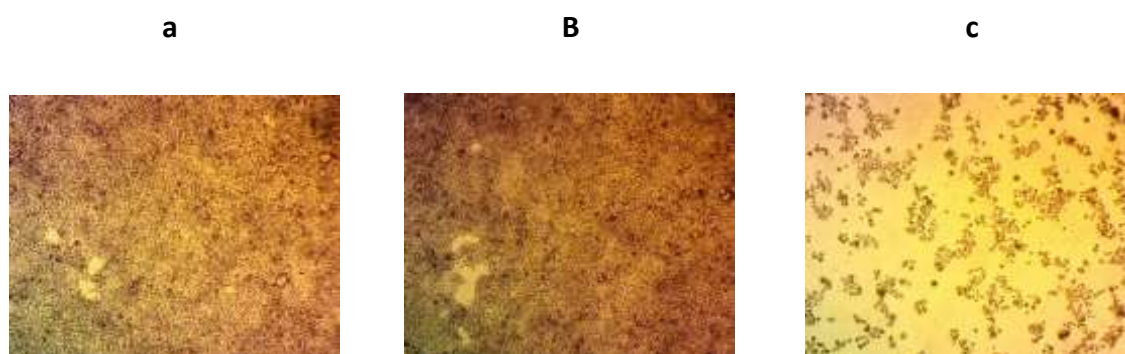


Figure 4. 22. Microscopic imaging showing the cell viability at different 2.53 concentrations against BNL cell line, with 2.53 concentrations of (a) 0 $\mu\text{g/ml}$ as the control; (b) 3 $\mu\text{g/ml}$; (c) 30 $\mu\text{g/ml}$; and (d) 100 $\mu\text{g/ml}$. The dots represent the viable cells which decrease in number with the increase in compound 2.53 concentration.

a B c



Figure 4. 23. Microscopic imaging showing the cell viability at different 2.53 concentrations against Caco-2 cell line, with 2.53 concentrations of (a) 0 µg/ml as the control; (b) 3 µg/ml; (c) 30 µg/ml; and (d) 100 µg/ml. The dots represent the viable cells which decrease in number with the increase in compound 2.53 concentration.

4.4.6. MTT assay of 2.58 against BNL and Caco-2 cells

Less than 30% decrease in cell viability after the BNL cell line was treated with compound 2.58 at concentrations of up to 30 µg/ml for 48 hours. Viable BNL cells decreased to 50% at a drug concentration of 36.52 µg/ml (Figure 4.24.). Caco-2 cell lines displayed higher sensitivity to this compound 2.58, where an IC₅₀ of 14.89 µg/ml was obtained (Figure 4.25.). Microscopic images of the treated cells against the BNL and Caco-2 cell lines after drug exposure to 3 µg/ml, 30 µg/ml, and 100 µg/ml concentrations are shown in Figure (4.26.) and Figure (4.27.).

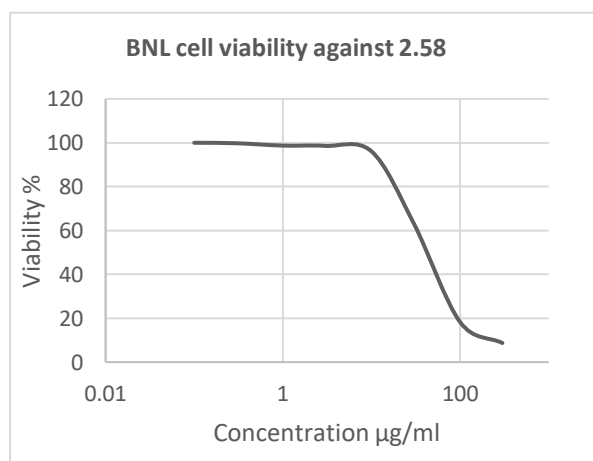


Figure 4. 25. Graph showing the plot of BNL cell viability % vs concentration of 2.58

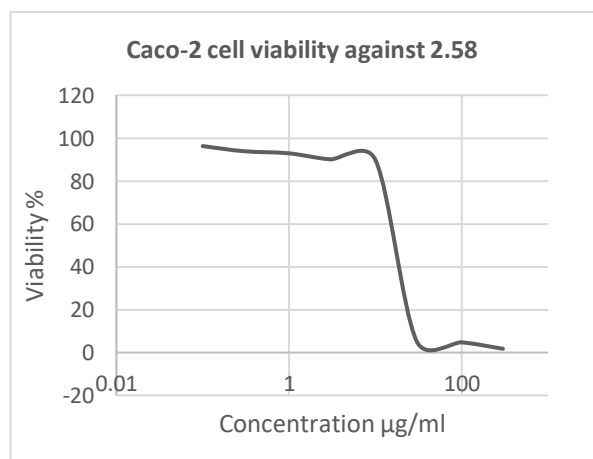


Figure 4. 24. Graph showing the plot of Caco-2 cell viability % vs concentration of 2.58

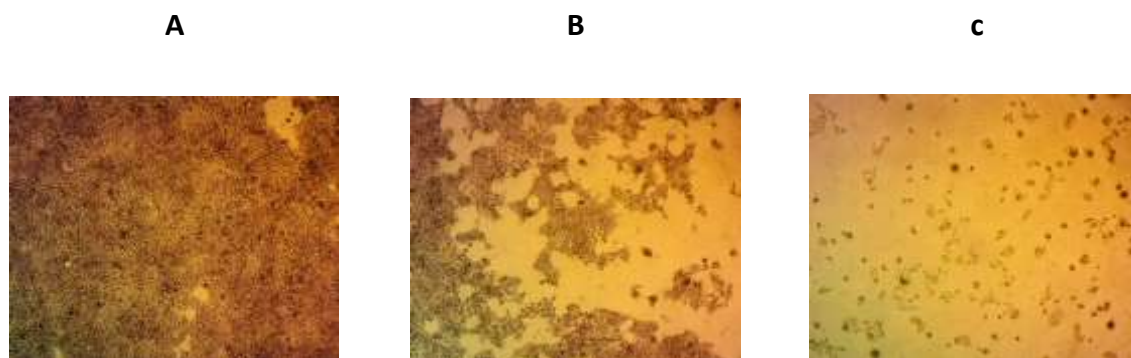


Figure 4. 26. Microscopic imaging showing the cell viability at different 2.58 concentrations against the BNL cell line, with 2.58 concentrations of (a) 0 $\mu\text{g/ml}$ as the control; (b) 3 $\mu\text{g/ml}$; (c) 30 $\mu\text{g/ml}$; and (d) 100 $\mu\text{g/ml}$. The dots represent the viable cells that decrease in number with the increase in compound 2.58 concentration.

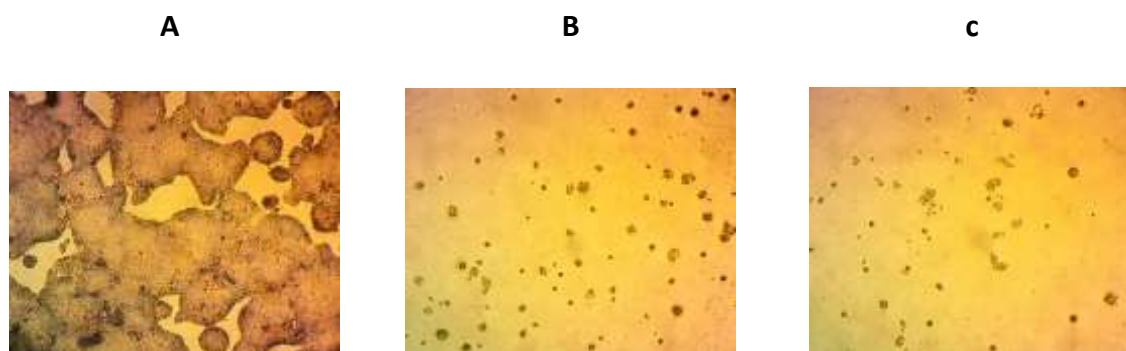


Figure 4. 27. Microscopic imaging showing the cell viability at different 2.58 concentrations against the Caco-2 cell line, with 2.58 concentrations of (a) 0 $\mu\text{g/ml}$ as the control; (b) 3 $\mu\text{g/ml}$; (c) 30 $\mu\text{g/ml}$; and (d) 100 $\mu\text{g/ml}$. The dots represent the viable cells that decrease in number with the increase in compound 2.58 concentration.

4.4.7. MTT assay of 2.20 against BNL and Caco-2 cells

Less than 25% decrease in cell viability after the BNL cell line was treated with compound 2.20 at concentrations of up to 30 $\mu\text{g/ml}$ for 48 hours. Viable BNL cells decreased to 50% at a drug concentration of 43.75 $\mu\text{g/ml}$ (Figure 4.28.). Caco-2 cell lines displayed a slightly higher sensitivity to this compound 2.20, where an IC_{50} of 32.51 $\mu\text{g/ml}$ was obtained (Figure 4.29.). Microscopic images of the treated cells against the BNL and Caco-2 cell lines after drug exposure to 3 $\mu\text{g/ml}$, 30 $\mu\text{g/ml}$, and 100 $\mu\text{g/ml}$ concentrations are shown in figures (4.30.) and (4.31.).

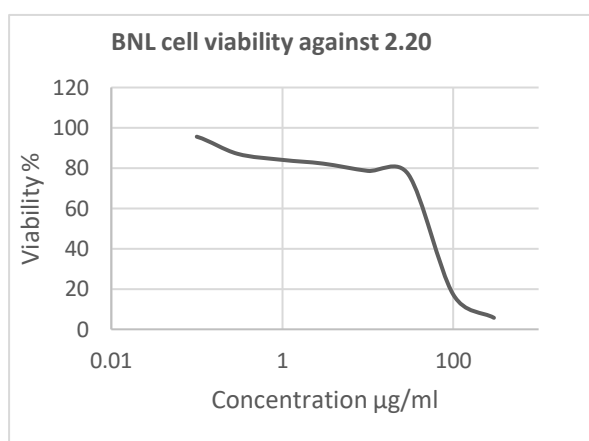


Figure 4. 29. Graph showing the plot of BNL cell viability % vs concentration of 2.20

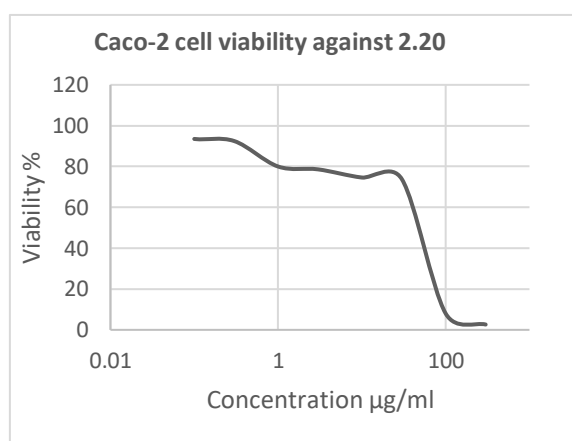


Figure 4. 28. Graph showing the plot of Caco-2 cell viability % vs concentration of 2.20

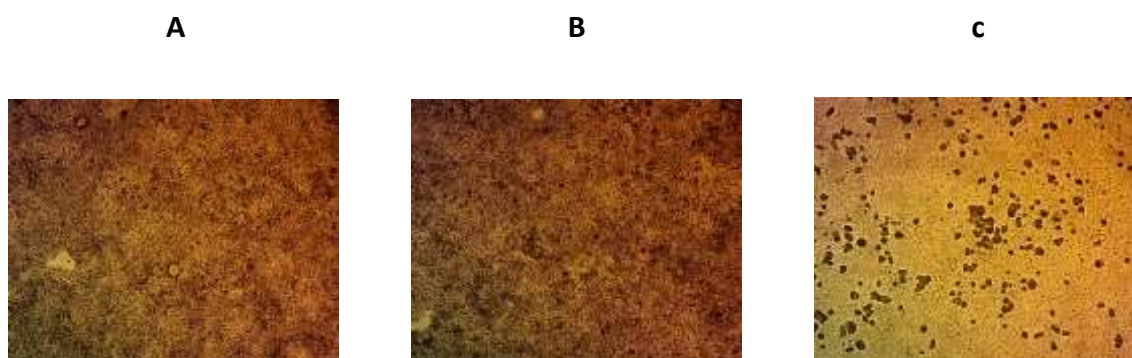


Figure 4. 30. Microscopic imaging showing the cell viability at different 2.20 concentrations against the BNL cell line, with 2.58 concentrations of (a) 0 $\mu\text{g/ml}$ as the control; (b) 3 $\mu\text{g/ml}$; (c) 30 $\mu\text{g/ml}$; and (d) 100 $\mu\text{g/ml}$. The dots represent the viable cell that decreases in number with the increase in compound 2.20

concentration.

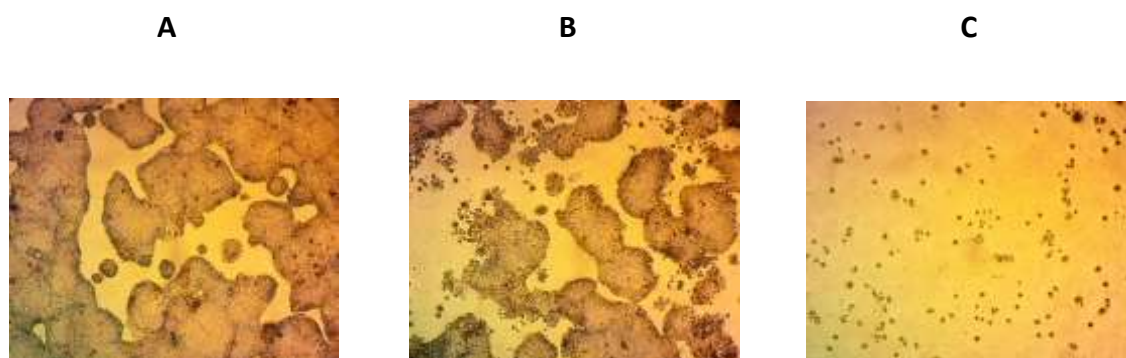


Figure 4. 31. Microscopic imaging showing the cell viability at different 2.20 concentrations against the Caco-2 cell line, with 2.58 concentrations of (a) 0 µg/ml as the control; (b) 3 µg/ml; (c) 30 µg/ml; and (d) 100 µg/ml. The dots represent the viable cells that decrease in number with the increase in compound 2.20 concentration.

4.5. Discussion

This chapter aimed to determine the *in vitro* effect of representative examples of the lead compounds prepared (Chapter 2) and evaluated (Chapter 3) on the viability of BNL and Caco-2 cell lines. The cytotoxicity was quantified by the MTT assay that allowed measurement of the IC₅₀ values summarised in (Figure 4.32.). The BNL cell line was selected for this study as the liver plays an important role in the selective uptake, metabolism, and excretion of most drugs and toxins. It is essential to examine the effect of any potential drug candidate on the liver before planning to introduce it into the body in any clinical trial study (Larson *et al.*, 2018). Sometimes the parent drug candidates themselves may exhibit hepatotoxicity. However, in most cases, the drug metabolites that form can cause drug-induced liver injury (DILI). Hepatocytic endoplasmic reticulum and other membrane-bound enzymes regulate the level of drug metabolites formed. The drug metabolism process produces water-soluble compounds for excretion through the bile (Vaja & Rana, 2020). Each drug may be transformed metabolically by discrete enzymes that control specific disposal pathways. For example, aromatic barbituric acid derivatives are mediated primarily by microsomal enzyme systems residing in the liver. Barbiturates are metabolised

by oxidation of substituents at the C5 position to terminate the pharmacological activity (Jurado, 2013).

Since all the synthesised compounds in this study were envisioned to target bacterial infection localised in the gut, the Caco-2 cell line was the appropriate choice to examine the cytotoxic properties of the representative lead compounds chosen in this chapter. Caco-2 cells represent a human colon epithelial cancer cell line that mimics the human intestinal compacted junction when cultured as a monolayer at the appropriate density. This unique characteristic enables the Caco-2 cells to act as a model to assess drug absorption and the paracellular motion through the monolayer. Unlike normal cells, Caco-2 cells lack the ability to express cytochrome P450 isozymes, and CYP3A4 is normally expressed excessively in the intestine. Supplying the Caco-2 cells with vitamin D₃ prompts the expression of higher quantities of CYP3A4 (Van Breemen & Li, 2005).

As mentioned in section 4.1., cell viability has a directly proportional correlation with the metabolic activity of cells and, consequently, any change in the metabolism will be a measure of the number of viable cells (Aslantürk, 2018). An incubation period of 24 hours was recommended as a prerequisite before the MTT assay (Yaacoub *et al.*, 2021, Tsai *et al.*, 2021). This step was adopted in this study to provide sufficient time for the cells to adhere to the plate, enabling washes and media changes to be successfully made by manual aspiration. This step reduces the risk of cell loss encountered with the washes and accelerates the speed of the assay. Moreover, this incubation period provides the cells with sufficient time to recover from the harvest and seeding phases. It is essential to perform this assay during the log phase of cell proliferation in order to occur within the linear range of absorbance measurement (van Meerloo *et al.*, 2011).

After 48 hours of exposure to the drug or test compound, treatment was washed from the wells with PBS before adding MTT. This washing step was made to eliminate the possible intrusion of the constant drug exposure with the reduction of MTT during incubation; thus, the viability data correspond to an exact drug exposure period. By adhering to the original protocol established by Mosmann at the beginning of the 1980s, the removal of unreduced MTT before applying the solubilising reagent was not necessary as the excess MTT does not hinder the absorption (Ghasemi *et al.*, 2021). The formazan crystals produced from MTT reduction have raised some concerns as the possible introduction of false positive results

through overestimation of cell viability has been reported (Young *et al.*, 2005). This issue was overcome by introducing blank wells into the experiment design, where the correct absorbance was calculated by subtracting the absorbance of the cells-containing wells incubated with MTT from the MTT-incubated media free from cells. Many researchers put forward hypotheses to rationalise the presence of extracellular formazan including breakage of the cell membrane via the crystal formation, the diffusion of intracellular formazan by exocytosis (Liu *et al.*, 1997), or other molecular interactions (Diaz *et al.*, 2007). Washing out the extracellular formazan following MTT incubation might lead to an underestimation of the viable cell count. Moreover, the presence of any damage in the cell membrane might aggravate the effect of the excess formazan at high drug concentrations or longer drug exposure. The precise absorbance values and cell viability percentage can be measured by excluding the washing step preceding the solubilisation of both the intracellular and extracellular formazan (Ghasemi *et al.*, 2021). Adequate solubilisation of the formazan crystals was a fundamental consideration to decrease any deviation that may take place from one well to another thereby ensuring that the absorbance lay in a detectable range. The addition of organic solvents such as DMSO in the MTT assay was essential owing to the lipophilic nature of formazan which prevents its solubilisation in aqueous media (Riss *et al.*, 2013).

The previously stated data represents a dose-dependent loss of cell viability for BNL and Caco-2 cells. This decline in cell viability was correlated with cell exposure to representatives of the most potent and selective drugs in the library of synthesised compounds. Doxorubicin was used as a positive control for a comparative study against the representative compounds prepared in the thesis work. Despite being derived from *Streptomyces peucetius*, doxorubicin has been used primarily as a chemotherapeutic agent since the early 1960s (Belger *et al.*, 2024). After 48 hours of exposure to doxorubicin, BNL cells exhibited high sensitivity against the drug which reduced viable cell count by 50% at a drug concentration of 0.21 µg/ml. This finding is in agreement with the clinical study that showed that incidences of hepatotoxicity are usually accompanied by doxorubicin administration to breast cancer patients (Damodar *et al.*, 2014). Caco-2 cells showed less sensitivity towards doxorubicin after 48 hours of exposure, where the IC₅₀ value was judged to be 34.32 µg/ml.

Four of the most potent compounds in the compound library possess a common structural feature which is the presence of a nitro-group, either in the para-position of a six-membered ring or at C 5 position of a five-membered heterocyclic ring; furan or thiophene. The cytotoxic effect of the nitro-containing compounds (**2.7**, **2.16**, **2.53**, and **2.58**) against BNL cells was evident from the IC₅₀ values that varied between 36.52 and 117.98 µg/ml. In comparison with the positive control drug, doxorubicin, all the synthesised compounds showed a notably lower effect against BNL cells; moreover, the observed IC₅₀ values were notably higher than their antimicrobial MIC values (Chapter 3). Hence, these representative compounds are less toxic to BNL cells which serve as a mimic of human liver cells. However, three out of four compounds showed lower IC₅₀ values against Caco-2 cells when compared to the positive control drug doxorubicin. The only aryl nitro derivative that displayed a reduced effect against Caco-2 cells was **2.53** (IC₅₀ of 38.88 µg/ml).

The presence of a nitro-containing aryl ring as a structural feature in known and widely used drugs may sometimes be accompanied by a risk of carcinogenicity, mutagenicity, and teratogenicity. These side effects occur due to the intracellular conversion of the nitro group to a reactive nitroso group which subsequently leads to the destruction of the DNA, RNA, and proteins by nucleophilic reactions. Unfortunately, these effects are undisputed to occur both in bacteria and in the human host. Despite their possible drastic side effects, some aryl nitro group containing drugs such as metronidazole and nitrofurantoin remain in a popular and widely traded market where metronidazole, a frontline treatment for CD infection, and nitrofurantoin are used for the treatment of uncomplicated urinary tract infections (Blass, 2021). The reason behind the continued prescribing of nitrofurantoin is its unique pharmacokinetic properties as 100 mg of the oral dose gets rapidly eliminated after absorption. Only around 25% of the dose becomes excreted, uncharged into the urinary tract as the remaining 75% of the quantity taken undergoes first-pass metabolism. The distributed plasma concentration of nitrofurantoin in all body parts is estimated to be less than 1 µg/ml except in the urinary tract where the concentration can reach more than 200 µg/ml. This concentration far exceeds that needed to successfully treat the bacterial infection. The pharmacokinetic characteristics of nitrofurantoin; localisation in the urinary tract, limits the total systemic, restricting the possible damage attributed to the drug through its usual mode of action (Blass, 2021).

Cytotoxicity is also associated with the metabolic derivatives formed from metronidazole. Metronidazole is a nitroimidazole derivative and retains its first-line status as a treatment for GIT-correlated infections and inflammatory disorders such as colitis caused by *C. difficile*. Even after six decades, research has not succeeded in defining the exact metabolic fragment(s) that contribute to the elevation of the cytotoxicity profile of metronidazole. Upon the activation of prodrugs such as the nitroimidazoles via the reduction of the nitro group under anaerobic conditions, imidazole fragmentation and cytotoxicity occur. Whether cytotoxicity is associated with the nitroimidazole activation stage or the successive fragments of the imidazole ring, or the metabolites only arbitrate cytotoxicity, has still to be determined (Dingsdag & Hunter, 2018).

Despite the possible toxic effects possessed by the nitro-substituted aryl-containing compounds synthesised in this library, those effects could be minimised in the clinic and practice by administering low concentrations of the compounds. It is reassuring to see that the MIC values (Chapter 3) of the four nitro-aryl-containing derivatives were lower than their IC₅₀ values.

The MIC value of compound **2.7** against the targeted microorganism *C. difficile* was 6 times lower than the scored IC₅₀ against Caco-2 cells; according to the reported data retention of 80% cell viability was observed at the MIC value of 2 µg/ml. While the MIC value of compound **2.16** against *C. difficile* was more than 27 times lower than their IC₅₀ against Caco-2 cells; according to the reported data less than 7% cell death was observed at the MIC value of 0.5 µg/ml. Compound **2.53** exhibited the least toxic effect among the nitro-aryl-containing derivatives against Caco-2 cells, its MIC value against *C. difficile* was 10 times lower than its IC₅₀ against Caco-2 cells where approximately 83% cell viability was scored at the MIC value of 4 µg/ml. As for compound **2.58**, a MIC value of 0.125 µg/ml was scored against *C. difficile*. The MIC value was approximately 119 times higher than the IC₅₀ value against Caco-2 cells.

The two nitro-free derivatives showed low efficacy against BNL cells, where the IC₅₀ of **2.8** was 590 times higher than doxorubicin, while BR1-44 showed an IC₅₀ of 43.75 µg/ml, which is 208 times higher than doxorubicin. On the other hand, an IC₅₀ of 150 µg/ml was observed for **2.8** against Caco-2; 4 times the concentration observed for doxorubicin. As for BR144, an IC₅₀ of 32.51 µg/ml was calculated against Caco-2 cells which is slightly lower than that

observed for doxorubicin. Since the IC_{50} of compound **2.20** against *C. difficile* was 0.25 $\mu\text{g/ml}$, administering this drug at concentrations lower than the IC_{50} may prevent the possible toxic effect. Generally, compound **2.8** showed the lowest IC_{50} values against both BNL and Caco-2 cells and was considered as possibly the safest if used in practice compared with the other 5 compounds tested.

A qualitative SAR correlation was determined based on the degree of cytotoxic activity against both BNL and Caco-2 cell lines. Compound **2.53** showed fewer toxic effects against both cell lines compared to **2.7**, whereas compound **2.16** exhibited less of a toxic effect against the BNL line compared to **2.58** without significant differences against Caco-2 cells. Thus, the replacement of NH groups at positions 1 and 3 by oxygen, and the substitution of the carbonyl group at C2 with the dimethyl group, decreased the toxic side effects evidenced by the increase in the IC_{50} values (Figure 4.31.). As previously mentioned, the presence of the nitro-aryl moiety in the structure increases the toxicity irrespective of antimicrobial activity. This characteristic can be further established by comparing compounds **2.20** and **2.16**, upon the replacement of the nitro group at C5 by hydrogen in the furyl ring, the toxic effect against Caco-2 decreased (2-fold) accompanied by a moderate decrease in the toxic effect against BNL cells (Figure). Substitution of the sulfur at position 1 in compound **2.20** with oxygen in compound **2.8** resulted in a decrease of the toxic effect against BNL cells by 3-fold, and a nearly 4-fold decrease in cytotoxicity against Caco-2 cells. In conclusion, the tested compounds showed high potency and selectivity against *C. difficile*, as well as acceptable cytotoxicity against BNL and Caco-2 cell lines. Compounds **2.8** showed the least cytotoxic effect against the two cell lines; whereas the toxic effects accompanied by the aryl nitro group containing compounds could be overcome by administering doses lower than the IC_{50} .

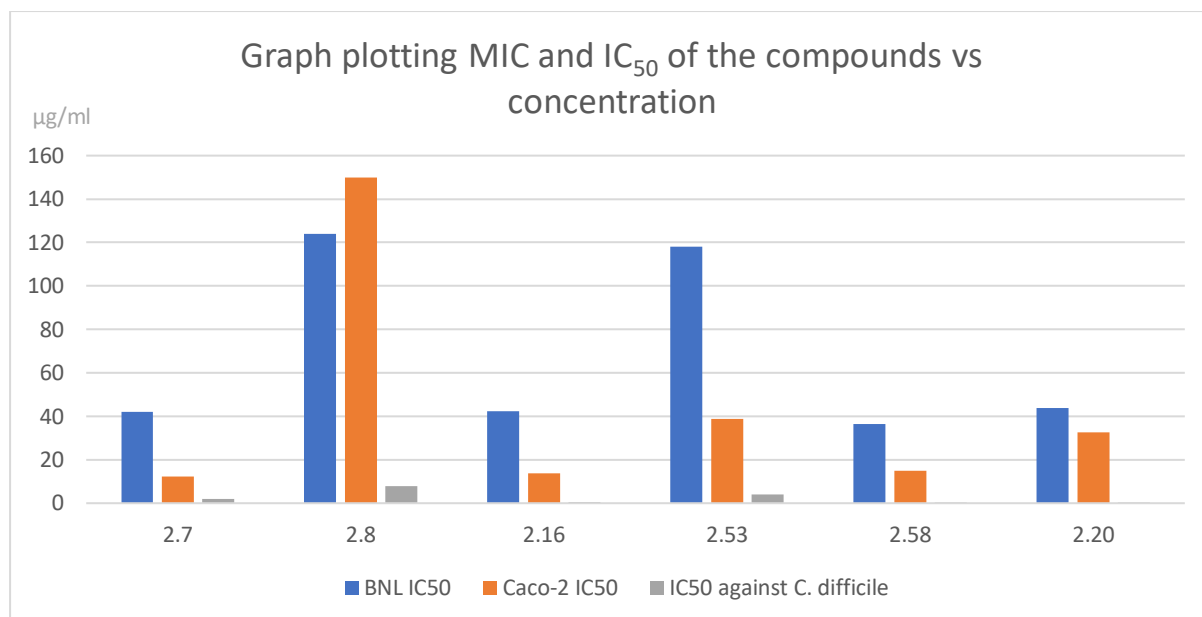


Figure 4. 32. Graph summarising the MIC and IC₅₀ values of the test compounds against the BNL and Caco-2 cell lines.

4.6. Limitations of the study

The study was performed on BNL and Caco-2 cell lines only. Further, cytotoxicity studies on other cell lines as Human Embryonic Kidney (HEK 293), for a better understanding and prevention of the possible side effects that may be accompanied by the drugs at certain concentrations is required. Moreover, the cytotoxic evaluation of only six of the most potent, and selective compounds in the library of compounds synthesised (Chapter 2) and evaluated (Chapter 3) were tested. The remaining compounds that show high potency and selectivity against *C. difficile* ought to be tested to make certain of the best drug candidates to progress in further studies. It would be useful to compare the activities of metronidazole and nitrofurantoin here as measured in the same viability assay as the synthesised compounds.

References

- Abutaleb, N., and Seleem, M. (2020). Auranofin, at a clinically achievable dose, protects mice and prevents the recurrence of *Clostridioides difficile* infection. *Scientific Reports*, **10**(1), 7701.
- Ahmed, M. and Baptiste, K. (2018). Vancomycin-resistant enterococci: a review of antimicrobial resistance mechanisms and perspectives of human and animal health. *Microbial Drug Resistance*, **24**(5), 590-606.
- Aleman, V. and Handler, P. (1967). Dihydroorotate Dehydrogenase: I. GENERAL PROPERTIES. *Journal of Biological Chemistry*, **242**(18), 4087-4096.
- Aljaafari, M., Alkhoori, M., Hag-Ali, M., Cheng, W., Lim, S., Loh, J. and Lai, K. (2022). Contribution of aldehydes and their derivatives to antimicrobial and immunomodulatory activities. *Molecules*, **27**(11), 3589.
- Amaning Danquah, C., Minkah, P., Osei Duah Junior, I., Amankwah, K. and Somuah, S. (2022). Antimicrobial compounds from microorganisms. *Antibiotics*, **11**(3), 285.
- Andersen, P. Jansen, P. and Hammer, K. (1994). Two different dihydroorotate dehydrogenases in *Lactococcus lactis*. *Journal of Bacteriology*, **176**(13), 3975-3982.
- Arakaki, T., Buckner, F., Gillespie, J., Malmquist, N., Phillips, M., Kalyuzhniy, O., Luft, J., DeTitta, G., Verlinde, C., Van Voorhis, W. and Hol, W. (2008). Characterization of *Trypanosoma brucei* dihydroorotate dehydrogenase as a possible drug target; structural, kinetic and RNAi studies. *Molecular Microbiology*, **68**(1), 37-50.
- Argyrou, A., Washabaugh, M. and Pickart, C. (2000). Dihydroorotate dehydrogenase from *Clostridium oroticum* is a class 1B enzyme and utilizes a concerted mechanism of catalysis. *Biochemistry*, **39**(34), 10373-10384.
- Asai, T., O'Sullivan, W., Kobayashi, M., Gero, A., Yokogawa, M. and Tatibana, M. (1983). Enzymes of the de novo pyrimidine biosynthetic pathway in *Toxoplasma gondii*. *Molecular and Biochemical Parasitology*, **7**(2), 89-100.
- Aslam, B., Wang, W., Arshad, M. I., Khurshid, M., Muzammil, S., Rasool, M. H., Nisar, M. A., Alvi, R. F., Aslam, M. A., Qamar, M. U., Salamat, M. K. F., and Baloch, Z. (2018). Antibiotic resistance: a rundown of a global crisis. *Infection and Drug Resistance*, **11**, 1645–1658. Available at: <https://doi.org/10.2147/IDR.S173867>
- Aslantürk, Ö. (2018). In Vitro Cytotoxicity and Cell Viability Assays: Principles, Advantages, and Disadvantages. Genotoxicity - A Predictable Risk to Our Actual World. *InTechOpen*. Available at: <http://dx.doi.org/10.5772/intechopen.71923>.
- Ayub, K. and Ludwig, R. (2016). Gas hydrates model for the mechanistic investigation of the Wittig reaction “on water”, *Royal Society of Chemistry Advances*, **6** (28), 23448-23458.
- Barakat, A., Islam, M., Al-Majid, A., Soliman, S., Mabkhot, Y., Al-Othman, Z., Ghabbour, H. and Fun, H. (2015). Synthesis of novel 5-monoalkylbarbiturate derivatives: new access to 1, 2-oxazepines. *Tetrahedron Letters*, **56**(50), 6984-6987.

Belger, C., Abrahams, C., Imamdin, A. and Lecour, S. (2024). Doxorubicin-induced cardiotoxicity and risk factors. *IJC Heart & Vasculature*, **50**, 101332.

Blass, B. E. (2021). Case studies in drug discovery. *Basic Principles of Drug Discovery and Development*, 625–664. Available at: <https://doi.org/10.1016/B978-0-12-817214-8.00014-2>

Borriello, S. (1990). The influence of the normal flora on *Clostridium difficile* colonisation of the gut. *Annals of Medicine*, **22**(1), 61–67. Available at: <https://doi.org/10.3109/07853899009147244>.

Brosge, F., Singh, P., Almqvist, F. and Bolm, C. (2021). Selected applications of Meldrum's acid—a tutorial. *Organic & Biomolecular Chemistry*, **19**(23), 5014-5027.

Brown, H. and Brown, C. (1962). A new convenient technique for the hydrogenation of unsaturated compounds. *Journal of the American Chemical Society*, **84**(8), 1495-1495.

Bryant, C., and DeLuca, M. (1991). Purification and characterization of an oxygen-insensitive NAD(P)H nitroreductase from *Enterobacter cloacae*. *The Journal of Biological Chemistry*, **266**(7), 4119–4125.

Bukhari, S., Abdelgawad, M., Ahmed, N., Amjad, M., Hussain, M., Elsherif, M., Ejaz, H., Alotaibi, N., Filipović, I., and Janković, N. (2023). Synthesis, Characterization, and Biological Evaluation of Meldrum's Acid Derivatives: Dual Activity and Molecular Docking Study. *Pharmaceuticals*, **16**(2), 281.

Bukhari, S., Abdelgawad, M., Ahmed, N., Amjad, M., Hussain, M., Elsherif, M., Ejaz, H., Alotaibi, N., Filipović, I. and Janković, N. (2023). Synthesis, Characterization, and Biological Evaluation of Meldrum's Acid Derivatives: Dual Activity and Molecular Docking Study. *Pharmaceuticals*, **16**(2), 281.

Byrne, P. (2012). Introduction to the Wittig Reaction and Discussion of the Mechanism. In: Investigation of Reactions Involving Pentacoordinate Intermediates. Springer Theses. Springer, Berlin, Heidelberg, 1-56. Available at: https://doi.org/10.1007/978-3-642-32045-3_1

Chen, L., Wang, Z., Liu, L., Qu, S., Mao, Y., Peng, X., Li, Y. and Tian, J. (2019). Cinnamaldehyde inhibits *Candida albicans* growth by causing apoptosis and its treatment on vulvovaginal candidiasis and oropharyngeal candidiasis. *Applied Microbiology and Biotechnology*, **103**, 9037-9055.

Chou, Y., Chen, Y., Lin, L. and Liu, Y. (2017). Thermosetting Resins Based on a Self-Crosslinkable Monomer/Polymer Possessing Meldrum's Acid Groups. *Macromolecular Chemistry and Physics*, **218**(17), 1700147.

Church, D., and Laishley, E. (1995). Reduction of metronidazole by hydrogenase from clostridia. *Anaerobe*, **1**(2), 81–92.

Church, D., Rabin, H., and Laishley, E. (1988). Role of hydrogenase 1 of *Clostridium pasteurianum* in the reduction of metronidazole. *Biochemical Pharmacology*, **37**(8), 1525–1534.

Clinical and Laboratory Standards Institute. (2006). Performance standards for antimicrobial susceptibility testing; sixteenth informational supplement. *CLSI document M100-S16CLSI*, Wayne, PA.

Cordeiro, A., Feliciano, P., Pinheiro, M. and Nonato, M. (2012). Crystal structure of dihydroorotate dehydrogenase from *Leishmania major*. *Biochimie*, **94**(8), 1739-1748.

Czepiel, J., Drózdź, M., Pituch, H., Kuijper, E. J., Perucki, W., Mielimonka, A., Goldman, S., Wultańska, D., Garlicki, A., & Biesiada, G. (2019). Clostridium difficile infection: review. *European Journal of Clinical Microbiology and Infectious Diseases*, **38**, 1211-1221. Available at: <https://doi.org/10.1007/s10096-019-03539-6>

Czepiel, J., Drózdź, M., Pituch, H., Kuijper, E.J., Perucki, W., Mielimonka, A., Goldman, S., Wultańska, D., Garlicki, A. and Biesiada, G. (2019). Clostridium difficile infection. *European Journal of Clinical Microbiology & Infectious Diseases*, **38**, 1211-1221.

Damodar, G., Smitha, T., Gopinath, S., Vijayakumar, S. and Rao, Y.A. (2014). An evaluation of hepatotoxicity in breast cancer patients receiving injection Doxorubicin. *Annals of Medical and Health Sciences Research*, **4**(1), 74-79.

Dandia, A., Parewa, V., Kumari, S., Bansal, S. and Sharma, A. (2016). Imposed hydrophobic interactions by NaCl: accountable attribute for the synthesis of spiro [acenaphthylene-1, 5'-pyrrolo [1, 2-c] thiazole] derivatives via 1, 3-dipolar cycloaddition reaction in aqueous medium. *Green chemistry*, **18**(8), 2488-2499.

Daneshvar, N., Shirini, F., Langarudi, M. and Karimi-Chayjani, R. (2018). Taurine as a green bio-organic catalyst for the preparation of bio-active barbituric and thiobarbituric acid derivatives in water media. *Bioorganic Chemistry*, **77**, 68-73.

Diaz, G., Melis, M., Musinu, A., Piludu, M., Piras, M. and Falchi, A. (2007). Localization of MTT formazan in lipid droplets. An alternative hypothesis about the nature of formazan granules and aggregates. *European Journal of Histochemistry*, **51**(3), 213-218.

Dingsdag S., & Hunter N. (2018). Metronidazole: an update on metabolism, structure-cytotoxicity and resistance mechanisms. *Journal of Antimicrobial Chemotherapy*, **73**(2):265-279.

Dumas, A., and Fillion, E. (2010). Meldrum's acids and 5-Alkylidene Meldrum's acids in catalytic carbon-carbon bond-forming processes. *Accounts of Chemical Research*, **43**(3), 440-454.

Eggertson L. (2004). C. difficile hits Sherbrooke, Que., hospital: 100 deaths. *Canadian Medical Association Journal*, **171**(5), 436. Available at: <https://doi.org/10.1503/cmaj.1041250>

Ehlhardt, W., Beaulieu Jr, B. and Goldman, P. (1987). Formation of an amino reduction product of metronidazole in bacterial cultures: lack of bactericidal activity. *Biochemical pharmacology*, **36**(2), 259-264.

Ehlhardt, W., Beaulieu, B., & Goldman, P. (1987). Formation of an amino reduction product of metronidazole in bacterial cultures: lack of bactericidal activity. *Biochemical Pharmacology*, **36**(2), 259-264.

European Committee for Antimicrobial Susceptibility Testing (EUCAST) of the European Society of Clinical Microbiology and Infectious Diseases (ESCMID). (2003). Determination of minimum inhibitory concentrations (MICs) of antibacterial agents by broth dilution. *Clinical Microbiology Infection*, **9**, ix–xv.

Fagan, R., and Palfey, B. (2009). Roles in binding and chemistry for conserved active site residues in the class 2 dihydroorotate dehydrogenase from *Escherichia coli*. *Biochemistry*, **48**(30), 7169-7178.

Fahad, M. (2022). Barbituric Acids: A Review of Preparation, Reactions and Biological Applications. *Biomedicine and Chemical Sciences*, **1**(4), 295-305.

Fang, J., Uchiumi, T., Yagi, M., Matsumoto, S., Amamoto, R., Takazaki, S., Yamaza, H., Nonaka, K. and Kang, D. (2013). Dihydro-orotate dehydrogenase is physically associated with the respiratory complex and its loss leads to mitochondrial dysfunction. *Bioscience Reports*, **33**(2), p.e00021.

Farkas, M., Rodríguez, R., Longo, C., Monasterios, M., Ortega, M., Rivas, A., Pardey, A., Lopez, R., and Moya, S. (2006). Reduction of 5-nitrofurans catalysed by a rhodium complex immobilized on poly(4-vinylpyridine): a relationship with antibacterial activity. *Journal of the Chilean Chemical Society*, **51**(1), 829-835. Available at: <http://dx.doi.org/10.4067/S0717-97072006000100014>

Fatima, R. and Aziz, M. (2019). The hypervirulent strain of *Clostridium difficile*: NAP1/B1/027-a brief overview. *Cureus*, **11**(1).

Ferreira, J., Resende Filho, J., Batista, P., Teotonio, E. and Vale, J. (2018). Rapid and efficient uncatalysed Knoevenagel condensations from binary mixture of ethanol and water. *Journal of the Brazilian Chemical Society*, **29**, 1382-1387.

Figueroa-Villar, J. and Vieira, A. (2013). Nuclear magnetic resonance and molecular modeling study of exocyclic carbon-carbon double bond polarization in benzylidene barbiturates. *Journal of Molecular Structure*, **1034**, 310-317.

Fox, J. and Shugar, D. (1952). Absorption spectra and structure of barbituric acid derivatives as a function of pH. *Bulletin des Sociétés Chimiques Belges*, **61**(1-2), 44-63.

Fraser, W., Suckling, C. and Wood, H. Latent inhibitors. Part 7. Inhibition of dihydro-orotate dehydrogenase by spirocyclopropanobarbiturates. *Journal of the Chemical Society*, 3137-3144.

Friedmann, H. and Vennesland, B. (1960). Crystalline dihydroorotic dehydrogenase. *Journal of Biological Chemistry*, **235**(5), 1526-1532.

Frost, C. and Hartley, B. (2009). Lewis base-promoted hydrosilylation of cyclic malonates: synthesis of β -substituted aldehydes and γ -substituted amines. *The Journal of Organic Chemistry*, **74**(9), 3599-3602.

Frost, C., Penrose, S. and Gleave, R. (2009). A Practical Synthesis of α -Substituted tert-Butyl Acrylates from Meldrum's Acid and Aldehydes. *Synthesis*, **2009**(04), 627-635.

Gallagher, J., Reilly, J., Navalkele, B., Downham, G., Haynes, K., & Trivedi, M. (2015). Clinical and economic benefits of fidaxomicin compared to vancomycin for *Clostridium difficile* infection. *Antimicrobial Agents and Chemotherapy*, **59**(11), 7007–7010.

Gallardo-Garrido, C., Cho, Y., Cortés-Rios, J., Vasquez, D., Pessoa-Mahana, C.D., Araya-Maturana, R., Pessoa-Mahana, H. and Faundez, M. (2020). Nitrofurans beyond redox cycling: Evidence of Nitroreduction-independent cytotoxicity mechanism. *Toxicology and Applied Pharmacology*, **401**, 115104.

Garrity, A. (2006). List of new names and new combinations previously effectively, but not validly, published. *Genetic Engineering and Biotechnology News*, **56**(1), 1-6.

Ge, I., Fevrier, H., Conell, C., Kheraj, M., Flint, A., Smith, D., & Herrinton, L. (2018). Reducing risk of *Clostridium difficile* infection and overall use of antibiotic in the outpatient treatment of urinary tract infection. *Therapeutic Advances in Urology*, **10**(10), 283–293. Available at: <https://doi.org/10.1177/1756287218783871>

Ghasemi, M., Turnbull, T., Sebastian, S. and Kempson, I. (2021). The MTT assay: utility, limitations, pitfalls, and interpretation in bulk and single-cell analysis. *International Journal of Molecular Sciences*, **22**(23), 12827.

Gorovoy, A., Guyader, D. and Lejon, T. (2014). Highly efficient synthesis of trioxopyrimidine-based chalconoids under solvent-free conditions. *Synthetic Communications*, **44**(9), 1296-1300.

Guerin, D., Mazeas, D., Musale, M., Naguib, F., Al Safarjalani, O., el Kouni, M. and Panzica, R. (1999). Uridine phosphorylase inhibitors: chemical modification of benzyloxybenzyl-barbituric acid and its effects on urdpase inhibition. *Bioorganic & medicinal chemistry letters*, **9**(11), 1477-1480.

Guery, B., Galperine, T., and Barbut, F. (2019). *Clostridioides difficile*: Diagnosis and treatments. *The British Medical Journal*, **366**. Available at: <https://doi.org/10.1136/BMJ.L4609>

Hall, I. and O'toole, E. (1935). Intestinal flora in new-born infants: with a description of a new pathogenic anaerobe, *Bacillus difficilis*. *American Journal of Diseases of Children*, **49**(2), 390-402.

Hayashi, Y., Itoh, T. and Ishikawa, H. (2011). Oxidative and Enantioselective Cross-Coupling of Aldehydes and Nitromethane Catalyzed by Diphenylprolinol Silyl Ether. *Angewandte Chemie International Edition*, **17**(50), 3920-3924.

Herzog, U. and Reinshagen (1977). New Meldrum's acid derivatives with antimicrobial properties. *Chemischer Informationsdienst*, **8**(10).

Huttner, A and Harbarth, S. (2017). Miscellaneous Agents: Fusidic Acid, Nitrofurantoin and Fosfomycin. *Infectious Diseases*, **2**(149), 1277-1279. Available at: <https://doi.org/10.1016/B978-0-7020-6285-8.00149-0>

Insuasty, B., Torres, H., Abonia, R., Quiroga, J., Low, J., Sanchez, A., Cobo, J. and Noguera, M. (2005). Unexpected synthesis of 4-R-phenylallylidene Meldrum's acid derivatives. *Heterocyclic Communications*, **11**(1), 55-60.

Jurado, C. (2013). Blood. *Encyclopedia of Forensic Sciences* (Second Edition), 336-342. Available at: <https://doi.org/10.1016/B978-0-12-382165-2.00301-9>.

Kahler, A., Nielsen, F. and Switzer, R. (1999). Biochemical characterization of the heteromeric *Bacillus subtilis* dihydroorotate dehydrogenase and its isolated subunits. *Archives of Biochemistry and Biophysics*, **371**(2), 191-201.

Kalita, S. and Deka, D. (2018). 2-Phenyl-2, 3-dihydrobenzo [d] thiazole: A Mild, Efficient, And Highly Active In Situ Generated Chemoselective Reducing Agent For The One-Pot Synthesis Of 5-Monoalkylbarbiturates in Water. *Synlett*, **29**(04), 477-482.

Kelly, C. (1996). Immune response to *Clostridium difficile* infection. *European Journal of Gastroenterology & Hepatology*, **8**, 1048–53.

Kelly, C. and LaMont, J. (1998). *Clostridium difficile* infection. *Annual Review of Medicine*, **49**(1), 375-390.

Kelly, C., Pothoulakis C., Orellana J., and LaMont J. (1992). Human colonic aspirates containing immunoglobulin A antibody to *Clostridium difficile* toxin A inhibit toxin A-receptor binding. *Gastroenterology*, **102**, 35–40.

Kim, P., Iaconis, J., Rolfe R. (1987). Immunization of adult hamsters against *Clostridium difficile*-associated ileocectitis and transfer of protection to infant hamsters. *Infection and Immunity*, **55**, 2984–92.

Larson, A., Kaplan, M. and Bonis, P. (2018). Drugs and the liver: metabolism and mechanisms of injury. *UpToDate, Waltham, MA. Accessed, 16*.
Vaja, R., and Rana, M. (2020). Drugs and the liver. *Anaesthesia and Intensive Care Medicine*, **21**(10), 517–523. Available at: <https://doi.org/10.1016/j.mpaic.2020.07.001>

Lawson, P., Citron, D., Tyrrell, K. and Finegold, S., (2016). Reclassification of *Clostridium difficile* as *Clostridioides difficile* (Hall and O'Toole 1935) Prévot 1938. *Anaerobe*, **40**, 95-99.

Leffler, D. and Lamont, J. (2015). *Clostridium difficile* infection. *New England Journal of Medicine*, **372**(16), 1539-1548.

Libby, J., Jortner, B., Wilkins, T. (1982). Effects of the two toxins of *Clostridium difficile* in antibiotic-associated cecitis in hamsters. *Infection and Immunity*, **36**, 822–29.

Lieberman, I. and Kornberg, A. (1953). Enzymic synthesis and breakdown of a pyrimidine, orotic acid: I. Dihydro-orotic dehydrogenase. *Biochimica et Biophysica Acta*, **12**(1-2), 223-234.

Liu, Y., Peterson, D.A., Kimura, H. and Schubert, D. (1997). Mechanism of cellular 3-(4, 5-dimethylthiazol-2-yl)-2,5-diphenyltetrazolium bromide (MTT) reduction. *Journal of Neurochemistry*, **69**(2), 581-593.

Löffler, M., Knecht, W., Rawls, J., Ullrich, A. and Dietz, C. (2002). *Drosophila melanogaster* dihydroorotate dehydrogenase: the N-terminus is important for biological function in vivo but not for catalytic properties in vitro. *Insect Biochemistry and Molecular Biology*, **32**(9), 1159-1169.

LoPachin, R. and Gavin, T. (2014). Molecular mechanisms of aldehyde toxicity: a chemical perspective. *Chemical Research in Toxicology*, **27**(7), 1081-1091.

Lucas-Hourani, M., Dauzonne, D., Munier-Lehmann, H., Khiar, S., Nisole, S., Dairou, J., Helynck, O., Afonso, P., Tangy, F. and Vidalain, P. (2017). Original chemical series of pyrimidine biosynthesis inhibitors that boost the antiviral interferon response. *Antimicrobial Agents and Chemotherapy*, **61**(10), 10-1128.

Macbeth, A., Nunan, T. and Traill, D. (1926). The labile nature of the halogen atom in organic compounds. Part XII. Halogen compounds of barbituric acids, *J. Chem. Soc.*, **129**, 1248-1253

Maehara, Y., Anai, H., Tamada, R. and Sugimachi K. (1987). The APT assay is more sensitive than the succinate dehydrogenase inhibition test for predicting cell viability. *European Journal of Cancer and Clinical Oncology*, **23**(3), 273-276. Available at: [https://doi.org/10.1016/0277-5379\(87\)90070-8](https://doi.org/10.1016/0277-5379(87)90070-8)

Marcinkeviciene, J., Tinney, L., Wang, K., Rogers, M. and Copeland, R. (1999). Dihydroorotate dehydrogenase B of *Enterococcus faecalis*. Characterization and insights into chemical mechanism. *Biochemistry*, **38**(40), 13129-13137.

Maynert, E., and Van Dyke, H. (1950). The absence of localization of barbital in divisions of the central nervous system. *Journal of Pharmacology and Experimental Therapeutics*, **98**(2), 184-187.

McFarland, L., Surawicz, C., and Stamm, W. (1990). Risk factors for *Clostridium difficile* carriage and *C. difficile*-associated diarrhea in a cohort of hospitalized patients. *The Journal of Infectious Diseases*, **162**(3), 678-684. Available at: <https://doi.org/10.1093/infdis/162.3.678>

McNab, H. (1978). Meldrum's acid. *Chemical Society Reviews*, **7**(3), 345-358.

Meinig, J., Fu, L. and Peterson, B. (2015). Synthesis of fluorophores that target small molecules to the endoplasmic reticulum of living mammalian cells. *Angewandte Chemie*, **127**(33), 9832-9835.

Meldrum, A. (1908). A β -lactonic acid from acetone and malonic acid. *Journal of the Chemical Society, Transactions*. **93**, 598-601.

Mohite, A. and Bhat, R. (2013). A practical and convenient protocol for the synthesis of (E)- α , β -unsaturated acids. *Organic Letters*, **15**(17), 4564-4567.

Moore, R., Beckthold, B., and Bryan, L. (1995). Metronidazole uptake in *Helicobacter pylori*. *Canadian Journal of Microbiology*, **41**(8), 746-749.

Mullish, B., and Williams, H. (2018). *Clostridium difficile* infection and antibiotic-associated diarrhoea. *Clinical Medicine (London, England)*, **18**(3), 237-241.

Munier-Lehmann, H., Vidalain, P., Tangy, F. and Janin, Y. (2013). On dihydroorotate dehydrogenases and their inhibitors and uses. *Journal of Medicinal Chemistry*, **56**(8), 3148-3167.

Nathan, C. and Cars, O. (2014). Antibiotic resistance—problems, progress, and prospects. *New England Journal of Medicine*, **371**(19), 1761-1763.

Neumann, D., Cammarata, A., Backes, G., Palmer, G. and Jursic, B. (2014). Synthesis and antifungal activity of substituted 2, 4, 6-pyrimidinetrione carbaldehyde hydrazones. *Bioorganic & medicinal chemistry*, **22**(2), 813-826.

Nielsen, F., Andersen, P. and Jensen, K. (1996). The B form of dihydroorotate dehydrogenase from *Lactococcus lactis* consists of two different subunits, encoded by the pyrDb and pyrK genes, and contains FMN, FAD, and [FeS] redox centers. *Journal of Biological Chemistry*, **271**(46), 29359-29365.

Nobay, F., & Acquisto, N. M. (2014). Barbiturates. *Encyclopedia of Toxicology: Third Edition*, 363–367. Available at: <https://doi.org/10.1016/B978-0-12-386454-3.00696-5>

Norager, S., Jensen, K. F., Björnberg, O., & Larsen, S. (2002). E. coli Dihydroorotate Dehydrogenase Reveals Structural and Functional Distinctions between Different Classes of Dihydroorotate Dehydrogenases. *Structure*, **10**(9), 1211–1223. Available at: [https://doi.org/10.1016/S0969-2126\(02\)00831-6](https://doi.org/10.1016/S0969-2126(02)00831-6)

Norager, S., Jensen, K. F., Björnberg, O., & Larsen, S. (2002). E. coli Dihydroorotate Dehydrogenase Reveals Structural and Functional Distinctions between Different Classes of Dihydroorotate Dehydrogenases. *Structure*, **10**(9), 1211–1223. Available at: [https://doi.org/10.1016/S0969-2126\(02\)00831-6](https://doi.org/10.1016/S0969-2126(02)00831-6)

O'Neill, J. (2016). Review on Antimicrobial Resistance. Tackling drug-resistant infections globally., *Who*, 11. Available at: https://amr-review.org/sites/default/files/160525_Final_paper_with_cover.pdf (Accessed: 17 July 2019).

O'Brien, R., and Morris, J. (1971). The Ferredoxin-dependent reduction of chloramphenicol by *Clostridium acetobutylicum*. *Journal of General Microbiology*, **67**(3), 265–271.

O'Donovan, G. and Neuhard, J. (1970). Pyrimidine metabolism in microorganisms. *Bacteriological Reviews*, **34**(3), 278-343.

Othman, L., Sleiman, A. and Abdel-Massih, R.M. (2019). Antimicrobial activity of polyphenols and alkaloids in middle eastern plants. *Frontiers In Microbiology*, **10**, 911.

Ovung, A. and Bhattacharyya, J. (2023). Bacterial infections: Antimicrobial mechanism of action and bacterial resistance. In *Viral, Parasitic, Bacterial, and Fungal Infections*, 479-487.

Owen, L. (1950). Heterocycles. X. Syntheses of ethanal- and phenyl barbituric acids. *Journal Of Organic Chemistry*, **15**, 998-93.

Owens, R., Donskey, C., Gaynes, R., Loo, V., and Muto, C. (2008). Antimicrobial-Associated Risk Factors for *Clostridium difficile* Infection. *Clinical Infectious Diseases*, **46**, 19–31. Available at: <https://doi.org/10.1086/521859>

Paparella, A., Aboulache, B., Harijan, R., Potts, K., Tyler, P. and Schramm, V. (2021). Inhibition of *Clostridium difficile* TcdA and TcdB toxins with transition state analogues. *Nature communications*, **12**(1),6285.

Popat, V. and Padhiyar, N. (2013). Kinetic study of bechamp process for P-nitrotoluene reduction to P-toluidine. *International Journal of Chemical Engineering and Applications*, **4**(6), 401-405.

Public Health England (2017) Health matters: antimicrobial resistance - GOV.UK, Public Health England. Available at: <https://www.gov.uk/government/publications/health-matters-antimicrobial-resistance/health-matters-antimicrobial-resistance> (Accessed: 11 August 2022).

Quraishi, M., Widlak, M., Bhala, N., Moore, D., Price, M., Sharma, N. and Iqbal, T. (2017). Systematic review with meta-analysis: the efficacy of faecal microbiota transplantation for the treatment of recurrent and refractory *Clostridium difficile* infection. *Alimentary Pharmacology & Therapeutics*, **46**(5), 479-493.

Read, A. and Woods, R. (2014). Antibiotic resistance management. *Evolution, medicine, and Public Health*, **1**, 147.

Reddy, C. and Nagaraj, A. (2007). Knoevenagel condensation of α , β -unsaturated aromatic aldehydes with barbituric acid under non-catalytic and solvent-free conditions. *Chinese Chemical Letters*, **18**(12), 1431-1435.

Reichard, P. (1952). The function of orotic acid in the biogenesis of pyrimidines in slices from regenerating liver. *Journal of Biological Chemistry*, **197**(1), 391-398.

Reis, R., Calil, F., Feliciano, P., Pinheiro, M., Cristina M. (2017). The dihydroorotate dehydrogenases: Past and present, *Archives of Biochemistry and Biophysics*, **632**, 175-191.

Reis, R., Lorenzato, E., Silva, V. and Nonato, M. (2015). Recombinant production, crystallization and crystal structure determination of dihydroorotate dehydrogenase from *Leishmania (Viannia) braziliensis*. *Acta Crystallographica Section F: Structural Biology Communications*, **71**(5), 547-552.

Releniy, A., Wallick, D., and Streit, J. (1986). Process for the preparation of Meldrum's acid, Dow Chemical Co, U.S. Patent 4,613,671.

Riss, T., Moravec, R., Niles, A., Benink, H., Worzella, T. and Minor, L. (2013). Cell Viability Assays. *Assay Guidance Manual*.

Roldán, M., Pérez-Reinado, E., Castillo, F., & Moreno-Vivián, C. (2008). Reduction of polynitroaromatic compounds: the bacterial nitroreductases. *FEMS Microbiology Reviews*, **32**(3), 474–500.

Schmidt, N., Carlson, P., Mullany, P., Zhu, D., Sorg, J. A., and Sun, X. (2018). *Clostridioides difficile* Biology: Sporulation, Germination, and Corresponding Therapies for *C. difficile* Infection. *Frontiers in Cellular and Infection Microbiology*, **8**, 29. Available at: <https://doi.org/10.3389/fcimb.2018.00029>

Singer, A., Shaw, H., Rhodes, V. and Hart, A. (2016). Review of antimicrobial resistance in the environment and its relevance to environmental regulators. *Frontiers In Microbiology*, **7**, 1728.

Singh, A., Maqbool, M., Mobashir, M. and Hoda, N. (2017). Dihydroorotate dehydrogenase: a drug target for the development of antimalarials. *European Journal of Medicinal Chemistry*, **125**, 640-651.

- Singh, A., Maqbool, M., Mobashir, M., & Hoda, N. (2017). Dihydroorotate dehydrogenase: A drug target for the development of antimalarials. *European Journal of Medicinal Chemistry*, **125**, 640-651.
- Sivagnanam, S., and Deleu, D. (2003). Red man syndrome. *Critical care (London, England)*, **7**(2), 119–120. Available at: <https://doi.org/10.1186/cc1871>
- Sørensen, P. and Dandanell, G. (2002). A new type of dihydroorotate dehydrogenase, type 1S, from the thermoacidophilic archaeon *Sulfolobus solfataricus*. *Extremophiles*, **6**, 245-251.
- Spellberg, B. and Gilbert, D. (2014). The future of antibiotics and resistance: a tribute to a career of leadership by John Bartlett. *Clinical Infectious Diseases*, **59**, S71-S75.
- Srivastava, B., Jain, M., Solanki, M., Soni, R., Valani, D., Gupta, S., Mishra, B., Takale, V., Kapadnis, P., Patel, H. and Pandya, P. (2008). Synthesis and in vitro antibacterial activities of novel oxazolidinones. *European Journal of Medicinal Chemistry*, **43**(4), 683-693.
- Srivastava, S., Aggarwal, H. and Gupta, R. (2015). Three-dimensional heterometallic coordination networks: syntheses, crystal structures, topologies, and heterogeneous catalysis. *Crystal Growth & Design*, **15**(8), 4110-4122.
- Sykes, D., Kfoury, Y., Mercier, F., Wawer, M., Law, J., Haynes, M., Lewis, T., Schajnovitz, A., Jain, E., Lee, D. and Meyer, H. (2016). Inhibition of dihydroorotate dehydrogenase overcomes differentiation blockade in acute myeloid leukemia. *Cell*, **167**(1), 171-186.
- Sykes, D., Kfoury, Y., Mercier, F., Wawer, M., Law, J., Haynes, M., Lewis, T., Schajnovitz, A., Jain, E., Lee, D. and Meyer, H. (2016). Inhibition of dihydroorotate dehydrogenase overcomes differentiation blockade in acute myeloid leukemia. *Cell*, **167**(1), 171-186.
- Tahmassebi, D., Wilson, L. and Kieser, J. (2009). Knoevenagel condensation of aldehydes with Meldrum's acid in ionic liquids. *Synthetic Communications*, **39**(14), 2605-2613.
- Takashima, E., Inaoka, D., Osanai, A., Nara, T., Odaka, M., Aoki, T., Inaka, K., Harada, S. and Kita, K. (2002). Characterization of the dihydroorotate dehydrogenase as a soluble fumarate reductase in *Trypanosoma cruzi*. *Molecular and Biochemical Parasitology*, **122**(2), 189-200.
- Tally, F., Goldin, B., Sullivan, N., Johnston, J., and Gorbach, S. (1978). Antimicrobial activity of metronidazole in anaerobic bacteria. *Antimicrobial Agents and Chemotherapy*, **13**(3), 460–465.
- Tantawy, A. and Gad, L. (1991). Imidazodiazepine derivatives of chemotherapeutic interest. *Mansoura Journal of Pharmaceutical Sciences*, **7**(1), 134-145.
- Taylor, W. and Taylor, M. (1964). Enzymes of the pyrimidine pathway in *Escherichia coli* II: Intracellular Localization and Properties of Dihydroorotic Dehydrogenase. *Journal of Bacteriology*, **88**(1), 105-110.
- Tedesco, F., Barton, R. and Alpers, D. (1974). Clindamycin-associated colitis: a prospective study. *Annals of Internal Medicine*, **81**(4), 429-433.

Tran, A., Huynh, V., Friz, E., Whitney, S. and Cordes, D. (2009). A general method for the rapid reduction of alkenes and alkynes using sodium borohydride, acetic acid, and palladium. *Tetrahedron Letters*, **50**(16), 1817-1819.

Tsai, H., Tsou, H., Lin, C., Chen, S., Cheng, H., Liu, T., Chen, W., Jiang, J., Yang, S., Chang, S. and Teng, H. (2021). Acrolein contributes to human colorectal tumorigenesis through the activation of RAS-MAPK pathway. *Scientific Reports*, **11**(1), 12590.

Van Breemen, R., and Li, Y. (2005). Caco-2 cell permeability assays to measure drug absorption. *Expert Opinion on Drug Metabolism & Toxicology*, **1**(2), 175–185. Available at: <https://doi.org/10.1517/17425255.1.2.175>

Van Meerloo, J., Kaspers, G. and Cloos, J. (2011). Cell sensitivity assays: the MTT assay. *Cancer Cell Culture: Methods and Protocols*, 237-245.

Van Tonder, A., Joubert, A. and Cromarty, A. (2015). Limitations of the 3-(4, 5-dimethylthiazol-2-yl)-2, 5-diphenyl-2H-tetrazolium bromide (MTT) assay when compared to three commonly used cell enumeration assays. *BMC Research Notes*, **8**, 1-10.

Vardanyan, R. S., and Hruby, V. J. (2006). Antibiotics. *Synthesis of Essential Drugs*, 425–498. Available at: <https://doi.org/10.1016/B978-044452166-8/50032-7>

Vedejs, E., and Peterson, M. (1994). Stereochemistry and mechanism in the Wittig reaction. *Topics in Stereochemistry*, **21**, 1–157.

Vernallis, A., Worthington, T., Lambert, P. and Fraser, W. (2010). *Preparation of Pyrimidine Derivatives for Use as Antibiotics, Specifically as Bacterial Dihydroorotate Dehydrogenase (DHODase) Inhibitors*. WIPO Patent 2010136804.

Vieira, A., Gomes, N., Matheus, M., Fernandes, P. and Figueroa-Villar, J. (2011). Synthesis and in vivo evaluation of 5-chloro-5-benzobarbiturates as new central nervous system depressants. *Journal of the Brazilian Chemical Society*, **22**, 364-371.

Waller, D. and Sampson, A. (2018). Chemotherapy of infections. *Medical Pharmacology and Therapeutics*, 581-629.

Wang, H. (2010). "Béchamp Reduction". *Comprehensive Organic Name Reactions*, **2**, 11-20.

Wang, S., Vorotnikov, V. and Vlachos, D.G., (2014). A DFT study of furan hydrogenation and ring opening on Pd (111). *Green Chemistry*, **16**(2), 736-747.

Warny, M., Vaerman, J., Avesani, V., Delmee, M. (1994). Human antibody response to *Clostridium difficile* toxin A in relation to clinical course of infection. *Infection & Immunity*, **62**, 384–89.

Weir C., Le J. (2023). Metronidazole. StAPTearls Publishing, Treasure Island, FL.

WHO (2017). Global priority list of antibiotic-resistant bacteria to guide research, discovery, and development of new antibiotics, *Who*, 7. Available at: <http://www.cdc.gov/drugresistance/threatreport-2013/> (Accessed: 30 June 2020).

Wiegand, I., Hilpert, K. and Hancock, R. (2008). Agar and broth dilution methods to determine the minimal inhibitory concentration (MIC) of antimicrobial substances. *Nature Protocols*, **3**(2), 163-175.

Wilcox, M. H. (2017). Nitroimidazoles, Metronidazole, Ornidazole and Tinidazole; and Fidaxomicin. *Infectious Diseases*, **2**, 1261-1263. Available at: <https://doi.org/10.1016/B978-0-7020-6285-8.00147-7>

Wood, J. and Anderson, E. (1909). CXI.—The constitution of the salts of barbituric acid. *Journal of the Chemical Society, Transactions*, **95**, 979-984.

Worsley, M. (1998). Infection control and prevention of Clostridium difficile Infection. *The Journal of Antimicrobial Chemotherapy*, **41**(3): 59-66.

Yaacoub, C., Rifi, M., El-Obeid, D., Mawlawi, H., Sabatier, J.M., Coutard, B. and Fajloun, Z. (2021). The cytotoxic effect of Apis mellifera venom with a synergistic potential of its two main components—Melittin and PLA2—On colon cancer HCT116 cell lines. *Molecules*, **26**(8), 2264.

Yang, Y., Han, B., Dong, F., Lv, J., Lu, H., Sun, Y., Lei, Z., Yang, Z. and Ma, H. (2022). A Cost-Effective Way to Produce Gram-Scale 18O-Labeled Aromatic Aldehydes. *Organic Letters*, **24**(24), 4409-4414.

Yarlagadda, V., Akkapeddi, P., Manjunath, G. and Haldar, J. (2014). Membrane active vancomycin analogues: a strategy to combat bacterial resistance. *Journal of Medicinal Chemistry*, **57**(11), 4558-4568.

Appendix

Dox. against BNL

Dox	Raw data			Blank Corrected Data			Viability %			Mean	STD
	Conc	1	2	3	1	2	3	1	2		
c	0.7535	0.7373	0.7784	0.7175	0.7013	0.7424	100	100	100	100	0
0.03	0.6995	0.6551	0.6854	0.6635	0.6191	0.6494	92.1016	85.9384	90.1444	89.3948	2.5713546
0.1	0.6778	0.6185	0.6244	0.6418	0.5825	0.5884	89.0894	80.8579	81.6768	83.8747	3.7024742
0.3	0.3151	0.3021	0.3034	0.2791	0.2661	0.2674	38.7424	36.9378	37.1183	37.5995	0.8114917
1	0.0995	0.0981	0.1102	0.0635	0.0621	0.0742	8.81455	8.62021	10.2998	9.24486	0.7501831
3	0.0951	0.0679	0.0725	0.0591	0.0319	0.0365	8.20378	4.4281	5.06663	5.8995	1.65009
Blank	0.0377	0.0348	0.0355	Blank Average		0.036	Control average		0.7204		

Dox	Raw data			Blank Corrected Data			Viability %			Mean	STD
	Conc	1	2	3	1	2	3	1	2		
c	0.7535	0.7373	0.7784	0.7175	0.7013	0.7424	100	100	100	100	0
10	0.0725	0.0654	0.0644	0.0365	0.0294	0.0284	5.06663	4.08107	3.94225	4.36332	0.5005357
30	0.0451	0.0551	0.0717	0.0091	0.0191	0.0357	1.26319	2.6513	4.95558	2.95669	1.5228016
100	0.1398	0.1517	0.1369	0.1038	0.1157	0.1009	14.4087	16.0605	14.0061	14.8251	0.8889013
300	0.303	0.3219	0.324	0.267	0.2859	0.288	37.0627	39.6863	39.9778	38.9089	1.3108712
Blank	0.0377	0.0348	0.0355	Blank Average		0.036	Control average		0.7204		

Synthesised compounds against BNL

BRO-23	Raw data			Blank Corrected Data			Viability %			Mean	STD
	Conc	1	2	3	1	2	3	1	2		
c	0.8643	0.8724	0.8485	0.8283	0.8364	0.8125	100	100	100	100	0
0.03	0.8556	0.8763	0.8654	0.8196	0.8403	0.8294	99.2572	101.764	100.444	100.488	1.0239039
0.1	0.8747	0.8541	0.8547	0.8387	0.8181	0.8187	101.57	99.0756	99.1482	99.9314	1.1592903
0.3	0.8621	0.8564	0.8114	0.8261	0.8204	0.7754	100.044	99.3541	93.9044	97.7676	2.7462158
1	0.8114	0.8232	0.8544	0.7754	0.7872	0.8184	93.9044	95.3334	99.1119	96.1166	2.1968884
3	0.843	0.7893	0.7971	0.807	0.7533	0.7611	97.7313	91.228	92.1726	93.7106	2.8690772
Blank	0.0377	0.0348	0.0355	Blank Average		0.036	Control average		0.82573		

BRO-23	Raw data			Blank Corrected Data			Viability %			Mean	STD
	Conc	1	2	3	1	2	3	1	2		
c	0.8643	0.8724	0.8485	0.8283	0.8364	0.8125	100	100	100	100	0
10	0.7848	0.7675	0.7995	0.7488	0.7315	0.7635	90.683	88.5879	92.4633	90.5781	1.583842
30	0.5998	0.5828	0.6403	0.5638	0.5468	0.6043	68.2787	66.2199	73.1834	69.2274	2.9209089
100	0.1243	0.1229	0.1595	0.0883	0.0869	0.1235	10.6935	10.524	14.9564	12.058	2.0506706
300	0.2289	0.2422	0.2558	0.1929	0.2062	0.2198	23.3611	24.9717	26.6188	24.9839	1.3299822
Blank	0.0377	0.0348	0.0355	Blank Average		0.036	Control average		0.82573		

BR1-93	Raw data			Blank Corrected Data			Viability %			Mean	STD
	Conc	1	2	3	1	2	3	1	2		
c	0.8643	0.8724	0.8774	0.82943	0.83753	0.84253	100	100	100	100	0
0.03	0.8898	0.9021	0.90225	0.85493	0.86723	0.86738	102.204	103.674	103.692	103.19	0.6974241
0.1	0.8776	0.9017	0.8343	0.84273	0.86683	0.79943	100.745	103.626	95.5688	99.9801	3.3336043
0.3	0.8541	0.8847	0.8629	0.81923	0.84983	0.82803	97.9358	101.594	98.9878	99.5059	1.5376801
1	0.8332	0.8502	0.8232	0.79833	0.81533	0.78833	95.4373	97.4696	94.2419	95.7163	1.3323972
3	0.8084	0.8021	0.8114	0.77353	0.76723	0.77653	92.4726	91.7195	92.8312	92.3411	0.4633072
Blank	0.0342	0.0352	0.0352	Blank Average		0.03487	Control average		0.8365		

BR1-93	Raw data			Blank Corrected Data			Viability %			Mean	STD
	Conc	1	2	3	1	2	3	1	2		
c	0.8643	0.8724	0.8774	0.82943	0.83753	0.84253	100	100	100	100	0
10	0.8021	0.7998	0.8121	0.76723	0.76493	0.77723	91.7195	91.4445	92.9149	92.0263	0.6382991
30	0.7871	0.7998	0.8114	0.75223	0.76493	0.77653	89.9263	91.4445	92.8312	91.4007	1.1863504
100	0.5662	0.5565	0.5954	0.53133	0.52163	0.56053	63.5186	62.359	67.0094	64.2957	1.976401
300	0.052	0.0515	0.0501	0.01713	0.01663	0.01523	2.04822	1.98844	1.82108	1.95258	0.0961334
Blank	0.0342	0.0352	0.0352	Blank Average		0.03487	Control average		0.8365		

BR1-141	Raw data			Blank Corrected Data			Viability %			Mean	STD
	Conc	1	2	3	1	2	3	1	2		
c	0.8253	0.8151	0.8221	0.79043	0.78023	0.78723	100	100	100	100	0
0.03	0.8321	0.8235	0.8121	0.79723	0.78863	0.77723	101.433	100.339	98.8888	100.221	1.0422318
0.1	0.8255	0.8121	0.8256	0.79063	0.77723	0.79073	100.594	98.8888	100.606	100.03	0.8067164
0.3	0.7995	0.8021	0.8559	0.76463	0.76723	0.82103	97.2857	97.6165	104.462	99.7879	3.3075281
1	0.8121	0.8121	0.808	0.77723	0.77723	0.77313	98.8888	98.8888	98.3672	98.715	0.2459085
3	0.7869	0.8142	0.828	0.75203	0.77933	0.79313	95.6826	99.156	100.912	98.5835	2.1728728
Blank	0.0342	0.0352	0.0352	Blank Average		0.03487	Control average		0.78597		

BR1-141	Raw data			Blank Corrected Data			Viability %			Mean	STD
	Conc	1	2	3	1	2	3	1	2		
c	0.8253	0.8151	0.8221	0.79043	0.78023	0.78723	100	100	100	100	0
10	0.7866	0.7753	0.8087	0.75173	0.74043	0.77383	95.6444	94.2067	98.4563	96.1025	1.7648424
30	0.5232	0.5321	0.541	0.48833	0.49723	0.50613	62.1316	63.2639	64.3963	63.2639	0.924571
100	0.1515	0.1995	0.1841	0.11663	0.16463	0.14923	14.8395	20.9466	18.9872	18.2578	2.5460222
300	0.0999	0.1006	0.1097	0.06503	0.06573	0.07483	8.27431	8.36337	9.52118	8.71962	0.567954049
Blank	0.0342	0.0352	0.0352	Blank Average		0.03487	Control average		0.78597		

BR1-27	Raw data			Blank Corrected Data			Viability %			Mean	STD
	Conc	1	2	3	1	2	3	1	2		
c	0.9548	0.9279	0.9263	0.91993	0.89303	0.89143	100	100	100	100	0
0.03	0.8551	0.8658	0.8954	0.82023	0.83093	0.86053	90.9888	92.1757	95.4593	92.8746	1.890790137
0.1	0.862	0.8651	0.8854	0.82713	0.83023	0.85053	91.7542	92.0981	94.3499	92.7341	1.151195857
0.3	0.8362	0.8447	0.8745	0.80133	0.80983	0.83963	88.8922	89.8351	93.1408	90.6227	1.8217135
1	0.8332	0.8554	0.8514	0.79833	0.82053	0.81653	88.5594	91.022	90.5783	90.0532	1.0717399
3	0.8336	0.8415	0.8414	0.79873	0.80663	0.80653	88.6038	89.4801	89.469	89.1843	0.4105255
Blank	0.0342	0.0352	0.0352	Blank Average		0.03487	Control average		0.90147		

BR1-27	Raw data			Blank Corrected Data			Viability %			Mean	STD
	Conc	1	2	3	1	2	3	1	2		
c	0.9548	0.9279	0.9263	0.91993	0.89303	0.89143	100	100	100	100	0
10	0.8147	0.8226	0.8325	0.77983	0.78773	0.79763	86.5072	87.3835	88.4817	87.4575	0.8078051
30	0.8175	0.7905	0.7695	0.78263	0.75563	0.73463	86.8178	83.8227	81.4931	84.0445	2.1794353
100	0.6773	0.6062	0.6464	0.64243	0.57133	0.61153	71.2653	63.3782	67.8376	67.4937	3.2290828
300	0.0877	0.0942	0.091	0.05283	0.05933	0.05613	5.86082	6.58187	6.22689	6.22319	0.2943779

Dox against Caco-2

Dox	Raw data			Blank Corrected Data			Viability %			Mean	STD
	Conc	1	2	3	1	2	3	1	2		
c	0.7588	0.7547	0.7884	0.72453	0.72043	0.75413	100	100	100	100	0
0.03	0.7556	0.7658	0.7695	0.72133	0.73153	0.73523	98.4039	99.7954	100.3	99.4998	0.8018503
0.1	0.7223	0.7454	0.7784	0.68803	0.71113	0.74413	93.8611	97.0124	101.514	97.4626	3.1405522
0.3	0.7168	0.7495	0.7669	0.68253	0.71523	0.73263	93.1108	97.5717	99.9454	96.876	2.8332581
1	0.7225	0.7441	0.7495	0.68823	0.70983	0.71523	93.8884	96.8351	97.5717	96.0984	1.5913783
3	0.7393	0.7321	0.7441	0.70503	0.69783	0.70983	96.1803	95.198	96.8351	96.0711	0.6727567
Blank	0.0341	0.0346	0.0341	Blank Average			0.03427	Control average			0.73303

Dox	Raw data			Blank Corrected Data			Viability %			Mean	STD
	Conc	1	2	3	1	2	3	1	2		
c	0.7588	0.7547	0.7884	0.72403	0.71993	0.75363	100	100	100	100	0
10	0.693	0.674	0.6954	0.65823	0.63923	0.66063	89.8571	87.2634	90.1847	89.1017	1.3067864
30	0.5295	0.5537	0.5669	0.49473	0.51893	0.53213	67.5373	70.8409	72.6429	70.3404	2.1141776
100	0.3842	0.3751	0.3521	0.34943	0.34033	0.31733	47.702	46.4598	43.32	45.8273	1.8440259
300	0.2885	0.333	0.3261	0.25373	0.29823	0.29133	34.6378	40.7126	39.7707	38.3737	2.6695177
Blank	0.0364	0.0339	0.034	Blank Average			0.03477	Control average			0.73253

Synthesised compounds against Caco-2

BRO-23	Raw data			Blank Corrected Data			Viability %			Mean	STD
	Conc	1	2	3	1	2	3	1	2		
c	0.6954	0.6954	0.6854	0.6594	0.6594	0.6494	100	100	100	100	0
0.03	0.6995	0.6854	0.6556	0.6635	0.6494	0.6196	101.133	98.9838	94.4416	98.1862	2.7893738
0.1	0.6115	0.6321	0.6286	0.5755	0.5961	0.5926	87.7197	90.8597	90.3262	89.6352	1.3718306
0.3	0.5898	0.5954	0.5996	0.5538	0.5594	0.5636	84.4122	85.2657	85.9059	85.1946	0.6118918
1	0.5602	0.5831	0.589	0.5242	0.5471	0.553	79.9004	83.3909	84.2902	82.5272	1.8933405
3	0.5547	0.5332	0.5551	0.5187	0.4972	0.5191	79.0621	75.785	79.1231	77.99	1.5594119
Blank	0.0377	0.0348	0.0355	Blank Average			0.036	Control average			0.65607

BRO-23	Raw data			Blank Corrected Data			Viability %			Mean	STD
	Conc	1	2	3	1	2	3	1	2		
c	0.6954	0.6954	0.6854	0.6594	0.6594	0.6494	100	100	100	100	0
10	0.5112	0.5023	0.5214	0.4752	0.4663	0.4854	72.4317	71.0751	73.9864	72.4977	1.1894463
30	0.145	0.1246	0.17	0.109	0.0886	0.134	16.6142	13.5047	20.4248	16.8479	2.8299194
100	0.0953	0.1391	0.0921	0.0593	0.1031	0.0561	9.03872	15.7149	8.55096	11.1015	3.2682045
300	0.0848	0.0878	0.1021	0.0488	0.0518	0.0661	7.43827	7.89554	10.0752	8.46967	1.1505257
Blank	0.0377	0.0348	0.0355	Blank Average			0.036	Control average			0.65607

BR1-27	Raw data			Blank Corrected Data			Viability %			Mean	STD
	Conc	1	2	3	1	2	3	1	2		
c	0.6525	0.6665	0.6521	0.61763	0.63163	0.61723	100	100	100	100	0
0.03	0.6415	0.6251	0.6121	0.60663	0.59023	0.57723	97.5033	94.8674	92.7779	95.0496	1.9334407
0.1	0.6021	0.6051	0.6029	0.56723	0.57023	0.56803	91.1706	91.6528	91.2992	91.3742	0.2038714
0.3	0.5954	0.5854	0.5745	0.56053	0.55053	0.53963	90.0938	88.4865	86.7345	88.4383	1.3718231
1	0.5651	0.5321	0.5412	0.53023	0.49723	0.50633	85.2237	79.9196	81.3823	82.1752	2.2367796
3	0.5115	0.5332	0.5621	0.47663	0.49833	0.52723	76.6086	80.0964	84.7415	80.4822	3.3314152
Blank	0.0342	0.0352	0.0352	Blank Average			0.03487	Control average			0.62217

BR1-27	Raw data			Blank Corrected Data			Viability %			Mean	STD
	Conc	1	2	3	1	2	3	1	2		
c	0.6525	0.6665	0.6521	0.61763	0.63163	0.61723	100	100	100	100	0
10	0.51125	0.5102	0.5021	0.47638	0.47533	0.46723	76.5684	76.3997	75.0978	76.022	0.6571227
30	0.50215	0.5129	0.5021	0.46728	0.47803	0.46723	75.1058	76.8336	75.0978	75.6791	0.816409
100	0.5021	0.4998	0.5141	0.46723	0.46493	0.47923	75.0978	74.7281	77.0265	75.6175	1.0077171
300	0.0741	0.0765	0.0764	0.03923	0.04163	0.04153	6.30592	6.69167	6.6756	6.55773	0.1781761
Blank	0.0342	0.0352	0.0352	Blank Average			0.03487	Control average			0.62217

BR1-82	Raw data			Blank Corrected Data			Viability %			Mean	STD
	Conc	1	2	3	1	2	3	1	2		
c	0.6652	0.6425	0.6321	0.63033	0.60763	0.59723	100	100	100	100	0
0.03	0.6514	0.6651	0.6251	0.61653	0.63023	0.59023	100.785	103.024	96.4854	100.098	2.7132396
0.1	0.6221	0.6214	0.6112	0.58723	0.58653	0.57633	95.995	95.8806	94.2132	95.3629	0.8143289
0.3	0.61251	0.6221	0.6102	0.57764	0.58723	0.57533	94.4273	95.995	94.0497	94.824	0.8422433
1	0.6118	0.60214	0.6021	0.57693	0.56727	0.56723	94.3112	92.7321	92.7256	93.2563	0.74595
3	0.555	0.5434	0.606	0.52013	0.50853	0.57113	85.0262	83.1299	93.3631	87.1731	4.444966
Blank	0.0342	0.0352	0.0352	Blank Average			0.03487	Control average			0.61173

BR1-82	Raw data			Blank Corrected Data			Viability %			Mean	STD
	Conc	1	2	3	1	2	3	1	2		
c	0.6652	0.6425	0.6321	0.63033	0.60763	0.59723	100	100	100	100	0
10	0.5121	0.5124	0.5092	0.47723	0.47753	0.47433	78.0133	78.0623	77.5392	77.8716	0.2358856
30	0.0654	0.0898	0.0661	0.03053	0.05493	0.03123	4.99128	8.97995	5.10571	6.35898	1.8538927
100	0.0561	0.0508	0.0541	0.02123	0.01593	0.01923	3.47101	2.60462	3.14407	3.07323	0.3572315
300	0.0743	0.0451	0.0433	0.03943	0.01023	0.00843	6.44616	1.67284	1.3786	3.16587	2.322628344
Blank	0.0342	0.0352	0.0352	Blank Average			0.03487	Control average			0.61173

BR1-93	Raw data			Blank Corrected Data			Viability %			Mean	STD
	Conc	1	2	3	1	2	3	1	2		
c	0.7442	0.7325	0.7332	0.70933	0.69763	0.69833	100	100	100	100	0
0.03	0.7112	0.7215	0.7321	0.67633	0.68663	0.69723	96.3758	97.8435	99.354	97.8578	1.215885945
0.1	0.7021	0.7211	0.7217	0.66723	0.68623	0.68683	95.0791	97.7865	97.872	96.9126	1.29692738
0.3	0.7121	0.7025	0.7032	0.67723	0.66763	0.66833	96.5041	95.1361	95.2358	95.6253	0.6226922
1	0.6995	0.6854	0.6541	0.66463	0.65053	0.61923	94.7086	92.6994	88.2392	91.8824	2.7035582
3	0.6325	0.6021	0.6321	0.59763	0.56723	0.59723	85.1613	80.8293	85.1043	83.6983	2.0287873
Blank	0.0342	0.0352	0.0352	Blank Average			0.03487	Control average			0.70177

BR1-93	Raw data			Blank Corrected Data			Viability %			Mean	STD
	Conc	1	2	3	1	2	3	1	2		
c	0.7442	0.7325	0.7332	0.70933	0.69763	0.69833	100	100	100	100	0
10	0.6155	0.6114	0.6125	0.58063	0.57653	0.57763	82.7388	82.1546	82.3113	82.4016	0.2469043
30	0.5332	0.5221	0.5141	0.49833	0.48723	0.47923	71.0113	69.4295	68.2896	69.5768	1.115998
100	0.0692	0.0739	0.0665	0.03433	0.03903	0.03163	4.89241	5.56215	4.50767	4.98741	0.4356997
300	0.0512	0.0491	0.0488	0.01633	0.01423	0.01393	2.32746	2.02821	1.98547	2.11371	0.1521457